IN THE UNITED STATES PATENT AND TRADEMARK OFFICE

Applicant(s): Rosen	
Application No.: 09/937,192	
Filed: 9/21/2001	Group Art Unit: 1624
Title: Methods and Compositions for Degradation and for Inhibition of HER-Family Tyrosine Kinases	Examiner: Bruck Kifle
Attorney Docket No.: MSK.P-038	

BRIEF FOR APPELLANT

This brief is filed in support of Applicants' Appeal from the rejection mailed 3/10/2005.[1] Consideration of the application and reversal of the rejections are respectfully urged.

Real Party in Interest

The real party in interest is Sloan-Kettering Institute for Cancer Research

Related Appeals and Interferences

To Applicants' knowledge, there are no related appeals or interferences now pending. A prior Appeal was filed in this case, but the rejection was withdrawn upon filing of an Appeal Brief.

Status of Claims

Claims 3, 4, 6 and 9-34 are pending in this application. Claims 1, 2, 5, 7 and 8 have been canceled. No other claims have been presented.

---

[1] Although the rejection of March 10, 2005 is not a final rejection, claims in this application have been twice rejected, and the requirements for filing an Appeal as set forth in 37 CFR 41.31(a) are met.

Status of Amendments

All amendment made in this case have been entered.

Summary of Claimed Subject Matter

As set forth in claim 3, the present application relates to:

> A chemical compound comprising first and second hsp-binding moieties which bind to the pocket of hsp90 with which ansamycin antibiotics bind, said binding moieties being connected to one another by a linker, wherein the first and second hsp-binding moieties are each an ansamycin antibiotic and retain the ability in the chemical compound to bind to the pocket of hsp90.

Ansamycins are a known class of antibiotics that bind to a specific pocket of the chaperone protein hsp90. (Specification, page 1, lines 26-28). The composition of the present invention have two ansamycin moieties which interact this pocket of hsp90 and can thus be considered as dimers (homo- or hetero-). (Page 1, lines 1-3, Page 3, lines 14-20).

In the compound as defined in claim 3, the two ansamycin antibiotics are joined by a linker. The linker may be of varying lengths, and may include substituents such as amines, or double or triple bonds. (Page 4, lines 14-19). Specific example of linkers include alkyl chains of 4 to 12 carbons as shown in Table 1 (Page 6) and aryl linkers, and N-methyl amino linkers as shown in Fig. 1. Synthesis of such compounds is described in Fig. 1 and Example 1.

The compositions of the invention are useful in the destruction of cells expressing a HER-family tyrosine kinase (claim 12, Page 4, lines 29-31), and in the treatment of cancer (claim 13,) particularly in cancers that over-express a HER-family kinase. (Claim 30). (See, specification, Page 3, lines 17-28, Page 8, lines 1-25 and examples 2-5).

Grounds of Rejection to be reviewed on Appeal

Claims 3, 4, 6 and 9-34 stand rejected under 35 USC § 112, first paragraph, as lacking enablement.

Claims 3, 4, 6 and 9-34 stand rejected under 35 USC § 112, second paragraph, as indefinite.

Argument

I. The Enablement Rejection

Claims 3, 4, 6 and 9-34 stand rejected for lack of enablement. In making this rejection, the Examiner has paid no attention to the scope of the individual claims or the arguments presented, but has treated all claims as a group. This is improper, since the rejection plainly cannot apply to all of the mentioned claims.

A. Claims 10 and 11 are composition claims within the scope said to be enabled.

The Examiner acknowledges that the present specification is enabling for the "geldanamycin dimer, wherein the linker is $-(CH_2)_{4-12}$ and bonded to the 17-carbon of each geldanamycin, to treat breast cancer." (Office Action, page 2). Given this acknowledgment, the rejection of claims 10 and 11, which are compositions claims (and therefore not dependent on any particular use) and which specifically fall within the scope that the Examiner says are enabled, is clearly in error and suggests that the Examiner has failed to give due consideration to the claims and the application.

The Examiner also asserts a lack of enablement without identifying the claims rejected on this ground because "the specification does not provide enablement for the treatment of cancer generally." This ground for rejection cannot be applied to composition claims.

Accordingly, the rejection under 35 USC § 112, first paragraph, for lack of enablement should be reversed with respect to claims 10 and 11.

B. Composition Claims 3, 4, and 6

Claims 3, 4, 6 and 9 are also composition claims, but they broader in scope than claims 10 and 11. The argument with respect to enablement of treatment of cancer generally cannot apply to these claims, and therefore the only arguments of relevance to these claims are those made in connection with the composition claims. The Examiner refers to and incorporates the Official Action of June 25, 2004, and argues that "determining the compound claimed would require synthesis of millions of compounds and testing each to determine whether the compounds falls within the scope of claim 1." In prior Office Action the Examiner made the same statement, and Applicants responded

> The Examiner on page 9 of the official action [argues] that "the breadth of the claims includes billions of compounds with radically diverse structures which bind to the pocket of hsp90." Applicants challenge the Examiner to support this statement with compounds that don't venture into the absurd. The parts of the claims that the Examiner has omitted from his characterization specify that the molecule contains two ansamycin antibiotic moieties. The Examiner has not established that this is class containing a multiplicity of compounds of diverse structure as the Examiner argues.

(Amendment filed December 27, 2004) In response to this, the Examiner did not provide a reasoned basis for his allegation or argument.[2] He did not establish that ansamycin antibiotics are a diverse groups of compounds of diverse structure. This being the case, the Examiner's position is nothing more than an unsupported allegation which should carry no weight in assessing enablement.

The Examiner also stated in the Official Action of June 25, 2004 (page 8), that "the direction concerning how to make the claimed compounds is not found in the specification." Applicants disagree. Fig. 1 provides two synthetic routes to compositions of the invention, one shown for a geldanamycin homodimer and one for a geldanamycin-herbimycin heterodimer. In both cases, reactive groups on the anasmaycin antibiotic (the 17 methoxy group of geldanamycin,

---

[2] The Examiner new ground for rejection under 35 USC § 112, second paragraph, is not reasoned support for this position as discussed below.

for example) are reacted with an linker having primary amine functionality at one end and amine or some other functionality at the other. (See Page 20, lines 28, Fig. 2 and Example 1) This linker is then reacted with the second ansamycin (in a single or two separate reactions) to form the dimer. The Examiner has not said why this synthetic method is not sufficient to teach how to make compounds within the scope of the claims, for a person of ordinary skill in the art. The reaction discussed here are not intricate processes where stereochemistry is important. They are simply sticking two known molecules (anasmycin antibiotics) together with something (a linker) in between using standard organic synthesis techniques.

In the Office Action of June 24, 2004 (page 8), the Examiner also asserted that "there is one working example." This assertion is in error, since Fig 1 and Example 1 show both a homo-dimer and a heterodimer and a variety of linkers and functional groups on the unreacted linkers, and since dimers with different length linkers were made and tested using the same techniques. Further, the Examiner has not offered any reasoning as why the methods described which involve standard synthetic reactions would not allow persons skilled in the art to make additional compounds.

For these reasons, the rejection for lack of enablement of claims 3, 4, 6 and 9 should be reversed.

C. Composition Claim 9 is enabled.

Composition claim 9 is a composition claim. It recites that both of the ansamycin antibiotics are geldanamycin, but is broader in scope than claims 10 and 11 because the linker is not specifically defined. The argument with respect to enablement of treatment of cancer generally cannot apply to this claim, and therefore the only arguments of relevance are those made in connection with the linker.

The Examiner has stated that the application is enabling for linkers that are $(CH2)_{4-12}$ bonded to the 17-carbon of geldanamycin. The Examiner has not, however, explained why other linkers bonded to this position (as required in claim 9) are not enabled. Thus, the Examiner has

failed to meet his burden in presenting a meaningful rejection of this claim to which Applicants can respond. The rejection should therefore be reversed.

D. Method Claim 12 is enabled

Claim 12 is a method claim, but it is not directed to the treatment of cancer. Rather it is directed to a method for destruction of cells expressing a HER-kinase. The Examiner has offered no reasons why this method is lacking enablement, and therefore it is assumed that the rejection of this claim is based on the definition of the composition that is used in the method, which corresponds in scope to compounds of claim 3. For the same reasons as set forth above, in section I. B., this rejection is in error and should be reversed.

E. Method Claims 13, and 15-17 are enabled

Method claim 13 recites a method of treating cancer by administration of a compound which is defined in the same scope as composition claims 3, 4, 6 and 9. The arguments set forth in Section I. B above are applicable to the rejection to the extent it relates to the definition of the enablement of the compositions.

The remaining reasons for rejection of these claims is the assertion that "the specification does not provide enablement for treatment of cancer generally." The reason he makes this statement is the unsupported assertion that no one has ever found a compound capable of treating cancer generally before. While Applicants would agree that general lack of success in the past gives rise to a basis for skepticism, this does not absolve the Examiner of the obligation to look at the invention and the evidence in deciding enablement issues.

In this case, Applicants have on several occasions submitted exhibits consistent with the broad scope of effectiveness of the compositions of the present invention and why the scope of the claims is appropriate. Copies of these Exhibits are attached in the Appendix. The Exhibits were first submitted with the Amendment filed July 22, 2002. The Office Action of September 12, 2002 rejected the claims on the same ground now on Appeal, but made no mention of the

exhibits. No mention of the exhibits was made in the Office Action of April 23, 2003 (remailed on June 11, 2003). In Applicants response filed by facsimile on August 27, 2003, Applicants stated "Applicants further inquire **why** the Examiner has maintained the rejection while refusing to comment on the references showing the diverse activity of geldanamycin and related species against diverse types of cancer" and asked the Examiner to either withdrawn the rejection or address the merits of the exhibits and related arguments. The response was an Advisory Action mailed 9/10/2003 which maintained the rejection with out comment.

Applicants again pointed out the failure of the Examiner to respond to the evidence in an Appeal Brief filed on April 26, 2004. This Brief led to reopening of prosecution with the Official Action mailed on June 25, 2004. This Action contained included an enablement rejection, but no mention of the declaration evidence in the record. Therefore, in the response filed December 27, 2004 Applicants stated:

> It is also noted that the Examiner has, despite repeated requests by Applicants, once again not even mentioned the declarations and the exhibits A-O which are of record in this case. The Examiner cannot pick and choose among the evidence of record, but must consider all of the evidence. Accordingly, should the rejection of the present claims be maintained, Applicants DEMAND a statement by the Examiner that these materials have been considered and an explanation as to why the Examiner finds them insufficient.

The Examiner still has not even mentioned the Exhibits.

Applicants realize that the Examiner cannot reasonably be barred from submitting arguments concerning these papers in further proceedings, as might be the case if he were a party to litigation. Nevertheless, Applicants submit that given the failure to consider available evidence, the rejection should be reversed unless the Examiner does provide some reasoned explanation of his position.

The basis for the Examiner's argument is largely that the Examiner is classing cancer therapy with perpetual motion machines and assumes in assessing enablement that it is inherently unbelievable that a cancer therapy could work generally. Such may have been the case when *In*

re Buting, 163 USPQ 689 (CCPA 1969), cited by the Examiner, was decided in 1969, but the art and the law have progressed since then. The notion of automatic unbelievability is no longer credited. Indeed, as the Board of Appeals noted in 1987 in *Ex parte Rubin*, 5 USPQ2d 1461, 1462 (POBAI 1987), "'contemporary knowledge in the art ' has far advanced since the days when the any statement of utility in treating cancer was per se 'incredible.'" Here, the Examiner has not offered any reasoning as to why the assertions of general utility in this application, given the suggested mechanism of action. As such, the Examiner has failed to meet the burden discussed in *In re Marzocchi*, 169 USPQ 367, 369 (CCPA 1971), where it is noted that:

> a specification disclosure which contains a teaching of the manner and process of making and using the invention in terms which correspond to those used in describing and defining the subject matter sought to be patents *must* be taken as in compliance with the enabling requirement of the first paragraph of § 112, *unless* there is a reason to doubt the objective truth of the statements contained therein, which must be relied upon for an enabling disclosure.

An over thirty-year-old case, discussing the state of the art at that time, is not a reason to doubt the truth of the asserted utility here.

Turning now to the contents of the much-ignored evidence, Applicants have submitted copies of published papers showing that a monomeric ansamycin compound, 17-allylamino-geldanamycin (17-AAG), which is mentioned in the specification on Page 8, line 15 and other hsp90 inhibitors are efficacious in a variety of tumor types including breast cancer, ovarian cancer, pancreatic cancer and gastric cancer (the cancer types specifically mentioned on Page 8, lines 9-11 of the application), other HER kinase overexpressing tumors, and tumors which do not over express HER kinase. For example, Yang et al. (Exhibit A), report inhibition of glioma (brain tumor) cells with 17-AAG. Okabe et al. (Exhibit B) reports *in vivo* activity of herbimycin A (an ansamycin antibiotic) against leukemia cells. Kelland *et al* (Exhibit C, JNCI 91: 1940, 1999) achieved tumor cytostasis in two human colorectal carcinomas, HT29 and BE for the July 7, 2005 duration of drug treatment with 17-AAG. Burger *et al* (Exhibit D Proc. AACR, 41: Abstract # 2844, 2000) reported potent effects of 17-AAG against a melanoma xenograft and,

interestingly, preliminary data from the London arm of the 17-AAG trial indicates that melanoma (2/6 objective responses) may be a responsive tumor (Exhibit E Banerji *et al*, Proc. ASCO, Abstract # 326, 2001) 17-AAG has also been used in studies with prostate cancers, and it has been shown that this administration resulted in dose-dependent inhibition of androgen-dependent and -independent prostate cancer xenografts. (Exhibit F Solit et al., *Clin. Cancer Res.* 8: 986-993, 2002). 17-AAG has also been shown to enhance paclitaxel-mediated cytotoxicity in lung cancer cells (Exhibit G Nguyen et al, *Ann. Thorac. Surg.* 72: 371-379, 2001); and to modulate metastasis phenotypes in non-small cell lung cancer (Exhibit H Nguyen et al., *Ann. Thorac. Surg.* 70: 1853-60, 2000). Thus, the efficacy of compounds that bind to the hsp90 receptor span a wide range of unrelated cancers, thereby refuting the Examiner's statement that generalized cancer therapy is inherently unbelievable.

The Examiner has not offered any **reasoning** as to why the assertions of general utility in this application, given the suggested mechanism of action, and the evidence of involvement of the targeted species in numerous different cancer types. As such, the Examiner has failed to meet the burden discussed in *In re Marzocchi.* For these reasons, Applicants submit that the rejection of claims 13 and 15-17 should be reversed.

F. Claims 18, 19 and 20 are enabled.

Claims 18, 19 and 20 have composition limitations which correspond to the limitations of claims 9, 10 and 11 discussed above in sections I.A. and I.C, and method scope comparable to that of claim 13 discussed in I.E. These arguments are applicable to claims 18, 19 and 20, and form the basis for reversal of the enablement rejection of these claim.

G. Claims 14 and 30 are enabled.

Claim 14 has composition limitations comparable to claim 3, and the arguments of Section I.B are therefore applicable. The arguments of Section I.E are also applicable. Further, claim 14 limits the scope of the cancer treated to cancers that are positive for HER-kinase. This

is a subset of "all cancers." Despite repeated requests, the Examiner has never explained why the argument that claims are not enabled for all cancers is applied to claim 14 which is a method of treating less than all cancers. Applicants provide a specific mechanism of action that is believed to explain the activity of the compounds against Her-kinase positive tumors (Page 4, line 29 - page 5, line 13). The Examiner has not explained why this mechanism combined with evidence of activity of ansamycin compounds against HER-positive cells is insufficient to establish enablement of the scope of claim 14.

Similarly, claim 30 states that the cancer is one that overexpresses a HER-family kinase. The same arguments apply to this claim, and the rejection should be reversed.

H. Claims 21-23 are enabled.

Claims 21-23 correspond in scope of compound to claims 4 and 6, and in scope of cancers treated to claim 14. Accordingly, the arguments of sections I.B and I.G are applicable and establish that these claims are enabled.

I. Claim 24 is enabled.

Claim 24 is dependent on claim 12, and recite a composition scope comparable to claim 9. Accordingly, the arguments of sections I.B. and I.D. are applicable and form the basis for reversal of the rejection of these claims.

J. Claim 25 and 26 are enabled.

Claims 25 and 26 are dependent on claim 12, and recite a composition scope comparable to claims 10 and 11. Accordingly, the arguments of sections I.A. and I.D. are applicable and form the basis for reversal of the rejection of these claims.

K. Claims 27 - 29 are enabled.

Claims 27 -29 are dependent on claim 12, and recite a composition scope comparable to claims 4 and 6. Accordingly, the arguments of sections I.B. and I.D. are applicable and form the basis for reversal of the rejection of these claims.

L. Claims 31-34 are enabled

Claims 31-34 depend from claim 13, but recite specific types of cancer. The argument concerning treatment all cancers is plainly not applicable to these claims. Thus, the only basis for the enablement rejection applicable to these claims relates to the scope of the compositions to which the argument of section I.B is applicable and establishes enablement.

II. The Definiteness Rejection

Claims 3, 4, 6 and 9-34 stand rejected under 35 USC § 112, second paragraph, as indefinite. The Examiner has cited three grounds for this rejection: (1) the meaning of the term ansamycin, (2) the nature of the linker; and (3) the assertion that the scope of the compounds is not determinable. Applicants submit that these grounds a are without merit and that the rejection should be reversed.

A. The term Ansamycin Antibiotic is Definite
(Claims 3, 4, 6, 12-17, 21-23, 27-34)

The Examiner has rejected the claims as indefinite based on the assertion that "the metes and bounds of the 'ansamycin' is unknown." This rejection cannot be applicable to claims 9-11, 18-20 and 24-26 in which the term ansamycin antibiotic is further defined as geldanamycin.

The term "ansamycin antiobiotic" is a recognized term of art, as is apparent from searches on the internet or in the USPTO full text search engine. For example, US Patent No. 4,247,462, entitled "Ansamycin Antibiotic" states that:

> The ansamycins constitute a class of antibiotics characterized by an aliphatic bridge linking two nonadjacent positions of an aromatic nucleus. The rifamycins and streptovaricins are well known members of this class of antibiotics. The chemistry of the ansamycin antibiotics is reviewed by K. L. Rinehart, Jr. and L. S. Shield in Progress in the Chemistry of Organic Natural Products, published by Springer-Verlag, Vienna-New York (1976).

See also, US Patent No. 4,738,958 entitled "Ansamycin antibiotic and its use as a medicament." A copy of the Rinehart paper which is referenced in this quotation is attached in the Exhibit Appendix.

When one takes the structure of geldanamycin for example, these definitions are applied as follows:

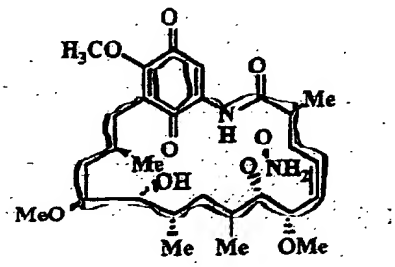

Geldanamycin (GM)

where the organic nucleus is indicated in red and the ansa ring is indicated in green.

Notwithstanding this evidence that the art recognizes a class of antibiotics as anasamycin antibiotics, the Examiner says a person skilled in the art does not know what an ansamycin antibiotic is. For example, he takes the language "The ansamycins constitute a class of antibiotics characterized by an aliphatic bridge linking two nonadjacent positions of an aromatic nucleus." that appears in an issued US Patent, and makes up a compound that meets the bare limit of this definition and asks if this is an ansamycin. There is no evidence or reason to imagine that this compound (1) exists, and (2) is an antibiotic, Applicants submit that this approach is inappropriate. Further it is noted that the compositions are not merely defined as

including "ansamycin antibiotics." They require that these ansamycin antibiotics bind to the same known pocket on hsp90 to which other ansamycin antibiotics bind.

The standard of definiteness does not require a person skilled in the art to be able to name every compound that falls within the scope of the claim. Rather, it requires a person skilled in the art to consider an actual compound, and determine whether it falls within the scope of the claims. See, *In re Johnson*, 194 U.S.P.Q. 187, 194 (C.C.P.A. 1977)(observing that claim is definite where "those skilled in the art would have no trouble ascertaining whether any particular polymer falls within the scope of the claim."). The art has an understanding of the meaning of the term "ansamycin antibiotic." That is may not meet some absolute standard does not mean that the term is not definite to persons skilled in the art.

B. The term "linker" is Definite

The Examiner also rejected the claims based on the term linker, asserting that "nature of the linker is unknown." From the Examiner's recitation of possible linker options, it is apparent that the Examiner is equating breadth with lack of definiteness. Case law is clear, however, that the two are not the same. See, In re Skoll, 187 U.S.P.Q. 481 (C.C.P.A. 1975). The specification states that "the two hsp-binding moieties are joined by a linker." (Page 4, lines 14-15). Thus, the recitation of a linker in the claims requires that there be something in between the two ansamycin antibiotics. The person skilled in the art would have no difficulty looking at a particular compound and see if there was something (a linker) present. Thus, there is no lack of definiteness based on this term in the claims.

The Examiner also states that the characterization of the linker as having a length of 4-7 carbons is unclear. The linker extends from one ansamycin antibiotic to the other. The specification states that "in general the linker will be 1 to 9 carbon atoms in length" (Page 4, lines 16-17) and provides examples of dimers where the linker is 4 to 12 carbons in length (Table 1) . The specification further refers on Page 5 to the linkers of differing lengths depicted in Fig. 2. Thus, a person skilled in art, having read the specification would undertand that the phrase "a length of 4 to 7 carbon atoms" is indicative of a chain of 4 to 7 carbon atoms that extends between the two ansamycin antibiotics. There may or may not be substitutions on this chain, or unsaturation (for example a double bond) as indicated on Page 4, line lines 17-19, and Fig. 1.

C. The term "bind" is not indefinite
(Claims 3, 4, 6, 12-17, 21-23, 27-34)

This ground for rejection is not applicable to claims 9-11, 18-20 and 24-26 in which the term ansamycin antibiotic, and thus the hsp-binding moiety is further defined as geldanamcyin.

The Examiner asserts that the scope of the compounds claimed is indeterminate because the term "bind" is indefinite. Applicants submit that this basis for rejection is in error.

In support of his position, the Examiner argues that "there is no way of knowing whether a given compound would bind," and that "binding is a process which cannot be observed, merely inferred, which is unreliable." Applicants point out, however, that the art of record in this case establishes that persons skilled in the art have been observing the interaction between ansamycin antibiotics such as geldanamycin with hsp90 for some time, and calling this interaction "binding." For example, the Stebbins reference (of record, attached in the Exhibit Appendix) refers to binding of geldanamycin to hsp90 as an observed phenomenon, and then determines the crystal structure of hsp90 and the location of the binding pocket.[3] Thus, both the meaning of binding, and the specific pocket referred to are clear.

The Examiner has not established why a person skilled in the art would have difficulty understanding whether a given compound falls within the scope of the claims. Accordingly, the rejection under 35 USC § 103 should be reversed.

---

[3] It is noted that the crystallographic observation of the geldanamycin - hsp90 complex contradicts the Examiner's assertion that the binding cannot be observed. However, such observation is not necessary for the claims to be definite.

III. Conclusion

Applicants submit that the rejections of the present claims under 35 USC § 112, first and second paragraphs, are in error and should be reversed.

Respectfully submitted,

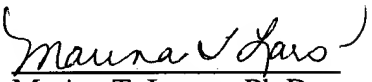

Marina T. Larson Ph.D.
PTO Reg. No. 32,038
Attorney for Applicant
(970) 468-6600

Claims Appendix

3. A chemical compound comprising first and second hsp-binding moieties which bind to the pocket of hsp90 with which ansamycin antibiotics bind, said binding moieties being connected to one another by a linker, wherein the first and second hsp-binding moieties are each an ansamycin antibiotic and retain the ability in the chemical compound to bind to the pocket of hsp90.

4. The chemical compound of claim 3, wherein at least one of the hsp-binding moieties is geldanamycin, and the linker is connected to the 17-carbon of the geldanamycin .

6. The chemical compound of claim 4, wherein the linker has a length of 4 to 7 carbon atoms.

9. The chemical compound of claim 3, wherein the first and second hsp-binding moieties are geldanamycin and the linker is connected to the 17-carbons of the geldanamycins.

10. The chemical compound of claim 9, wherein the linker has a length of 4 to 7 carbons atoms.

11. The chemical compound of claim 10, wherein the linker has a length of 4 carbon atoms.

12. A method for destruction of cells expressing a HER-family tyrosine kinase, comprising administering to the cells a chemical compound comprising first and second hsp-binding moieties which bind to the pocket of hsp90 with which ansamycin antibiotics bind, said binding moieties being connected to one another by a linker, wherein the first and second hsp-binding moieties are each an ansamycin antibiotic and retain the ability in the chemical compound to bind to the pocket of hsp90.

13. A method for treating cancer in a patient suffering from cancer, comprising administering to the patient a therapeutic composition comprising a chemical compound comprising first and second hsp-binding moieties which bind to the pocket of hsp90 with which ansamycin antibiotics bind, said binding moieties being connected to one another by a linker, wherein the first and second hsp-binding moieties are each an ansamycin antibiotic and retain the ability in the chemical compound to bind to the pocket of hsp90.

14. The method of claim 13, wherein the cancer is an HER-positive cancer.

15. The method according to claim 13, wherein at least one of the hsp-binding moieties is geldanamycin, and the linker is connected to the 17-carbon of the geldanamycin.

16. The method according to claim 15, wherein the linker has a length of 4 to 7 carbon atoms.

17. The method according to claim 16, wherein the linker has a length of 4 carbon atoms.

18. The method according to claim 13, wherein the first and second binding moieties are geldanamycin, and the linker is connected to the 17-carbons of the geldanamycins.

19. The method according to claim 18, wherein the linker has a length of 4 to 7 carbon atoms.

20. The method according to claim 19, wherein the linker has a length of 4 carbon atoms.

21. The method according to claim 14, wherein at least one of the hsp-binding moieties is geldanamycin, and the linker is connected to the 17-carbon of the geldanamycin.

22. The method according to claim 21, wherein the linker has a length of 4 to 7 carbon atoms.

23. The method according to claim 22, wherein the linker has a length of 4 carbon atoms.

24. The method according to claim 12, wherein the first and second binding moieties are geldanamycin, and the linker is connected to the 17-carbons of the geldanamycins.

25. The method according to claim 24, wherein the linker has a length of 4 to 7 carbon atoms.

26. The method according to claim 25, wherein the linker has a length of 4 carbon atoms.

27. The method according to claim 12, wherein at least one of the hsp-binding moieties is geldanamycin, and the linker is connected to the 17-carbon of the geldanamycin.

28. The method according to claim 27, wherein the linker has a length of 4 to 7 carbon atoms.

29. The method according to claim 28, wherein the linker has a length of 4 carbon atoms.

30. The method of claim 13, wherein the cancer is one in which the cancer cells overexpress a HER-family kinase.

31. The method of claim 13, wherein the cancer is breast cancer.

32. The method of claim 13, wherein the cancer is ovarian cancer.

33. The method of claim 13, wherein the cancer is pancreatic cancer.

34. The method of claim 13, wherein the cancer is gastric cancer.

Evidence Appendix

Yang et al. (Exhibit A)
Okabe et al. (Exhibit B)
Kelland *et al* (Exhibit C)
Burger *et al* (Exhibit D)
Banerji et al. (Exhibit E)
Solit et al. (Exhibit F)
Nguyen et al. (Exhibit G)
Nguyen et al. (Exhibit H)
Stebbins Article
Rinehart Article

[CANCER RESEARCH 61, 4010–4016, May 15, 2001]

Disruption of the EF-2 Kinase/Hsp90 Protein Complex: A Possible Mechanism to Inhibit Glioblastoma by Geldanamycin[1]

(4) Glioma

Jun Yang, Jin-Ming Yang, Marie Iannone, Weichung Joe Shih, Yong Lin, and William N. Hait[2]

University of Medicine and Dentistry of New Jersey-Robert Wood Johnson Medical School, Departments of Medicine and Pharmacology, The Cancer Institute of New Jersey [J. Y., J-M. Y., M. I., W. N. H.] and School of Public Health [W. J. S., Y. L.], New Brunswick, New Jersey, 08901

ABSTRACT

Glioblastoma multiforme is the most treatment-resistant brain tumor. Elongation factor-2 (EF-2) kinase (calmodulin kinase III) is a unique protein kinase that is overexpressed in glioma cell lines and in human surgical specimens. Several mitogens activate this kinase and inhibitors block mitogen activation and produce cell death. Geldanamycin (GA) is a benzoquinone ansamycin antibiotic that disrupts Hsp90-protein interactions. Because EF-2 kinase is chaperoned by Hsp90, we investigated the effects of GA on the viability of glioma cells, the expression of EF-2 kinase protein, and the interaction between Hsp90 and EF-2 kinase. GA was a potent inhibitor of the clonogenicity of four glioma cells lines with IC_{50}s ranging from 1 to 3 nM. 17-allylamino-17-demethoxygeldanamycin (17-AAG), a less toxic and less potent derivative of GA, inhibited the clonogenicity of glioma cells with IC_{50} values of 13 nM in C6 cells and 35 nM in T98G cells. Treatment of cell lines for 24–48 h of GA or 17-AAG disrupted EF-2-kinase/Hsp90 interactions as measured by coimmunoprecipitation, resulting in a decreased amount of recoverable kinase in cell lysates. The ability of GA to inhibit the growth of glioma cells was abrogated by overexpressing EF-2 kinase. In addition, 17-AAG significantly inhibited the growth of a glioma xenograft in nude mice. These studies demonstrate for the first time the activity of GAs against human gliomas *in vitro* and *in vivo* and suggest that destruction of EF-2 kinase may be an important cytotoxic mechanism of this unique class of drug.

INTRODUCTION

Glioblastoma multiforme is a highly resistant, lethal malignancy of the central nervous system that represents an increasingly important cause of death from cancer in adults and children (1). Current therapy with surgery, radiation, and chemotherapy rarely, if ever, cures the disease and infrequently prolongs life for more than 1 year (2). Therefore, our laboratory has been investigating new signal transduction proteins as potential targets for drug development.

Activation of tyrosine kinases through receptor occupation or mutation initiates several signal transduction pathways that culminate in cell division. The epidermal growth factor receptor is frequently overexpressed or mutated in human glioblastoma (3–5). Activation of phospholipase C by the epidermal growth factor receptor produces two second messengers, diacylglycerol and inositol-1,4,5-triphosphate. Whereas the former can participate in mitogen-activated protein kinase signaling, the latter activates calmodulin-dependent pathways through the release of intracellular calcium (6–9).

We previously found that calmodulin-dependent phosphorylation of eEF-2[3] was markedly increased in glioblastoma because of the increased activity of calmodulin-dependent protein kinase 3 (10), also known as EF-2 kinase (11–13). EF-2 kinase phosphorylates eEF-2 in response to elevation in intracellular calcium, which leads to the inactivation of this translation factor (14, 15). Additional studies defined EF-2 kinase as a proliferation-dependent and mitogen-activated enzyme in a variety of normal and malignant cell types (16, 17).

The cloning and sequencing of EF-2 kinase led to the realization that it represented a unique enzyme family (13). Except for the ATP binding site, EF-2 kinases from several different species exhibit no sequence homology to any Ca^{2+}/calmodulin-dependent protein kinase, or to any member of the eukaryotic protein kinase superfamily. However, EF-2 kinase does have homology to the catalytic domain of myosin heavy chain kinase A (MHCK A) from *Dictyostelium*. The unique structural features of EF-2 kinase, together with its increased activity in malignancy and cell-cycle dependency, makes it a novel target for anticancer therapies.

In fact, several lines of evidence suggest that inhibiting the activity of EF-2 kinase can kill cancer cells. For example, Parmer *et al.* (18), demonstrated that rottlerin, an EF-2 kinase inhibitor, blocked glioma cells at the G_1-S phase interface and killed a variety of cell lines at concentrations (1–10 nM) that were consistent with IC_{50}s for enzyme inhibition (18). Antisense RNA to calmodulin (19) and EF-2 kinase[4] markedly decreased the clonogenicity of rat and human glioma cell lines. Therefore, identification of new drugs that block the function of EF-2 kinase may lead to new types of anticancer drugs.

During the purification of EF-2 kinase (20), we found the enzyme to be tightly associated with Hsp90 as previously demonstrated by Palmquist *et al.* (21). Hsp90 is a protein chaperone responsible for maintaining proper protein folding and stability (22). Recently, a new class of drug, the GAs was found to disrupt Hsp90/protein interactions (23). These benzoquinone ansamycin antibiotics were shown to have antitumor effects in cell culture and experimental animals (24). Recently, 17-AAG, a less toxic and less potent derivative of GA, has entered Phase I clinical testing (25–27).

Because the activity of EF-2 kinase is markedly increased in human glioblastoma and is chaperoned by Hsp90, we examined the effects of the GAs on this lethal malignancy of the central nervous system.

MATERIALS AND METHODS

Cell Culture. The C6 *N*-nitrosomethylurea-induced rat glioma line and the human cell lines T98G (glioblastoma), Daoy (medulloblastoma), and SKNSH (neuroblastoma) were obtained from The American Type Culture Collection. TJY1-R and TJY2-D cell lines were derived from T98G cells by stable transfection with either antisense or sense cDNA of EF-2 kinase. These two cell lines expressed either low or high amounts of EF2-K protein, respectively, relative to the parental line. T98G and Daoy cells were grown in a 1:10, DMEM:Ham's F-10 media, supplemented with 10% fetal bovine serum and 100 units/ml penicillin and 100 mg/ml streptomycin. TJY1-R and TJY2-D cell lines were maintained in the same medium as T98G, but were supplemented with 200 μg/ml G418. C6 and SKNSH cells were cultured in supplemented DMEM. Cell cultures were maintained in a humidified incubator at 37°C with 5% CO_2. Cells in log phase were grown in 100-mm tissue culture plates and treated with GA or 17-AAG as indicated in the figure legend.

Received 10/6/00; accepted 3/16/01.

The costs of publication of this article were defrayed in part by the payment of page charges. This article must therefore be hereby marked *advertisement* in accordance with 18 U.S.C. Section 1734 solely to indicate this fact.

[1] Supported by USPHS Grant CA43888 and National Cancer Institute (NIH) Grant CA72720.

[2] To whom requests for reprints should be addressed, at The Cancer Institute of New Jersey, 195 Little Albany Street, New Brunswick, New Jersey 08901. Phone: (732) 235-8064; Fax: (732) 235-8094; E-mail: haitwn@umdnj.edu.

[3] The abbreviations used are: eEF-2, elongation factor 2; EF-2 kinase, elongation factor 2 kinase; 17-AAG, 17-allylamino-17-demethoxygeldanamycin; BCNU, 1,3-bis(2-chloroethyl)-1-nitrosourea; GA, geldanamycin; Hsp90, heat shock protein 90; PMSF, phenylmethylsulphonyl fluoride.

[4] S. Hua, J. Yang, and W. N. Hait, unpublished observations.

Exhibit A

Drugs. GA and 17AAG were obtained from Drug Synthesis and Chemistry Branch, Developmental Therapeutics Program, Division of Cancer Treatment and Diagnosis of the National Cancer Institute in the form of a lyophilized powder. They were stored in dark, airtight containers at 4°C and reconstituted in DMSO immediately before use.

Clonogenic Assays. Cytotoxicity of GA and 17AAG was determined by clonogenic assay. Four × 10^2 C6 cells or 6 × 10^2 T98G cells were plated in 60-mm tissue culture dishes and allowed to adhere overnight. The cells were then exposed to various concentrations of drug ranging from 0.05–100 nM (control cultures were treated with 0.01% DMSO) and incubated for 24–48 h at 37°C. The medium was then removed and replaced with fresh medium free of drug. After 7–10 days of growth, colonies were fixed and stained with 0.5% methylene blue. Colonies with diameters of 2 mm and larger were counted using an electronic counting pencil.

Preparation of Cell Homogenates for Detection of Cellular EF-2 Kinase. Cell monolayers were washed twice in PBS (pH 7.4), scraped into 15-ml centrifuge tubes in 5 ml of PBS, and then centrifuged at 1,000 × *g* for 5 min. Cell pellets were homogenized with 15 strokes in ice-cold HOMO buffer [25 mM HEPES (pH 7.4), 100 mM sodium chloride, 20 mM sodium PP_i, 2 mM EDTA, 0.1 mM PMSF, 10 μg/ml leupeptin, 2 μg/ml pepstatin A, and 0.1 mM sodium orthovanadate], using a Polytron homogenizer. The homogenates were then centrifuged at 15,000 × *g* for 30 min at 4°C. The protein concentration of the supernatants was determined according to the method of Bradford using a Bio-Rad protein assay kit (Bio-Rad Laboratories, Richmond, CA). Twenty μg of protein from each sample were used for EF-2 kinase detection. Sample volumes were adjusted with HOMO buffer. Samples were boiled with 3× Laemmli buffer [190 mM Tris (pH 6.8), 6% SDS, 30% glycerol, 15% 2-mercaptoethanol, and 0.003% bromphenol blue dye] for 5 min before resolution by 7.5% SDS-PAGE.

Immunoprecipitations. Cell monolayers were washed twice with PBS and lysed with NET lysis buffer [50 mM Tris-HCl (pH7.4), 150 mM NaCl, 0.1% NP40, 1.0 mM EDTA, 1 mM PMSF, and 1% aprotinin] at 4°C for 30 min. Cells were scraped into 1.5-ml microcentrifuge tubes and incubated at 4°C with rotation for 30 min, passed through a 25-gauge needle, and then centrifuged at 15,000 × *g* at 4°C for 30 min. The protein concentration of the supernatants was determined using the Bio-Rad protein assay kit.

Immunoprecipitations were performed using 2 mg (C6 cells) or 1 mg (T98G cells) of protein from total cell lysates as starting material. Reaction volumes were equalized using NET buffer. For Hsp90 precipitation, 4 μg of anti-Hsp90 polyclonal antibody (Santa Cruz Biotechnology, Santa Cruz, CA) were added to each sample. For EF-2 kinase precipitation, 4 μl of anti-EF-2 kinase rabbit serum (kindly provided by Dr. A. C. Nairn of Rockefeller University, New York, NY) was used. Immunoprecipitation of samples with preimmune sera was used as a control. After 1–4 h of rotating incubation at 4°C, 80 μl of Protein A-Sepharose CL-4G (50% NET buffer; Amersham Pharmacia Biotech, Piscataway, NJ) were added. Tubes were incubated overnight at 4°C with rotation. At the end of the incubation, samples were centrifuged at 15,000 × *g* at 4°C for 2 min, and the supernatant was discarded. Beads were washed twice with NET buffer and twice with PBS containing 1% aprotinin and 1 mM PMSF. After the final wash, 30 μl of Laemmli buffer were added, and the samples were boiled for 5 min. After a 3-min spin at 15,000 × *g*, supernatants were loaded onto a 8% SDS-PAGE gel.

Western Blot Analysis. Proteins resolved on SDS-PAGE were transferred to nitrocellulose membranes (Hybond ECL; Amersham Pharmacia Biotech). Membranes were first blocked with 10% milk in PBS-T (PBS/0.1% Tween) and then were incubated with anti-EF-2 kinase rabbit antiserum in 10% milk/PBS-T for EF-2 kinase detection. For detection of Hsp90, the anti-Hsp90 rabbit antiserum was used. An anti-β-actin monoclonal mouse ascites (Sigma Chemical Co., St. Louis, MO) was used for detection of β-actin. After a 2-h incubation with the primary antibodies, membranes were washed in PBS-T, incubated with horseradish peroxidase conjugated secondary antibodies (Amersham-Life Science), and washed again with PBS-T. M_r standards (Bio-Rad Laboratories, Richmond, CA) and authentic EF-2 kinase were used to determine the position of the proteins of interest. Proteins were visualized using Amersham-Pharmacia ECL detection reagents. Blots were scanned by UMAX Magic Scan 4.3 program, and the intensity of protein bands was quantified by Molecular Analyst software.

Generation of Stable Cell Lines Expressing Different Levels of EF-2 Kinase. pSTAR vector was originally constructed to mediate tetracycline-induced gene expression in mammalian cells (28). However, this vector conferred constitutive expression of target genes in most stable clones that we have tested, which was likely attributable to the use of two strong promoters, cytomegalovirus and SV40, in this vector system. A full-length human EF-2 kinase cDNA was inserted into the multiple cloning site region of pSTAR in both antisense (AS) and sense (S) orientations. Constructs expressing AS (pJYH1) and sense (pJYH2) EF-2 kinase mRNA were introduced into T98G human glioma cells by liposome-mediated transfection (Life Technologies, Inc., Rockville, MD). Transfectants were selected in 500 μg/ml G418. G418-resistant colonies were expanded and maintained in 200 μg/ml G418. Cytosolic extracts of each clone were collected by homogenization and centrifugation and were analyzed for EF-2 kinase expression by Western blot. The TJY1-R clone was found to express low amounts of EF-2 kinase protein. The TJY2-D clone expressed high levels of sense EF-2 kinase mRNA and protein compared with that of TJY1-R.

Treatment of Glioma Xenografts with 17-AAG. C6 cells grown at logarithmic phase were removed from culture flasks by trypsinization, then washed and resuspended in PBS at density of 1.6 × 10^7 cells/ml. Cells (1.6 × 10^6/100 μl) were injected into the flank of each of 16 Swiss nude ($^{nu/nu}$) mice (male, 5 weeks old; Taconic, Germantown, NY). The s.c. grown tumors were measured daily with a Vernier caliper. The length (*L*) and width (*W*; in mm) of the tumors were taken and used to calculate the volume (*V*), using the formula: $V = (W^2 \times L)/2$. On the 12th day after inoculation, when the median tumor volume reached 60 mm^3, the mice were paired by the similarity of the tumor volumes. Within each pair, mice were randomly assigned to either 17-AAG or vehicle. Animals received i.p. injections of 17-AAG (80 mg/kg) or vehicle on days 2, 3, 4, 5, and 8, 9, 10, 11, and 12.

Statistical Analysis. The two-sample *t* test was used to compare tumor volumes between the two treatment groups at treatment day 1. Logs(tumor volume) on day 5 to day 22 were analyzed using the repeated-measurement model with treatment and day as factors and the first order autoregressive correlation structure (29).

RESULTS

Effect of GA on Cell Growth and Viability. We investigated the effects of a 48-h incubation with GA and 17-AAG on the clonogenicity of human T98G (glioblastoma), Daoy (medulloblastoma) and SKNSH (neuroblastoma) cells. GA inhibited T98G, Daoy, and SKNSH cell viability with IC_{50} values of 3 nM, 1 nM, and 1 nM, respectively (Fig. 1*A*; Table 1). GA also inhibited the clonogenicity of the C6 rat glioma line (IC_{50}, 1.5 nM).

17-AAG also decreased the clonogenicity of glioma cells, but was ~10-fold less potent than GA against the same cell lines. IC_{50} value for C6 cells was 13 nM and for T98G cells was 35 nM (Fig. 1*B*; Table 1).

For comparison, we also performed clonogenic assays of C6 cells treated with BCNU, a standard chemotherapeutic drug used to treat glioblastoma. Fig. 1*C* and Table 1 show that the IC_{50} of BCNU against C6 cells was 5 μM, ~3000-fold greater than the IC_{50} value of GA against the same cell line.

Effect of GA and 17-AAG on EF-2 Kinase Protein Content. To analyze the role of EF-2 kinase in the cytotoxicity of GAs, we tested whether or not GA or 17-AAG affected EF-2 kinase content in glioma cells. T98G cells were incubated with 0–40 nM GA for 24 h (Fig. 2*A*, *left panel*). Cell homogenates were collected and EF-2 kinase measured by Western blot. Fig. 2 demonstrates that there was a >50% decrease in EF-2 kinase at a concentration of 10 nM and a >80% decrease after treatment with 20 nM GA. We chose the 24-h incubation time to avoid problems in interpretation of data obtained using a dying population of cells (Fig. 1). Similar results were observed in C6 cells treated with GA for 24 h (Fig. 2*B*); EF-2 kinase was reduced by 70% after treatment with 1–10 nM GA. 17-AAG (20–40 nM) decreased EF-2 kinase by 40–50% (Fig. 2*A*, *right panel*).

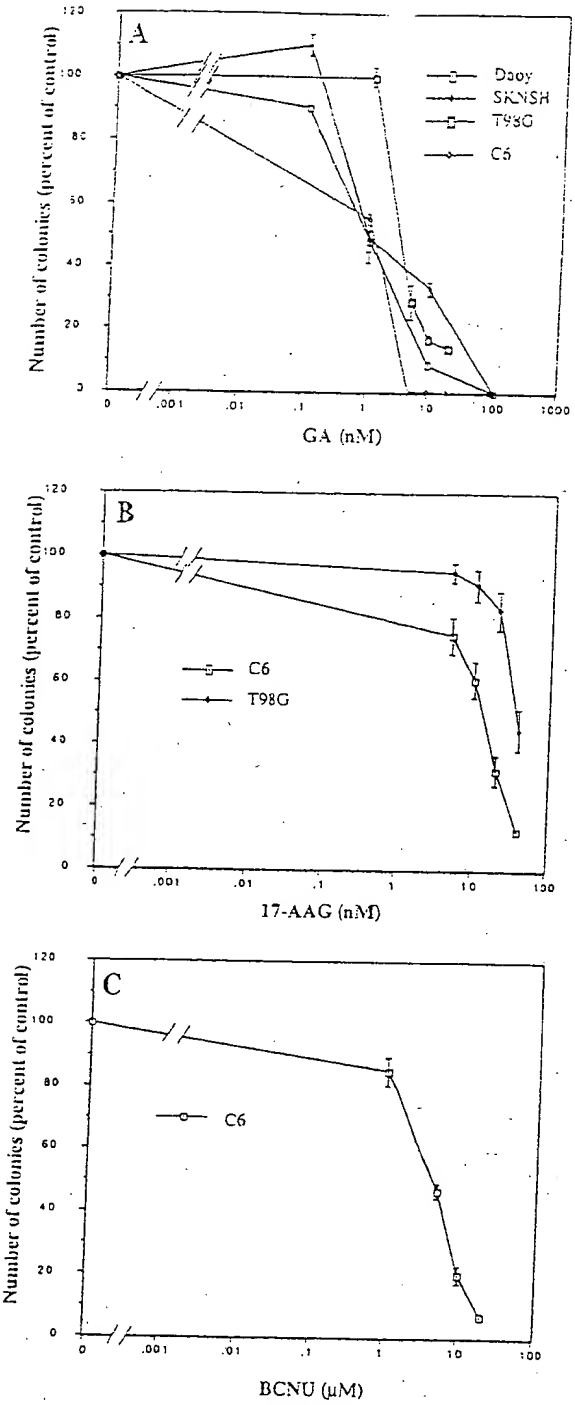

Fig. 1. Effect of GA, 17-AAG, and BCNU on the clonogenic survival of glioma and other cell lines of neurogenic origin. Murine glioma (*C6*), human glioblastoma (*T98G*), human neuroblastoma (*SKNSH*), and human medulloblastoma (*Daoy*) were cultured as described in "Materials and Methods." Cell lines were exposed for 48 h in varying concentrations of GA (*A*), 17-AAG (*B*), and BCNU (*C*). Cells were then cultured in drug-free medium and allowed to grow for another 7–10 days. Colonies were stained with methylene blue and counted with an electron counting pencil. Each point represents the mean of three determinations from one of three similar experiments; *bars*, ± SE. Controls (vehicle-treated cells) usually contained 100–300 colonies.

Effect of GA and 17-AAG on Hsp90/EF-2 Kinase Interactions. We next carried out coimmunoprecipitation experiments to investigate the effects of GA and 17-AAG on Hsp90/EF-2 kinase protein interactions. T98G (Fig. 3*A*) and C6 cells (Fig. 3*B*) were treated with 10 nM GA, 40 nM 17-AAG, or vehicle (0.1% DMSO) for 24 h (the optimal conditions for reducing the cellular content of EF-2 kinase as shown above). Cell lysates were incubated with anti-Hsp90 rabbit antiserum or preimmune serum and protein-A beads to immunoprecipitate Hsp90. After Western transfer, the membranes were first blotted with anti-EF-2 kinase polyclonal antibody and then were stripped and reblotted with anti-Hsp 90 polyclonal antibody. Fig. 3, *A* and *B*, demonstrate that approximately equal amounts of Hsp90 (*bottom panels*) were precipitated under each condition. EF-2 kinase (*upper panels*) was coprecipitated with Hsp90 in vehicle-treated cells (*Lane 1*) but not with preimmune serum (data not shown), which confirmed the association of the kinase with Hsp90 in both T98G and C6 cells. Treatment with GA (*Lane 2*) or 17-AAG (*Lane 3*) significantly reduced the amount of EF-2 kinase that was coprecipitated with Hsp90 in both cell lines.

To exclude the possibility that the apparent decrease of Hsp90 association with EF-2 kinase was merely the result of decreased overall EF-2 kinase protein, we investigated the effect of shorter incubation times with higher concentrations of drug. In these experiments, cells were incubated with 3 μM GA (*Lane 4*) or 6 μM 17-AAG (*Lane 5*) for 3 h. Fig. 3*C* demonstrates that the amount of EF-2 kinase in T98G or C6 cells was not significantly changed under these conditions. The amount of EF-2 kinase that was coimmunoprecipitated with Hsp90 under these conditions was markedly decreased (Fig. 3, *A* and *B*, *Lanes 4* and *5*).

We next determined whether antibodies to EF-2 kinase could immunoprecipitate Hsp90 and whether GA disrupted the interaction. Immunoprecipitation was performed using an anti-EF-2 kinase anti-

Table 1 *Effect of GAs on the clonogenicity of glioma and other cell lines of neurogenic origin*

Cell lines, grown in tissue culture, were treated with varying concentrations of drugs or vehicles, and clonogenic survival was measured as described in "Materials and Methods." Each value represents the mean of at least two experiments having less than 10% variation between them.

Cell line	GA IC_{50} (nM)	17-AAG IC_{50} (nM)	BCNU IC_{50}
C6	2 ± 0.1	13 ± 1.8	5 ± 0.2
T98G	3 ± 0.2	35 ± 4.0	
SKNSH	1 ± 0.1		
Daov	1 ± 0.1		
TJY1-R	0.4 ± 0.04		
TJY2-D	2 ± 0.1		

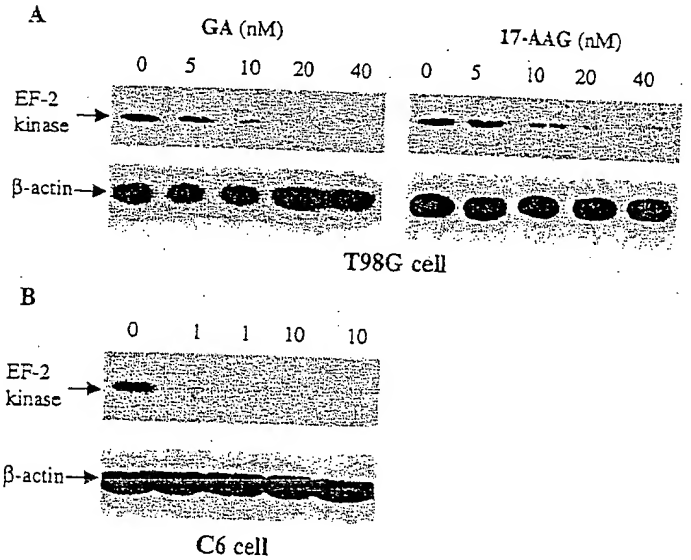

Fig. 2. Effect of GAs on the content of EF-2 kinase in glioblastoma cell lines. T98G (*A*) and C6 cells (*B*) were grown in culture as described in "Materials and Methods." Following a 24-h incubation with drug or appropriate vehicle, cell homogenates containing 20 μg of total protein were assayed for the content of elongation factor 2 kinase and β-actin by Western blot analysis. The figure represents the results of one of three similar experiments.

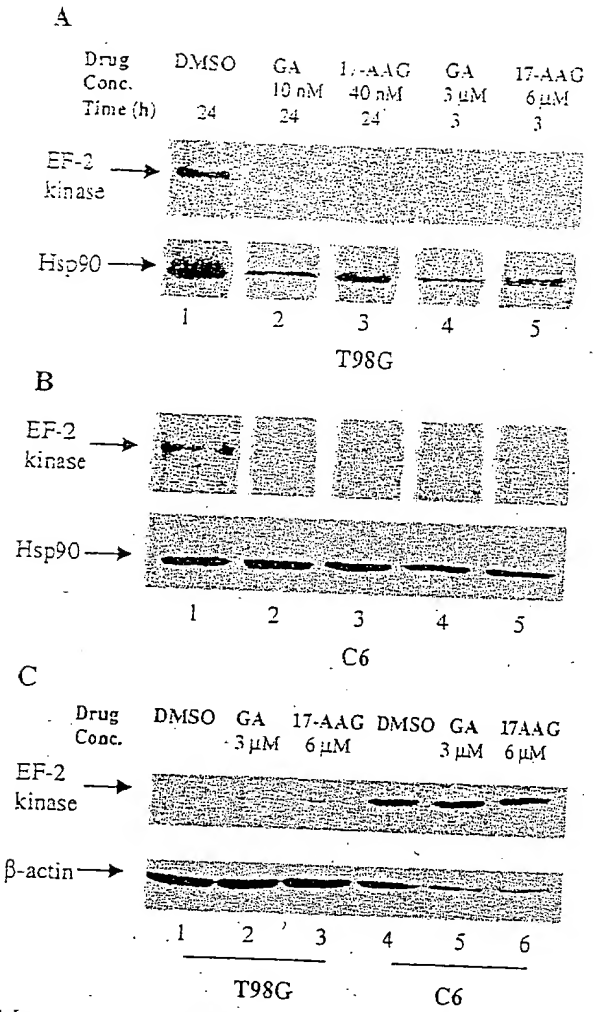

Fig. 3. Immunoprecipitation of EF-2 kinase by antibodies against Hsp90 in cell lysates treated with GAs. T98G (*A*) and C6 (*B*) cells were treated with 10 nM GA (*Lane 2*), 40 nM 17-AAG (*Lane 3*), or vehicle (0.1% DMSO, *Lane 1*) for 24 h. Cells were also treated with 3 μM GA (*Lane 4*) or 6 μM 17-AAG (*Lane 5*) for 3 h. Cell lysates were incubated with anti-Hsp90 rabbit antiserum and protein-A beads to immunoprecipitate Hsp90. After Western transfer, the membranes were first probed with anti-EF-2 kinase polyclonal antibody, then were stripped and reprobed with anti-Hsp90 polyclonal antibody. *C*, Western blot analysis of EF-2 kinase in T98G and C6 cells treated with GA or 17-AAG in high concentration and shorter incubation time. Cells were incubated with vehicle (*Lanes 1* and *4*), 3 μM GA (*Lanes 2* and *5*), or 6 μM 17-AAG (*Lanes 3* and *6*) for 3 h. Each blot is representative of three similar experiments.

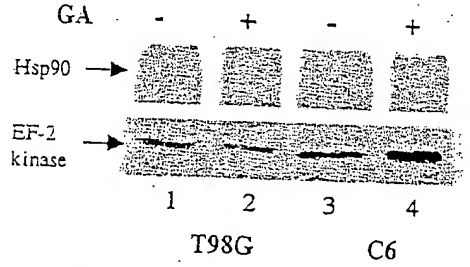

Fig. 4. Immunoprecipitation of Hsp90 by antibodies against EF-2 kinase in cell lysates treated with GAs. T98G and C6 cells were treated with either 3 μM GA or vehicle (0.1% DMSO) for 3 h. Cell lysates were incubated with anti-EF-2 kinase rabbit antiserum and protein-A beads as described in "Materials and Methods." After Western transfer, the membrane was first probed with anti-Hsp90 polyclonal antibody, then was stripped and reprobed with anti-EF-2 kinase polyclonal antibody. These data are representative of two similar experiments.

body and cell lysates from T98G and C6 were treated with either vehicle or 3 μM GA for 3 h (Fig. 4). Similar amounts of EF-2 kinase were recovered under each condition (*lower panel*). Hsp90 was co-precipitated with EF-2 kinase in vehicle controls (*Lanes 1* and *3*) but was absent in t mmune-complex from GA-treated cell lysates (*Lanes 2* and *4*).

Effect of Overexpression of EF-2 Kinase on GA Activity. We next determined whether the effect of GA on cytotoxicity could be abrogated by overexpressing EF-2 kinase. In these experiments, we compared the sensitivity to GA in two cell lines that express different levels of EF-2 kinase. TJY1-R and TJY2-D cell lines were isolated after stable transfection of T98G cells with either antisense or sense EF-2 kinase expression vectors. TJY1-R was selected based on low kinase expression after transfection with antisense RNA; TJY2-D was selected as a clone expressing high EF-2 kinase after transfection with sense RNA. The Western blot in Fig. 5*A* shows that TJY2-D cells express ~6-fold more EF-2 kinase protein as compared with that of TJY1-R cells.

Clonogenic assays were performed on TJY1-R and TJY2-D cells treated with different concentrations of GA for 24 h. Overall, we noted a decreased viability of clones transfected with EF-2 kinase antisense. Of the several clones identified, TJY1-R was the most robust based on morphology and a doubling time that was consistent with the sense transfectants (data not shown). Fig. 5*B* and Table 1 demonstrate that cells that overexpress EF-2 kinase were 5-fold less sensitive to the cytotoxic effects of GA (IC_{50}, 2 nM) than isogenic cells with less EF-2 kinase content (IC_{50}, 0.4 nM).

Effect of 17-AAG on Glioma Growth in Mice. To test whether GAs remained active against glioma cell lines *in vivo*, we evaluated the effect of 17-AAG on the growth of C6 glioma cells in nude mice. C6 cells were implanted in sixteen mice in the dorsal flank; tumors were allowed to form for 12 days and reached 60 mm^3 in size before

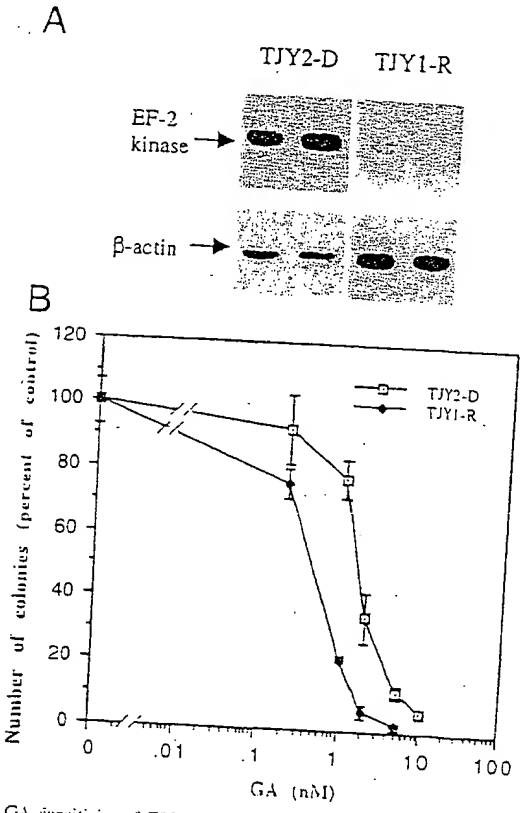

Fig. 5. GA sensitivity of T98G cell derivatives expressing different levels of EF-2 kinase. *A*, expression of EF-2 kinase in T98 cells transfected with EF-2 kinase sense (*TJY2-D*) or antisense (*TJY1-R*) expression vectors. EF-2 kinase and β-actin were detected by Western blot analysis. *B*, effect of GA on the clonogenic survival of TJY2-D and TJY1-R cell lines. Drug sensitivity was determined by exposing cells to 0–10 nM GA for 24 h, by washing and allowing the cells to grow for another 7–10 days, and by staining with methylene blue. Colonies were then enumerated using an electronic counting pencil as described in "Materials and Methods." Each point represents the mean from a representative of two similar experiments; *bars*, ± SE.

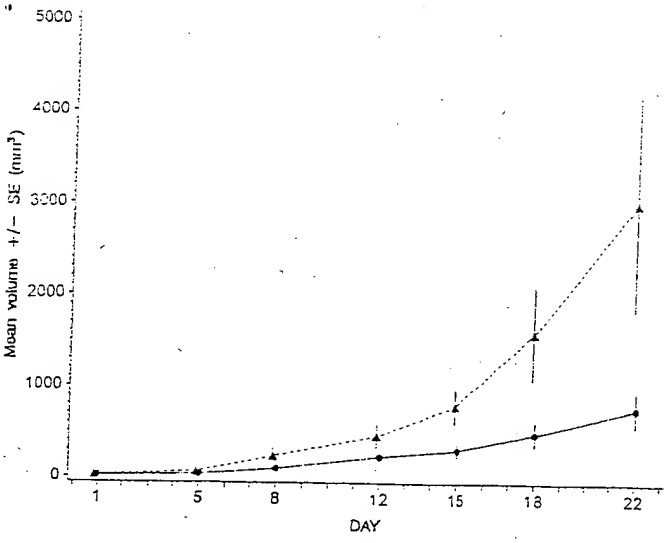

Fig. 6. Effect of 17-AAG on the growth of C6 glioma xenografts.C6 cells (1.6×10^6cells/mouse) were implanted into the flank of 16 Swiss nude ($^{nu/nu}$) mice. On the 12th day after inoculation (day 1 in Fig. 6), the mice were paired in two groups and were randomly assigned to treatment. 17-AAG (80 mg/kg) or vehicle were injected via the intraperitoneal route on days 2, 3, 4, 5, 8, 9, 10, 11, and 12. Each point represents the mean volume of the eight animals in each group; *bars*, ± SE. The differences in tumor volumes between the two treatment groups were statistically significant ($P \leq 0.017$) at all time points from day 5 to day 22 [least-square mean of log(tumor volume), 0.91 ± 0.33 (mean ± SE)].

treatment began. Fig. 6 demonstrates the ability of 17-AAG to significantly inhibit the growth of C6 glioma. The mean tumor volumes of the two treatment groups were not statistically different before drug treatment (day 1; $P > 0.752$). The differences in tumor volumes between the two treatment groups were statistically significant ($P \leq 0.017$) at all time points from day 5 to day 22 [least-square means of log(tumor volume), 0.91 ± 0.33 (mean ± SE)]. No significant weight loss, changes in activity or deaths were observed during the period of drug treatment.

DISCUSSION

The need for new treatments for glioblastoma is highlighted by its devastation to both children and adults. Despite the recent introduction of an oral alkylating agent, temozolomide (30–32), very little has been added to prospects for increasing overall survival in patients with this disease.

Disruption of Hsp90 chaperoning represents a novel approach to developing new anticancer therapies. Numerous proteins induced in the growth of malignant cells associate with Hsp90 (22, 33). Interference with this interaction targets the nonassociated protein for degradation (34–38). Therefore, it may be possible to target proteins important for the growth of malignant cells by disrupting their association with Hsp90.

EF-2 kinase is an attractive target for the treatment of high-grade astrocytomas and perhaps other malignancies. The markedly increased activity of this enzyme in glioblastoma multiforme (17) and the cytotoxicity of specific and nonspecific inhibitors for this kinase support this concept (18). Because EF-2 kinase is chaperoned by Hsp90 (20, 21), we examined the effects of GAs on glioma and other malignant cell lines of neurogenic origin and found these drugs to be potent cytotoxic agents that disrupt Hsp90/EF-2 kinase interactions.

GA is a potent inhibitor of the clonogenicity of several cell lines including T98G and C6 glioblastoma, Daoy medulloblastoma, and SKNSH neuroblastoma (Fig. 1). Table 1 lists the IC_{50} values obtained after a 48-h exposure to GA that ranged from 1 to 3 nM. For C6 cells, GA is 2500 times more potent than BCNU, a standard chemotherapy for glioblastoma (39–42). 17-AAG, a less potent inhibitor of Hsp90/protein interactions (25, 26) compared with GA, is also a less potent inhibitor of clonogenicity in T98G and C6 cells, with IC_{50} values ranging from 13 to 35 nM (Fig. 1; Table 1). It is nevertheless a potent compound when compared with BCNU.

To determine whether or not the cytotoxicity of GAs was attributable, at least in part, to inhibition of EF-2 kinase activity through disruption of Hsp90 chaperoning, we carried out a series of experiments to measure both the association and depletion of the enzyme. These studies revealed a good correlation between the concentration of drug required to disrupt Hsp90/EF-2 kinase interactions and effects on clonogenic survival. For example, after a 24 h incubation of T98G cells with 10 nM GA there is a >50% decrease in EF-2 kinase (Fig. 2*A*), which correlates with the IC_{50} of 3 nM obtained by clonogenic assay after exposing the cells to drug for 48 h (Fig. 1; Table 1).We chose the shorter incubation period to evaluate the effect of drug exposure on kinase degradation to avoid the pitfalls of studying the effects of drug in a population in which one-half the cells were dead or dying. Similarly, we found a 70% decrease in EF-2 kinase in C6 cells exposed for 24 h to 10 nM GA, which correlates with the IC_{50} value of 2 nM obtained by clonogenic assay after exposing the cells to drug for 48 h. The IC_{50}s in clonogenic assays for 17-AAG were 5- to 10-fold greater than those of GA, which correlates to the decreased potency of this derivative in producing loss of the kinase (Fig. 2*A*).

Interference with the chaperoning function of Hsp90 is known to be detrimental to associated kinases. GA disrupts the binding of EF-2 kinase to Hsp90 as measured by coimmunoprecipitation (Fig. 3 and 4). The disruption of this interaction is associated with decreased EF-2 kinase protein content (Fig. 2). Schulte *et al.*, demonstrated that the serine/threonine kinase, raf-1, is rapidly destabilized on addition of GA, which disrupts the Raf-1/Hsp90 molecular complex (38). The disappearance of EF-2 kinase in glioma cells treated with GA is likely caused by this mechanism. These data are consistent with a proposed mechanism by which GAs disrupt the chaperoning of critical cellular proteins leading to targeted degradation (38, 43, 44). Further insight may be gained by investigating the mechanism by which the EF-2 kinase protein is degraded. Published reports (45–47) point toward the role of GA in targeting proteins for proteosome degradation.

GAs are likely to affect numerous intracellular targets that are critical for cell viability. In addition to raf-1 (26, 48–50), both GA and 17-AAG deplete cells of the transmembrane protein tyrosine kinase $p185^{erB-2}$, which has been implicated in oncogenic transformation (45, 51). Treatment of lung cancer cell lines expressing p185 with paclitaxel and 17-AAG showed synergistic activity (52). 17-AAG also destabilizes mutant forms of p53 (47). Therefore, to understand the importance of EF-2 kinase among these other targets, we transfected parental T98G cells with either sense or antisense EF-2 kinase expression vectors. As expected, overexpression of antisense mRNA and subsequent decrease in EF-2 kinase (Fig. 5*A*) reduced the viability and subsequent recovery of transfected clones (53). Nonetheless, we were able to study drug sensitivity by choosing our most robust antisense clone for these experiments and compared this with a sense clone obtained during the same round of transfections. We then chose a shorter drug exposure time (24 h) to measure effects on clonogenicity and repeatedly found the antisense clone to be more sensitive to GA (Fig. 5*B*). This result is consistent with EF-2 kinase being an important target for the cytotoxicity of GAs in glioma cell lines. However, despite the excellent correlation between EF-2-kinase content and drug sensitivity (Fig. 5, *A* and *B*), given the difficulty in recovering viable antisense clones, we cannot rule out the

possibility that these are indirect effects resulting from clonal selection.

Numerous drugs kill cancer cells in tissue culture but far fewer retain activity in animal xenografts. We studied 17-AAG against xenografted C6 glioma because it is a less toxic compound that has already entered clinical testing (26, 27). 17-AAG significantly inhibits the growth of established gliomas in animals. Treatment that is started after 12 days of growth significantly inhibits the growth of the xenografts (Fig. 6). This is particularly promising because the drug is highly lipid-soluble and likely to penetrate the blood-brain barrier.

In summary, our results demonstrate that GAs represent a new class of anticancer drug that have potent activity against glioblastoma and other malignant cell lines of neurogenic origin. The compounds disrupt the interaction of EF-2 kinase with Hsp90, leading to the destruction of this unique protein kinase member of the calmodulin-mediated pathway of signal transduction.

REFERENCES

1. Prados, M. D., and Levin, V. Biology and treatment of malignant glioma. Semin. Oncol., *27:* 1–10, 2000.
2. Madajewicz, S., Chowhan, N., Tfayli, A., Roque, C., Meek, A., Davis, R., Wolf, W., Cabahug, C., Roche, P., Manzione, J., Iliya, A., Shady, M., Hentschel, P., Atkins, H., and Braun, A. Therapy for patients with high grade astrocytoma using intra-arterial chemotherapy and radiation therapy. Cancer (Phila.), *88:* 2350–2356, 2000.
3. Ekstrand, A. J., Longo, N., Hamid, M. L., Olson, J. J., Liu, L., Collins, V. P., and James, C. D. Functional characterization of an EGF receptor with a truncated extracellular domain expressed in glioblastomas with *EGFR* gene amplification. Oncogene, *9:* 2313–2320, 1994.
4. Libermann, T. A., Nusbaum, H. R., Razon, N., Kris, R., Lax, I., Soreq, H., Whittle, N., Waterfield, M. D., Ullrich, A., and Schlessinger, J. Amplification, enhanced expression, and possible rearrangement of *EGF* receptor gene in primary human brain tumours of glial origin. Nature (Lond.), *313:* 144–147, 1985.
5. Malden, L. T., Novak, U., Kaye, A. H., and Burgess, A. W. Selective amplification of the cytoplasmic domain of the epidermal growth factor receptor gene in glioblastoma multiforme. Cancer Res., *48:* 2711–2714, 1988.
6. Berridge, M. J. Inositol lipids and cell proliferation. Biochim. Biophys. Acta, *907:* 33–45, 1987.
7. Streb, H., Irvine, R. F., Berridge, M. J., and Schulz, I. Release of Ca^{2+} from a nonmitochondrial intracellular store in pancreatic acinar cells by inositol-1,4,5-trisphosphate. Nature (Lond.), *306:* 67–69, 1983.
8. Joseph, S. K., Williams, R. J., Corkey, B. E., Matschinsky, F. M., and Williamson, J. R. The effect of inositol trisphosphate on Ca^{2+} fluxes in insulin-secreting tumor cells. J. Biol. Chem., *259:* 12952–12955, 1984.
9. Joseph, S. K., Thomas, A. P., Williams, R. J., Irvine, R. F., and Williamson, J. R. myo-Inositol 1,4,5-trisphosphate. A second messenger for the hormonal mobilization of intracellular Ca^{2+} in liver. J. Biol. Chem., *259:* 3077–3081, 1984.
10. Bagaglio, D. M., Cheng, E. H., Gorelick, F. S., Mitsui, K., Naim, A. C., and Hait, W. N. Phosphorylation of elongation factor 2 in normal and malignant rat glial cells. Cancer Res., *53:* 2260–2264, 1993.
11. Naim, A. C., Bhagat, B., and Palfrey, H. C. Identification of calmodulin-dependent protein kinase III and its major M_r 100,000 substrate in mammalian tissues. Proc. Natl. Acad. Sci. USA, *82:* 7939–7943, 1985.
12. Naim, A. C., and Palfrey, H. C. Identification of the major M_r 100,000 substrate for calmodulin-dependent protein kinase III in mammalian cells as elongation factor-2. J. Biol. Chem., *262:* 17299–17303, 1987.
13. Ryazanov, A. G., Ward, M. D., Mendola, C. E., Pavur, K. S., Dorovkov, M. V., Wiedmann, M., Erdjument-Bromage, H., Tempst, P., Parmer, T. G., Prostko, C. R., Germino, F. J., and Hait, W. N. Identification of a new class of protein kinases represented by eukaryotic elongation factor-2 kinase. Proc. Natl. Acad. Sci. USA, *94:* 4884–4889, 1997.
14. Proud, C. G. Peptide-chain elongation in eukaryotes. Mol. Biol. Rep., *19:* 161–170, 1994.
15. Redpath, N. T., and Proud, C. G. Cyclic AMP-dependent protein kinase phosphorylates rabbit reticulocyte elongation factor-2 kinase and induces calcium-independent activity. Biochem. J., *293:* 31–34, 1993.
16. Bagaglio, D. M., and Hait, W. N. Role of calmodulin-dependent phosphorylation of elongation factor 2 in the proliferation of rat glial cells. Cell Growth Differ., *5:* 1403–1408, 1994.
17. Parmer, T. G., Ward, M. D., Yurkow, E. J., Vyas, V. H., Kearney, T. J., and Hait, W. N. Activity and regulation by growth factors of calmodulin-dependent protein kinase III (elongation factor 2-kinase) in human breast cancer. Br. J. Cancer., *79:* 59–64, 1999.
18. Parmer, T. G., Ward, M. D., and Hait, W. N. Effects of rottlerin, an inhibitor of calmodulin-dependent protein kinase III, on cellular proliferation, viability, and cell cycle distribution in malignant glioma cells. Cell Growth Differ., *8:* 327–334, 1997.
19. Prostko, C. R., Zhang, C., and Hait, W. N. The effects of altered cellular calmodulin expression on the growth and viability of C6 glioblastoma cells. Oncol. Res., *9:* 13–17, 1997.
20. Hait, W. N., Wat[illegible] D., Trakht, I. N., and Ryazanov, A. G. Elongation factor-2 kinase: immunolo[illegible] evidence for the existence of tissue-specific isoforms. FEBS Lett., *397:* 55–60, 1996.
21. Palmquist, K., Riis, B., Nilsson, A., and Nygard, O. Interaction of the calcium and calmodulin regulated eEF-2 kinase with heat shock protein 90. FEBS Lett., *349:* 239–242, 1994.
22. Buchner, J. Hsp90 & Co.—a holding for folding. Trends Biochem. Sci., *24:* 136–141, 1999.
23. Roe, S. M., Prodromou, C., O'Brien, R., Ladbury, J. E., Piper, P. W., and Pearl, L. H. Structural basis for inhibition of the Hsp90 molecular chaperone by the antitumor antibiotics radicicol and geldanamycin. J. Med. Chem., *42:* 260–266, 1999.
24. Sasaki, K., Yasuda, H., and Onodera, K. Growth inhibition of virus transformed cells *in vitro* and antitumor activity *in vivo* of geldanamycin and its derivatives. J. Antibiot. (Tokyo), *32:* 849–851, 1979.
25. Schnur, R. C., Corman, M. L., Gallaschun, R. J., Cooper, B. A., Dee, M. F., Doty, J. L., Muzzi, M. L., Moyer, J. D., DiOrio, C. I., and Barbacci, E. G. Inhibition of the oncogene product p185erbB-2 *in vitro* and *in vivo* by geldanamycin and dihydrogeldanamycin derivatives. J. Med. Chem., *38:* 3806–3812, 1995.
26. Schulte, T. W., and Neckers, L. M. The benzoquinone ansamycin 17-allylamino-17-demethoxygeldanamycin binds to Hsp90 and shares important biologic activities with geldanamycin. Cancer Chemother. Pharmacol., *42:* 273–279, 1998.
27. Kelland, L. R., Sharp, S. Y., Rogers, P. M., Myers, T. G., and Workman, P. DT-diaphorase expression and tumor cell sensitivity to 17-allylamino,17-demethoxygeldanamycin, an inhibitor of heat shock protein 90. J. Natl. Cancer Inst. (Bethesda), *91:* 1940–1949, 1999.
28. Zeng, Q., Tan, Y. H., and Hong, W. A single plasmid vector (pSTAR) mediating efficient tetracycline-induced gene expression. Anal. Biochem., *259:* 187–194, 1998.
29. Lindsey, J. K. Models for Repeated Measurements 85–88. Oxford: Clarendon Press, 1993.
30. Prados, M. D. Future directions in the treatment of malignant gliomas with temozolomide. Semin. Oncol., *27:* 41–46, 2000.
31. Yung, W. K., Albright, R. E., Olson, J., Fredericks, R., Fink, K., Prados, M. D., Brada, M., Spence, A., Hohl, R. J., Shapiro, W., Glantz, M., Greenberg, H., Selker, R. G., Vick, N. A., Rampling, R., Friedman, H., Phillips, P., Bruner, J., Yue, N., Osoba, D., Zaknoen, S., and Levin, V. A. A Phase II study of temozolomide vs. procarbazine in patients with glioblastoma multiforme at first relapse. Br. J. Cancer, *83:* 588–593, 2000.
32. Yung, W. K. Temozolomide in malignant gliomas. Semin. Oncol., *27:* 27–34, 2000.
33. Pratt, W. B. The role of the Hsp90-based chaperone system in signal transduction by nuclear receptors and receptors signaling via MAP kinase. Annu. Rev. Pharmacol. Toxicol., *37:* 297–326, 1997.
34. Scheibel, T., and Buchner, J. The Hsp90 complex—a super-chaperone machine as a novel drug target. Biochem. Pharmacol., *56:* 675–682, 1998.
35. Supino-Rosin, L., Yoshimura, A., Yarden, Y., Elazar, Z., and Neumann, D. Intracellular retention and degradation of the epidermal growth factor receptor, two distinct processes mediated by benzoquinone ansamycins. J. Biol. Chem., *275:* 21850–21855, 2000.
36. Lewis, J., Devin, A., Miller, A., Lin, Y., Rodriguez, Y., Neckers, L., and Liu, Z. G. Disruption of Hsp90 function results in degradation of the death domain kinase, receptor-interacting protein (RIP), and blockage of tumor necrosis factor-induced nuclear factor-κB activation. J. Biol. Chem., *275:* 10519–10526, 2000.
37. Schneider, C., Sepp-Lorenzino, L., Nimmesgern, E., Ouerfelli, O., Danishefsky, S., Rosen, N., and Hartl, F. U. Pharmacologic shifting of a balance between protein refolding and degradation mediated by Hsp90. Proc. Natl. Acad. Sci. USA, *93:* 14536–14541, 1996.
38. Schulte, T. W., Blagosklonny, M. V., Ingui, C., and Neckers, L. Disruption of the Raf-1-Hsp90 molecular complex results in destabilization of Raf-1 and loss of Raf-1-Ras association. J. Biol. Chem., *270:* 24585–24588, 1995.
39. Johnson, D. B., Thompson, J. M., Corwin, J. A., Mosley, K. R., Smith, M. T., de los Reyes, R. A., Daly, M. B., Petty, A. M., Lamaster, D., Pierson, W. P., *et al.* Prolongation of survival for high-grade malignant gliomas with adjuvant high-dose BCNU and autologous bone marrow transplantation. J. Clin. Oncol., *5:* 783–789, 1987.
40. Phillips, G. L., Wolff, S. N., Fay, J. W., Herzig, R. H., Lazarus, H. M., Schold, C., and Herzig, G. P. Intensive 1,3-bis (2-chloroethyl)-1-nitrosourea (BCNU) monochemotherapy and autologous marrow transplantation for malignant glioma. J. Clin. Oncol., *4:* 639–645, 1986.
41. Walker, M. D., Alexander, E., Jr., Hunt, W. E., MacCarty, C. S., Mahaley, M. S., Jr., Mealey, J., Jr., Norrell, H. A., Owens, G., Ransohoff, J., Wilson, C. B., Gehan, E. A., and Strike, T. A. Evaluation of BCNU and/or radiotherapy in the treatment of anaplastic gliomas. A cooperative clinical trial. J. Neurosurg., *49:* 333–343, 1978.
42. Walker, M. D., Green, S. B., Byar, D. P., Alexander, E., Jr., Batzdorf, U., Brooks, W. H., Hunt, W. E., MacCarty, C. S., Mahaley, M. S., Jr., Mealey, J., Jr., Owens, G., Ransohoff, J. D., Robertson, J. T., Shapiro, W. R., Smith, K. R., Jr., Wilson, C. B., and Strike, T. A. Randomized comparisons of radiotherapy and nitrosoureas for the treatment of malignant glioma after surgery. N. Engl. J. Med., *303:* 1323–1329, 1980.
43. Ochel, H. J., Schulte, T. W., Nguyen, P., Trepel, J., and Neckers, L. The benzoquinone ansamycin geldanamycin stimulates proteolytic degradation of focal adhesion kinase. Mol. Genet. Metab., *66:* 24–30, 1999.
44. Neckers, L., Schulte, T. W., and Mimnaugh, E. Geldanamycin as a potential anticancer agent: its molecular target and biochemical activity. Investig. New Drugs, *17:* 361–373, 1999.

45. Mimnaugh, E. G., Chavany, C., and Neckers, L. Polyubiquitination and proteasomal degradation of the p185c-erbB-2 receptor protein-tyrosine kinase induced by geldanamycin. J. Biol. Chem., *271:* 22796–22801, 1996.
46. Schulte, T. W., An, W. G., and Neckers, L. M. Geldanamycin-induced destabilization of Raf-1 involves the proteasome. Biochem. Biophys. Res. Commun., *239:* 655–659, 1997.
47. Whitesell, L., Sutphin, P., An, W. G., Schulte, T., Blagosklonny, M. V., and Neckers, L. Geldanamycin-stimulated destabilization of mutated p53 is mediated by the proteasome *in vivo*. Oncogene, *14:* 2809–2816, 1997.
48. Khan, S. M., Oliver, R. H., Dauffenbach, L. M., and Yeh, J. Depletion of *Raf-1* proto-oncogene by geldanamycin causes apoptosis in human luteinized granulosa cells. Fertil. Steril., *74:* 359–365, 2000.
49. Stancato, L. F., Silverstein, A. M., Owens-Grillo, J. K., Chow, Y. H., Jove, R., and Pratt, W. B. The Hsp90-binding antibiotic geldanamycin decreases Raf levels and epidermal growth factor signaling without disrupting formation of signaling complexes or reducing the specific enzymatic activity of Raf kinase. J. Biol. Chem., *272:* 4013–4020, 1997.
50. An, W. G., Schnur, R. C., Neckers, L., and Blagosklonny, M. V. Depletion of p185erbB2, Raf-1, and mutant p53 proteins by geldanamycin derivatives correlates with antiproliferative activity. Cancer Chemother. Pharmacol., *40:* 60–64, 1997.
51. Miller, P., DiOrio, C., Moyer, M., Schnur, R. C., Bruskin, A., Cullen, W., and Moyer, J. D. Depletion of the *erb*B-2 gene product p185 by benzoquinoid ansamycins. Cancer Res., *54:* 2724–2730, 1994.
52. Nguyen, D. M., Chen, A., Mixon, A., and Schrump, D. S. Sequence-dependent enhancement of paclitaxel toxicity in non-small cell lung cancer by 17-allylamino 17-demethoxygeldanamycin. J. Thorac. Cardiovasc. Surg., *118:* 908–915, 1999.
53. Yang, J., Hua, S., Yang, J. M., and Hait, W. N. Inhibition of elongation factor-2 kinase in human glioma cells by antisense oligodeoxynucleotides and vector-expressed antisense RNA. Proc. Amer. Assoc Cancer Res., *42:* 3910, 2001.

Pergamon

(4) BCR-ABL-driven mouse leukemia

Leukemia Research Vol. 18, No. 11, pp. 867–873, 1994
Elsevier Science Ltd
Printed in Great Britain
0145-2126/94 $7.00 + 0.00

0145-2126(94)00094-8

IN VIVO ANTITUMOR ACTIVITY OF HERBIMYCIN A, A TYROSINE KINASE INHIBITOR, TARGETED AGAINST BCR/ABL ONCOPROTEIN IN MICE BEARING BCR/ABL-TRANSFECTED CELLS

Mihiro Okabe,* Yoshimasa Uehara,† Takayuki Noshima,‡ Toshiyuki Itaya,* Yasuyuki Kunieda,* and Mitsutoshi Kurosawa*

*The Third Department of Internal Medicine; ‡The Second Department of Pathology, Hokkaido University School of Medicine, Sapporo 060, Japan; and †The Department of Bioactive Molecules, National Institute of Health, Tokyo 162, Japan

(*Received* 7 *March* 1994. *Revision accepted* 1 *July* 1994)

Abstract—Herbimycin A, a benzoquinoid ansamycin antibiotic, has been shown to reverse the oncogenic phenotype of $p60^{v\text{-}src}$ transformed cells because of the inhibition of src protein tyrosine kinase. We previously demonstrated that herbimycin A displayed antitumor activity on the *in vitro* growth of Philadelphia chromosome-positive leukemia cells and BCR/ABL-transfected murine hematopoietic FDC-P2 cells through the inhibition of BCR/ABL protein tyrosine kinase. In this study, the transformed FDC-P2 cells were demonstrated to be tumorigenic in syngeneic DBA/2 mice. The intraperitoneal (i.p.) injection of the transformed tumor cells into DBA/2 mice induced infiltrations of abdominal organs, and then all of the mice died within time periods proportional to the cell numbers of inoculation. In mice that received an i.p. inoculation with greater than 1×10^5 cells, *in vivo* administration of herbimycin A by i.p. injection inhibited tumor formation and significantly prolonged survival time, and further, in mice inoculated with 1×10^4 cells, herbimycin A completely suppressed the *in vivo* growth of transformant FDC-P2 cells and brought about a complete remission. The present study revealed the *in vivo* efficacy of herbimycin A in mice bearing BCR/ABL-transfected cells.

Key words: Herbimycin A, BCR/ABL oncoprotein, protein tyrosine kinase, tyrosine kinase inhibitor, *in vivo* antitumor activity.

Introduction

The *bcr/abl* oncogene is the product of the Philadelphia chromosome (Ph^1), resulting from the reciprocal translocation between chromosomes 9 and 22 which are found in Ph^1-positive leukemias which mainly constitutes more than 90% of chronic myelogenous leukemia (CML) and approximately 20% of adult acute lymphocytic leukemia (ALL) [1–5]. The *bcr/abl* fusion proteins generating from the hybrid *bcr/abl* genes, $P210^{bcr/abl}$ and $P190^{bcr/abl}$ exhibit the deregulated tyrosine kinase activity of ABL and oncogenic activity *in vitro* and *in vivo* [6–9].

Recent progress in the study of the *bcr/abl* gene and its product in Ph^1-positive leukemia offers an opportunity for developing several strategies for specific therapy targeted against BCR/ABL [10–14]. Herbimycin A, an inhibitor of protein tyrosine kinase (PTK) that we isolated on the basis of its ability to cause rat kidney cells transformed by *v-src* to revert to normal morphology with a loss of PTK activity of the transforming protein of $p60^{src}$[15], was shown to display a relatively selective antitumor activity for transformed cells by oncogenes coding PTK[16]. In fact, we demonstrated that herbimycin A displayed a preferential antitumor activity on the *in vitro* growth of Ph^1-positive cells by reducing BCR/ABL PTK [12]. In order to determine whether or not herbimycin A may offer a new therapeutic potential for Ph^1-positive leukemia, we have investigated the antitumor activity of *in vivo* administration of herbimycin A in syngeneic DBA/2 mice inoculated with BCR/ABL oncoprotein-transformed murine FDC-P2 cells. Here, we report the *in vivo* efficacy of herbimycin A on mice bearing BCR/ABL oncoprotein-associated tumors.

Correspondence to: Mihiro Okabe, M.D., Third Department of Internal Medicine, Hokkaido University School of Medicine, Kita-15, Nishi-7, Kita-ku, Sapporo 060, Japan (Tel: (011) 716–1161, Ext. 5920; Fax: (011) 706–7867).

Materials and Methods

Murine hematopoietic cell lines

The murine IL-3 dependent hematopoietic cell line FDC-P2 [17] was used in this study. As control cells, P815,

Exhibit B

mastcytoma cell line, and P388, lymphoma cell line, were used.

Transfection of retroviral vector expressing P210$^{bcr/abl}$ into IL-3-dependent FDC-P2 cells

Five million FDC-P2 cells were cultured by the addition of a mixture of 30 μl Lipofectin (Gibco, Berlin, Germany) and 4 μg of pGD210 retroviral vectors expressing P210$^{bcr/abl}$ oncoprotein [8] for 16 h in serum-free Opti-MEM (Gibco) in the presence of recombinant murine IL-3 (rmIL-3) which was prepared from COS-1 cells transfected with p*SV2neo* containing mIL-3 cDNA. The cells were selected in a RPMI-1640 medium to which 10% fetal bovine serum (FBS) and 600 μg/ml geneticin (G418 sulfate; Gibco) were added in the presence of rmIL-3 for 10 days, and were then further selected in a medium lacking rmIL-3 for IL-3-independent growth. In the absence of mIL-3, parental or mock pZIPNeoSV(X)-transfected FDC-P2 cells died within 72 h, but G418-resistant pGD210$^{bcr/abl}$-transfected cells were able to grow autonomously in a medium which lacked mIL-3. As previously described in detail [12], transformed FDC-P2 cells expressed *bcr/abl* and *neo* mRNAs and the P210$^{bcr/abl}$ oncoprotein.

In vitro *growth testing for herbimycin A*

The assay of cellular proliferation was carried out by using the colorimeric MTT method. The cells (2×10^4/well) were seeded in triplicate in 100 μl of 10% FBS-added RPMI 1640 with or without herbimycin A, and cultured for 3–5 days in a humidified atmosphere with 5% CO_2 at 37 °C. After the addition of 10 μl of a 5 mg/ml stock solution of MTT (3-(4,5-dimethylthiazol-2,5-diphenyl tetrazolium bromide) (Sigma Co. Ltd., Munich, FRG) into each well for the last 4 h, formazan crystals were solibilized in 100 μl of isopropanol–0.04 N HCl, and then the plates were measured on a MTP-100 microplate reader (Corona Electric, Tokyo, Japan) using a test wavelength of 570 nm with a reference wavelength of 630 nm.

Western blotting and immune complex kinase assay of BCR/ABL

Transformant FDC-P2 cells were cultured for 16 h in the presence or absence of 0.2 μg/ml of herbimycin A, where cell viabilities of both groups were more than 90%. The cells were lysed in the presence of kinase and phosphatase inhibitors, as previously described by Longo [18]. The lysate was clarified by centrifugation at 4°C, and 20 μg of proteins in the supernatant were separated by SDS-PAGE in reducing conditions (100 mM dithiothreitol). Proteins were blotted onto a polyvinylidene difluoride (Millipore) membrane. The BCR/ABL oncoprotein was identified using a monoclonal anti-ABL protein (Ab-3, Oncogene Science, Mineola, NY).

The immune complex kinase assay was carried out by using a modified method of that described by Kurzrock *et al.* [19, 20]. In brief, the cells (1×10^7) were harvested, washed with phosphate-buffered saline (PBS), and then lysed at 4°C by sonication in 50 mM Tris–HCl pH 7.5, containing 0.15 mM NaCl, 0.1% SDS, 1% Triton X-100, 0.5% sodium deoxycholate, 1 mM PMSF. The diluted sample was treated with mouse monoclonal antibody against c-*abl*, Ab-3 (Oncogene Science), for 1 h at room temperature and was incubated overnight at 4°C. Immune complexes with anti-ABL antibody were precipitated with mouse anti-IgG antibody-coated protein A (Zymed Laboratories, San Francisco, CA), and immunoprecipitates were then reacted with 5 μCi of (γ – ^{32}P) ATP for 10 min on ice. Next, immune complexes were analyzed on 7.5% SDS-polyacryiamide gels, followed by autoradiography with an intensifying screen.

Animals

Seven-week-old female DBA/2 mice were supplied by Oriental Kobo Co. Ltd (Tokyo, Japan).

Examination of tumor cells and tissues

Tissues were processed for histological examination and for Southern blot analysis. High molecular DNAs derived from tissues and tumors were digested with restriction enzymes, electrophoresed through 0.8% agarose gel, and then transferred to nylon membranes. The hybridization with a human 3′-*bcr* genomic DNA probe (*bcr*-1: Oncogene Science) was carried out by the method previously described [21].

Administration of herbimycin A

Herbimycin A was isolated as described previously [15], and was dissolved in phosphate-buffered saline containing 1% (V/V) of Tween-20. Various concentrations of herbimycin A were then administrated by i.p. injections daily from days 2–6 and from day 12 to day 16 after either transformed FDC-P2 cells, P518 cells or P388 cells at cell numbers of 1×10^4–1×10^6 were inoculated intraperitoneally into syngeneic DBA/2 mice on the first day.

Expression of results

Unless otherwise indicated, mean values ± one S.D. for measurements from triplicate culture have been presented. Bars in figures indicate one S.D. The statistical analysis was carried out using a Student's *t*-test, and results were interpreted to be significantly different when $p < 0.001$.

Results

In vitro *antitumor effect of herbimycin A on BCR/ABL-transformed murine cells*

We investigated the *in vitro* effect of herbimycin A against P210$^{bcr/abl}$ oncoprotein-associated autonomous growth of FDC-P2 cells transformed by a transfection of the *bcr/abl* gene. Herbimycin A showed no significant inhibition of the growth of parental FDC-P2 cells in the presence of the culture supernatant of WEHI cells containing mIL-3, but did display an inhibitory effect on the growth of transformant FDC-P2 cells at doses showing no toxicity on murine P815 cells and P388 cells (Fig. 1).

Effect of herbimycin A on BCR/ABL oncoprotein and tyrosine kinase

We previously reported that the antitumor activity of herbimycin A on Ph^1-positive leukemia cells seems to be associated with an inhibition on the activity of BCR/ABL PTK in spite of having no effect on the expression of BCR/ABL oncoprotein [12]. Similarly, the immune complex kinase assay of BCR/ABL revealed that herbimycin A dramatically suppressed

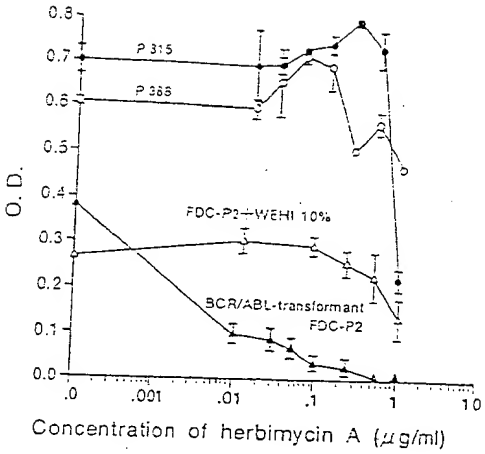

Fig. 1. Effects of herbimycin A on the *in vitro* growth of parental FDC-P2 cells, BCR/ABL-transfected FDC-P2 cells and syngeneic murine hematopoietic malignant cells. Effects of herbimycin A on IL-3-dependent growth of parental FDC-P2 cells in the presence of the culture supernatant obtained from WEHI cells and autonomous growth of transformant FDC-P2 cells by a transfection with BCR/ABL were assayed by MTT proliferation assay after culturing for 72 h. In P815 and P388 cells, MTT proliferation assay was carried out after the 72 h and 5 day cultures, respectively. The growth of P815 cells and P388 cells was not significantly inhibited at low doses of herbimycin A showing an inhibitory effect on the growth of transformant FDC-P2 cells in the 72 h and 5 day cultures. The results of 5 day cultures of P815 and P388 cells are shown.

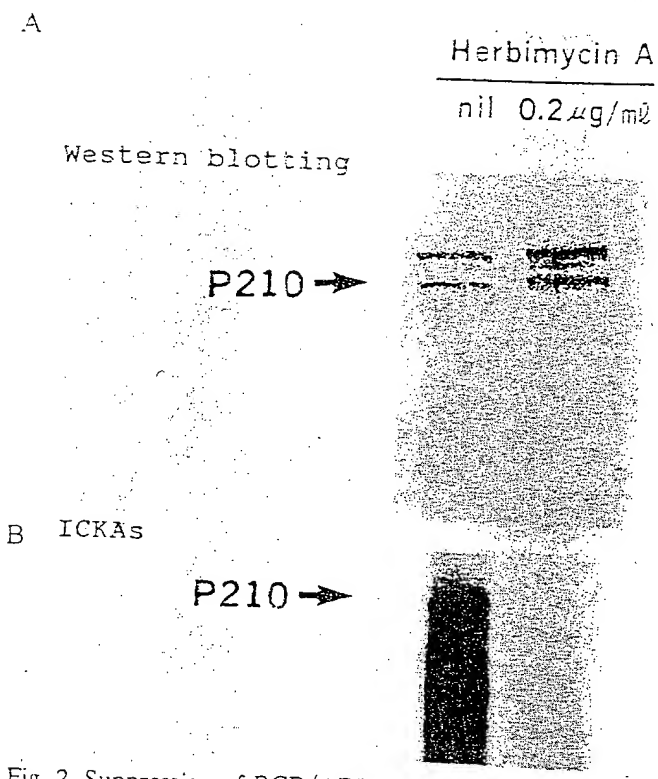

Fig. 2. Suppression of BCR/ABL PTK activity by herbimycin. (A) For the western blotting of BCR/ABL oncoprotein, transformant FDC-P2 cells were cultured for 16 h in the presence or absence of 0.2 μg/ml of herbimycin A, and then cellular protein was isolated. Twenty micrograms of protein were subjected to western blotting. (B) For the immune complex kinase assay (ICKAs), transformant FDC-P2 cells were treated with or without 0.2 μg/ml of herbimycin for 16 h. After this the cell extracts were immunoprecipitated with anti-c-*abl* monoclonal antibody. The resulting immune complexes were analyzed for their autophosphorylation activities.

the autophosphorylation activity of $P210^{bcr/abl}$ tyrosine kinase in BCR/ABL-transformed FDC-P2 cells, while it did not affect the amount of BCR/ABL oncoprotein (Fig. 2).

Mice bearing tumor cells transfected with BCR/ABL

Transformant FDC-P2 cells were transplantable by either i.p. or i.v. injection into syngeneic DBA/2 mice, whereas parental FDC-P2 cells were not transplanted. Mice inoculated with transformant FDC-P2 cells by i.p. injections exhibited a gradual increase of abdominal tumors and died within 5–11 weeks post-inoculation. Postmortem examinations revealed that tumor cells formed masses on the abdominal walls and infiltrated mainly into mesentric and retroperitoneal lymph nodes (Fig. 3(A)). The invasions were observed in the liver, spleen, pancreas and peritoneum (Fig. 3(A)), but were not noted in other organs including the lungs and kidneys. The presence of the *bcr/abl* gene in tumors was confirmed by Southern blot analysis with a human *bcr* probe (Fig. 3(B)).

In vivo efficacy of herbimycin A in mice bearing BCR/ABL oncoprotein-associated tumors

The study regarding determination of lethal dose in DBA/2 mice has revealed that LD_{50} of a single i.p. injection of herbimycin A is approximately 20 mg/kg body weight. The intraperitoneal injection of herbimycin daily for 5 days at less than 2.0 mg/kg body weight was well tolerated with no obvious toxicity. A marked reduction in subsequent tumor formation and a prolongation in the survival rates were evident following herbimycin treatment at doses of 1.0–2.0 mg/kg body weight in mice inoculated with greater than 1×10^5 of transformant cells (Fig. 4(A)). Furthermore, the i.p. administration with herbimycin A at 2.0 mg/kg body weight completely protected against tumor formation and brought about cures in all mice inoculated with 1×10^4 cells, whereas the i.p. administration at 1.0 mg/kg protected against tumor formation in two out of five mice (Fig. 4(B)). In contrast, P815 cells and P388 cells, which were not sensitive to herbimycin A *in vitro*, were transplantable into syngeneic DBA/2 mice, and all mice inoculated i.p. with amounts of greater than 1×10^4

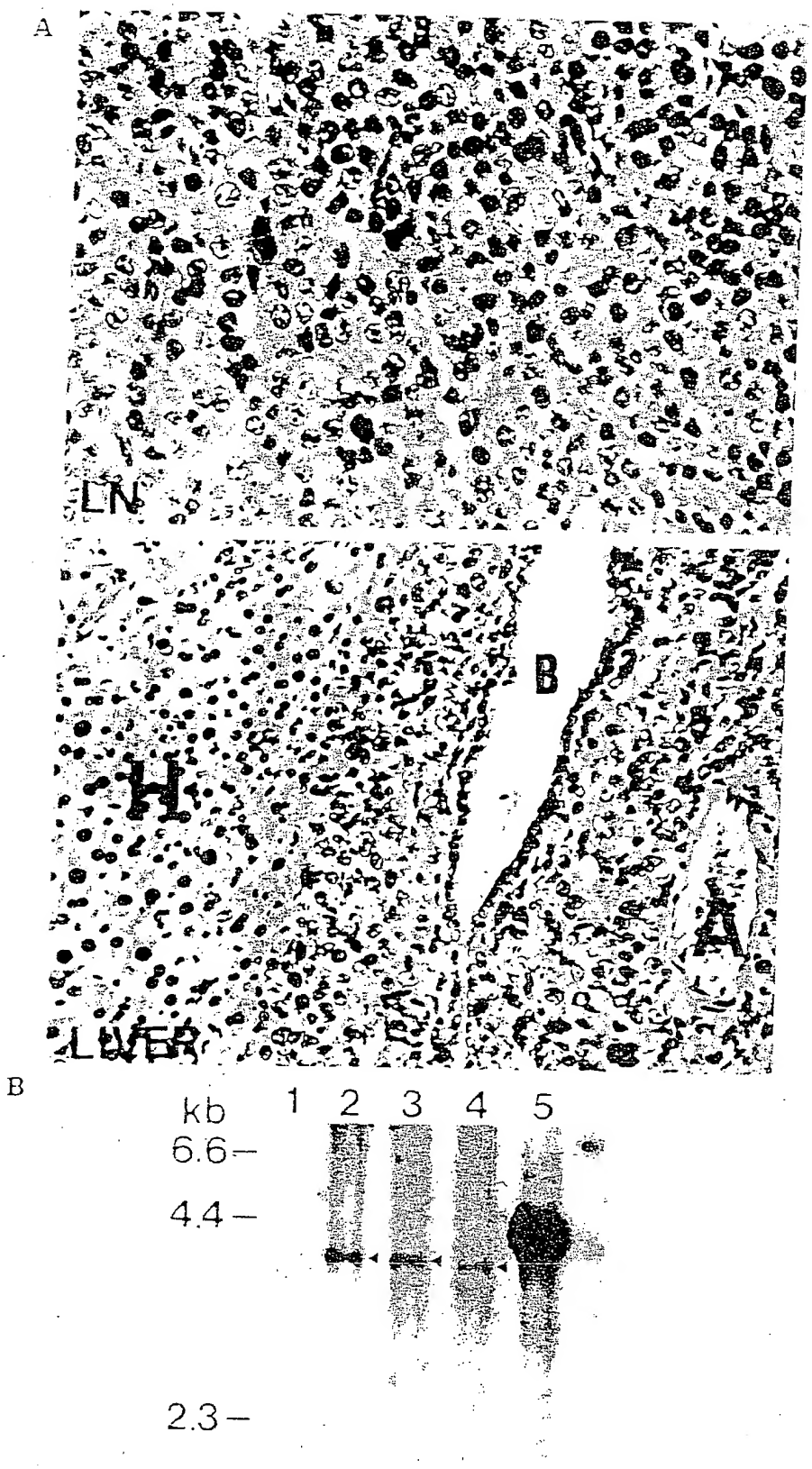

Fig. 3. Histological examination of tumors. (A) Pathological findings of the lymph nodes and the liver. Micrograph of the retroperitoneal lymph node (LN) showing the replacement by tumor cells. Small polygonal cells with prominent nuclei are evident (HE, ×350). Micrograph of the liver: tumor cells are observed throughout the portal tract (HE, ×200). B, bile duct; A, hepatic artery; H, normal hepatocytes. (B) Southern blot analysis revealed the presence of the *bcr/abl* gene. High-molecular weight DNAs isolated from tissues were digested with *Hind*III and were subjected to the Southern blot using 3′ M-*bcr* genomic DNA probe. Lane 1, parental FDC-P2 cells; lane 2, transformed FDC-P2 cells; lane 3, lymph nodes; lane 4, liver; lane 5, human placenta DNA. Arrows indicate the signals derived from *bcr/abl* gene.

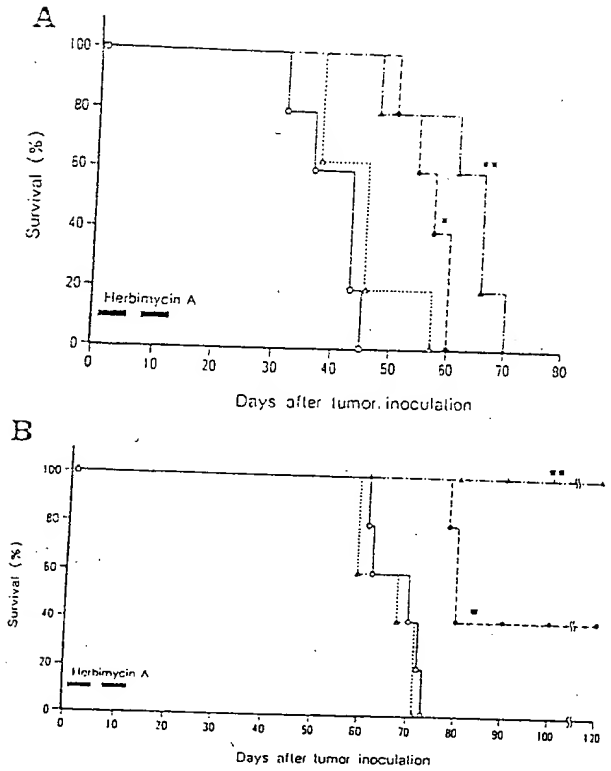

Fig. 4. Therapeutic effects of herbimycin A on DBA/2 mice inoculated with BCR/ABL-transformed FDC-P2 cells. Five DBA/2 mice per group were administered i.p. with herbimycin A (0.1 mg/kg body weight, △----△; 1.0 mg/kg body weight, ●----●; 2.0 mg/kg body weight, ▲----▲) on days 1–5 and 8–12 after i.p. inoculation of 1×10^6 tumor cells (A) or 1×10^4 tumor cells (B). Control groups (○-○) were administered with vehicle only. ■, ■■: significant, $p < 0.001$ (Student's *t*-test).

cells died within 12 weeks. In this case, herbimycin A administration had no effect on their survival rates.

Discussion

PTK activity has been demonstrated to be associated with stimulatory effects of many growth factors and with transforming oncogenes such as *src*, *abl*, *ros*, *fps*, *yes*, and *fes*. These findings indicate that a variety of PTK may play a critical role in the proliferation and differentiation of cells [22] as well as in some malignant transformations of cells, where Ph^1-positive leukemia is representative in human malignancies. Until now, several tyrosine kinase inhibitors including genistein, erbstain and lavendustin have been developed on the basis of inhibition of EGF-associated tyrosine kinase. In contrast to these inhibitors of receptor-type tyrosine kinase, herbimycin A, which was isolated from the cultured filtrate of *Streptomyces* sp. MH237-CF-8, was capable of causing a reversion of the transformed Rous sarcoma virus-infected rat kidney cell to normal morphology at modest concentrations via reduction of $p60^{src}$ PTK activity [15]. Furthermore, we previously demonstrated that herbimycin A preferentially suppressed Ph^1-positive leukemia cell growth and BCR/ABL oncoprotein-associated transformed murine cells via the inhibition of BCR/ABL PTK activity [12].

In this study, we evaluated the *in vivo* efficacy of herbimycin A in a murine model bearing BCR/ABL oncoprotein-expressing transformed cells. The transformed FDC-P2 cells by a transfection of BCR/ABL grew autonomously *in vitro* and were tumorigenic in syngeneic DBA/2 mice, in which the i.p. inoculation of transformant FDC-P2 cells showed the induction of massive swelling of abdominal lymph nodes and the infiltration of abdominal organs and brought about fatal outcomes in mice. In this murine model bearing the BCR/ABL-associated tumors, the i.p. administration of herbimycin A at concentrations of less than 2 mg/kg body weight for 5 days consecutively for 2 weeks significantly prolonged the survival times of the mice when they were inoculated with more than 1×10^5 tumor cells and, furthermore, completely protected against *in vivo* tumor formation in mice that received 1×10^4 cells with no overt side effects. Similarly, Honma has previously described the *in vivo* antitumor effect of herbimycin A in the murine model inoculated with highly v-*abl*-expressing murine myeloid cell lines, Cl cells [23]. Recently, it has been shown that herbimycin A also is a potent cytotoxin against malignant human tumors with primitive neural features, and the tumorigenicity in nude mice of these sensitive cell lines can be markedly reduced by systemic or topical administration of herbimycin A without any apparent toxicity to the whole animal [24].

More recently, erbstain and tyrphostins, derivative synthetics of erbstain, provided an important insight into future therapeutic developments against various types of cancers with amplified ErbB-1 (EGF-R) and ErbB-2 (Neu) through inhibiting PTK activity [25–27]. Furthermore, it has been noted that PTK blockers from the tyrphostin family can discriminate between normal ABL and transforming ABL proteins [28]. In addition to these studies, our development and study of herbimycin A, and further development of chemical modifications might provide an important insight into future therapeutic development according to a new strategy of *bcr abl* oncoprotein-targeted therapy against Ph^1-positive leukemia.

Acknowledgements—We are grateful to Dr R. A. van Etten and Dr. G. Q. Daley (Massachusetts Institute of Technology) for providing pGD210 plasmid construct and Dr M. Kobayashi (Hokkaido University School of Medicine) for providing pSV2*neo* containing murine IL-3 cDNA.

This study is supported in part by a Grant-in-Aid for Scientific Research from the Ministry of Education, Science and Culture of Japan.

References

1. Kurzrock R., Gutterman J. U. & Talpaz M. (1989) The molecular genetics of Philadelphia chromosome-positive leukemias. *New Engl. J. Med.* 319, 990.
2. Groffen J., Stephenson J. R., Heistekamp N., Klein A. de, Bartram C. R. & Grosveld G. (1984) Philadelphia chromosomal breakpoints are clustered within a limited region, *bcr*, on chromosome 22. *Cell* 36, 93.
3. Hermans A., Heisterkamp N., Lindern M. von, Groffen J., Boostma D. & Grosveld G. (1987) Unique fusion of *bcr* and *abl* genes in Philadelphia chromosome positive acute lymphoblastic leukemia. *Cell* 51, 33.
4. Clark L. C., McLaughlin J., Crist W. M., Champlin T. & Witte O. N. (1987) Unique form of the *abl* tyrosine kinase distinguish Ph^1-positive CML from Ph^1-positive ALL. *Science* 235, 1985.
5. Kurzrock R., Shtarlid M., Romero P., Kloetzer W. S., Talpas M., Trujillo J. M., Blick M., Beran M. & Gutterman J. U. (1987) A novel c-*abl* protein product in Philadelphia-positive acute lymphoblastic leukemia. *Nature* 325, 631.
6. Daley G. Q. & Baltimore D. (1988) Transformation of an interleukin 3-dependent hematopoietic cell line by the chronic myelogenous leukemia-specific P210$^{bcr/abl}$. *Proc. natn. Acad. Sci. U.S.A.* 85, 9312.
7. Lugo T. G., Pendergast A-M., Muller A. J. & Witte O. N. (1990) Tyrosine kinase activity and transformation potency of *bcr-abl* oncogene products. *Science* 247, 1079.
8. Daley G. Q., Van Etten R. A. & Baltimore D. (1990) Induction of chronic myelogenous leukemia in mice by the P210$^{bcr/abl}$ gene of the Philadelphia chromosome. *Science* 247, 824.
9. Heisterkamp N., Jenster G., Hoeve J. ten, Zovich D., Pattengale P. & Groffen J. (1990) Acute leukemia in BCR/ABL transgenic mice. *Nature* 344, 251.
10. Szczylik C., Skorski T., Nicolaides N. C., Manzella L., Malaguarnera L., Venturelli D., Gewirtz A. M., & Calabretta B. (1991) Selective inhibition of leukemia cell proliferation by BCR-ABL antisense oligodeoxynucleotides. *Science* 253, 562.
11. Okabe M., Kuni-eda Y., Sugiura T., Tanaka M., Miyagishima T., Saiki I., Minagawa T., Kurosawa M., Itaya T. & Miyazaki T. (1991) Inhibitory effect of interleukin-4 on *in vitro* growth of Ph^1-positive acute lymphoblastic leukemia. *Blood* 78, 1574.
12. Okabe M., Uehara Y., Miyagishima T., Itaya Y., Tanaka M., Kuni-eda Y., Kurosawa M. & Miyazaki T. (1992) Effect of herbimycin A, an antagonist of tyrosine kinase, on BCR/ABL oncoprotein-associated cell proliferation: abrogative effect on the transformation of murine hematopoietic cells by transfection of a retroviral vector expressing oncoprotein P210^{210} and preferential inhibition of *in vitro* growth of Ph^1-positive leukemia cells. *Blood* 80, 1330.
13. Dolnick B. J. (1991) Antisense agents in cancer research and therapeutics. *Cancer Invest.* 9, 185.
14. Maeriat P., Lewalle P., Taj A. S., Philippe M., Larondelle Y., Vaerman J. L., Wildmann C., Goldman J. M. & Miahaux J. L. (1993) Retrovirally transduced antisense sequences stably suppress P210$^{bcr/abl}$ expression and inhibit the proliferation of BCR/ABL-containing cell lines. *Blood* 81, 502.
15. Uehara Y., Hori M., Takeuchi T. & Umezawa T. (1985) Screening of agents with converted transformed morphology of Rous sarcoma virus-infected rat kidney cells to normal morphology: identification of an active agent as herbimycin and its inhibition of intracellular *src* kinase. *Jpn. J. Cancer Res.* 76, 672.
16. Uehara Y., Murakami Y., Mizuno S. & Kawai S. (1989) Inhibition of transforming activity of tyrosine kinase oncogene by herbimycin A. *Virology* 164, 294.
17. Dexter T. M., Garland J., Scott D., Scolnick E. & Metcalf D. (1980) Growth of factor-dependent hemopoietic precursor cell lines. *J. exp. Med.* 152, 1036.
18. Longo N., Shuster R. C., Griffin L. D., Langley S. D. & Elsas L. J. (1992) Activation of insulin receptor signaling by a single amino acid substitution in the transmembrane domain. *J. biol. Chem.* 267, 12,416.
19. Kurzrock R., Kloetzer W. S., Talpas M., Blick M., Walters R. & Arlinghaus R. B. (1987) Identification of molecular variants of P210$^{bcr/abl}$ in chronic myelogenous leukemia. *Blood* 70, 233.
20. Okabe M., Kawamura K., Miyagishima T., Itaya T., Goodwyn D., Shoji M., Vogler W. R., Sakurada K., Uehara Y. & Miyazaki T. (1994) Effect of herbimycin A, an inhibitor of tyrosine kinase, on protein tyrosine kinase activity and phosphotyrosyl proteins of Ph^1-positive leukemia cells. *Leukemia Res.* 18, 213.
21. Okabe M., Matsushima S., Morioka M., Kobayashi M., Abe S., Sakurada K., Kakinuma M. & Miyazaki T. (1987) Establishment and characterization of a cell line, TOM-1, derived from a patient with Philadelphia chromosome-positive acute lymphocytic leukemia. *Blood* 69, 990.
22. Koch C. A., Anderson D., Moran M. F., Ellis C. & Pawson T. (1993) SH2 and SH3 domains: elements that control interactions of cytoplasmic signaling proteins. *Science* 252, 668.
23. Honma Y., Okabe-kado J., Kasukabe T., Hozumi M., Kodama H., Kajigaya S., Suda T. & Miura Y. (1992) Herbimycin A, an inhibitor of tyrosine kinase, prolongs survival of mice inoculated with myeloid leukemia Cl cells with high expression of v-*abl* tyrosine kinase. *Cancer Res.* 52, 4017.
24. Whitesell L., Shifrin S. D., Schwab G. & Neckers L. M. (1992) Benzoquinonoid ansamycins possess selective tumoricidal activity unrelated to *src* kinase inhibition. *Cancer Res.* 52, 1721.
25. Yaish P., Gazit A., Gilon C. & Levizki A. (1991) Blocking of EGF-dependent cell proliferation by EGF receptor kinase inhibitors. *Science* 242, 933.
26. Toi M., Mukaida H., Wada T., Hirabayashi N., Toge T., Hori T. & Umezawa K. (1990) Antineoplastic effect of erbstain on human mammary and oesophageal tumors in athymic nude mice. *Eur. J. Cancer* 26, 722.
27. Yoneda T., Lyall R. M., Alsina M. M., Persons P. E., Spada A. P., Levitzki A., Zilberstein A. & Mundy G. R. (1991) The antiproliferative effects of tyrosine

kinase inhibitors tyrphostins on a human squamous cell carcinoma *in vitro* and in nude mice. *Cancer Res.* 51, 4430.

28. Anafi M., Gazit A., Gilon C., Ben-Neriah Y. & Levitzki A. (1992) Selective interactions of transforming and normal *abl* proteins with ATP, tyrosine-copolymer substrates, and tyrphostins. *J. biol. Chem.* 267, 4518.

(34) McWhorter WP, Mayer WJ. Black/w[illegible]fferences in type of initial breast cancer treatment and implication[illegible]survival. Am J Public Health 1987;77:1515–7.
(35) Diehr P, Yergan J, Chu J, Feigl P, Glaefke G, Moe R, et al. Treatment modality and quality differences for black and white breast-cancer patients treated in community hospitals. Med Care 1989;27:942–58.
(36) Whittle J, Conigliaro J, Good CB, Lofgren RP. Racial differences in the use of invasive cardiovascular procedures in the Department of Veterans Affairs medical system. N Engl J Med 1993;329:621–7.
(37) Mandelblatt J, Andrews H, Kao R, Wallace R, Kerner J. The late-stage diagnosis of colorectal cancer: demographic and socioeconomic factors. Am J Public Health 1996;86:1794–7.
(38) Liff JM, Chow WH, Greenberg RS. Rural–urban differences in stage at diagnosis. Possible relationship to cancer screening. Cancer 1991;67:1454–9.
(39) Weaver P, Harrison B, Eskander G, Jahan MS, Tanzo V, Williams W, et al. Colon cancer in blacks: a disease with a worsening prognosis. J Natl Med Assoc 1991;83:133–6.
(40) Tejeda HA, Green SB, Trimble EL, Ford L, High JL, Ungerleider RS, et al. Representation of African-Americans, Hispanics, and whites in National Cancer Institute cancer treatment trials. J Natl Cancer Inst 1996;88:812–6.
(41) Watanabe ME. "Amid criticism, NCI tries to boost minority clinical-trial recruitment." The Scientist 1996;10:7 p. 1, 4–5, April 1.
(42) Brown KS. "Sci[illegible]. African-American clergy join forces for trial recruitment." The [illegible]ist 1997;11:4 p. 1, 10, February 17.
(43) Macdonald JS. Adjuvant therapy for colon cancer. CA Cancer J Clin 1997;47:243–56.

NOTES

[1]*Editor's note:* SEER is a set of geographically defined, population-based, central cancer registries in the United States, operated by local nonprofit organizations under contract to the National Cancer Institute (NCI). Registry data are submitted electronically without personal identifiers to the NCI on a biannual basis, and the NCI makes the data available to the public for scientific research.

Supported by Public Health Service grants U10CA69651 and U10CA12027 from the National Cancer Institute, National Institutes of Health, Department of Health and Human Services; and by grant ACS-R-13 from the American Cancer Society.

We thank Carol Ursiny, Certified Clinical Research Associate, for her contributions in maintaining the NSABP colon cancer trials database.

Manuscript received June 1, 1999; revised September 15, 1999; accepted September 17, 1999.

(1) $7 \times 7 \times 7 \times 0.5 \simeq 200\,mm^3$

DT-Diaphorase Expression and Tumor Cell Sensitivity to 17-Allylamino,17-demethoxygeldanamycin, an Inhibitor of Heat Shock Protein 90

(4) 2 human CC lines

Lloyd R. Kelland, Swee Y. Sharp, Paul M. Rogers, Timothy G. Myers, Paul Workman

Background: To our knowledge, 17-allylamino,17-demethoxygeldanamycin (17AAG) is the first inhibitor of heat shock protein 90 (Hsp90) to enter a phase I clinical trial in cancer. Inhibition of Hsp90, a chaperone protein (a protein that helps other proteins avoid misfolding pathways that produce inactive or aggregated states), leads to depletion of important oncogenic proteins, including Raf-1 and mutant p53 (also known as TP53). Given its ansamycin benzoquinone structure, we questioned whether the antitumor activity of 17AAG was affected by expression of the NQO1 gene, which encodes the quinone-metabolizing enzyme DT-diaphorase. *Methods:* The antitumor activity of 17AAG and other Hsp90 inhibitors was determined by use of a sulforhodamine B-based cell growth inhibition assay in culture and by the arrest of xenograft tumor growth in nude mice. DT-diaphorase activity was determined by use of a spectrophotometric assay, and protein expression was determined by means of western immunoblotting. *Results:* In two independent *in vitro* human tumor cell panels, we observed a positive relationship between DT-diaphorase expression level and growth inhibition by 17AAG. Stable, high-level expression of the active NQO1 gene transfected into the DT-diaphorase-deficient (by NQO1 mutation) BE human colon carcinoma cell line resulted in a 32-fold increase in 17AAG growth-inhibition activity. Increased sensitivity to 17AAG in the transfected cell line was also confirmed in xenografts. The extent of depletion of Raf-1 and mutant p53 protein confirmed that the Hsp90 inhibition mechanism was maintained in cells with high and low levels of DT-diaphorase. 17AAG was shown to be a substrate for purified human DT-diaphorase. *Conclusion:* These results suggest that the antitumor activity and possibly the toxicologic properties of 17AAG in humans may be influenced by the expression of DT-diaphorase. Careful monitoring for NQO1 polymorphism and the level of tumor DT-diaphorase activity is therefore recommended in clinical trials with 17AAG. [J Natl Cancer Inst 1999;91:1940–9]

Benzoquinone ansamycins, such as herbimycin and geldanamycin (Fig. 1), exhibit anticancer activity by binding to heat shock protein 90 (Hsp90), a molecular chaperone, and its homologue GRP94 *(1,2)*. In this interaction, geldanamycin competes with adenosine triphosphate at the N-terminal-binding site

Affiliations of authors: L. R. Kelland, S. Y. Sharp, P. M. Rogers, P. Workman, Cancer Research Campaign Centre for Cancer Therapeutics, The Institute of Cancer Research, Surrey, U.K.; T. G. Myers, Developmental Therapeutics Program, Information Technology Branch, National Cancer Institute, Bethesda, MD.

Correspondence to: Paul Workman, Ph.D., Cancer Research Campaign Centre for Cancer Therapeutics, The Institute of Cancer Research, 15 Cotswold Rd., Sutton, Surrey SM2 5NG, U.K. (e-mail-paulw@icr.ac.uk).

See "Notes" following "References."

Exhibit C

of Hsp90 *(3)*. The interaction results in th[illegible]osome-mediated degradation of several important oncogenic proteins, including Raf-1, c-ErbB2, and mutant (but not wild-type) p53 (also known as TP53) *(4–6)*. Clearly, this molecular profile offers considerable potential for antitumor activity. However, both herbimycin and geldanamycin have limitations as drug candidates because of poor stability and hepatotoxicity *(7)*. This has resulted in efforts to discover improved synthetic analogues *(8)*.

One such compound, the 17-allylamino,17-demethoxy analogue of geldanamycin (17-allylamino,17-demethoxygeldanamycin; 17AAG) (Fig. 1), has also been shown to bind to Hsp90 *(9)*. Although, in rodent and dog toxicology studies, 17AAG retains some of geldanamycin's toxicity in the liver, gallbladder, and kidney [*(10)* and National Cancer Institute [NCI] drug data file on 17AAG] it has a better therapeutic index. For example, 17AAG exerts antitumor activity against some human melanoma xenografts at nontoxic doses [NCI drug data file on 17AAG and *(11)*]. Preclinical pharmacokinetic studies show that pharmacologically active concentrations can be achieved in plasma and tissues [NCI drug data file on 17AAG and *(12)*] and that the major liver microsomal metabolite (shown in Fig. 1) is 17-amino,17-demethoxygeldanamycin *(13)*. In view of its novel mechanism of action and its good therapeutic index, 17AAG has now entered phase I clinical trials as first-in-class Hsp90 inhibitor under the auspices of the U.S. NCI and the U.K. Cancer Research Campaign (CRC). Recently, the structurally distinct macrocyclic antifungal compound radicicol (Fig. 1) has been shown to bind to Hsp90 and inhibit its activity *(14–17)*.

DT-diaphorase, an obligate two-electron-reducing enzyme [reduced nicotinamide-adenine dinucleotide (phosphate):quinone oxidoreductase; EC 1.6.99.2], catalyzes the reduction of various quinones *(18)*. As a result, cells rich in DT-diaphorase are especially sensitive to quinone-containing bioreductive anticancer agents, such as mitomycin C and the indoloquinone EO9, which act as prodrugs for activation to toxic forms by DT-diaphorase *(19–21)*. Some tumor types (notably, colon and non-small-cell lung cancers) have been shown to contain relatively high levels of DT-diaphorase *(22–26)*. Thus, these cancers may be particularly suitable for treatments that use a DT-diaphorase prodrug approach. Although previous studies *(27)* have shown that geldanamycin is a substrate for DT-diaphorase, a cell line derived from human colorectal cancer and expressing DT-diaphorase did not appear to be particulary sensitive to geldanamycin. However, it is not known whether cells expressing high levels of DT-diaphorase show altered sensitivity to 17AAG.

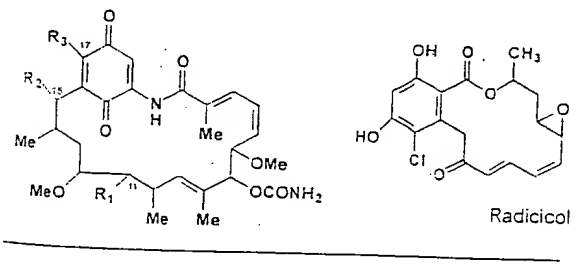

	R_1	R_2	R_3
Geldanamycin	OH	H	OMe
17AAG	OH	H	CH_2=$CHCH_2NH$
17-amino	OH	H	NH_2
Herbimycin	OMe	OMe	H

Fig. 1. Chemical structures of geldanamycin, 17-allylamino,17-demethoxygeldanamycin (17AAG), 17-amino,17-demethoxygeldanamycin (17-amino), radicicol, and herbimycin.

The primary aim of this study was to investigate whether DT-diaphorase activity has a role in the sensitivity of human tumor cells to 17AAG. Initially, sensitivity to 17AAG was determined by use of the CRC/Institute of Cancer Research (ICR) panel of 15 human colorectal and 11 ovarian carcinoma cell lines, including some resistant to classical agents. Comparative data were obtained in selected lines for the 17-amino metabolite and the additional Hsp90-binding agents geldanamycin and radicicol. The correlation between sensitivity and DT-diaphorase activity seen in a subset of the CRC/ICR panel (selected to span the range of sensitivity to 17AAG) was then examined and confirmed with data from the NCI panel of 60 human tumor cell lines *(28)*. This led to the hypothesis that high DT-diaphorase expression was a major factor in determining cellular sensitivity to 17AAG but not to geldanamycin or radicicol. To provide further conclusive data, sensitivity to 17AAG was determined in a newly established isogenic pair of cell lines that differ only in the expression of the active NQO1 gene. This pair is composed of the human colon BE line [which contains a disabling point mutation in the NQO1 gene encoding DT-diaphorase *(29)*] and a subline stably transfected with the NQO1 gene and expressing high levels of functional DT-diaphorase. Finally, evidence that the Hsp90 inhibitory mechanism was retained by 17AAG in colon cell lines expressing high and low levels of DT-diaphorase was obtained by immunoblot analysis of Raf-1, mutant p53, Hsp70, and Hsp90 proteins. The results suggest that determination of patients' NQO1 genotype and of tumor DT-diaphorase activity should be included in the clinical evaluation of 17AAG because variations in these characteristics could affect the toxicity and efficacy of the drug.

Materials and Methods

Cell Lines

We used panels of human colon and ovarian cell lines. We obtained cell lines from commercial cell culture collections or derived them in-house as described previously *(30)*. In some cases, we used sublines derived from a particular parent line with acquired drug resistance to cisplatin (CH1cisR and A2780cisR ovarian lines) or to doxorubicin (CH1doxR and an SKOV-3 subline stably overexpressing the multidrug-resistance protein MRP1) *(30–32)*. All lines were grown as monolayers in Dulbecco's modified Eagle medium containing 10% fetal calf serum, 2 m*M* glutamine, and 0.5 μg/mL hydrocortisone in 6% CO_2/94% air. All lines were free of *Mycoplasma* contamination.

Drugs and Chemicals

Geldanamycin, 17AAG, and 17-amino,17-demethoxygeldanamycin were supplied by E. Sausville (NCI). The remaining drugs (herbimycin, radicicol, streptonigrin, and dicoumarol) and chemicals were obtained from Sigma Chemical Co. (Poole, U.K.).

Growth Inhibition Studies

We used the sulforhodamine B assay as described previously *(30–32)* for growth inhibition studies. Briefly, we seeded tumor cells into 96-well microtiter plates, allowed the cells to attach overnight, and then added the drug to quadru-

plicate wells as indicated. Unless otherwise indicated, we exposed cells to a drug for 4 days. Thereafter, the cell number in treated versus control wells was estimated after treatment with 10% trichloroacetic acid and staining with 0.4% sulforhodamine B in 1% acetic acid. The IC_{50} was calculated as the drug concentration that inhibits cell growth by 50% compared with control growth.

Stable Transfection of the NQO1 Gene Into the BE Human Colon Carcinoma Cell Line

BE cells contain a point mutation in the NQO1 gene and thus have no functional DT-diaphorase enzyme activity *(29)*. We used the bicistronic expression vector pEFIRES-P *(33)* to express the NQO1 gene in BE cells. Lipofectamine (Life Technologies, Inc. [GIBCO BRL], Gaithersburg, MD) for transfection, and puromycin (0.5 μg/mL) for selection. Resulting clones were screened for DT-diaphorase enzyme activity or protein by an enzyme assay or immunoblotting, respectively (*see below*). Full details of the vector construction and the biologic properties of the stable transfectants will be published elsewhere (Sharp SY, Kelland LR, Valenti MR, Brunton LA, Hobbs S, Workman P: unpublished results). The stable transfectants, designated BE-F397 clone 2 and BE-F397 clone 5, were used in these studies.

DT-Diaphorase Assay

To determine whether 17AAG was a good substrate for DT-diaphorase, we used the standard cytochrome *c* assay, as described previously for the bioreductive indoloquinone EO9 *(34)* and geldanamycin *(27)*, but replaced menadione with 17AAG as the substrate and intermediate electron acceptor. We assayed extracts of the human colon cell line HT29 or purified human DT-diaphorase protein (from J. Skeily, ICR). For preparation of cell extracts, 2×10^7 cells were trypsinized, washed twice in ice-cold phosphate-buffered saline (PBS), and centrifuged (MSE Centaur I; 1100 rpm for 5 minutes at room temperature). The cell pellet then was resuspended in 0.5–1 mL of lysis buffer (PBS containing 1% Triton X-114 and 500 μ*M* phenylmethylsulfonyl fluoride) and left on ice for 30 minutes. After centrifugation (MSE Microcentrifuge; 12 000 rpm for 5 minutes at room temperature), the supernatant was used for protein determination and the enzyme assay. Results obtained for 17AAG were compared with those for geldanamycin, EO9, and streptonigrin, an excellent substrate for DT-diaphorase *(35)*. For all drugs, the difference in reduction of the menadione substrate in the absence and presence of dicoumarol (100 μ*M*), a standard inhibitor of DT-diaphorase, was determined *(27)*.

Immunoblotting

This analysis was performed as described previously *(30–32)*. Briefly, 5×10^6 cells were trypsinized, washed with PBS, and lysed in 100 μL of lysis buffer at 4 °C for 1 hour. Lysis buffer contained 10 mL of 150 m*M* NaCl–50 m*M* Tris–HCl (pH 7.5), 500 μL of 20 m*M* phenylmethylsulfonyl fluoride, 2 μL of aprotinin (10 mg/mL, stock solution), 2 μL of leupeptin (10 mg/mL, stock solution), 100 μL of 10 m*M* sodium orthovanadate, 100 μL of Nonidet P-40, and 100 μL of 20% sodium dodecyl sulfate (SDS). Lysates were centrifuged (MSE Microcentrifuge; 12 000 rpm for 15 minutes at 4 °C), and the resulting protein extracts were separated (50 μg/lane) by SDS–polyacrylamide gel electrophoresis and electroblotted to nitrocellulose filters. Antibodies to Hsp90 and Hsp70 were obtained from StressGen (Victoria, Canada), and antibodies to Raf-1 and p53 (DO1) were from Santa Cruz Biotechnology (Santa Cruz, CA). A monoclonal antibody to the rat DT-diaphorase (which cross-reacts with human diaphorase) was supplied by R. Knox (previously at CRC/ICR, now at Enzacta Ltd., Salisbury, U.K.). Antibody binding was identified with horseradish peroxidase-labeled secondary antibodies combined with enhanced chemiluminescence reagents (Amersham, Buckinghamshire, U.K.) and autoradiography.

In Vivo Effects

BE vector control cells and BE-F397 clone 2 cells were established as subcutaneous xenografts by injection of 5×10^6 cells into the flanks of adult female athymic nude (nu/nu) mice. The antitumor effect of 17AAG was determined in mice bearing comparably sized tumors (6–8 mm in diameter) derived from these cells. Animals were randomly assigned to receive vehicle alone (five or six mice) or 17AAG (five animals; dose schedule = 80 mg/kg per day in 10% dimethyl sulfoxide and 90% egg phospholipid by intraperitoneal injection on days 1–4 and days 7–11). Before this clinical formulation was available, 17AAG was administered to mice bearing HT29 xenografts in 10% dimethyl sulfoxide–0.05% Tween 20–90% NaCl, with a dose schedule of 80 mg/kg per day on days 0–3 and days 6–10. This dose and schedule were derived from previously performed experiments [NCI drug data file on 17AAG and *(11)*].

Tumor size was determined twice weekly by caliper measurements, and tumor volumes were calculated (volume = $[a \times b^2 \times \pi]/6$, where a and b are orthogonal tumor diameters). Tumor volumes were then expressed as a percentage of the volume at the start of treatment (relative tumor volume). The effect of the drug was determined by the growth delay, i.e., the difference in days required for the volume of tumors in control and treated animals to double. All procedures involving animals were performed within the guidelines set out by the Institute's Animal Ethics Committee and the United Kingdom Coordinating Committee for Cancer Research's *ad hoc* Committee on the Welfare of Animals in Experimental Neoplasia *(36)*.

Statistical Analyses

Where indicated, errors are presented as standard deviation ($n \geq 3$). Correlation tests and linear regression analyses were computed with SAS JMP (SAS Institute, Cary, NC). We assessed correlations with a Spearman calculation for the CRC/ICR panel and with a Pearson calculation for the NCI panel. Although the Spearman statistic is technically more robust, the Pearson statistic was used for correlations in the NCI panel for historic continuity. The likelihood test for linear model comparison was performed with S-Plus (Mathsoft, Seattle, WA). All P values are two-sided.

RESULTS

In Vitro Growth Inhibition

The *in vitro* growth inhibition properties of geldanamycin, 17AAG, and radicicol against panels of human colon (12 lines) and ovarian (11 lines) carcinoma cell lines are shown in Table 1, A. The IC_{50} value for 17-amino,17-demethoxygeldanamycin, the major metabolite of 17AAG, is also included for some lines. In most cell lines, all four compounds potently inhibited growth, with IC_{50} values of less than 2.5 μ*M*. Notably, one ovarian cell line (the 41M line) was relatively resistant (IC_{50} >2.5 μ*M*) to all four Hsp90-interactive compounds. On average, geldanamycin was the most potent agent (mean IC_{50} = 50.1 n*M*), with similar values obtained for 17-amino,17-demethoxygeldanamycin (mean IC_{50} = 47 n*M* in a subset of nine cell lines). 17AAG showed intermediate potency (mean IC_{50} = 220.4 n*M*), and the least potent agent was radicicol (mean IC_{50} = 587.4 n*M*).

Bar graphs showing the IC_{50} values (Fig. 2) reveal some interesting differences in the patterns of response for geldanamycin, 17AAG, and radicicol. Notably, some cell lines (e.g., BE and LoVo colon cells) are relatively resistant to 17AAG but not to geldanamycin (or radicicol). In contrast, the colon cell lines LS174T and KM12 were relatively resistant to geldanamycin but not to 17AAG. We have compared patterns of response for 25 cell lines (excluding 41M because this line was resistant to all compounds) by use of the Spearman analysis. Positive, but not statistically significant, correlations were observed between geldanamycin and radicicol (r = .36; P = .08) and between geldanamycin and 17AAG (r = .33; P = .11). There was, however, no correlation between 17AAG and radicicol (r = −.08; P = .72). Results indicate relatively distinct patterns of response for the three compounds. 17-Amino,17-demethoxygeldanamycin was studied in only a few lines in the panel. With the exception of LS174T colon cells, which are relatively resistant to geldanamycin and more sensitive to the 17-amino metabolite, the two compounds behaved similarly across the panel.

Activity in Acquired Anticancer Drug-Resistant Cell Lines

The *in vitro* potencies of geldanamycin, 17AAG, and radicicol have also been evaluated in various anticancer drug-resistant

Table 1. *In vitro* human tumor cell growth inhibi 17AAG and other heat shock protein inhibitors

A. Summary of growth inhibition (drug concentrations that inhibit growth by 50% [IC_{50}]) of geldanamycin, 17AAG, radicicol, and 17-amino against the CRC/ICR panel of human colon and ovarian tumor cells,†*

Cell line	IC_{50}, nM			
	Geldanamycin	17AAG	Radicicol	17-Amino
Colon				
BE	19.3 ± 3.1	773 ± 30.6	190	18
HT29	46.7 ± 9	8.9 ± 2.9	3100	6.3 ± 1.8
COLO205	3.8	7.2	1400	ND
DLD-1	78	140	290	ND
HCA-7	1.8	72	120	ND
HCC2998	98	78	650	ND
HCT15	83	490	280	ND
HCT116	67	99	240	ND
HT5	11.3	13.5	390	17
KM12	54	9	135	ND
LIM1215	9	77	100	20.5
LS174T	245	78.5	780	33.5
LoVo	21.9	1130	360	42
MAWI	6.2	58	1850	ND
SW620	3.1	68	110	ND
Ovarian				
A2780	11.5	12	115	43
CH1	104.5	1055	325	190
HX62	47	670	2500	ND
IGROV-1	94	92	295	ND
OVCAR-3	5	58	69	ND
OVCAR-4	9.6	295	540	ND
OVCAR-5	88	40	660	ND
OVCAR-8	15.5	67	230	ND
PXN94	84	43	1450	ND
SKOV-3	46	76	395	58
41M	>2500	5200	2350	>2500

B. Growth inhibitory properties of geldanamycin, 17AAG, and radiciol against anticancer drug-resistant human tumor cell lines,†*

Cell line	IC_{50}, nM		
	Geldanamycin	17AAG	Radicicol
A2780	7.1	2.4	115
A2780cisR	9.1	1.9	270
RF	1.3	0.8	2.3
CH1	49	960	325
CH1cisR	17	1220	88
RF	0.35	1.3	0.27
CH1doxR (Pgp)	2500	>2500	565
RF	51	>2.6	1.7
SKOV-3 puro	97.3	46	280
SKOV-3 S2 (MRP)	337	142	280
RF	3.5	3.1	1.0

*17AAG = 17-allylamino,17-demethoxygeldanamycin; 17-Amino = 17-amino,17-demethoxygeldanamycin; CRC = Cancer Research Campaign; ICR = Institute of Cancer Research; MRP = multidrug-resistance protein; Pgp = P-glycoprotein; puro = puromycin; ND = not done; RF = resistance factor (IC_{50}-resistant or -transfected line/parent/vector control line).

†Data are either the mean ± standard deviation (n = 3) or the mean of two determinations.

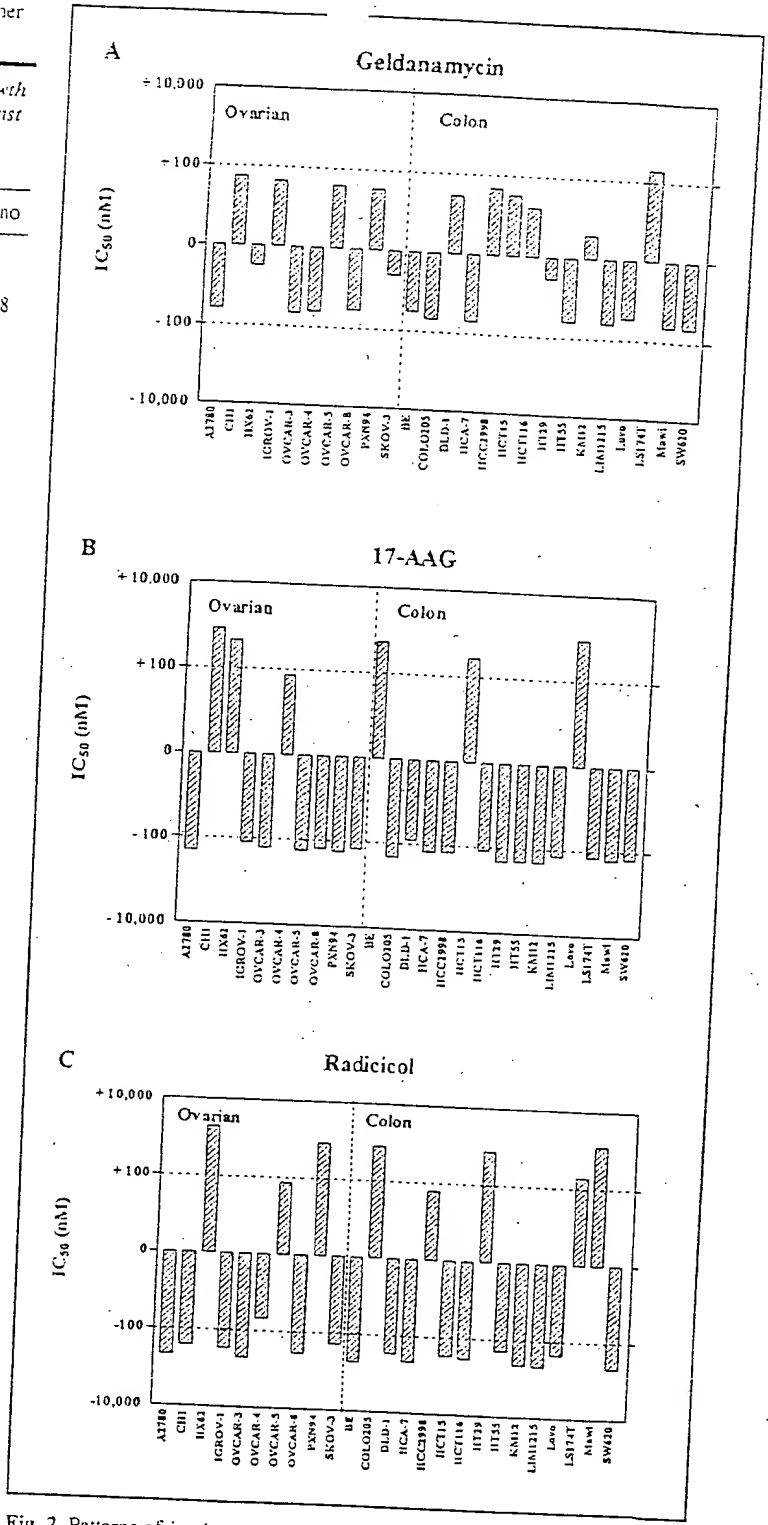

Fig. 2. Patterns of *in vitro* growth inhibition response across 25 human colon or ovarian carcinoma cell lines (as indicated) for geldanamycin (A), 17-allylamino,17-demethoxygeldanamycin (17-AAG) (B), and radicicol (C). Results are displayed as the extent to which the IC_{50} value (mean drug concentrations that inhibit growth by 50% for a 96-hour exposure) for a given cell line was greater or lower than the mean IC_{50} calculated for the entire panel. Values for the mean IC_{50} across the whole panel were as follows: 50.1 n*M* for geldanamycin, 220.4 n*M* for 17-AAG, and 587.4 n*M* for radicicol.

ublines. These lines possess acquired resistance to cisplatin cisR lines) or to doxorubicin through overexpression of P-lycoprotein (doxR line) or of MRP1 (SKOV-3 S2) (Table 1, B). lthough little cross-resistance to geldanamycin was observed the cisplatin-resistant cell lines, geldanamycin was markedly ss potent in the P-glycoprotein-overexpressing cell lines and in e MRP1-overexpressing cell lines than in the parent lines, ggesting that geldanamycin is a substrate for these multidrug-resistant efflux proteins. The picture is rather less clear for 17AAG because the parental CH1 ovarian cell line is relatively resistant to 17AAG, although there is at least a 2.5-fold cross-resistance to 17AAG in CH1doxR. The level of cross-resistance

for geldanamycin and 17AAG is similar in the MRP-overexpressing ovarian line. Like geldanamycin, 17AAG retains full activity in the cisplatin-resistant lines.

Growth Inhibition and DT-Diaphorase Enzyme Activity

Because geldanamycin and 17AAG are quinone-based compounds and BE cells have a disabling point mutation in the NQO1 gene *(29)*, the lack of DT-diaphorase activity in these cells could be involved in their surprisingly high relative resistance to 17AAG and low relative resistance to geldanamycin. To explore this possibility, we measured DT-diaphorase enzyme activity and IC_{50} values for geldanamycin, 17AAG, and radicicol in 11 cell lines (selected from those shown in Table 1), with a broad spectrum of responses to these compounds (Fig. 3). A statistically significant negative Spearman correlation was apparent for 17AAG ($r = -.81$; $P = .002$). Cells with marginal DT-diaphorase levels were relatively resistant to 17AAG, but there was no statistically significant correlation between sensitivity to geldanamycin or radicicol and DT-diaphorase levels ($P = .33$ and .76, respectively). Thus, we have identified the potential for a causal link between expression of DT-diaphorase and sensitivity to 17AAG, but not geldanamycin, in the CRC/ICR panel of colorectal and ovarian cell lines.

We then repeated this analysis with the NCI panel of 60 cell lines, which are derived from a diverse group of human cancers *(28)*. We have reported previously the DT-diaphorase activities for this panel of cells *(23)* as the logarithmically transformed values that are normally used for analysis in the NCI panel. We used correlation tests to explore the hypothesis that DT-diaphorase levels could be directly responsible for the sensitivity differences observed among the cell lines. The Pearson correlation coefficient indicated a weak positive relationship between DT-diaphorase expression and sensitivity to 17AAG ($r = .11$). The correlation between DT-diaphorase and geldanamycin was also weak, with possibly a negative trend ($r = -.15$). Neither correlation was statistically significant ($P = .43$ and .24, respectively). We then tested the hypothesis that, although DT-diaphorase activity may not predict sensitivity to 17AAG directly, it might explain why some cell lines are more sensitive to 17AAG than to geldanamycin. We tested this hypothesis by comparing the following two linear regression models: 1) 17AAG sensitivity = geldanamycin sensitivity + error, and 2) 17AAG sensitivity = geldanamycin sensitivity + DT-diaphorase activity + error. Because 17AAG and geldanamycin are reasonably well correlated ($r = .50$; $P<.001$), both models fit the data well. However, more important, inclusion of DT-diaphorase caused a statistically significant ($P = .03$) improvement in the fit as measured with a likelihood ratio test (analysis of variance by use of the F statistic). Thus, DT-diaphorase is a statistically significant factor when the sensitivity patterns of 17AAG are compared with those of geldanamycin. Addition of multidrug resistance protein status, as measured functionally by rhodamine efflux, did not improve the above model (data not shown).

Activity in Isogenic BE Colon Cell Lines That Contain or Lack the Active NQO1 Gene

To more directly investigate the role of DT-diaphorase in mediating the cytotoxicity of 17AAG, we stably transfected the BE cell line with the NQO1 gene encoding DT-diaphorase. As shown by immunoblotting, the resulting BE-F397 clone 2 and

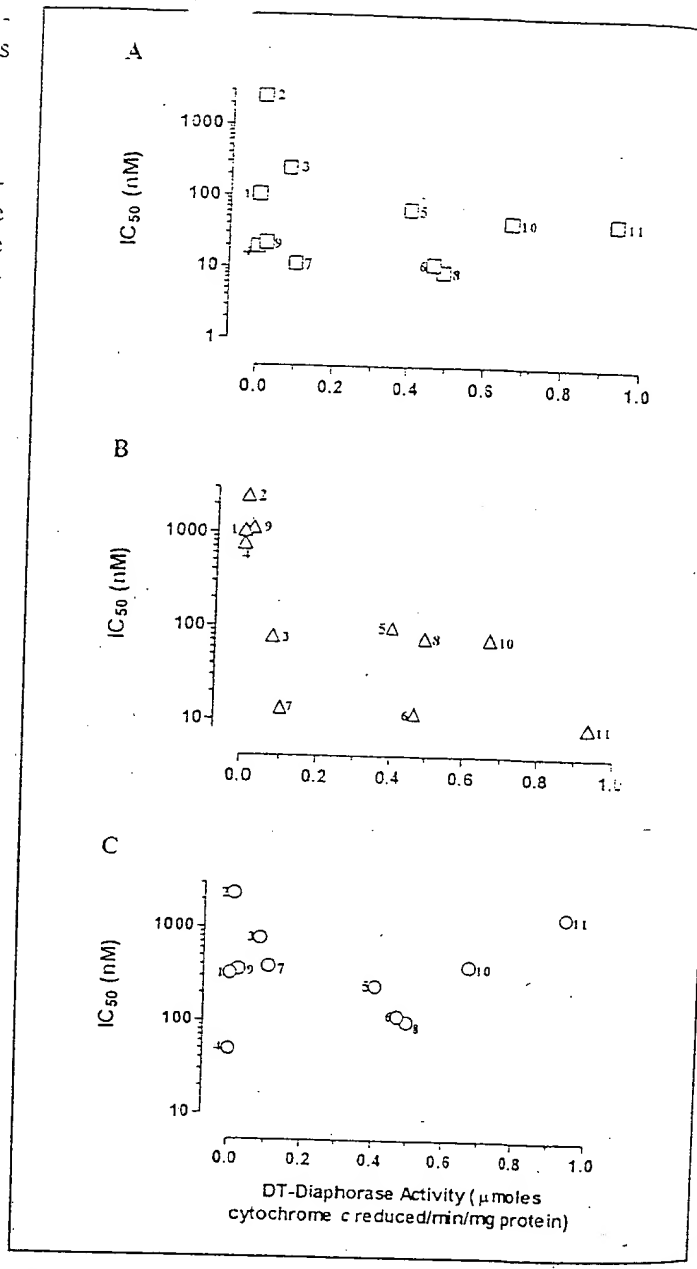

Fig. 3. Relationship between *in vitro* growth inhibition and DT-diaphorase expression for heat shock protein 90 inhibitors. The results are displayed as a plot of IC_{50} (mean drug concentrations that inhibit growth by 50% [illegible] 96-hour exposure) versus DT-diaphorase enzyme activity and DT-diaphorase enzyme activity for geldanamycin (A), 17-allylamino,17-demethoxygeldanamycin (B), and radicicol (C) in the following 11 human tumor cell lines: 1 = CH1 (ovarian); 2 = 41M (ovarian); 3 = LS174T (colon); 4 = BE (colon); 5 = HCT116 (colon); 6 = A2780 (ovarian); 7 = HT55 (colon); 8 = LIM1215 (colon); 9 = LoVo (colon); 10 = SKOV-3 (ovarian); and 11 = HT29 (colon).

the naturally high DT-diaphorase-containing colon line HT29 possess similar levels of DT-diaphorase protein (unpublished results). Enzyme activity data supported the immunoblotting observations. Values (measured as the dicoumarol-inhibitable reduction of menadione and expressed as micromoles of cytochrome *c* reduced per minute per milligram of protein) are as follows: BE vector control cells, unmeasurable activity (<0.002); BE-F397 clone 2, 1.4 ± 0.5; BE-F397 clone 5, 1.3 ± 0.2; and HT29, 0.94 ± 0.2. This HT29 activity is similar to the activity obtained previously with the same assay *(27)*. Functional validation of the model was provided by the observation

that introduction of the DT-diaphorase gene into BE cells substantially enhanced the potency of streptonigrin, an excellent DT-diaphorase substrate and bioreductive agent. The degree of potentiation correlated with DT-diaphorase levels and activity (117-fold potentiation in BE-F397 clone 5 and 142-fold potentiation in BE-F397 clone 2). Further details will be published elsewhere.

Dose–response curves for geldanamycin and 17AAG in BE vector control cells and BE-F397 clone 2 are shown in Fig. 4, A. Although the two lines showed similar sensitivity to geldanamycin, BE vector control cells lacking DT-diaphorase were markedly less sensitive to 17AAG. The degrees of potentiation (in terms of IC_{50} values) for geldanamycin, 17AAG, 17-amino,17-demethoxygeldanamycin, radicicol, and herbimycin observed when DT-diaphorase was introduced into the BE colon cell line are shown in Fig. 4, B. Notably, a 32-fold potentiation was observed with 17AAG, whereas a less than threefold potentiation was observed for all other compounds evaluated. In a second test of the effect of DT-diaphorase on the growth inhibitory properties of these compounds (Fig. 4, B), HT29 colon cells (naturally high in DT-diaphorase activity) were compared with BE parent cells (no measurable DT-diaphorase activity). Results generally mirrored those results observed with the isogenic-transfected pair of BE lines, with only 17AAG, of the Hsp90 inhibitors tested, showing a marked DT-diaphorase-mediated differential effect (87-fold potentiation). It is of interest in this pair of lines that HT29 cells had a strikingly greater sensitivity to radicicol than did BE cells, an effect not seen with the isogenic BE cell line pair.

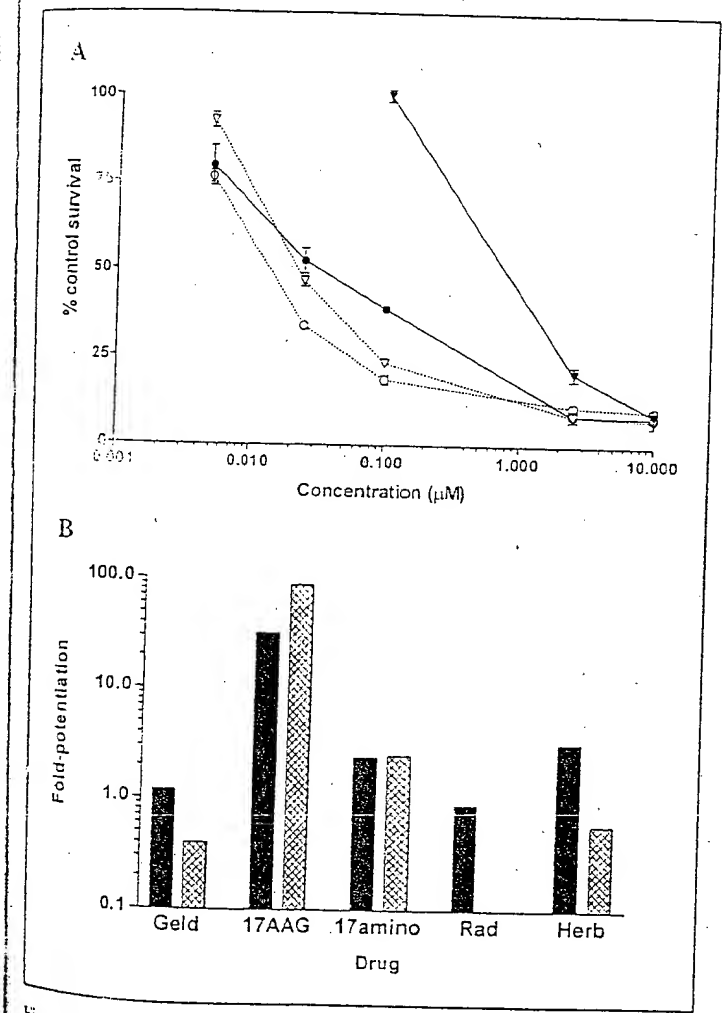

Fig. 4. Effects of DT-diaphorase gene (NQO1) transfection on response to heat shock protein 90 (Hsp90) inhibitors. A) Dose–response curves for BE vector control (▼, ▽) and BE-F397 clone 2 (●, ○) for geldanamycin (Geld; open symbols, broken lines) and 17-allylamino,17-demethoxygeldanamycin (17AAG; solid symbols, continuous lines). B) Extent of potentiation in high compared with low DT-diaphorase-expressing cells for the Hsp90 inhibitors geldanamycin, 17AAG, 17-amino,17-demethoxygeldanamycin (17amino), radicicol (Rad), and herbimycin (Herb). Fold-potentiation = drug concentrations that inhibit growth by 50% (IC_{50}) in cells expressing low levels of DT-diaphorase (BE parental or BE vector control line)/IC_{50} in cells expressing a high level of DT-diaphorase (BE-F397 or HT29 colon line). Solid bars = BE vector control/BE-F397 cells; cross-hatched bars = BE/HT29 cells.

Reduction of 17AAG by Purified Human DT-Diaphorase

Having demonstrated a potentially important role for DT-diaphorase in cellular sensitivity to 17AAG, we used a menadione substrate replacement assay as described previously *(27,34)* to determine the ability of this agent, geldanamycin, and 17-amino,17-demethoxygeldanamycin to act as substrates for purified human DT-diaphorase (Table 2). Streptonigrin *(35)*, an excellent substrate for DT-diaphorase, was also included in the comparison. We found that 17AAG was a reasonable substrate for DT-diaphorase, but it is not appreciably better than geldanamycin or 17-amino,17-demethoxygeldanamycin. This is perhaps surprising in view of the cellular data. The DT-diaphorase-mediated reduction rate was similar for all three analogues, each at a substrate concentration of 10 μM. At 50 μM, 17AAG and 17-amino,17-demethoxygeldanamycin gave twofold to threefold higher rates than geldanamycin, and the difference was even greater at 100 μM. Geldanamycin at 100 μM resulted in substrate inhibition, which was not observed with the other two analogues at 100 μM. The latter two concentrations, however, are much higher than the pharmacologically relevant range. It also should be noted that all three of the ansamycin analogues gave reaction rates that were substantially lower than rates observed for streptonigrin (Table 2). With the structurally distinct Hsp90 inhibitor radicicol, which lacks a quinone moiety, no reduction was observed.

Effects of 17AAG on Hsp90, Hsp70, and Oncogenic Proteins

To determine whether the mode of action of 17AAG was the same in cells expressing low and high levels of DT-diaphorase and to guide the choice of molecular pharmacodynamic markers in the imminent clinical trial, we measured the levels of Raf-1, mutant p53, Hsp90, and Hsp70 proteins in vector control cells and transfected BE cells treated with 17AAG (or geldanamycin). Levels of these proteins 6 and 24 hours after the addition of equitoxic (continuous exposure to 5× and 10× IC_{50}) or equimolar (0.15 and 0.3 μM) geldanamycin or 17AAG are shown in Fig. 5. No change in Hsp90 protein levels was observed. A similar marked reduction, especially at 24 hours, was observed for Raf-1 and p53 proteins in the BE vector control cells and BE-F397 clone 2 cells at equitoxic concentrations. By contrast, an increase in Hsp70 levels was observed. For geldanamycin or 17AAG at equimolar concentrations (0.15 or 0.3 μM), no change in any of the four proteins was observed in the BE vector control cells expressing low levels of DT-diaphorase, consistent with their cellular resistance at these concentrations.

Table 2. Reduction of geldanamycin, 17-allylamino,17-demethoxygeldanamycin (17AAG), and 17-amino,17-demethoxygeldanamycin (17-amino) by purified human DT-diaphorase (at 20 μg/mL)*,†

Substrate	Reduction of substrate,* μmol of cytochrome *c* reduced per minute per mg of protein
Menadione, 10 μ*M*	1188.5 ± 163.7
Streptonigrin, 50 μ*M*	206.1 ± 6.0
Streptonigrin, 25 μ*M*	159.1 ± 9.0
Streptonigrin, 10 μ*M*	176.6 ± 69.5
Geldanamycin, 100 μ*M*	1.5 ± 0.8
Geldanamycin, 50 μ*M*	7.2 ± 3.3
Geldanamycin, 25 μ*M*	7.0 ± 1.0
Geldanamycin, 10 μ*M*	4.3 ± 0.6
17AAG, 100 μ*M*	20.5 ± 2.1
17AAG, 50 μ*M*	15.0 ± 7.9
17AAG, 25 μ*M*	8.3 ± 1.3
17AAG, 10 μ*M*	3.6 ± 0.6
17-Amino, 100 μ*M*	17.6 ± 5.3
17-Amino, 50 μ*M*	22.8 ± 3.6
17-Amino, 25 μ*M*	11.7 ± 4.3
17-Amino, 10 μ*M*	6.8 ± 3.5
Radicicol	ND

*Values are individual or mean ± standard deviation (n = 3).
†ND = not detectable at all concentrations tested.

In Vivo Effects of 17AAG

We determined the effect of 17AAG on the response of the BE vector control cells and BE-F397 cells when grown subcutaneously as solid tumor xenografts in nude mice. 17AAG was administered at the maximum tolerated dose of 80 mg/kg per day intraperitoneally on days 0–4 and days 7–11, a schedule that is active on sensitive xenografts [NCI drug data file on 17AAG and *(11)*]. The xenograft tumor grown from the transfected BE-F397 cells (Fig. 6, B) was more sensitive than the BE vector control cells (Fig. 6, A). The growth delays, calculated from the time required to reach twice the treatment volume, were 11.4 days for the BE-F397 xenograft and 5.8 days for the vector control. For the HT29 xenograft (and a similar schedule of 80 mg/kg per day intraperitoneally on days 0–3 and days 6–10), a growth delay of 16.6 days was observed (Fig. 6, C). Experiments (not shown) confirmed that the differences in DT-diaphorase expression seen *in vitro* were maintained in the xenograft (data not shown). Thus, the HT29 line with a naturally high level of DT-diaphorase and also the transfected BE-F397 line were more sensitive *in vivo* than the BE vector control cells that have a low level of DT-diaphorase activity.

Discussion

17AAG is currently entering phase I clinical trial as the first-in-class Hsp90 inhibitor, under the auspices of the NCI and CRC. Treatment with this drug results in the depletion of a number of important oncogenic proteins, including Raf-1, ErbB2, and mutant p53 proteins, from tumor cells *(1,4–6,9)*. In this article, we show that the levels of DT-diaphorase activity in a tumor cell are an important and statistically significant determinant of how well 17AAG will inhibit the growth of that tumor cell. Evidence for this role of DT-diaphorase comes from the following three observations: 1) There was a statistically significant correlation between DT-diaphorase activity and sensitivity to 17AAG for 11 human colon and ovarian cancer cell lines from the CRC/ICR panel. 2) Subsequent interrogation of data from the NCI panel of 60 human tumor cell lines supported the hypothesis that the level of DT-diaphorase activity was a contributory factor in the differences in the sensitivity of tumor cell lines to 17AAG compared with geldanamycin. [In an analogous way, the differences in sensitivity between methotrexate and trimetrexate in the NCI 60 human tumor cell line panel have been explained by differences in the levels of reduced folate carrier protein *(37)*.] 3) Transfection of DT-diaphorase into the BE human colon cancer cell line, thereby creating pairs of isogenic cell lines differing only in DT-diaphorase expression, resulted in a marked increase in 17AAG-induced growth inhibition *in vitro* and an increased response to 17AAG *in vivo*. The degree

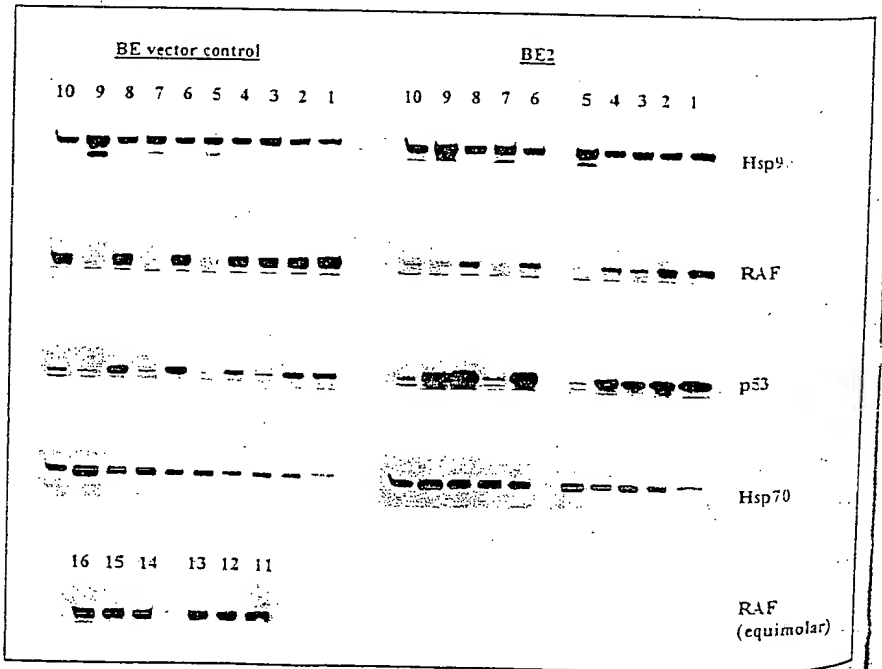

Fig. 5. Representative immunoblots for heat shock protein 90 (Hsp90), RAF-1, p53, and Hsp70 (as indicated) in BE vector control or BE clone 2 cells exposed to equitoxic concentrations (5× or 10× drug concentrations that inhibit growth by 50% [IC_{50}]) of geldanamycin (0.2 and 0.4 μ*M* for 5× and 10× IC_{50} in BE vector control cells and 0.1 and 0.2 μ*M* for 5× and 10× IC_{50} in BE-F397 clone 2 cells, respectively) or 17-allylamino,17-demethoxygeldanamycin (17AAG; 7 and 14 μ*M* for 5× and 10× IC_{50} in BE vector control cells and 0.15 and 0.3 μ*M* for 5× and 10× IC_{50} in BE-F397 clone 2 cells, respectively). Two fixed concentrations of 17AAG (0.15 and 0.3 μ*M*) are also shown for RAF-1 in the BE vector control cells. Cells were exposed to drug for 2 hours and harvested 6 and 24 hours after exposure. Lane 1 = 6-hour incubation of untreated cells; lane 2 = 6-hour incubation in geldanamycin (5× IC_{50}); lane 3 = 24-hour incubation in geldanamycin (5× IC_{50}); lane 4 = 6-hour incubation in geldanamycin (10× IC_{50}); lane 5 = 24-hour incubation in geldanamycin (10× IC_{50}); lane 6 = 6-hour incubation in 17AAG (5× IC_{50}); lane 7 = 24-hour incubation in 17AAG (5× IC_{50}); lane 8 = 6-hour incubation in 17AAG (10× IC_{50}); lane 9 = 24-hour incubation in 17AAG (10× IC_{50}); and lane 10 = 24-hour incubation of untreated cells. Blots for the BE vector control cells and 17AAG are also shown. Lane 11 = 6-hour incubation of untreated cells; lane 12 = 6-hour incubation in 0.15 μ*M* 17AAG; lane 13 = 24-hour incubation in 0.15 μ*M* 17AAG; lane 14 = 6-hour incubation in 0.3 μ*M* 17AAG; lane 15 = 24-hour incubation in 0.3 μ*M* 17AAG; and lane 16 = 24-hour incubation of untreated cells.

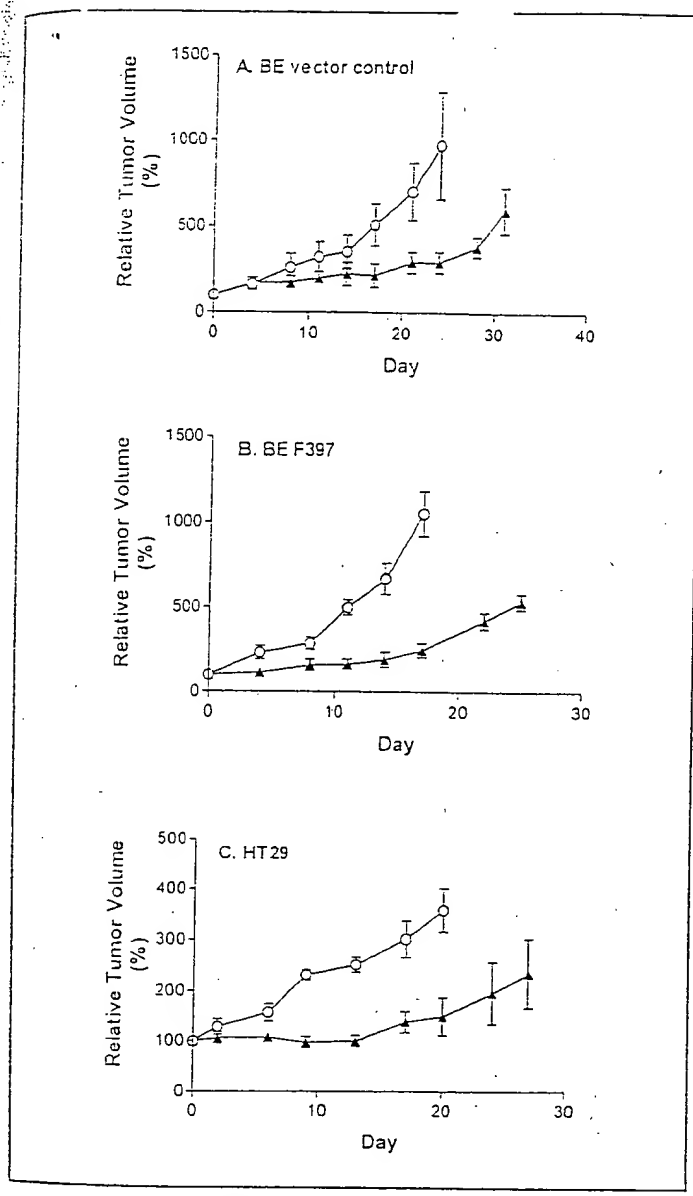

Fig. 6. Effect of DT-diaphorase expression on the response of human tumor xenografts *in vivo* to 17-allylamino,17-demethoxygeldanamycin (17AAG). Tumor growth curves for mice bearing BE vector control (A), BE-F397 clone 2 (B), or HT29 (C) xenografts after treatment with 17AAG. The dosing schedule was 80 mg/kg per day intraperitoneally daily on days 1–4 and days 7–11 for BE tumors and on days 0–3 and days 6–10 for HT29 tumors. ▲ = 17AAG; ○ = control. Data for relative tumor volumes are the means (± standard deviation) from five animals.

of *in vitro* growth inhibition correlated with the level of enzyme expression, being 32-fold higher in the transfected cell line with the higher levels of DT-diaphorase and 22-fold higher in the transfected cell line with somewhat lower levels. Of interest, the DT-diaphorase effect was not observed with geldanamycin, results in agreement with data from a nonisogenic pair *(27)*. Moreover, the effect was not seen with 17-amino,17-demethoxygeldanamycin, which was identified as the major 17AAG metabolite in human and mouse hepatic preparations *(13)* and confirmed as such *in vivo* (NCI drug data file on 17AAG). DT-diaphorase activity also appeared unrelated to the potency of radicicol, the structurally distinct Hsp90-binding antibiotic. Indeed, BE cells that express a low level of DT-diaphorase were almost 10-fold more sensitive to radicicol than were HT29 cells, which express a naturally high level of DT-diaphorase. There was no difference with radicicol in the isogenic transfected BE cell line pair.

The correlation seen between expression of DT-diaphorase activity and sensitivity to 17AAG but not to geldanamycin or radicicol shows that the effect is not generic across all Hsp90 inhibitors or, indeed, across all benzoquinone ansamycins. The precise mechanism by which high levels of DT-diaphorase in tumor cells result in sensitivity to 17AAG is not clear. The observation that DT-diaphorase activity affects tumor cell sensitivity to 17AAG but not to geldanamycin or 17-amino,17-demethoxygeldanamycin is not explicable in terms of their respective behavior as substrates for the purified human enzyme. Although we have demonstrated that 17AAG is a reasonable substrate for human DT-diaphorase, it was not appreciably better than geldanamycin or 17-amino,17-demethoxygeldanamycin, particularly at more relevant drug concentrations. Only at the markedly suprapharmacologic concentrations of 50 and 100 μM was 17AAG reduced at a statistically significantly faster rate than geldanamycin. For 17-amino,17-demethoxygeldanamycin, there was no appreciable difference in rate compared with geldanamycin.

Given the close structural similarity of 17AAG, 17-amino,17-demethoxygeldanamycin, and geldanamycin (Fig. 1), it is clear that it is the allyl substitution on the amino group at position 17 that is responsible for the DT-diaphorase effect. Preliminary results with a range of 17AAG analogues are consistent with this observation. We hypothesize that the behavior of the reduction product of 17AAG must differ from the reduction products derived from geldanamycin analogues with other substituents.

The xenograft experiment confirmed that DT-diaphorase-transfected BE-F397 cells were more sensitive than BE vector control cells in a solid tumor *in vivo*. The naturally high DT-diaphorase-containing HT29 xenograft was also more sensitive than the BE vector control xenograft. Dose–response data were not generated in these experiments. However, it seems likely that the differences seen in the *in vivo* xenografts were not as large as those observed in the same lines *in vitro*. One factor that would tend to decrease the contribution of DT-diaphorase levels in the xenograft experiments is the metabolism of 17AAG to the 17-amino derivative, which is the major metabolite in the mouse *(13)*. This could be important because we show in this article that sensitivity to the 17-amino metabolite is not affected by DT-diaphorase. Formation of the 17-amino metabolite is catalyzed by cytochrome P450, specifically CYP3A4 in human microsomes *(13)*. Thus, we propose that the sensitivity of a given patient's tumor to 17AAG may be affected by the balance between DT-diaphorase and CYP3A4 metabolism. Consequently, we urge that both enzymes (or surrogates thereof) be monitored in the clinical studies that are now under way with 17 AAG.

We determined that 17AAG was operating through the Hsp90 protein to stimulate degradation of the oncogenic client proteins Raf-1 and mutant p53 by use of 17AAG at equitoxic and equimolar concentrations and cells expressing high and low levels of DT-diaphorase. The depletion of client proteins reported previously for both 17AAG and geldanamycin *(4–6,9)* was seen in cells expressing high and low levels of DT-diaphorase. At equitoxic concentrations of 17AAG or geldanamycin (5× and 10× IC_{50}) in the isogenic BE cell lines after 6 hours and, especially, after 24 hours of drug exposure, there was a similar and marked reduction in Raf-1 and mutant p53 proteins. At the fixed

concentrations of 0.15 or 0.3 μM 17AAG, which inhibited growth of wild-type NQO1-transfected cells but not BE vector control cells, there was no reduction in Raf-1 or p53 protein in cells with low levels of DT-diaphorase, whereas depletion was seen in the cells with high levels of DT-diaphorase that did respond to these concentrations. Thus, target activity was maintained in the presence of the respective active concentrations of 17AAG, independent of the expression of DT-diaphorase. This rules out the possibility that different target mechanisms operate in cells expressing low and high levels of DT-diaphorase. Rather, DT-diaphorase expression increases the potency of 17AAG via client protein depletion.

In contrast to effects reported in melanoma xenografts after administration of 17AAG *(11)*, no difference in the levels of Hsp90 was observed in our experiments. Hsp70 levels, however, were increased, consistent with the removal of Hsp90-induced transcriptional repression of Hsp70 when Hsp90 is inhibited *(38)*. Again, this effect was seen at equitoxic concentrations of 17AAG in both high and low DT-diaphorase lines, consistent with retention of the Hsp90-binding mechanism.

The high constitutive expression of p53 in BE cells suggests a mutant p53 genotype. Effects on mutant p53 were consistent with cell cycle effects of geldanamycin reported in cell lines expressing wild-type or mutant p53 *(39)*. In our own studies on the A2780 human ovarian carcinoma cell line (wild-type for p53) and a subline stably transfected with the viral p53-inactivating gene HPVE6 *(40)*, we found no difference in sensitivity to geldanamycin or 17AAG. Overall, the results indicate that p53 status is unlikely to influence sensitivity to 17AAG.

In summary, although uncertainties remain regarding the precise mechanism involved, our results clearly show that expression of DT-diaphorase can influence a tumor's sensitivity to 17AAG. It is also possible that NQO1 expression could affect toxicity of 17AAG toward normal tissues. There are obvious implications for the clinical evaluation of 17AAG as an anticancer agent because 5%–20% of the population (depending on ethnicity) is homozygous for the genetic polymorphism used in this study, the DT-diaphorase-disabling point mutation in the NQO1 gene present in the BE colon cell line *(41)*. In addition, the expression of DT-diaphorase in human tumors is very variable *(25,26)*, as it is in the cell lines studied herein and elsewhere *(22–24)*. We suggest that, in addition to measuring degradation of oncogenic client proteins and/or an increase in Hsp70 after treatment with 17AAG as potential markers of activity and therapeutic response, NQO1/DT-diaphorase genotype, CYP3A4 status, and also tumor DT-diaphorase levels should be determined. In particular, we propose that these measurements may provide useful indicators of efficacy and/or toxicity and should be considered for the phase I clinical trials of 17AAG that have recently begun under the auspices of the NCI and CRC.

REFERENCES

(1) Whitesell L, Mimnaugh EG, De Costa B, Myers CE, Neckers LM. Inhibition of heat shock protein HSP90-pp60v-src heteroprotein complex formation by benzoquinone ansamycins: essential role for stress proteins in oncogenic transformation. Proc Natl Acad Sci U S A 1994;91:8324–8.

(2) Stebbins CE, Russo AA, Schneider C, Rosen N, Hartl FU, Pavletich NP. Crystal structure of an Hsp90-geldanamycin complex: targeting of a protein chaperone by an antitumor agent. Cell 1997;89:239–50.

(3) Prodromou C, Roe SM, O'Brien RO, Ladbury JE, Piper PW, Pearl LH. Identification and structural characterization of the ATP/ADP-binding site in the Hsp90 molecular chaperone. Cell 1997;90:65–75.

(4) An WG, Schnur RC, Neckers L, Blagosklonny MV. Depletion of p185^{erbB2}, Raf-1 and mutant p53 proteins by geldanamycin derivatives correlates with antiproliferative activity. Cancer Chemother Pharmacol 1997;40:60–4.

(5) Dasgupta G, Momand J. Geldanamycin prevents nuclear translocation of mutant p53. Exp Cell Res 1997;237:29–37.

(6) Whitesell L, Sutphin PD, Pulcini EJ, Martinez JD, Cook PH. The physical association of multiple molecular chaperone proteins with mutant p53 is altered by geldanamycin, an hsp90-binding agent. Mol Cell Biol 1998;18:1517–24.

(7) Supko JG, Hickman RL, Grever MR, Malspeis L. Preclinical pharmacologic evaluation of geldanamycin as an antitumor agent. Cancer Chemother Pharmacol 1995;36:305–15.

(8) Schnur RC, Corman ML, Gallaschun RJ, Cooper BA, Dee MF, Doty JL, et al. erbB-2 oncogene inhibition by geldanamycin derivatives: synthesis, mechanism of action, and structure–activity relationships. J Med Chem 1995;38:3813–20.

(9) Schulte TW, Neckers LM. The benzoquinone ansamycin 17-allylamino-17-demethoxygeldanamycin binds to HSP90 and shares important biologic activities with geldanamycin. Cancer Chemother Pharmacol 1998;42:273–9.

(10) Page J, Heath J, Fulton R, Yalkowsky E, Tabibi E, Tomaszewski J, et al. Comparison of geldanamycin (NSC-122750) and 17-allylamino-geldanamycin (NSC-330507D) toxicity in rats [abstract]. Proc Am Assoc Cancer Res 1997;38:A2067.

(11) Burger AM, Fiebig HH, Newman DJ, Camalier RF, Sausville EA. Antitumor activity of 17-(allylamino)-17-demethoxygeldanamycin (NSC 330507) in melanoma xenografts is associated with decline in Hs[illegible]0 protein expression [abstract]. Annals Oncol 1998;9(Suppl 2):abstract 504.

(12) Eiseman JL, Sentz DL, Zuhowski EG, Ramsland TS, Rosen DM, Reyna SP, et al. Plasma pharmacokinetics and tissue distribution of 17-allylaminogeldanamycin (NSC 330507), a prodrug for geldanamycin, in CD_2F_1 mice and Fisher 344 rats [abstract]. Proc Am Assoc Cancer Res 1997;38:A2063.

(13) Egorin MJ, Rosen DM, Wolff JH, Callery PS, Musser SM, Eiseman JL. Metabolism of 17-(allylamino)-17-demethoxygeldanamycin (NSC 330507) by murine and human hepatic preparations. Cancer Res 1998;58:2385–96.

(14) Sharma SV, Agatsuma T, Nakano H. Targeting of the protein chaperone, HSP90, by the transformation suppressing agent, radicicol. Oncogene 1998;16:2639–45.

(15) Soga S, Kozawa T, Narumi H, Akinaga S, Irie K, Matsumoto K, et al. Radicicol leads to selective depletion of Raf kinase and disrupts K-Ras-activated aberrant signaling pathway. J Biol Chem 1998;273:822–8.

(16) Schulte TW, Akinaga S, Soga S, Sullivan W, Stensgard B, Toft D, et al. Antibiotic radicicol binds to the N-terminal domain of Hsp90 and shares important biologic activities with geldanamycin. Cell Stress Chaperones 1998;3:100–8.

(17) Roe SM, Prodromou C, O'Brien R, Ladbury JE, Piper PW, Pearl LH. Structural basis for inhibition of the Hsp90 molecular chaperone by the antitumor antibiotics radicicol and geldanamycin. J Med Chem 1999;42:260–6.

(18) Ernster L. DT-diaphorase: a historical review. Chemica Scripta 1987;27A:1–13.

(19) Workman P. Enzyme-directed bioreductive drug development revisited: a commentary on recent progress and future prospects with emphasis on quinone anticancer agents and quinone metabolising enzymes, particularly DT-diaphorase. Oncol Res 1994;6:461–75.

(20) Riley RJ, Workman P. DT-diaphorase and cancer chemotherapy. Biochem Pharmacol 1992;43:1657–69.

(21) Stratford IJ, Workman P. Bioreductive drugs into the next millennium. Anticancer Drug Des 1998;13:519–28.

(22) Robertson N, Stratford IJ, Houlbrook S, Carmichael J, Adams GE. The sensitivity of human tumor cells to quinone bioreductive drugs: what role for DT-diaphorase? Biochem Pharmacol 1992;44:409–12.

(23) Fitzsimmons SA, Workman P, Grever M, Paull K, Camalier R, Lewis AD. Reductase enzyme expression across the National Cancer Institute Tumor Cell Line Panel: correlation with sensitivity to mitomycin C and EO9. J Natl Cancer Inst 1996;88:259–69.

(24) Ross D, Beall HD, Siegel D, Traver RD, Gustafson DL. Enzymology of bioreductive drug activation. Br J Cancer Suppl 1996;27:S1–8.

(25) Schlager JJ, Powis G. Cytosolic NAD(P)H:(quinone acceptor)oxidoreduc-

tase in human normal and tumor tissue: effects of cigarette smoking and alcohol. Int J Cancer 1990;45:403–9.

(26) Marin A, Lopez de Cerain A, Hamilton ... Lewis AD, Martinez-Penuela JM, Idoate MA, et al. DT-diaphorase and cytochrome b_5 reductase in human lung and breast tumours. Br J Cancer 1997;76:923–9.

(27) Brunton VG, Steele G, Lewis AD, Workman P. Geldanamycin-induced cytotoxicity in human colon-cancer cell lines: evidence against the involvement of c-Src or DT-diaphorase. Cancer Chemother Pharmacol 1998;41: 417–22.

(28) Monks A, Scudiero DA, Johnson GS, Paull KD, Sausville EA. The NCI anti-cancer drug screen: a smart screen to identify effectors of novel targets. Anticancer Drug Des 1997;12:533–41.

(29) Traver RD, Horikoshi T, Danenberg KD, Stadlbauer THW, Danenberg PV, Ross D, et al. NAD(P)H : quinone oxidoreductase gene expression in human colon carcinoma cells: characterization of a mutation which modulates DT-diaphorase activity and mitomycin sensitivity. Cancer Res 1992;52: 797–802.

(30) Holford J, Sharp SY, Murrer BA, Abrams M, Kelland LR. *In vitro* circumvention of cisplatin resistance by the novel sterically hindered platinum complex AMD473. Br J Cancer 1998;77:366–73.

(31) Sharp SY, Rowlands MG, Jarman M, Kelland LR. Effects of a new antioestrogen, idoxifene, on cisplatin- and doxorubicin-sensitive and -resistant human ovarian carcinoma cell lines. Br J Cancer 1994;70:409–14.

(32) Sharp SY, Smith V, Hobbs S, Kelland LR. Lack of a role for MRP1 in platinum drug resistance in human ovarian cancer cell lines. Br J Cancer 1998;78:175–80.

(33) Hobbs S, Jitrapakdee S, Wallace JC. Development of a bicistronic vector driven by the human polypeptide chain elongation factor 1α promotor for creation of stable mammalian cell lines that express very high levels of recombinant proteins. Biochem Biophys Res Commun 1998;252: 368–72.

(34) Walton MI, Smith PJ, Workman P. The role of NAD(P)H : quinone reductase (EC 1.6.99.2, DT-diaphorase) in the reductive bioactivation of the novel indoloquinone antitumor agent EO9. Cancer Commun 1991;3: 199–206.

(35) Beall HD, Liu Y, Siegel D, Bolton EM, Gibson NW, Ross D. Role of NAD(P)H : quinone oxidoreductase (DT-diaphorase) in cytotoxicity and induction of DNA ... e by streptonigrin. Biochem Pharmacol 1996;51: 645–52.

(36) Workman P, Twentyman P, Balkwill F, Balmain A, Chaplin D, Double J, et al. United Kingdom Co-ordinating Committee on Cancer Research guidelines for the welfare of animals in experimental neoplasia. 2nd ed. Br J Cancer 1998;77:1–10.

(37) Moscow JA, Connolly T, Myers TG, Cheng CC, Paull K, Cowan KH. Reduced folate carrier gene (RFC1) expression and anti-folate resistance in transfected and non-selected cell lines. Int J Cancer 1997;72:184–90.

(38) Zou J, Guo Y, Guettouche T, Smith DF, Voellmy R. Repression of heat shock transcription factor HSF1 activation by HSP90 (HSP90 complex) that forms a stress-sensitive complex with HSF1. Cell 1998;94: 471–80.

(39) McIlwrath AJ, Brunton VG, Brown R. Cell-cycle arrests and p53 accumulation induced by geldanamycin in human ovarian tumour cells. Cancer Chemother Pharmacol 1996;37:423–8.

(40) Walton MI, Pestell KE, Valenti MR, Brunton LA, Kelland LR, Workman P. A comparison of *in vitro* and *in vivo* techniques for assessing chemosensitivity in a genetically engineered cell line [abstract]. Proc Am Assoc Cancer Res 1999;40:407.

(41) Kelsey KT, Ross D, Traver RD, Christiani DC, Zuo ZF, Spitz MR, et al. Ethnic variation in the prevalence of a common NAD(P)H quinone oxidoreductase polymorphism and its implications for anti-cancer chemotherapy. Br J Cancer 1997;76:852–4.

NOTES

Supported by the U.K. Cancer Research Campaign (CRC; SP2330/0201) and by a Public Health Service grant from the National Cancer Institute, National Institutes of Health, Department of Health and Human Services. P. Workman is a CRC Life Fellow.

We thank Dr. E. Sausville at the NCI for helpful discussion and the supply of geldanamycin and derivatives, Drs. A. Monks and N. Scudeiro at the NCI for providing NCI cell screen data, M. Valenti and L. Brunton for technical assistance with the xenograft experiment, and Dr. M. Walton for discussion of data.

Manuscript received April 17, 1999; revised September 10, 1999; accepted September 17, 1999.

tion by reducing the surface expression of KDR on HUVECs, or the affinity or total amount of VEGF binding to KDR on HUVECs. Instead, it appears that the durable effect of SU5416 may be due to a residual pool of inhibitor, which is concentrated in cells, that remains associated with cells. The sub-cellular localization and kinetics of elimination of the inhibitor are currently under investigation.

#2843 INHIBITION OF NF-κB BY A NOVEL PROTEASOME INHIBITOR AND ANTI-TUMOR ACTIVITY IN SQUAMOUS CELL CARCINOMA. J B Sunwoo, Z Chen, G Dong, C V Crowl-Bancroft, N Yeh, J Adams, J Mitchell, E Sausville, and C Van Waes, *Leukosite, Inc, Cambridge, MA, and National Inst of Health, Bethesda, MD*

Squamous cell carcinoma (SCC) of the head and neck has an elevated constitutive activation of the NF-κB transcriptional regulator. We have evidence suggesting that this activation is important for cell survival, tumor development, and protection from ionizing radiation. Activation of NF-κB depends on the proteolysis of the inhibitory protein IκB by the 26S proteasome. In this study, a novel proteasome inhibitor, PS-341 (Leukosite, Inc.), was used to inhibit NF-κB, and its anti-tumor effects were examined in a variety of murine and human SCC cell lines. A 50% inhibition of NF-κB was demonstrated by reporter gene and electrophoretic mobility shift assays at 10^{-8} M concentration. This correlated with anti-proliferation assays, demonstrating an IC_{50} of 10^{-8} M. Flow cytometry was used to show that cytotoxicity was preceded by a cell cycle block at the G2/M transition. Anti-tumor activity was also examined *in vivo*, and a significant dose-dependent response was observed. Because exposure to PS-341 induced a cell cycle block at G2/M and was also found to inhibit induction of NF-κB by ionizing radiation, we examined the utility of this compound as a sensitizer to ionizing radiation. We found a 30% increase in radiosensitivity by colonogenic assay after accounting for direct cytotoxic effects of the compound. These results suggest that the use of proteasome inhibitors to target the inhibition of NF-κB may be a useful therapeutic strategy in patients with squamous cell carcinoma of the head and neck.

#2844 RESPONSE OF HUMAN MELANOMAS TO 17-AAG IS ASSOCIATED WITH MODULATION OF THE MOLECULAR CHAPERONE FUNCTION OF HSP90. Angelika Maria Burger, Edward A Sausville, Richard F Camalier, David J Newman, and Heinz H Fiebig, *National Cancer Inst, Bethesda, MD, Tumor Biology Ctr, Freiburg, Germany, and Univ of Freiburg, Freiburg, Germany*

17-allylaminogeldanamycin (17-AAG, NSC 330507) is a new antitumor agent identified by the NCI which has entered phase I clinical trials in the US. Antitumor activity of geldanamycins has been described to result from degradation of signaling proteins and nuclear hormone receptors by binding their molecular chaperone Hsp90. In this study, two human melanoma xenografts, the 17-AAG sensitive MEXF 276 (T/C = 6%), the resistant MEXF 514 (T/C = 60%), and cell lines derived thereof, were chosen to elucidate 17-AAG effects on its potential target Hsp90 and down-stream effector proteins in a time and concentration dependent manner. Tumor tissues were collected after 48h, 72h, and 10d under 17-AAG treatment (at MTD = 80mg/kg/d, for 2x Qdx5). Cell lines were exposed to drug concentrations which cause total growth inhibition (TGI = 375nM in MEXF 276L, 10μM in MEXF 514L cells). By using immunohistochemistry and Western blot analysis we found Hsp90 abundantly expressed in 17-AAG responsive MEXF 276 tumors, but at lower levels in resistant MEXF 514 and in normal tissues. Moreover, whilst 17-AAG treatment did not affect Hsp90 expression in MEXF 514, it caused a rapid decline of Hsp90 in MEXF 276 cells. In latter, this was accompanied by translocation of Hsp90 from cytoplasm and nuclei to cell membranes. In contrast, Hsp72 levels were not changed in either melanoma. As a result of Hsp90 depletion in MEXF 276L cells, down-regulation of Raf-1 and HER-2/neu was observed 8h after drug addition. In MEXF 276 tissues, decrease of Hsp90 was further associated with occurrence of apoptosis. The apoptotic index rose from 9% (48h) over 12% (72h) to 45% (10d) under drug treatment. Our data suggest that the efficacy of 17-AAG is related to its ability to inhibit Hsp90 chaperone function.

#2845 ANTICANCER EFFECTS OF LIPOSOME-ASSOCIATED L AND D STEREOISOMERS OF ET-18-OCH_3. I. Ahmad, G. R Masters, J. Nguyen, J. J Schupsky, A. S Janoff, and E. Mayhew, *The Liposome Company (TLC), Princeton, NJ*

TLC ELL-12 is a liposome based formulation of ET-18-OCH_3 (1–O–octadecyl–2–O–methyl–*sn*–glycero–3–phosphocholine), and is currently in Phase I clinical trials. The L isomer of ET-18-OCH_3 is the active ingredient of ELL-12. We have previously shown the therapeutic efficacy of ELL-12 against several experimental mouse tumors. The aim of the present investigation was to determine any difference in toxicity or therapeutic efficacy of ELL-12 when formulated with L or D stereoisomers of ET-18-OCH_3. The L isomer liposome formulation of ELL-12 significantly reduced toxicity compared to the D isomer liposome formulation when administered once daily, i.v. x 5. L and D isomer formulations of ELL-12 were found to be equally effective in prolonging mean survival time against P388 murine leukemia. However, the L isomer liposome formulation, when administered against established B16/F10 lunge tumors, significantly ($p < 0.05$) reduced the mean number of tumor nodules when compared to control or the D isomer liposome formulation. These studies indicate that ELL-12 formulated with the L isomer of ET-18-OCH_3 is less toxic and more effective against B 16/F10 tumor than the D isomer liposomes.

#2846 THE APOPTOTIC EFFECT OF LONG-CHAIN FATTY AMINES ON HUMAN PANCREATIC CANCER CELLS IS MEDIATED BY SIGNALING PATHWAYS INCLUDING MAPK FAMILY AND CASPASES. Mizukami Yusuke, H. Ura, T. Obara, T. Izawa, N. Yanagawa, S. Tanno, Y. Fujimoto, and Y. Kohgo, *Asahikawa Med Coll, Hokkaido, Japan*

Farnesyl transferase inhibitor (FTI) is usually ineffective n Ki-ras transformed cells. However, we have shown that farnesylamine (FA), one of FTI could induce apoptosis in Ki-ras transformed fibroblasts and human pancreatic cancer cell lines (Mol Carcinogenesis, 1998). Therefore, we speculated that FA may have an another apoptotic mechanism in addition to the inhibition of farnesylation. Considering the chemical formula of FA, the "long-chain fatty amine (LFA)" structure may have a critical role for this mechanism. In this experiment, we used oleylamine (OA) as LFA and examined the signaling pathways to induce apoptosis in Ki-ras transformed fibroblasts and human pancreatic cancer cell lines. In both cells, apoptosis was nduced by OA and JNK activity was increased as well as by FA, but not in parent fibroblast (NIH3T3). Although the OA-induced apoptosis was caspase-dependent, caspase inhibitors did not affect JNK activation. The blockage of JNK activity by dominant negative mutant significantly abrogated the cytotoxic effect of OA and DNA laddering. 0A did not act as FTI, but decreased the upregulated ERK activity. In contrast to indispensable effect of JNK in OA-induced apoptosis, attenuated ERK activity alone was not sufficient, but might be required, because MEK inhibitor PD98059 alone did not induce apoptosis. The kinase activity of Akt, which transduce p21 ras mediated survival signaling, resulted in no marked change. Multiple signaling pathways including JNK, ERK, and their downstream caspases mediate the apoptosis and might be shared, at least in part, in FA-induced selective cytotoxicity on Ki-ras mutant cells.

#2847 PHARMACOLOGICAL INDUCTION OF PHOSPHATIDYLINOSITOL ACCUMULATION IS ASSOCIATED WITH CYTOLYSIS OF NEOPLASTIC CELLS. Robert E Finney, E Nudelman, S A Shaffer, T White, S Bursten, L L Leer, N Wang, D Waggoner, J W Singer, and R A Lewis, *Cell Therapeutics, Inc, Seattle, WA*

De novo phospholipid biosynthesis is required for growth of tumor cells. Here, we demonstrate that phospholipid biosynthesis through phosphatidic acid (PA) in neoplastic cells can be exploited for development of cytotoxic anti-cancer agents. PA is a key intermediate for biosynthesis of phosphatidylcholine (PC), phosphatidylethanolamine (PE), and phosphatidylserine (PS) through a diacylglycerol (DAG) intermediate and for biosynthesis of the anionic phospholipids, cardiolipin (CL) and phosphatidylinositol (PI), through a cytidinediphosphate-DAG intermediate. In addition to de novo PA production from lysophosphatidic acid (LPA), production of PA by phospholipase D has been cited among the effects of certain oncogenes (e.g. ras, fps, and src) and growth factors (e.g. PDGF, EGF, FGF, Insulin). CT-2584, a cancer chemotherapeutic drug candidate currently in Phase II clinical trials, decreased utilization of PA for PC biosynthesis and increased PA utilization for PI biosynthesis. A two to three-fold increase in PI was observed in tumor cell lines derived from breast, lung and prostate, was associated with cytotoxic concentrations of CT-2584, and occurred well prior to cytolysis of the tumor cell lines. In contrast, cytotoxic concentrations of cisplatin did not induce accumulation of PI, indicating that PI elevation by CT-2584 was not a general consequence of chemotherapy-induced cell death. Consistent with this mechanism of action, propranolol, an inhibitor of phosphatidic acid phosphohydrolase and PC biosynthesis, was also cytotoxic to tumor cell lines, induced PI accumulation, and was synergistic with CT-2584 in cytotoxicity assays. As expected from the biophysical properties of anionic phospholipids on cellular membranes, CT-2584 cytotoxicity was associated with disruption and swelling of endoplasmic reticulum and mitochondria. We conclude that CT-2584 effects a novel mechanism of action involving modulation of phospholipid metabolism in cancer cells.

#2848 THE EFFECTS OF LYSOPHOSPHATIDYLCHOLINE ON TNF-α PRODUCTION INDUCED BY LIPOSOMAL ET-18-OCH3. Marina Y Pushkareva, Andrew S Janoff, and Eric Mayhew, *The Liposome Co , Inc, Princeton, NJ*

The incorporation of 1-*o*-octadecyl-2-*o*-methyl-*sn*-glycero-3-phosphocholine (ET-18-OCH3) into optimized liposomes (ELL-12) overcomes the non-specific hemolytic effects of ET-18-OCH3 while maintaining or enhancing anti-cancer efficacy. ELL-12 is currently in Phase I clinical trial. We showed previously that *in vitro* ELL-12 induced growth inhibition is associated with a time- and dose-dependent production of tumor necrosis alpha (TNF-α). As lysophosphatidylcholine (lysoPC) has been shown to modulate the growth inhibiting effects of ELL-12, it was of interest to determine the effects of lysoPC on ELL-12-induced TNF-α production by U-937 cells. We treated U-937 cells with different concentrations of ELL-12 and lysoPC for various times. Maximum of TNF-α production (0.78±0:17 ng per 10^6 cells) was observed after 48 hours of incubation of U-937 cells with 3-4 μM ELL-12. LysoPC prevented induction of TNF-α production in dose-dependent manner. For example, 20 μM of lysoPC completely prevented TNF-α production at 48 hours, whereas 2 μM lysoPC produced 50 % inhibition. The effects on TNF-α production were not directly coupled to the effects of lysoPC on reduction of ELL-12-induced growth inhibition, since 2 μM lysoPC did not significantly affect ELL-12-induced growth inhibition. ET-18-OCH3 and lysoPC share structural similarity and have common cellular targets including inhibition of *de novo* phosphatidylcholine synthesis. The possible mechanism of inhibition of ELL-12-induced TNF-α production by lysoPC will be discussed.

Exhibit D

(4) - clinical / melanoma

Notes on 17-AAG clinical trials from ASCO meeting, May 2001, San Francisco
L. Fritz

1. Banerji et al (Workman group, UK). (Abstract 326)

Enrolled 21 patients; 6 melanoma (most of any type). 2 patients showed stable disease (both melanoma, at 320 mg/). Drug comes as 25 mg/ml in DMSO.

PD measurements: HSP70 increased
Raf decreased
In one melanoma patient, CDK4 went down and HSP70 went up (no Raf in that tumor)

PK: at 320 mg/ m^2: Cmax = 5-10 uM

Has good xenograft data.

No myelotoxicity even at peak doses.

2. Wilson et al (NIH arm of the study) (Abstract 325)

Richard Wilson presented the poster, but has returned to Northern Ireland. Jean Grem now heads the NIH arm of the clinical trial.

Patients entered:

Colorectal	6
Pancreatic	5
Renal	2
Various	1 each
Total	18 patients

Wilson says Len Neckers was wrong – no lung cancer response was seen – in fact, n9o0 lung cancer patient has been entered at NIH.

They have seen two patients with stable disease: 1 colorectal and 1 renal. But, Wilson says you see these types of patients stabilize spontaneously.

PD measurements:

Had good degradation of Lck and Raf-1 in PBL's (by day 2) also, HSP70 up – all by Western (done by Neckers).

3

Regarding who at CTEP is in charge of the 17-AAG project:

Exhibit E

Louise Grachow Runs Investigative Drug Branch in CTEP

Susan Arbuck Runs Developmental Chemotherapy Section (runs it, or is in it?) Reports to Grachow. Is directly responsible for 17-AAG. Arbuck is the person we should contact

Dale Shoemaker He was mentioned, but I'm not sure what his role is.

Sherry Ansher Interacts with companies for CTEP. Jean Grem described her as "more like a lawyer".

3. Munster et al (MSKCC trial data) (Abstract 327)

Pam said she'd send us the slides that comprised her poster

4. Also spoke with the clinicain who runs the Mayo Clinic arm of the 17-AAG trial. He said they are having trouble reliably measuring Lck and Raf in their blood samples (Neckers had better gels – but said not all samples had Raf either). NCI seemed to have the best PD measurements of all the sites.

Advances in Brief

17-Allylamino-17-demethoxygeldanamycin Induces the Degradation of Androgen Receptor and HER-2/*neu* and Inhibits the Growth of Prostate Cancer Xenografts[1]

David B. Solit, Fuzhong F. Zheng, Maria Drobnjak, Pamela N. Münster, Brian Higgins,[2] David Verbel, Glenn Heller, William Tong, Carlos Cordon-Cardo, David B. Agus,[3] Howard I. Scher, and Neal Rosen[4]

Program in Cell Biology [D. B. S., F. F. Z., P. N. M., N. R.], and Departments of Medicine [D. B. S., B. H., D. B. A., H. I. S., N. R.], Pathology [M. D., C. C-C.], and Epidemiology and Biostatistics [D. V., G. H.], Memorial Sloan-Kettering Cancer Center, New York, New York 10021

Abstract

Purpose: Ansamycin antibiotics, including 17-allylamino-17-demethoxygeldanamycin (17-AAG), inhibit Hsp90 function and cause the selective degradation of signaling proteins that require this chaperone for folding. Because mutations in the androgen receptor (AR) and activation of HER2 and Akt may account, in part, for prostate cancer progression after castration or treatment with antiandrogens, we sought to determine whether an inhibitor of Hsp90 function could degrade these Hsp90 client proteins and inhibit the growth of prostate cancer xenografts with an acceptable therapeutic index.

Experimental Design: The effect of 17-AAG on the expression of Hsp90 regulated signaling proteins in prostate cancer cells and xenografts was determined. The pharmacodynamics of target protein degradation was associated with the toxicology and antitumor activity of the drug.

Results: 17-AAG caused the degradation of HER2, Akt, and both mutant and wild-type AR and the retinoblastoma-dependent G_1 growth arrest of prostate cancer cells. At nontoxic doses, 17-AAG caused a dose-dependent decline in AR, HER2, and Akt expression in prostate cancer xenografts. This decline was rapid, with a 97% loss of HER2 and an 80% loss of AR expression at 4 h. 17-AAG treatment at doses sufficient to induce AR, HER2, and Akt degradation resulted in the dose-dependent inhibition of androgen-dependent and -independent prostate cancer xenograft growth without toxicity.

Conclusions: These data demonstrate that, at a tolerable dose, inhibition of Hsp90 function by 17-AAG results in a marked reduction in HER2, AR, and Akt expression and inhibition of prostate tumor growth in mice. These results suggest that this drug may represent a new strategy for the treatment of prostate cancer.

Introduction

Prostate cancer can be eradicated when localized, but systemic disease remains incurable. Androgen ablation is the standard treatment for advanced disease, but despite dramatic clinical responses, virtually all of the patients relapse (1). The mechanisms responsible for disease progression after castration or treatment with antiandrogens are complex and not fully understood. The AR[5] is expressed at normal or amplified levels in most patients with androgen-independent disease, and several gain of function mutations have been characterized (2–4). These include mutations within the ligand-binding domain that alter ligand-binding specificity and have been associated with clinical progression after antiandrogen therapy (4).

In a majority of cases, changes in the AR gene have not been identified suggesting that other mechanisms must be involved. Recent studies show that activation of receptor tyrosine kinase signaling pathways leads to phosphorylation of steroid receptors and their activation in a ligand-independent manner (5–8). In one experimental system, selection for prostate tumor cells that grow at low levels of androgen was associated with overexpression of the HER2 receptor tyrosine kinase (9). Thus, prostate cancer tumor growth after castration or treatment with hormone receptor antagonists may be mediated by AR mutation or its ligand-independent activation by upstream tyrosine kinase pathways.

Ansamycin antibiotics, exemplified by GM, are natural products that bind to a conserved pocket in the Hsp90 family of chaperone proteins (10–12). Hsp90 is not required for general cotranslational protein folding but does play a role in the refolding of proteins in cells exposed to stress (13, 14). It is also required for the conformational maturation of Raf and steroid receptors (15, 16). High concentrations of ansamycins prevent

Received 11/26/01; revised 2/14/02; accepted 2/20/02.
The costs of publication of this article were defrayed in part by the payment of page charges. This article must therefore be hereby marked *advertisement* in accordance with 18 U.S.C. Section 1734 solely to indicate this fact.
[1] Supported in part by P50CA68425-02, CaPCURE, the PepsiCo Foundation, and the generous support of the Belfer Foundation. D.B.S. is supported in part by grant number CA09512 from the National Cancer Institute.
[2] Present address: Hoffmann-La Roche, Inc., Nutley, NJ 07110.
[3] Present address: Cedars-Sinai Medical Center, Los Angeles, CA 90048.
[4] To whom requests for reprints should be addressed, at Memorial Sloan-Kettering Cancer Center, Box 271, 1275 York Avenue, New York, NY 10021. Phone: (212) 639-2369; Fax: (212) 717-3627; E-mail: rosenn@mskcc.org.

[5] The abbreviations used are: AR, androgen receptor; GM, geldanamycin; 17-AAG, 17-allylamino-17-demethoxygeldanamycin; RB, retinoblastoma; PI3k, phosphatidylinositol 3-kinase; MAPK, mitogen-activated protein kinase; EPL, egg-phospholipid; PSA, prostate specific antigen.

Exhibit F

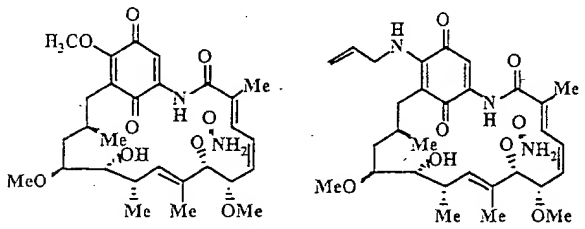

Geldanamycin (GM) 17-AAG

Fig. 1 Structures of GM and 17-AAG.

the binding of Hsp90 to its target proteins, which then cannot achieve their mature conformation (17). In addition, binding of ansamycins to the Hsp90-unfolded protein complex stabilizes the complex by preventing the ATP-dependent release of the chaperones (18, 19). The unfolded proteins in the complex are then ubiquinated and targeted for degradation in the proteasome (20, 21).

Occupancy of the Hsp90 pocket by GM causes the degradation of several signaling proteins important in mediating prostate cancer growth. These include AR and members of the HER family of receptor tyrosine kinases (15, 18, 20–22). Here we show that treatment of prostate cancer cell lines with the GM derivative 17-AAG (Fig. 1) results in the degradation of HER2, and both wild-type and mutant AR, growth arrest, and an RB-dependent G_1 block. Furthermore, at nontoxic doses, 17-AAG induces the degradation of AR and HER family tyrosine kinases in prostate tumors, and inhibits their growth. These data suggest that 17-AAG is effective in inhibiting pathways required for the growth of advanced prostate cancer. Moreover, ansamycins can inhibit Hsp90 function in mice without toxicity and, thus, may represent a new strategy for the treatment of this disease.

Materials and Methods

Materials. 17-AAG (NSC 330507) was obtained from the Drug Synthesis and Chemistry Branch, Developmental Therapeutics Program, National Cancer Institute (Bethesda, MD). Drug was dissolved in DMSO to yield 10 μM and 50 mg/ml stock solutions, and stored at −20°C. The following antibodies were used: Akt (Cell Signaling, Beverly, MA; 1:500), AR (PharMingen, San Diego, CA; 1:250 for immunoblot and 1:100 for immunofluorescence), HER2 (Santa Cruz Biotechnology, Santa Cruz, CA; C-18, 1:1000), HER3 (Santa Cruz Biotechnology; C-17, 1:1000), Hsp70 (StressGene, Victoria, British Columbia, Canada; 1:1000), Hsp90 (StressGene; 1:1000), MAPK (Cell Signaling; 1:1000), p85 subunit of PI3k (Upstate Biotechnology, Lake Placid, NY; 1:2000), and RB (PharMingen; 1:1000).

Cell Culture. The human prostate cancer cell lines LNCaP, DU-145, and PC-3 were obtained from the American Type Culture Collection (Rockville, MD) and maintained in RPMI 1640 supplemented with 5–10% heat-inactivated fetal bovine serum, 2 mM glutamine, and 50 units/ml of penicillin and streptomycin in a humidified 5% CO_2/air atmosphere at 37°C. LAPC-4 was generously provided by Charles Sawyers (UCLA, Los Angeles, CA) and maintained in Iscove's modified Dulbecco's medium supplemented with 10% fetal bovine serum and 10 nM R1881.

For the Alamar Blue proliferation assay, 2–4 × 10^3 cells were plated in 96-well plates. Later (48 h), cells were treated with 17-AAG for 96 h or 0.01% DMSO as control. On day 4, Alamar Blue viability assay (AccuMed, Westlake, OH) was performed as described elsewhere (23). IC_{50} and IC_{90}s were calculated as the doses of 17-AAG required to inhibit cell growth by 50 and 90%, respectively. Cell cycle distribution was assayed as described previously by Nusse *et al.* (24) with a Becton Dickinson fluorescence-activated cell sorter and analyzed by the Cell Cycle Multicycle system (Phoenix Flow System, San Diego, CA).

Immunoblotting. For immunoblotting, cells in culture were harvested in medium, washed twice in PBS, and then dissolved in SDS lysis buffer [50 mM Tris-HCl (pH 7.4) and 2% SDS], boiled for 10 min, and sonicated briefly. Cell lysates were cleared by centrifugation at 14,000 × *g* for 10 min, and supernatants were collected as the experimental samples. Lysates were added to sample buffer [0.3125 M Tris-HCl (pH 6.8), 10% SDS, 50% glycerol, and 77.5 mg/ml DTT], and equal amounts of protein were resolved by SDS-PAGE and transferred to nitrocellulose membranes. Blots were blocked in 5% nonfat milk in Tris-buffered saline [0.1% Tween 20, 10 mM Tris (pH 7.4), and 150 mM NaCl] and subsequently probed with the antibody of interest. After incubation with horseradish peroxidase-conjugated secondary antibodies, proteins were visualized by chemiluminescence (Amersham Corp., Piscataway, NJ). To prepare lysate from xenograft tumors, tumor tissue was homogenized in 2% SDS lysis buffer for 30 s then processed as above.

Immunofluorescence. For immunofluorescence, 5 × 10^3 cells were plated onto fibronectin-coated chamber slides (Fisher Scientific). Cells were then incubated with 17-AAG, 500 nM, or 0.01% DMSO (control). At the indicated time points, slides were washed twice with ice-cold PBS, and fixed with methanol and acetone solution (1:1) for 5 min. Fixed monolayers were rehydrated with water and then blocked with 3% BSA in PBS solution. After nonspecific blocking, cells were incubated with anti-AR monoclonal antibody in 1% BSA in PBS at room temperature then washed three times with PBS. Monolayers were then incubated with an Alexa-488 conjugated secondary antibody for 1 h at room temperature. Nuclei were stained with 0.5 μg/ml bis-benzimide (Hoechst 33342).

Animal Studies. Four- to six-week old *nu/nu* athymic male and female mice were obtained from the National Cancer Institute-Frederick Cancer Center (Frederick, MD) and maintained in ventilated caging. Experiments were carried out under an Institutional Animal Care and Use Committee-approved protocol, and institutional guidelines for the proper and humane use of animals in research were followed. Before administration, 17-AAG was dissolved in an EPL vehicle developed for this purpose by the National Cancer Institute. To aid in the identification of an optimal dose and schedule, nontumor bearing mice were treated by i.p. injection with 25–200 mg/kg of 17-AAG 5 days/week for 3 weeks or by the EPL vehicle alone. Serum samples were taken from each group, and equal volumes were pooled on days 5, 10, and 15 of treatment for serum

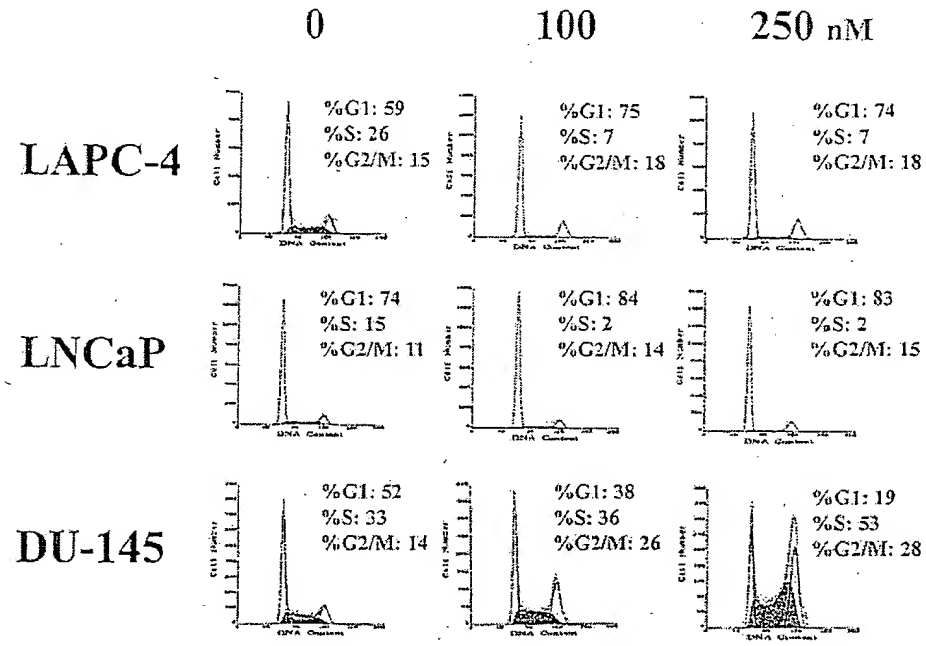

Fig. 2 17-AAG treatment of prostate cancer cell lines causes an RB-dependent cell cycle arrest. LAPC-4 (wild-type RB), LNCaP (wild-type RB), and DU-145 (mutant RB) cell lines were treated with 0 (0.01% DMSO), 100, or 250 nM 17-AAG for 48 h. Cell cycle distribution was assessed by fluorescence-activated cell sorter analysis. LAPC-4 and LNCaP cells arrested in G_1. By immunofluorescent staining, DU-145 cells arrested in mitosis (DNS).

chemistry and liver function analysis. At sacrifice, plasma samples were collected for complete blood count. A gross necropsy was performed on all of the mice, and a complete necropsy, including histopathology, was performed on 1 animal/group.

Male animals were inoculated s.c. with minced tumor tissue from donor mice bearing the androgen-dependent CWR22 xenograft line. Females were inoculated in the same way with the androgen-independent xenografts CWR22R and CWRSA6. These variants were derived from tumors that regrew after castration-induced regression of CWR22 tumors (25). Tumor cells were injected together with reconstituted basement membrane (Matrigel; Collaborative Research, Bedford, MA). To maintain stable serum testosterone levels, 12.5-mg 90-day sustained release testosterone pellets (Innovative Research of America, Sarasota, FL) were placed s.c. before inoculation with androgen-dependent tumor. Tumor dimensions were measured twice a week with vernier calipers, and tumor volumes were calculated with the formula: $\pi/6 \times$ larger diameter $\times$ (smaller diameter)^2. Mice with established tumors 4–5 mm in diameter were selected for study (n = 5–8 per treatment group). All of the mice received Augmentin (Amoxicillin/Clavulanate potassium; SmithKline Beecham) in their drinking water while on therapy. Mice were sacrificed by CO_2 euthanasia.

Both continuous and intermittent dosing schedules were studied. The "continuous" dosing schedule involved exposure to drug 5 days/week for 3 consecutive weeks. In the "intermittent" schedule, mice were treated with one 5-day cycle and then monitored for tumor progression. At progression, mice were treated with a second 5-day cycle of drug. In experiments with the androgen-dependent CWR22 tumor, serum PSA levels were measured with the PSA Assay kit (American Qualex Antibodies, San Clemente, CA).

In experiments designed to define the pharmacodynamic effects of 17-AAG on AR and HER-kinase expression, mice with established tumors were treated with 17-AAG at the doses specified or with EPL alone. At the time of sacrifice, serum was collected, and tumors were flash frozen or fixed in 10% buffered formalin. Immunohistochemistry for AR (clone F39.4.1; 2 μg/ml; BioGenex, San Ramon, CA) and HER2 (HercepTest; DAKO Corp., Carpinteria, CA) were performed as described previously (25, 26). Serum concentrations of 17-AAG and 17-amino-17-demethoxygeldanamycin were determined by high-performance liquid chromatography based on the method of Egorin *et al.* (27).

Statistical Analysis. A permutation test was used to compare the average tumor volume over time between groups, using 5000 resamples. The null hypothesis of this test is that there is no difference in the change in tumor volumes over time between treatment groups. The statistic used to test this hypothesis was the sum of the squared differences between mean tumor volume summed over all time points, which in effect, compares the trajectories of the average tumor volume between treatment groups. It is defined as follows:

$$SS\_DEV = \sum_{i=1}^{k} (\bar{x}_i - \bar{y}_i)^2 ,$$

where there are k time points and $\bar{x}_i$ and $\bar{y}_i$ are the average tumor volumes at time i in each treatment group. The Wilcoxon sum-rank test was used to compare treatment and control group serum PSA values.

Results

17-AAG Inhibited Prostate Cancer Cell Proliferation by Causing an RB-dependent G_1 Growth Arrest. 17-AAG is a less toxic derivative of GM now in clinical trial. We found that

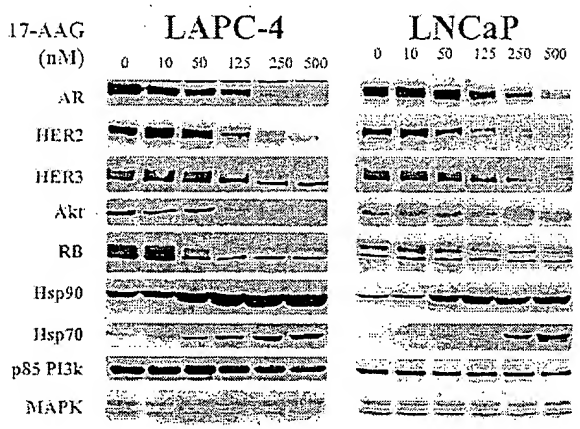

Fig. 3 Effect of 17-AAG on signaling proteins in LNCaP and LAPC-4 prostate cancer cells. Cells were treated for 24 h with 17-AAG at the indicated doses or DMSO (0.01%) as control. By immunoblot 17-AAG caused a dose-dependent decline in AR, HER2, HER3, and Akt expression and hypophosphorylation of RB. Levels of Hsp70 and Hsp90 were increased. No change in p85 PI3k or MAPK expression was noted.

17-AAG inhibited the anchorage-dependent growth of four representative prostate cancer cell lines. After 96 h of exposure, IC_{50}s ranged from 25–45 nM (LNCaP, 25 nM; LAPC-4, 40 nM; DU-145, 45 nM; and PC-3, 25 nM). At doses that caused complete growth arrest (75–125 nM for LNCaP and LAPC-4; and 150–200 nM for DU-145), prostate cell lines with intact RB (LNCaP, LAPC-4, and PC-3) arrested in G_1 after 17-AAG treatment, whereas DU-145, an androgen-independent cell line with mutated RB, arrested in mitosis (Fig. 2; data not shown). Growth arrest was accompanied by hypophosphorylation of RB (Fig. 3). These data are consistent with previous results in which we showed that the ansamycin Herbimycin A caused an RB-dependent G_1 block with RB-negative cells undergoing arrest in prometaphase (28, 29).

17-AAG Caused the Down-Regulation of HER2, HER3, and AR. Modulation of Hsp90 function by ansamycins causes the proteasomal degradation of a subset of cellular proteins. Most proteins and mRNAs are unchanged, as determined by evaluating multiple specific control proteins (PI3k and MAPK in Fig. 3 and DNS), the lack of change in the patterns of total cellular protein expression (DNS), and microarray analysis (30). HER2 is expressed at significant levels in both LAPC-4 and LNCaP, and is one of the most sensitive and rapidly degraded targets of 17-AAG (Fig. 3). HER3 and Akt levels also declined after 17-AAG treatment. 17-AAG increased the expression of the heat shock proteins Hsp90 and Hsp70.

Both wild-type AR (LAPC-4) and the Thr877Ala AR mutant found in LNCaP are sensitive to the drug as determined by immunoblot (Figs. 3 and 4). Exposure to 500 nM (24 h) of drug resulted in a 91% reduction in wild-type AR and a 92% reduction in the Thr877Ala AR mutant expressed by LNCaP cells. In LNCaP cells grown in serum-supplemented medium, most AR resides in the nucleus. Six and 12 h after 17-AAG treatment, nuclear AR staining was lost, and only faint cytoplasmic staining could be identified (Fig. 4). By 24 h, AR staining was again apparent with 52% of cells demonstrating detectable levels of nuclear AR by immunofluorescence. The intensity of nuclear AR staining within this population was heterogeneous with only 10% of cell demonstrating nuclear AR staining equivalent to control levels (Fig. 4).

Toxicology Studies. The degradation of mutant AR and HER2 by 17-AAG suggests that this agent may be useful in the treatment of advanced prostate cancers. We sought to determine whether inhibition of these pathways could be accomplished *in vivo* with nontoxic doses of 17-AAG. The GM-Hsp90 domain has been studied in various species (yeast, bacteria, *Drosophila*, mouse, and human) and is highly conserved across species (11). Specifically, human and murine Hsp 90α have >99% homology. Therefore, we evaluated the toxicity profile and pharmacology of 17-AAG in tumor and nontumor bearing *nu/nu* athymic mice. 17-AAG is metabolized by hepatic microsomes into at least five metabolites (27). The major metabolite, 17-AG, is active and is equally potent in degrading HER2 and AR in LNCaP and LAPC-4 cell lines.[6] We measured 17-AAG and 17-AG plasma concentrations after i.p. administration of one 50 mg/kg dose. 17-AAG was rapidly absorbed, and peak levels of >10 μM were achieved within 30 min. Serum levels of 17-AG >1 μM were also detectable by high-performance liquid chromatography. Both 17-AAG and 17-AG were then rapidly cleared with no detectable plasma levels 8 h after injection.

We found that the maximally tolerated dose of 17-AAG was schedule dependent and higher in control mice than in tumor-bearing mice. In nontumor bearing mice, treatment with three consecutive 5-day cycles of 75 mg/kg or more caused toxicity as evidenced by weight loss, elevated liver transaminase levels, anemia, and death (1 of 4 mice at the 75 mg/kg dose level, 3 of 4 mice at 125 mg/kg, and 4 of 4 mice at 200 mg/kg). Necropsy of mice after treatment with 17-AAG or the vehicle alone revealed peritonitis, possibly related to the i.p. route of administration, but no other gross or histological abnormalities. With less frequent dosing, up to 150 mg/kg/day of drug could be safely administered without evidence of toxicity (weight loss or death).

17-AAG Caused a Reduction in AR, HER2, and HER3 Expression in Prostate Cancer Xenograft Tumors. To determine whether nontoxic doses of 17-AAG could induce down-regulation of AR and HER kinases *in vivo*, we studied the effects of 17-AAG on the expression of these cellular proteins in the CWR22 xenograft model. In CWR22, the AR contains a mutation (histidine->tyrosine at residue 874) located within the ligand-binding pocket (31). Despite this mutation, androgens are still required for the growth of this tumor. Castration of CWR22 tumor-bearing mice causes tumor regression followed 80–200 days later by a resumption of tumor growth (25). Several of these variants have been serially passaged, and two (CWR22R and CWRSA6) were selected for additional use.

We treated mice bearing CWR22 or CWRSA6 (androgen-independent) tumors with 25 or 50 mg/kg 17-AAG or EPL diluent for 4 days. After the final dose (8 h), the mice were sacrificed and the tumors removed. Four days of 17-AAG treatment resulted in a dose-dependent reduction in the expression of AR, HER2, HER3, and Akt (Fig. 5*A*; CWR22 DNS). A dose of 50 mg/kg resulted in an 87% decline in AR, a 85% decline in HER2, a 50% decline in HER3, and a 60% decline in Akt

[6] F. Zheng, unpublished observations.

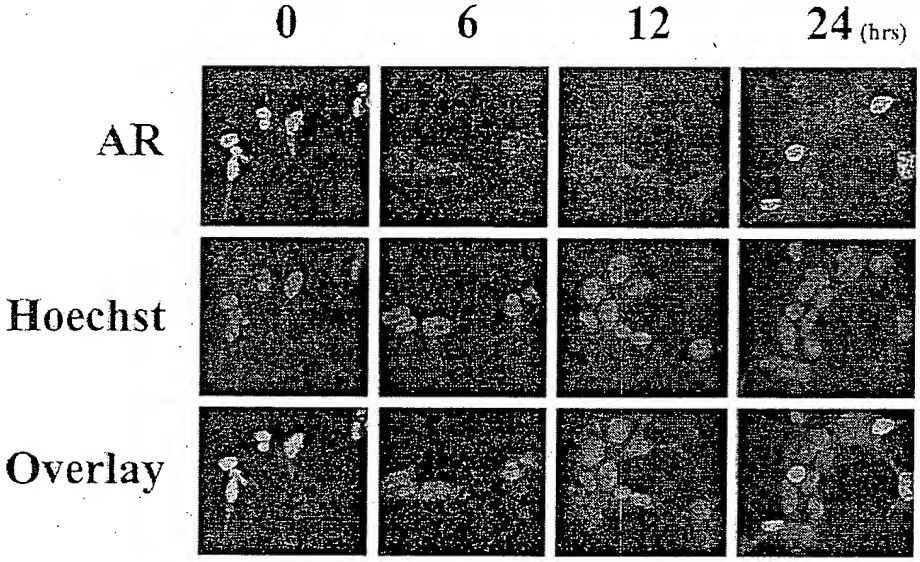

Fig. 4 Immunofluorescent staining of LNCaP cells for AR expression. Six and 12 h after treatment with 17-AAG (500 nM) LNCaP cells demonstrate a loss of nuclear AR expression. By 24 h a heterogeneous cell population is apparent with 52% of cells demonstrating at least partial recovery of AR staining.

expression in CWRSA6 tumors. Treatment was also associated with an 8-fold increase in Hsp70 and a 1.5-fold increase in Hsp90 levels. No change in the expression of PI3k was noted.

To characterize the kinetics of this effect, mice with well-established CWRSA6 tumors of comparable size were treated with a single dose of 17-AAG 50 mg/kg and sacrificed pretreatment and from 2 to 48 h afterward. A rapid, >50% decline in AR, HER2, and HER3 expression in the tumors was noted by 2 h (Fig. 5*B*). The maximal declines in AR and HER2 were noted at 4 h: a 97% reduction in HER2 and an 80% reduction in AR. By 24 h, AR expression returned to near baseline levels, whereas a rise in HER2 expression was not noted until 48 h after drug administration. The kinetics of HER2 recovery was similar in mice treated with 3 or 5 consecutive days of 17-AAG with its expression returning to near control levels 48 h after the final dose of therapy (DNS). With a single dose of therapy, the effect of 17-AAG on Akt expression was more delayed and less pronounced (maximum decline of 35% at 8 h) than that seen with AR, HER2, and HER3 (DNS).

In untreated CWRSA6 tumors, AR staining was compartmentalized in the nucleus (Fig. 5*C*). The frequency and intensity of this staining was diminished 4 and 8 h after 17-AAG administration. A steep decline in the mitotic index and a loss in membranous HER2 staining were also apparent at these time points. These data demonstrate that at nontoxic doses, 17-AAG induces the degradation of AR, HER2, HER3, and Akt in prostate tumors.

17-AAG Inhibited the Growth of Androgen-dependent and Androgen-independent Prostate Cancers. We studied the effects of two different dosing schedules of 17-AAG on the growth of CWR22, CWRSA6, and CWR22R tumors. The intermittent schedule consisted of a 5-day treatment cycle followed by a second cycle when definitive evidence of tumor regrowth occurred. The continuous schedule was comprised of three consecutive weekly 5-day cycles. Both regimens caused a dose-dependent delay in xenograft tumor growth in all three models (Table 1; Fig. 6). For example, with the continuous schedule, 50 mg/kg 17-AAG caused 80% growth inhibition of CWRSA6 tumor growth when assessed on the day the controls required sacrifice [Table 1; Fig. 6*A*, mean tumor volume (treatment group) *versus* mean tumor volume (control) on day 29; $P < 0.01$]. With the intermittent schedule, 17-AAG caused 87% growth inhibition of CWRSA6 tumor growth (Table 1; Fig. 6*B*; $P < 0.01$). Similar results were noted with the parental CWR22 model and with a second androgen-independent subline CWR22R. Furthermore, in mice bearing CWR22 tumors, 17-AAG treatment (50 mg/kg dose level) was associated in an ~60% reduction in serum PSA (Day 25 serum PSA; intermittent schedule: 61% reduction *versus* control, $P < 0.01$; continuous schedule: 62% reduction, $P < 0.01$). These data demonstrate that at tolerable doses, 17-AAG inhibits the growth of prostate cancer cells *in vivo*. Additionally, growth inhibition correlates with a reduction in HER2, HER3, Akt, and the mutated AR (His874Tyr) expressed in the tumor.

Discussion

In this report, we examined the effects of 17-AAG on prostate cancer growth using a panel of prostate cell lines and the CWR22 xenograft model. 17-AAG is a less-toxic derivative of the ansamycin GM and is now in clinical trial. We found that 17-AAG causes the selective degradation of a subset of proteins, many of them involved in mitogenic signaling. These included both wild-type (LAPC-4) and mutant (LNCaP, CWR22) ARs, and the HER2 and HER3 receptor tyrosine kinases. The expression of Akt, which is downstream of HER2 and which may modulate AR signaling in tumors with HER2 overexpression, is also down-regulated by the drug (8). Most cellular proteins including MAPK and PI3k were unaffected.

We have shown previously that exposure of cancer cells to the ansamycins GM and herbimycin A leads to a loss of cyclin D-associated kinase activity and an RB-dependent G_1 growth arrest (28). Cells lacking RB-function progress through G_1

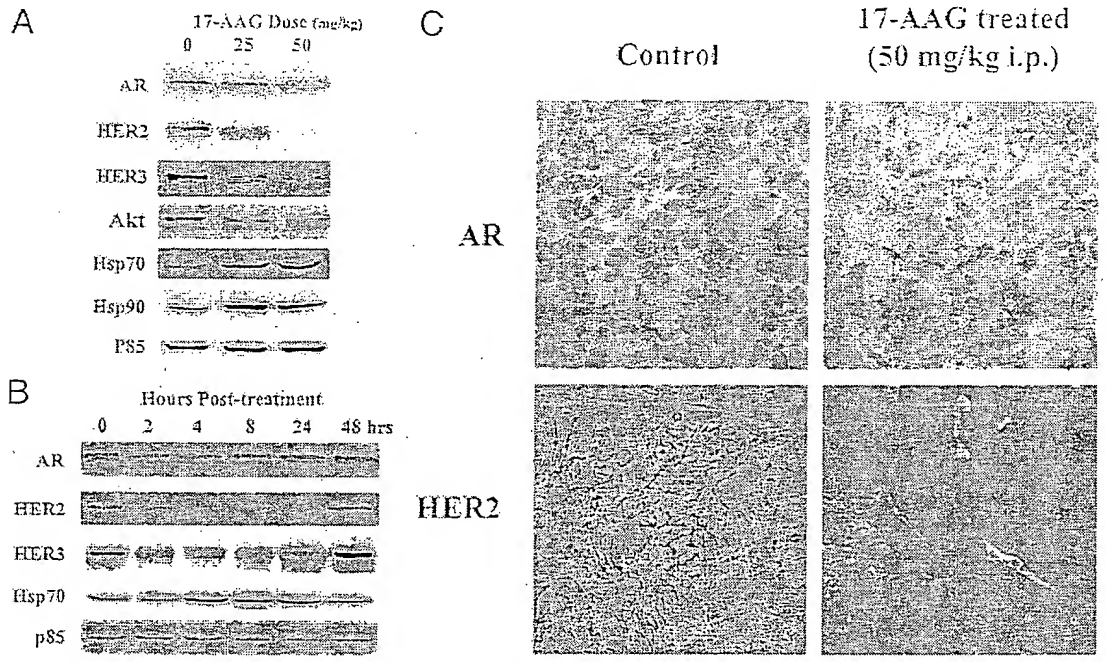

Fig. 5 *A*, changes in target protein expression of CWRSA6 xenograft tumors from mice treated with 17-AAG at doses of 25 mg/kg and 50 mg/kg daily for 4 days. Control mice received vehicle only. Mice were sacrificed 8 h after the final treatment on day 4. Immunoblot demonstrates a dose-dependent decline in AR, HER2, HER3, and Akt expression. Levels of Hsp70 and Hsp90 were increased. No change in the control protein p85 PI3k was noted. This experiment was repeated with a second set of animals with equivalent results. *B*, mice with established CWRSA6 xenograft tumors treated with one dose of 17-AAG 50 mg/kg. Pretreatment and at the time points specified, mice were sacrificed and tumors removed. By immunoblot, a rapid decline in HER2, HER3, and AR expression is evident within 2 h of treatment. No change in p85 PI3k expression occurred. This experiment was repeated with a second set of animals with equivalent results. *C*, immunohistochemistry of CWRSA6 xenograft tumors demonstrating a loss of nuclear AR staining, a loss in membranous HER2 staining, and a reduction in the mitotic index 4 h after treatment with one dose of 17-AAG 50 mg/kg. Similar findings were also noted 8 h after treatment.

Table 1 Effect of continuous and intermittent dosing schedules of 17:AAG on the growth of CWR22, CWR22R and CWRSA6 xenografts.

Tumor	Dose (mg/kg)	Dosing regimen	Percent (%) Inhibition (day)	*P*
CWR22	25	Continuous	42 (24)	<0.01
	50	Continuous	67 (24)	<0.01
	50	Intermittent	51 (25)	0.01
CWRSA6	25	Continuous	56 (29)	0.07
	50	Continuous	80 (29)	<0.01
	50	Intermittent	87 (30)	<0.01
CWR22R	25	Continuous	49 (21)	0.01
	50	Continuous	68 (21)	0.02
	50	Intermittent	67 (22)	<0.01

normally in the presence of drug and arrest in prometaphase before undergoing apoptosis. D-cyclins are not direct targets of ansamycins, but their expression is controlled at the post-transcriptional level by a PI3k/Akt kinase-dependent pathway (32). Consistent with these findings, LNCaP and LAPC-4 (wild-type RB) cells arrested in G_1, whereas DU-145, a cell line with mutant RB, arrested in mitosis.

We found that 17-AAG treatment reduced the expression of AR in prostate cancer xenografts and inhibited the growth of both androgen-dependent and -independent tumors. The maximum effect of 17-AAG on AR expression in the tumors was evident 4–8 h after treatment with receptor levels returning to baseline by 24 h. The degradation of wild-type and mutant AR by drug suggests that this class of agents may be particularly effective in the treatment of advanced androgen-independent prostate cancer. The mechanisms responsible for the emergence of androgen-independent disease are complex and not fully understood. In a subset of patients treated with AR antagonists, clinical progression is associated with AR gene amplification or mutation (4, 33). AR amplification may result in sufficient AR pathway activation to allow for tumor growth at low levels of testosterone. Mutations in AR may convert antagonists into agonists or lead to constitutive ligand-independent activation of the receptor. For example the missense mutation (Thr877Ala) found in LNCaP cells has been identified in patients treated previously with flutamide, and this AR exhibits altered ligand specificity (4). Hydroxyflutamide, adrenal androgens, and estrogens induce its activation and promote cell growth. In some patients, tumor regression may occur after flutamide withdrawal (4, 34). These data suggest that mutation or overexpression of AR may play a role in the progression to an androgen-independent state. Although the antiproliferative effects of ansamycins may be multifactorial and the result of inhibition of AR-independent pathways, the ability of ansamycins to degrade mutant as well as wild-type

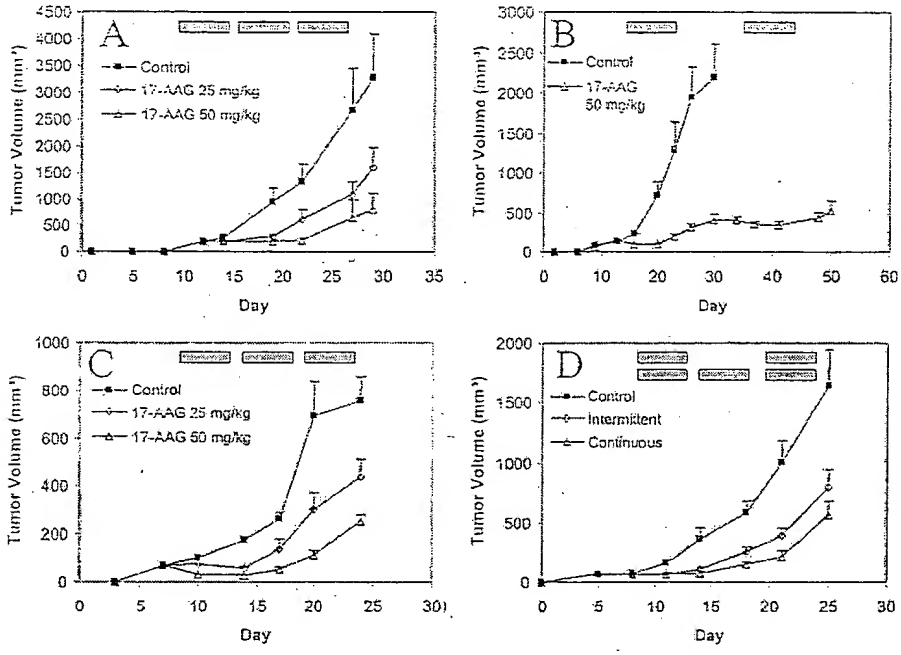

Fig. 6 *A* and *B*, response of CWRSA6 androgen-independent xenografts to 17-AAG. *C* and *D*, response of CWR22 androgen-dependent xenografts to 17-AAG. *Bars*, ± SE.

forms of AR suggest that they may be useful in the treatment of such patients.

In most patients whose tumors relapse after hormonal therapy, mutations or amplification of the AR gene have not been identified. Several recent studies suggest that modulation of AR activity by growth factor activated tyrosine kinase pathways allows for prostate cancer growth at low androgen levels. The epidermal growth factor, insulin-like growth factor-I, keratinocyte growth factor, and interleukin 6 all induce AR phosphorylation and the expression of PSA, a downstream target of AR (6, 35). Several lines of evidence suggest that HER2 may be important in this process. HER2 overexpression and gene amplification have been identified in a subset of patients with prostate cancer (36, 37). HER2 overexpression is more common in patients treated previously with hormonal therapy and those with androgen-independent metastatic disease (37). CWR22 and LNCaP both express high levels of HER2, and Herceptin (Trastuzumab), a humanized monoclonal antibody that binds to HER2, inhibits the growth of these xenografts (26). A mechanism for this effect has been proposed by Yeh *et al.* (7) who demonstrated that HER2 activates AR by inducing its phosphorylation by MAPK. As 17-AAG targets both the AR and HER2 for degradation and thus inactivation, tumors that depend on tyrosine kinase pathway-mediated phosphorylation of AR for growth and survival after androgen ablation may be particularly sensitive to this agent.

Akt, which is downstream of HER2, also phosphorylates AR and may modulate AR signaling in tumors with HER2 overexpression (8). We found that 17-AAG down-regulated the expression of Akt in a dose-dependent manner in the xenograft tumors, although this effect was delayed and of a lesser degree than the effect of 17-AAG on AR and HER2. Hsp90 has been reported recently to associate with Akt and regulate its activity (38). Therefore, Akt may be a direct target of 17-AAG. Alternatively, the reduction in Akt expression caused by 17-AAG could be secondary to down-regulation of other pathways by the drug.

In this report, we show that 17-AAG, an inhibitor of Hsp90 function, delays the growth of prostate tumors *in vivo* at nontoxic doses. The inhibition of growth correlated with reduced expression of AR and HER-family kinases in the tumor. The results suggest that ansamycins may represent a new strategy for the treatment of advanced prostate cancers that depend on AR mutations or activated tyrosine kinases for tumor progression. Human trials to evaluate the efficacy of 17-AAG in this setting are now in progress.

Acknowledgments

We thank Merna Timaul for technical assistance, and Drs. Thomas Pretlow and Charles Sawyers for generously providing the CWR22 and LAPC-4 cell lines.

References

1. Schröder, F. H: Endocrine treatment of prostate cancer–recent developments and the future. Part 1: maximal androgen blockade, early *vs.* delayed endocrine treatment and side-effects. BJU Int., *83:* 161–170, 1999.

2. van der Kwast, T. H., Schalken, J., Ruizeveld de Winter, J. A., van Vroonhoven, C. C., Mulder, E., Boersma, W., and Trapman, J. Androgen receptors in endocrine-therapy-resistant human prostate cancer. Int. J. Cancer, *48:* 189–193, 1991.

3. Visakorpi, T., Hyytinen, E., Koivisto, P., Tanner, M., Keinanen, R., Palmberg, C., Palotie, A., Tammela, T., Isola, J., and Kallioniemi, O. P. *In vivo* amplification of the androgen receptor gene and progression of human prostate cancer. Nat. Genet., *9:* 401–406, 1995.

4. Taplin, M. E., Bubley, G. J., Ko, Y. J., Small, E. J., Upton, M., Rajeshkumar, B., and Balk, S. P. Selection for androgen receptor mutations in prostate cancers treated with androgen antagonist. Cancer Res., *59:* 2511–2515, 1999.

5. Kato, S., Endoh, H., Masuhiro, Y., Kitamoto, T., Uchiyama, S., Sasaki, H., Masushige, S., Gotoh, Y., Nishida, E., Kawashima, H.,

Metzger, D., and Chambon, P. Activation of the estrogen receptor through phosphorylation by mitogen-activated protein kinase. Science (Wash. DC), *270:* 1491–1494, 1995.

6. Culig, Z., Hobisch, A., Cronauer, M. V., Radmayr, C., Trapman, J., Hittmair, A., Bartsch, G., and Klocker, H. Androgen receptor activation in prostate tumor cell lines by insulin-like growth factor-I, keratinocyte growth factor, and epidermal growth factor. Cancer Res., *54:* 5474–5478, 1994.

7. Yeh, S., Lin, H. K., Kang, H. Y., Thin, T. H., Lin, M. F., and Chang, C. From HER2/Neu signal cascade to androgen receptor and its coactivators: a novel pathway by induction of androgen target genes through MAP kinase in prostate cancer cells. Proc. Natl. Acad. Sci. USA, *96:* 5458–5463, 1999.

8. Wen, Y., Hu, M. C., Makino, K., Spohn, B., Bartholomeusz, G., Yan, D. H., and Hung, M. C. HER-2/neu promotes androgen-independent survival and growth of prostate cancer cells through the Akt pathway. Cancer Res., *60:* 6841–6845, 2000.

9. Craft, N., Shostak, Y., Carey, M., and Sawyers, C. L. A mechanism for hormone-independent prostate cancer through modulation of androgen receptor signaling by the HER-2/neu tyrosine kinase. Nat. Med., *5:* 280–285, 1999.

10. Grenert, J. P., Sullivan, W. P., Fadden, P., Haystead, T. A., Clark, J., Mimnaugh, E., Krutzsch, H., Ochel, H. J., Schulte, T. W., Sausville, E., Neckers, L. M., and Toft, D. O. The amino-terminal domain of heat shock protein 90 (hsp90) that binds geldanamycin is an ATP/ADP switch domain that regulates hsp90 conformation. J. Biol. Chem., *272:* 23843–23850, 1997.

11. Stebbins, C. E., Russo, A. A., Schneider, C., Rosen, N., Hartl, F. U., and Pavletich, N. P. Crystal structure of an Hsp90-geldanamycin complex: targeting of a protein chaperone by an antitumor agent. Cell, *89:* 239–250, 1997.

12. Prodromou, C., Roe, S. M., O'Brien, R., Ladbury, J. E., Piper, P. W., and Pearl, L. H. Identification and structural characterization of the ATP/ADP-binding site in the Hsp90 molecular chaperone. Cell, *90:* 65–75, 1997.

13. Nathan, D. F., Vos, M. H., and Lindquist, S. *In vivo* functions of the *Saccharomyces cerevisiae* Hsp90 chaperone. Proc. Natl. Acad. Sci. USA, *94:* 12949–12956, 1997.

14. Caplan, A. J. Hsp90's secrets unfold: new insights from structural and functional studies. Trends Cell Biol., *9:* 262–268, 1999.

15. Schulte, T. W., Blagosklonny, M. V., Romanova, L., Mushinski, J. F., Monia, B. P., Johnston, J. F., Nguyen, P., Trepel, J., and Neckers, L. M. Destabilization of Raf-1 by geldanamycin leads to disruption of the Raf- 1-MEK-mitogen-activated protein kinase signaling pathway. Mol. Cell Biol., *16:* 5839–5845, 1996.

16. Fang, Y., Fliss, A. E., Robins, D. M., and Caplan, A. J. Hsp90 regulates androgen receptor hormone binding affinity *in vivo*. J. Biol. Chem., *271:* 28697–28702, 1996.

17. Schulte, T. W., Blagosklonny, M. V., Ingui, C., and Neckers, L. Disruption of the Raf-1-Hsp90 molecular complex results in destabilization of Raf-1 and loss of Raf-1-Ras association. J. Biol. Chem., *270:* 24585–24588, 1995.

18. Schneider, C., Sepp-Lorenzino, L., Nimmesgern, E., Ouerfelli, O., Danishefsky, S., Rosen, N., and Hartl, F. U. Pharmacologic shifting of a balance between protein refolding and degradation mediated by Hsp90. Proc. Natl. Acad. Sci. USA, *93:* 14536–14541, 1996.

19. Young, J. C., and Hartl, F. U. Polypeptide release by hsp90 involves ATP hydrolysis and is enhanced by the co-chaperone p23. EMBO J., *19:* 5930–5940, 2000.

20. Mimnaugh, E. G., Chavany, C., and Neckers, L. Polyubiquitination and proteasomal degradation of the p185c-erbB-2 receptor protein-tyrosine kinase induced by geldanamycin. J. Biol. Chem., *271:* 22796–22801, 1996.

21. Whitesell, L., and Cook, P. Stable and specific binding of heat shock protein 90 by geldanamycin disrupts glucocorticoid receptor function in intact cells. Mol. Endocrinol., *10:* 705–712, 1996.

22. Schulte, T. W., and Neckers, L. M. The benzoquinone ansamycin 17-allylamino-17-demethoxygeldanamycin binds to HSP90 and shares important biologic activities with geldanamycin. Cancer Chemother. Pharmacol., *42:* 273–279, 1998.

23. White, M. J., DiCaprio, M. J., and Greenberg, D. A. Assessment of neuronal viability with Alamar blue and granule cell cultures. J. Neurosci. Methods, *70:* 195–200, 1996.

24. Nusse, M., Beisker, W., Hoffmann, C., and Tarnok, A. Flow cytometric analysis of G1- and G2/M-phase subpopulations in mammalian cell nuclei using side scatter and DNA content measurements. Cytometry, *11:* 813–821, 1990.

25. Agus, D. B., Cordon-Cardo, C., Fox, W., Drobnjak, M., Koff, A., Golde, D. W., and Scher, H. I. Prostate cancer cell cycle regulators: response to androgen withdrawal and development of androgen independence. J. Natl. Cancer Inst., *91:* 1869–1876, 1999.

26. Agus, D. B., Scher, H. I., Higgins, B., Fox, W. D., Heller, G., Fazzari, M., Cordon-Cardo, C., and Golde, D. W. Response of prostate cancer to anti-Her-2/neu antibody in androgen-dependent and -independent human xenograft models. Cancer Res., *59:* 4761–4764, 1999.

27. Egorin, M. J., Rosen, D. M., Wolff, J. H., Callery, P. S., Musser, S. M., and Eiseman, J. L. Metabolism of 17-(allylamino)-17-demethoxygeldanamycin (NSC 330507) by murine and human hepatic preparations. Cancer Res., *58:* 2385–2396, 1998.

28. Srethapakdi, M., Liu, F., Tavorath, R., and Rosen, N. Inhibition of Hsp90 function by ansamycins causes retinoblastoma gene product-dependent G1 arrest. Cancer Res., *60:* 3940–3946, 2000.

29. Munster, P. N., Srethapakdi, M., Moasser, M. M., and Rosen, N. Inhibition of heat shock protein 90 function by ansamycins causes the morphological and functional differentiation of breast cancer cells. Cancer Res., *61:* 2945–2952, 2001.

30. Clarke, P. A., Hostein, I., Banerji, U., Stefano, F. D., Maloney, A., Walton, M., Judson, I., and Workman, P. Gene expression profiling of human colon cancer cells following inhibition of signal transduction by 17-allylamino-17-demethoxygeldanamycin, an inhibitor of the hsp90 molecular chaperone. Oncogene, *19:* 4125–4133, 2000.

31. McDonald, S., Brive, L., Agus, D. B., Scher, H. I., and Ely, K. R. Ligand responsiveness in human prostate cancer: structural analysis of mutant androgen receptors from LNCaP and CWR22 tumors. Cancer Res., *60:* 2317–2322, 2000.

32. Muise-Helmericks, R. C., Grimes, H. L., Bellacosa, A., Malstrom, S. E., Tsichlis, P. N., and Rosen, N. Cyclin D expression is controlled post-transcriptionally via a phosphatidylinositol 3-kinase/Akt-dependent pathway. J. Biol. Chem., *273:* 29864–29872, 1998.

33. Wallen, M. J., Linja, M., Kaartinen, K., Schleutker, J., and Visakorpi, T. Androgen receptor gene mutations in hormone-refractory prostate cancer. J. Pathol., *189:* 559–563, 1999.

34. Scher, H. I., and Kelly, W. K. Flutamide withdrawal syndrome: its impact on clinical trials in hormone-refractory prostate cancer. J. Clin. Oncol., *11:* 1566–1572, 1993.

35. Hobisch, A., Eder, I. E., Putz, T., Horninger, W., Bartsch, G., Klocker, H., and Culig, Z. Interleukin-6 regulates prostate-specific protein expression in prostate carcinoma cells by activation of the androgen receptor. Cancer Res., *58:* 4640–4645, 1998.

36. Ross, J. S., Sheehan, C., Hayner-Buchan, A. M., Ambros, R. A., Kallakury, B. V., Kaufman, R., Fisher, H. A., and Muraca, P. J. HER-2/neu gene amplification status in prostate cancer by fluorescence *in situ* hybridization. Hum. Pathol., *28:* 827–833, 1997.

37. Signoretti, S., Montironi, R., Manola, J., Altimari, A., Tam, C., Bubley, G., Balk, S., Thomas, G., Kaplan, I., Hlatky, L., Hahnfeldt, P., Kantoff, P., and Loda, M. Her-2-neu expression and progression toward androgen independence in human prostate cancer. J. Natl. Cancer Inst., *92:* 1918–1925, 2000.

38. Sato, S., Fujita, N., and Tsuruo, T. Modulation of Akt kinase activity by binding to Hsp90. Proc. Natl. Acad. Sci. USA, *97:* 10832–10837, 2000.

Enhancement of Paclitaxel-Mediated Cytotoxicity in Lung Cancer Cells by 17-Allylamino Geldanamycin: In Vitro and In Vivo Analysis

Dao M. Nguyen, MD, Dominique Lorang, PhD, G. Aaron Chen, MS, John H. Stewart IV, MD, Esmail Tabibi, PhD, and David S. Schrump, MD

Sections of Thoracic Oncology and Surgical Metabolism, Surgery Branch, Division of Clinical Sciences, and Developmental Therapeutics Program, Pharmaceutical Resources Branch, Division of Cancer Therapeutics and Diagnostics, National Cancer Institute, National Institutes of Health, Bethesda, Maryland

Background. It has previously been demonstrated that 17-allylamino geldanamycin (17-AAG) enhances paclitaxel-mediated cytotoxicity and downregulates vascular endothelial factor expression in non-small cell lung cancer. This project was designed to evaluate the tumoricidal and antiangiogeneic effects of 17-AAG and paclitaxel in H358 non-small cell lung cancer cells grown as xenografts in nude mice.

Methods. In vitro cytotoxic drug combination effects were evaluated by (4, 5-dimethylthiazo-2-yl)-2, 5-diphenyl tetrazolium bromide-based proliferation assays. The combinations of 17-AAG and paclitaxel were administered intraperitoneally in nude mice bearing H358 tumor xenografts. Tumor volumes were measured weekly. Tumor expression of erbB2, vascular endothelial cell growth factor, von Willebrand factor (tumor microvasculature), and activated caspase 3 (apoptosis) were determined by immunohistochemistry.

Results. Five- to 22-fold enhancement of paclitaxel cytotoxicity was achieved by paclitaxel + 17-AAG combination that was paralleled with marked induction of apoptosis. This combination treatment profoundly suppressed tumor growth and significantly prolonged survival of mice bearing H358 xenografts. Immunohistochemical staining of tumor tissues indicated profound reduction of vascular endothelial cell growth factor expression associated with reduction of microvasculature in tumors treated with 17-AAG. Apoptotic cells were more abundant in tumors treated with 17-AAG + paclitaxel than in those treated with 17-AAG or paclitaxel alone.

Conclusions. Concurrent exposure of H358 cells to 17-AAG and paclitaxel resulted in supraadditive growth inhibition effects in vitro and in vivo. Analysis of molecular markers of tumor tissues indicated that therapeutic drug levels could be achieved with this chemotherapy regimen leading to significant biological responses. Moreover, 17-AAG-mediated suppression of vascular endothelial cell growth factor production by tumor cells may contribute to the antitumor effects of this drug combination in vivo.

(Ann Thorac Surg 2001;72:371–9)

Non-small cell lung cancers (NSCLC) frequently exhibit resistance to chemotherapy and ionizing radiation. Although dose-intensive regimens may increase response rates, they are frequently associated with severe systemic side effects. Treatment strategies designed to sensitize tumor cells to chemotherapeutic agents or radiation therapy may allow dose reduction, thereby diminishing systemic toxicity of cancer treatments.

The molecular basis of chemoresistance in cancer is complex and appears to involve both genetic and epigenetic factors, including overexpression of erbB1 and erbB2, encoding the epidermal growth factor receptor (EGFr) and the orphan receptor HER2/neu respectively. Inhibition of the function or the expression of the EGFr or HER2/neu sensitizes tumor cells, including those of NSCLC histology, to standard cytotoxic agents such as cisplatin or paclitaxel [1–3]. Previously we demonstrated that sensitivity to paclitaxel could be enhanced in NSCLC cells overexpressing erbB2 after treatment with 17-allylamino geldanamycin (17-AAG) [4]. This agent has been selected for clinical development at the National Cancer Institute because of its activity against cell lines derived from a variety of human malignancies [5, 6]; antitumor effects of this compound relate in part to its ability to inhibit the expression of various oncoproteins including EGFr and HER2/neu at nanomolar to micromolar concentrations [6, 7].

Overexpression of EGFr or HER2/neu oncoproteins in lung, esophageal, breast, and ovarian cancers correlates with locally advanced disease, distant metastases, and diminished survival in patients with these malignancies [8–10]. In vitro experimental data indicate that tumor cells overexpressing these oncoproteins exhibit one or more phenotypes associated with local invasion or dis-

Presented at the Thirty-seventh Annual Meeting of The Society of Thoracic Surgeons, New Orleans, LA, Jan 29–31, 2001.

Address reprint requests to Dr Nguyen, Section of Thoracic Oncology, Surgery Branch, NCI, NIH, Room 2B07, 10 Center Dr, Bethesda, MD 20892; e-mail: Dao_Nguyen@nih.gov.

Published by Elsevier Science Inc

0003-4975/01/$20.00
PII S0003-4975(01)02787-4

Exhibit G

tant metastasis in vivo, including downregulation of E-cadherin expression, increased expression of matrix metalloproteinases, and vascular endothelial growth factor (VEGF), as well as accelerated invasion through artificial extracellular matrix [11–13]. Conceivably, inhibition of erbB-mediated signal transduction by monoclonal antibodies, which antagonize receptor ligand binding, or compounds such as 17-AAG, which deplete erbB1/erbB2 expression, may effectively reduce the metastatic potential of cancer cells. Exploiting the latter approach, we have recently demonstrated that treatment of NSCLC cells with 17-AAG at nanomolar concentrations for 48 hours results in profound suppression of VEGF and matrix metalloproteinase-9 secretion, as well as inhibition of cell motility through the artificial extracellular matrix membrane Matrigel (Sigma, St. Louis, MO) [14]. The relevance of these findings, particularly the antiangiogenic effects of 17-AAG-mediated suppression of VEGF production, have not been defined.

In the present study, we sought to examine the in vivo effects of paclitaxel and 17-AAG using nude mice bearing H358 NSCLC xenografts. Herein, we demonstrate that 17-AAG + paclitaxel treatment mediates profound retardation of tumor growth, and significant prolongation of survival in tumor-bearing animals. The in vitro effects of 17-AAG on H358 cells were closely reproduced in vivo: diminished erbB2 and VEGF expression in xenografts correlated with reduced tumor capillary density in animals receiving treatments containing 17-AAG. Apoptosis was most pronounced in xenografts from animals treated with 17-AAG + paclitaxel. Collectively these data support further evaluation of 17-AAG in combination with paclitaxel in lung cancer patients.

Material and Methods

Cells and Reagents

The NSCLC cell line H358 was purchased from American Tissue Culture Collection (Manassas, VA). Cells were maintained in RPMI media supplemented with glutamine (1 mmol/L), streptomycin (100 μg/mL)/penicillin (100 U/mL), and 10% of fetal calf serum. Normal human bronchial epithelial cells were purchased from Clonetics Corp (Walkersville, MD) and maintained in bronchial epithelial cell basal media (Clonetics Corp). The 17-AAG, obtained from the Drug Synthesis & Chemistry Branch, Developmental Therapeutic Program, Division of Cancer Treatment, National Cancer Institute, Bethesda, MD, was dissolved in dimethylsulfoxide (DMSO) to yield a 100 μmol/L stock solution and stored at −70°C. The selective erbB2 tyrosine kinase inhibitor AG825 was obtained from Calbiochem/Oncogene Research Products (Cambridge, MA), dissolved in DMSO, and stored as 10 mmol/L stock solution. All experiments involving these two compounds were performed under subdued light conditions. Paclitaxel (Taxol, USP) was purchased from Bristol-Myers Squibb (Princeton, NJ). 4,5-Dimethylthiazo-2-yl-2,5-diphenyl tetrazolium bromide was purchased from Sigma (St. Louis, MO). Recombinant human epidermal growth factor (EGF) (R&D, Minneapolis, MN) and the anti-erbB1 and anti-erbB2 monoclonal antibodies (Calbiochem/Oncogene Research Products, Cambridge, MA) were constituted in phosphate-buffered saline and stored at 4°C as recommended by the manufacturers. Human VEGF enzyme-linked immunosorbent assay kit was obtained from R&D. A formulation of egg phospholipid emulsion in dextrose solution was used to dissolve 17-AAG for parenteral administration.

Immunofluorescent Staining and Flow Cytometric Analysis of erbB1 and erbB2 Expression

Surface expression of erbB1 and erbB2 on H358 or normal human bronchial epithelial cells was quantitated by flow cytometry using a Beckton-Dickinson fluorescence-activated cell sorter as described previously [14].

Quantitation of Vascular Endothelial Cell Growth Factor Production by H358 Cells

Cells were grown to 80% confluency in 12-well tissue culture plates, washed once with phosphate-buffered saline and media replenished with 1 mL of RPMI with 1% fetal calf serum with or without 20 ng/mL of EGF. In 17-AAG- or AG825-treated groups, appropriate aliquots of 17-AAG or AG825 stocks were added into the culture media to yield desired drug concentrations 2 hours before stimulating tumor cells with EGF. After 24 hours of incubation, conditioned media were harvested and frozen at −70°C. Cells from each well were collected and cellular protein was assayed by BCA technique (Pierce, Rockford, IL). The VEGF levels in the conditioned media were measured by enzyme-linked immunosorbent assay using a commercially available kit and expressed as picograms per milliliter per 24 hours per milligram of cellular protein.

In Vitro Evaluation of Drug Cytotoxicity

Cells were seeded in flat-bottom 96-well microtiter plates (4,000 cells/well). After an overnight incubation, cells were treated with either paclitaxel alone or 17-AAG + paclitaxel combination. Cells were exposed to various concentrations (ranging from 4 to 1,000 nmol/L) of paclitaxel for 90 minutes followed by 96 hours of further incubation in normal media or media containing 17-AAG (20 or 40 nmol/L). At the end of the incubation period, viable cells were quantitated by (4, 5-dimethylthiazo-2-yl)-2, 5-diphenyl tetrazolium bromide colorimetric assays as described by the manufacturer. Paclitaxel dose–response curves were plotted as a fraction of viable paclitaxel-treated cells relative to cells grown in normal media. The H358 cells treated with the 17-AAG + paclitaxel combination were plotted as fraction of viable cells relative to cells exposed to 17-AAG alone (to correct for the minor growth inhibitory effect of 17-AAG). Paclitaxel inhibitory concentration at 50% (IC_{50}) values for cells treated with paclitaxel alone or paclitaxel in combination with 17-AAG were derived from respective dose–response curves. A reduction of paclitaxel IC_{50} values in cells treated with the drug combination indicated increased cellular responsiveness to paclitaxel cytotoxic

effects mediated by 17-AAG. To further confirm the synergistic cytotoxic drug interaction effect of paclitaxel and 17-AAG, the combination index at 50% growth inhibition level (CI_{50}) was calculated [15]. The CI_{50} values less than 1, equal to 1, or more than 1 indicate synergistic, additive, or antagonistic cytotoxic drug interactions, respectively.

Apoptosis and Caspase 3 Activity

The H358 cells treated with paclitaxel alone (50 or 200 nmol/L) or paclitaxel with 17-AAG (20 nmol/L) were harvested at 48 and 60 hours after drug treatment for measurement of caspase 3 activity and apoptosis, respectively. Caspase 3 activity in cell lysates was measured by colorimetric assay (R&D). After normalization for total protein in the cell lysates, caspase 3 activity was expressed as fold increase over levels detected in untreated control cells. Apoptosis was quantitated by flow cytometry techniques using the Apo-BrdU kit (Pharmingen, San Diego, CA) and protocols contained therein.

In Vivo H358 Human Tumor Xenografts Model

The H358 human tumor xenografts were created in hind flanks of nude mice by inoculation of 10^7 cells suspended in 100 μL of phosphate-buffered saline. Palpable tumors of 170 to 200 mm^3 appeared approximately 4 weeks after tumor cell injection. Tumor-bearing animals then received either paclitaxel (1 mg/kg dissolved in 100 μL of phosphate-buffered saline once per week for 4 weeks), 17-AAG (10 or 25 mg/kg in 100 μL of carrier solution at three daily injections per week for 4 weeks) or paclitaxel + 17-AAG combinations (first doses of 17-AAG were administered concurrently with paclitaxel) by intraperitoneal injections. Control animals received phospholipid-based drug carrier solution alone. Orthogonal diameters of tumors were measured weekly. Animals were euthanized when tumors reached maximally allowable volumes of 2,500 to 2,800 mm^3. Tumor volumes were estimated using the following formula: $V = 0.52 \times a \times b \times c$, where a, b, c are orthogonal diameters.

Representative xenografts were harvested at the end of treatment for evaluation of cellular expression of VEGF, von Willebrand factor, erbB2, or activated caspase 3 using immunohistochemical techniques.

Data Analysis

Data were expressed as mean ± standard deviation of at least three independent experiments. Paired *t* test, Student's *t* test, and one-way analysis of variance (with Bonferroni test for pairwise comparisons) were performed for statistical analysis using Prism 2.0 software package (Graphpad Software, Inc, San Diego, CA).

Results

Depletion of erbB1 and erbB2 Expression on H358 Cells by 17-AAG

The H358 cells expressed high levels of erbB2 (approximately threefold higher than the level detected on normal human bronchial epithelial cells), with mean fluorescence intensity of 160 ± 11. Exposure of H358 cells to 20 or 80 nmol/L of 17-AAG for 24 hours resulted in a dose-dependent reduction of erbB2 mean fluorescence intensity to 80 ± 6 and 40 ± 8 ($p < 0.01$ versus baseline controls, n = 3) (Fig 1). Moreover, at the higher dose of 17-AAG, erbB2 expression was completely depleted in 65% of treated cells. In contrast, erbB1 expression in H358 cells was comparable to normal human bronchial epithelial cells, and depletion of erbB1 was achievable only at high concentration of 17-AAG. Exposure to 80 nmol/L of 17-AAG for 24 hours reduced erbB1 expression by 35% (mean fluorescence intensity of 110 ± 4 in treated cells versus 168 ± 12 in control cells, $p < 0.01$); all tumor cells remained positively stained for this receptor (Fig 1). Similar to a previously published report [16], 24-hour exposure of tumor cells to 17-AAG was more efficient in depleting erbB2 than erbB1 membrane expression. The 17-AAG also significantly inhibited H358 cell growth in vitro with the estimated IC_{50} value of 70 ± 5 nmol/L.

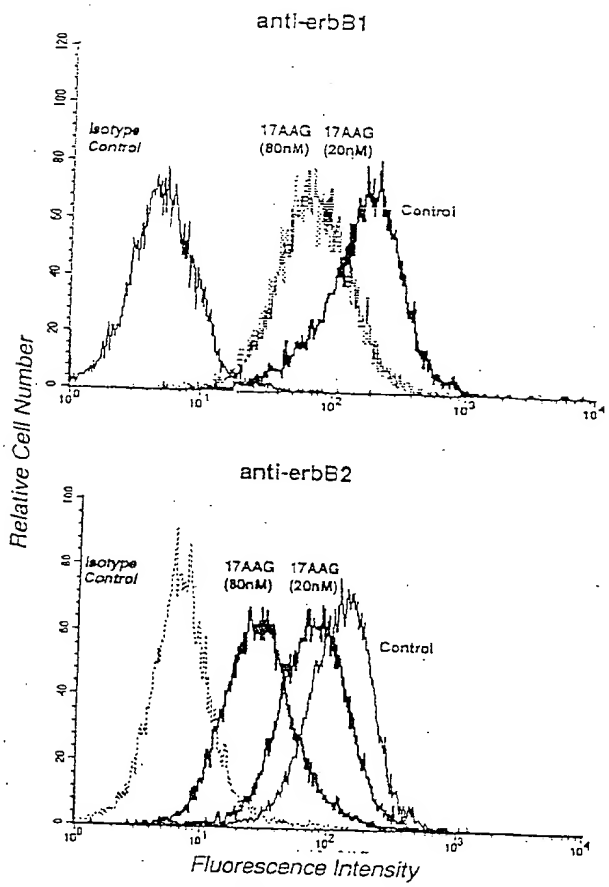

Fig 1. Immunofluorescence flow cytometric analysis of surface expression of erbB1 and erbB2 on H358 cells at baseline and after 24 hours of exposure to 17-allylamino geldanamycin (17-AAG) (20 or 80 nmol/L). Depletion of erbB1 (only at 80 nmol/L of 17-AAG) and erbB2 levels after 17-AAG treatment was indicated by significant reduction of erbB1 and erbB2 mean fluorescence intensity and shifting of the curves to the left. Representative data of three independent experiments that yielded similar results are shown.

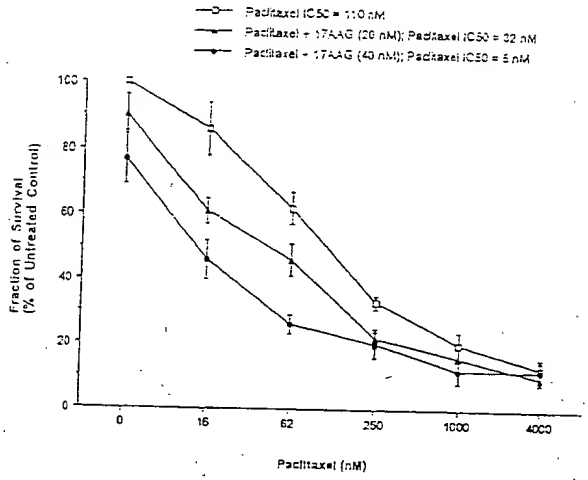

Fig 2. Enhancement of paclitaxel-mediated cytotoxicity in H358 cells by 17-allylamino geldanamycin (17-AAG) (20 or 40 nmol/L). The magnitude of growth inhibitory effect in cells treated with the drug combination was supraadditive, particularly at low doses of paclitaxel. Data are presented as mean ± standard deviation of four independent experiments, paclitaxel inhibitory concentration at 50% (IC50) values are indicated in the legends.

Enhancement of Paclitaxel Cytotoxicity by 17-AAG In Vitro

Figure 2 demonstrates the dose-dependent growth inhibitory effects of paclitaxel or paclitaxel + 17-AAG combination in H358 cells. Paclitaxel effectively inhibited tumor cell viability (IC_{50} = 110 ± 8 nmol/L). Concurrent exposure of H358 cells to paclitaxel and 17-AAG resulted in a drastic reduction of paclitaxel IC_{50} values (20 ± 3 and 5 ± 1 nmol/L at 20 nmol/L and 40 nmol/L of 17-AAG, respectively); these IC_{50} values were significantly lower than the paclitaxel IC_{50} value in cells treated with paclitaxel alone ($p < 0.001$). The increased suppression of cell growth by the addition of 17-AAG to paclitaxel treatment (30% to 40% at lower spectrum of paclitaxel dose range) was higher than the mild 17-AAG-mediated growth inhibition. This finding suggested that 17-AAG enhanced the susceptibility of tumor cell to the cytotoxic effect of paclitaxel. Furthermore, the synergistic cytotoxic effect of this drug combination was confirmed by the combination index CI_{50} values being significantly less than 1 (0.589 ± 0.078 and 0.630 ± 0.113 at 20 nmol/L and 40 nmol/L of 17-AAG, respectively, $p < 0.01$). The 17-AAG did not activate caspase 3 or induce apoptosis in H358 cells; in contrast, caspase 3 activity was evident in H358 cells after treatment with 17-AAG + paclitaxel, which was higher than that observed after exposure to paclitaxel alone (Fig 3A). This was accompanied by a higher magnitude of induction of apoptosis (Fig 3B). For instance, 55% ± 8% and 60% ± 4% of apoptotic cells were detected after treatment with 50 nmol/L and 200 nmol/L of paclitaxel in conjunction with 17-AAG compared to 22% ± 3% and 28% ± 4% of apoptotic cells after exposure to paclitaxel alone ($p < 0.01$).

Inhibition of Vascular Endothelial Cell Growth Factor Secretion From H358 Cells by 17-AAG and AG825 In Vitro

The H358 cells secreted high levels of VEGF into the culture media under basal conditions. Stimulation with EGF (20 ng/mL) resulted in a mild but significant elevation of VEGF (35,400 ± 3,750 versus 27,596 ± 2,500 pg/mL

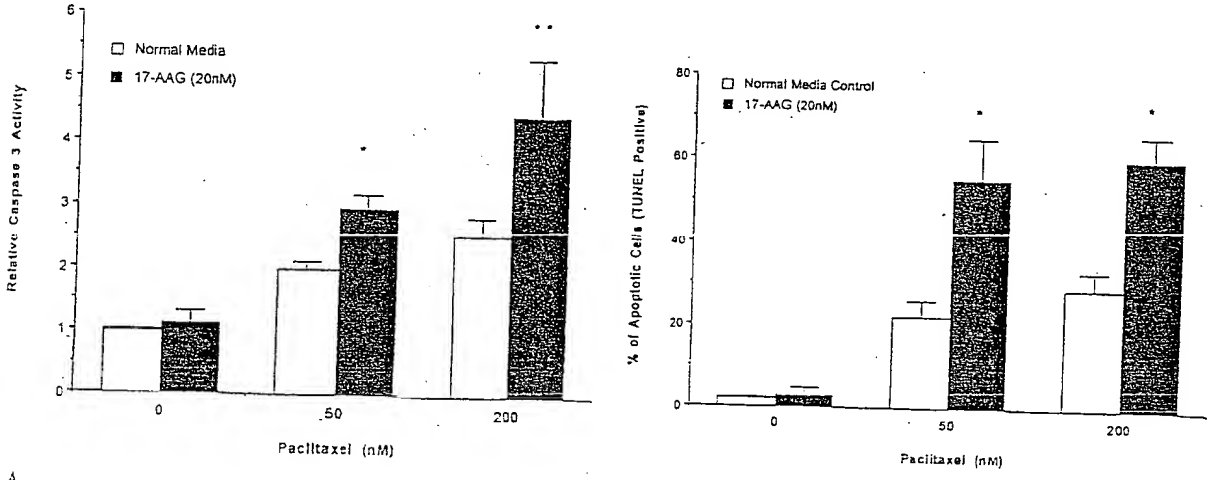

*Fig 3. (A) Caspase 3 activity in H358 cells treated with paclitaxel (50 or 200 nmol/L) alone or in combination with 17-allylamino geldanamycin (17-AAG) (20 nmol/L). Significantly higher levels of caspase 3 activity was observed in H358 cells treated with 17-AAG and paclitaxel combination than those treated with paclitaxel alone. Caspase 3 activity is expressed as fold of increase over baseline levels detected in control cells. Data are presented as mean ± standard deviation of four independent experiments, *$p < 0.01$, **$p < 0.001$. (B) Induction of apoptosis of H358 cells treated with paclitaxel (50 or 200 nmol/L) alone or in combination with 17-AAG (20 nmol/L). Apoptosis was quantitated in H358 cells harvested 60 hours after drug treatment by terminal deoxynucleotidyltransferase-mediated dUTP nick end-labeling (TUNEL) assay. Although 17-AAG at 20 nmol/L failed to induce apoptosis, combining 17-AAG with paclitaxel resulted in up to twofold increase in the induction of apoptosis. Data are presented as mean ± standard deviation of four independent experiments, *$p < 0.01$.*

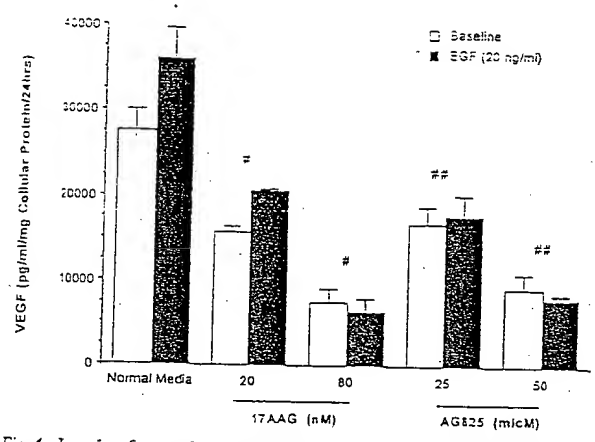

Fig 4. Levels of vascular endothelial cell growth factor (VEGF) in conditioned culture media of H358 cells at baseline or after stimulation with epidermal cell growth factor (EGF) (20 ng/mL) in the presence or absence of 17-allylamino geldanamycin (17-AAG) (20 or 80 nmol/L) or the selective erbB2 tyrosine kinase inhibitor AG825 (25 or 50 μmol/L). Not only did 17-AAG or AG825 strongly inhibit vascular endothelial cell growth factor production by H358 cells at baseline conditions but they also effectively abrogated the upregulation of vascular endothelial cell growth factor production by epidermal cell growth factor. Data are presented as mean ± standard deviation of four independent experiments. $^{\#}p < 0.01$, $^{\#\#}p < 0.001$.

per 24 hours per milligram of cellular protein, $p < 0.01$). Treating H358 cells with 17-AAG (20 or 80 nmol/L) for 24 hours suppressed both basal as well as EGF-mediated upregulation of VEGF expression (Fig 4) in a dose-dependent manner with the magnitude of inhibition ranging from 40% to 80%.

Inhibition of EGF-mediated upregulation of VEGF production by H358 cells after 17-AAG exposure may result from its effect on downregulating both erbB1 and erbB2 expression. The erbB2 receptor, although lacking a cognate ligand, modulates signaling from other members of the erbB superfamily [17]. To delineate further the role of erbB2 in EGF-mediated upregulation of VEGF production, additional experiments were performed using the selective erbB2 tyrosine kinase antagonist AG825 [18]. Treating H358 cells with AG825 (25 or 50 μmol/L) suppressed basal as well as EGF-mediated induction of VEGF secretion, to the same degree as observed after 17-AAG treatment (Fig 4).

In Vivo Tumoricidal Effect of Paclitaxel and 17-AAG

The in vivo experiment was designed to validate the in vitro findings of the synergistic cytotoxic effect and the potential antiangiogenic property of this combination (Fig 5). Parental administration of 17-AAG alone resulted in dose-dependent growth inhibition of H358 xenografts. Statistically significant reduction of tumor volumes and corresponding survival extensions were observed only in animals treated with the high dose of 17-AAG (25 mg/kg) (Fig 5 and Table 1). Significant inhibition of tumor growth and prolonged survivals were also noted in mice treated with paclitaxel (1 mg/kg) alone. More importantly, concurrent administration of 17-AAG (either at 10 or 25 mg/kg) and paclitaxel (1 mg/kg) resulted in a profound dose-dependent tumoricidal effects with 70% to 85% inhibition of tumor growth, and extension of survival from 3.5 months (low dose of 17-AAG with paclitaxel) to nearly 5 months (17-AAG 25 mg/kg and paclitaxel), representing a two- to threefold prolongation of life expectancy of tumor-bearing animals (Fig 5 and Table 1). The tumor volumes measured at 8 weeks after the beginning of combination chemotherapy were significantly less than those predicted by assuming additive drug effects (Table 1). Furthermore, the mean survival extensions of animals treated with 17-AAG + paclitaxel com-

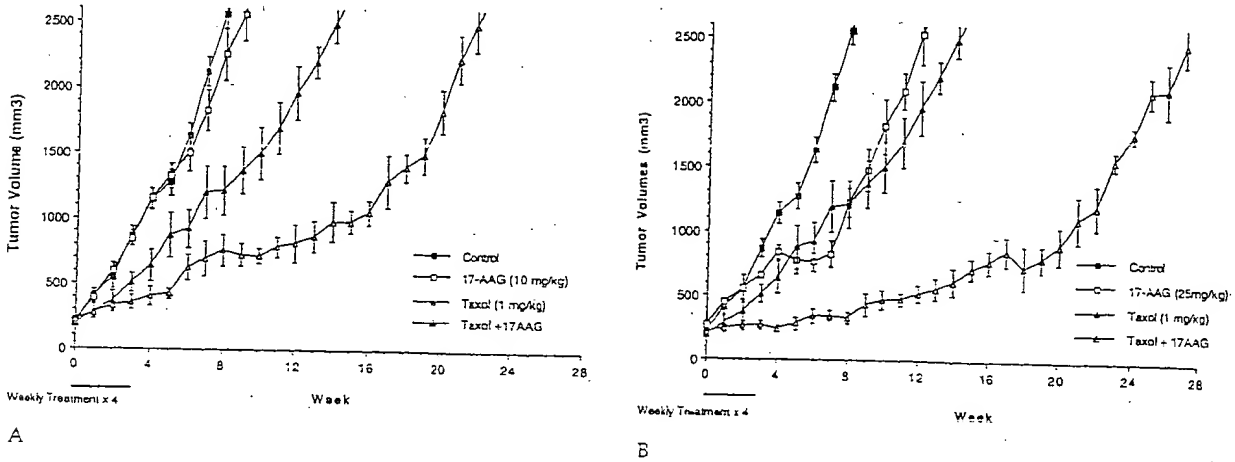

Fig 5. Enhancement of paclitaxel tumoricidal effect by 17-allylamino geldanamycin (17-AAG) in nude mice bearing H358 tumor xenografts. Animals were treated with either 10 mg/kg of 17-AAG (A) or 25 mg/kg of 17-AAG (B) in combination with paclitaxel (1 mg/kg) weekly for 4 weeks by intraperitoneal injections. Treatment schedule consisted of paclitaxel one injection/wk or 17-AAG three daily consecutive injections/wk for 4 weeks. Controls were animals treated with mock injection of the phospholipid-based carrier solution, with 17-AAG alone or with paclitaxel alone. Tumor dimensions were measured weekly until sacrifice. Data are presented as mean ± standard deviation, n = 8 per group. (Taxol = paclitaxel.)

Table 1. In Vivo Tumoricidal Effects of 17-AAG, Paclitaxel, and 17-AAG + Paclitaxel Combination

Group	Survival[a] (wk)	Mean Extension of Survival (wk)	Tumor Volumes at 8 Weeks (mm^3)
Control	7.8 ± 0.8	N/A	2,557 ± 110
17-AAG (10 mg/kg)	9.2 ± 1.6	1.4	2,370 ± 300
17-AAG (25 mg/kg)	13.5 ± 0.5[b]	5.7	1,077 ± 56
Paclitaxel (1 mg/kg)	14.3 ± 1.6[b]	6.5	1,210 ± 183
17-AAG (10) + paclitaxel	22.6 ± 1.6[b]	14.8	762 ± 120 (1174)[c]
17-AAG (25) + paclitaxel	26.8 ± 3.2[b]	19.0	328 ± 45 (508)[c]

Mean ± SD (n = 8 per group).

[a] Time elapsed from the onset of therapy to reaching tumor volumes of 2,500 mm^3. [b] $p < 0.001$ versus control by analysis of variance and Bonferroni test. [c] Predicted mean tumor volumes by assuming additive drug effects.

17-AAG = 17-allylamino geldanamycin.

binations were longer than the algebraic sums of the extensions resulting from each treatment alone (Table 1). Collectively, these data suggested in vivo synergistic tumoricidal drug effects.

Immunohistochemical analysis of erbB2 and VEGF expression, capillary density, and apoptosis in tumor nodules harvested 24 hours after completion of chemotherapy is shown in Figure 6. A profound reduction of membrane-bound erbB2 expression was observed in tumors from mice treated with either 17-AAG alone or 17-AAG + paclitaxel, suggesting that therapeutic levels of 17-AAG were achieved in xenografts. In parallel with in vitro observation of 17-AAG-mediated inhibition of VEGF production by H358 cells, cytoplasmic VEGF expression was also significantly decreased in tumors harvested from mice treated with 17-AAG or 17-AAG + paclitaxel (Table 2). Interestingly, mild-to-moderate reduction of cytoplasmic VEGF expression, was also noted in tumors treated with paclitaxel alone, similar to previously published observations [19]. Capillary density of tumor nodules was evaluated by staining for von Willebrand factor, which is expressed by capillary endothelial cells. Diffuse positive endothelial staining observed in control tumors was slightly diminished in tumors treated with paclitaxel. von Willebrand factor expression was markedly reduced in tumor treated with 17-AAG or 17-AAG + paclitaxel, indicating that reduction of VEGF expression coincided with diminished tumor angiogenesis (Table 2). Abundance of activated caspase 3-positive cells (indicative of ongoing apoptosis, dark brown staining cells) could be observed in tumors treated with the 17-AAG + paclitaxel drug combinations (Fig 6). Apoptotic cells were less frequently noted in paclitaxel-treated tumors, and rarely were they seen in control or 17-AAG-treated tumors.

Table 2. Semiquantitative Analysis of Immunohistochemical Staining of Tumor Tissues for Molecular Markers (n = 3)

Group	erbB2	VEGF	vW Factor	Activated Caspase 3
Control	+++	+++	+++	0
17-AAG (10 mg/kg)	++	++	++	0
17-AAG (25 mg/kg)	+	+	++	0
Paclitaxel (1 mg/kg)	+++	++	++	+
17-AAG (10) + paclitaxel	++	++	++	++
17-AAG (25) + paclitaxel	+	+	+	+++

17-AAG = 17-allylamino geldanamycin; VEGF = vascular endothelial cell growth factor; vW = von Willebrand.

Comment

Previous studies have demonstrated that members of the erbB superfamily (particularly erbB1 and erbB2, which are frequently overexpressed in NSCLC cells) play important roles in mediating the response of tumor cells to cytotoxic stress and modulating their susceptibility to chemotherapeutic agents. Overexpression of erbB2 in cancer cells enhances resistance to various cytotoxic agents including cisplatin and paclitaxel as well as irradiation. Upregulation of DNA repair mechanisms mediated by erbB2 overexpression contributes to chemotherapy and radiation resistance in cancer cells [3]. In contrast, upregulation of the cyclin-dependent kinase inhibitor p21, which inhibits progression of cells into the M phase of the cell cycle, is a major mechanism of paclitaxel resistance in cancer cells overexpressing erbB2 [20, 21]. Overexpression of erbB1 or activation of erbB1 receptor tyrosine kinase activity by EGF similarly renders tumor cells refractory to paclitaxel cytotoxicity [22]. Inhibition of the function or phenotypic expression of erbB1 or erbB2 by monoclonal antibodies or low molecular weight compounds abrogates chemoresistance mediated by erbB overexpression in cancer cells.

We have been interested in developing strategies to enhance the cytotoxic effects of conventional chemotherapeutic agents such as paclitaxel in lung or esophageal cancers by exploiting the current understanding of the relationship between the erbB signal transduction pathways and paclitaxel sensitivity. By targeting the erbB oncogenes using low molecular weight compounds such as 17-AAG we may avoid technical issues that may limit the efficacy of anti-erbB monoclonal antibodies, antisense constructs, or intracellular anti-HER2/neu single chain antibodies. Previously, we have demonstrated sequence-dependent enhancement of paclitaxel cytotoxicity in NSCLC by this compound [4]. Concurrent but not sequential 17-AAG/paclitaxel drug exposure significantly sensitized NSCLC cells expressing high levels of erbB2 to paclitaxel. This salutary effect has been extended to esophageal cancer cells expressing elevated levels of erbB2 (unpublished data). The in vivo experiments dem-

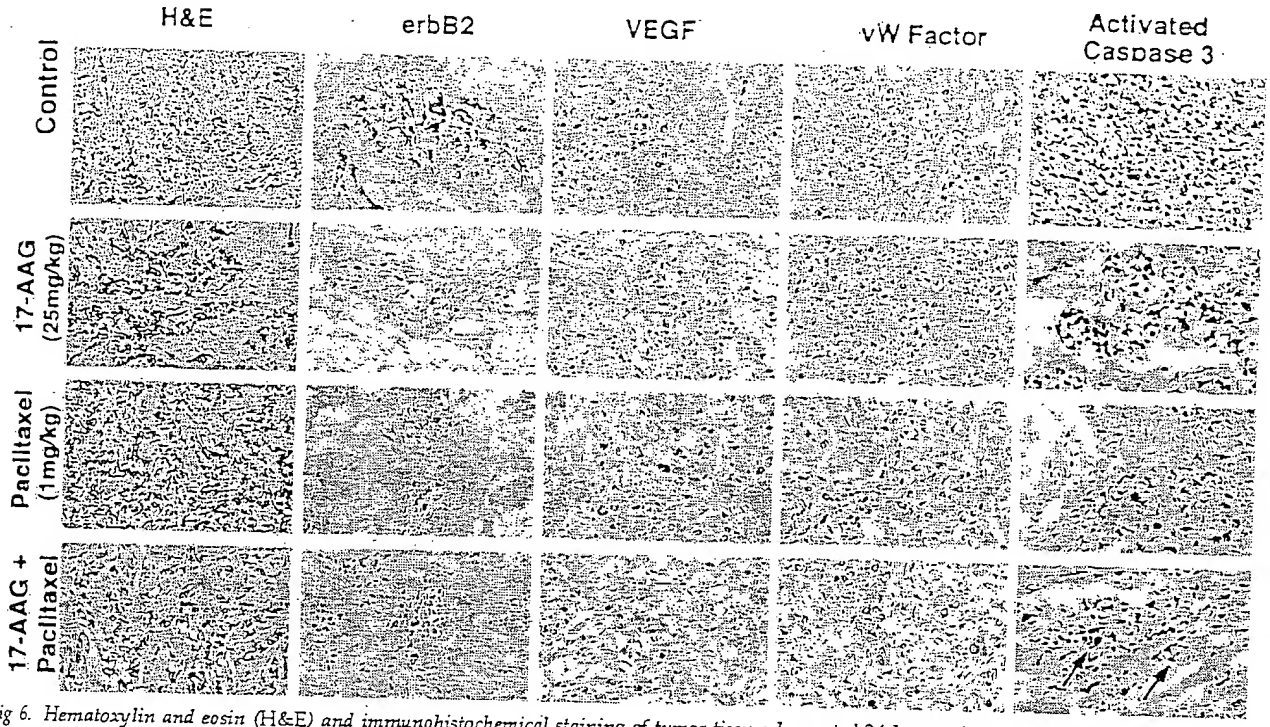

Fig 6. Hematoxylin and eosin (H&E) and immunohistochemical staining of tumor tissues harvested 24 hours after completion of the full 4-week course chemotherapy for molecular markers including erbB2, vascular endothelial cell growth factor (VEGF), von Willebrand (vW) factor (staining for endothelial cells to evaluate tumor microvasculature) and activated caspase 3 (only present in apoptotic cells). Representative photomicrographs of tumors treated with phosphate-buffered saline (control), 17-allylamino geldanamycin (17-AAG) (25 mg/kg), paclitaxel (1 mg/kg), or both are shown here. Hematoxylin and eosin: magnification, ×200; immunohistochemical staining: magnification, ×400.

onstrating profound tumoricidal effects of the paclitaxel and 17-AAG combination extended in vitro observations of synergistic cytotoxic drug interaction of these two agents. However, it is difficult to prove synergism of drug interactions in vivo. The observations that tumor volumes in animals treated by the drug combinations were smaller than predicted by assuming additive antitumor drug effects (Table 1) and the survivals of tumor-bearing animals treated with the drug combination were longer than the algebraic sums of the extension of survivals achieved by individual drug treatment alone strongly support the notion of potentiation of paclitaxel tumoricidal effect by 17-AAG.

In addition to being a chemotherapy sensitizer, our studies have shown that 17-AAG is a powerful inhibitor of VEGF production by tumor cells through its negative effect on erbB signal transduction pathways, which are known to transcriptionally regulate VEGF gene expression [13, 23]. Significant information was derived from the molecular analysis of tumor samples harvested after completion of a 4-week course of chemotherapy. This time point was chosen to clearly demonstrate the antiangiogeneic effect of 17-AAG. Whereas depletion of VEGF secretion by H358 cells occurs within hours of 17-AAG exposure, alteration of tumor microvasculature in response to reduced VEGF levels would take more time to develop. The in vivo effects of 17-AAG on erbB2 or VEGF expression and the induction of apoptosis by paclitaxel (with or without 17-AAG) were probably derived from the last treatment rather than a cumulative effect of the four cycles. Almost complete depletion of erbB2 expression in tumors treated with regimens containing 17-AAG provided direct proof that therapeutic drug levels were achieved using the treatment schedule discussed. In conjunction with depletion of erbB2 expression, significant reduction of VEGF cytoplasmic expression in H358 tumor cells and inhibition of angiogenesis were also observed. These data clearly demonstrate the biological significance of 17-AAG-mediated inhibition of VEGF production, and affirm our in vitro experiments that suggested that 17-AAG exhibits antiangiogenic effects. In this context, 17-AAG played the dual role of a paclitaxel-sensitizing and an antiangiogenic agent. This drug combination strategy appears quite analogous to recent anticancer regimens combining a cytotoxic agent and an antiangiogenic agent (either an anti-VEGF antibody or a VEGF receptor pharmacologic antagonist) [24, 25]. The individual contribution of the paclitaxel sensitization and the antiangiogenic properties of 17-AAG are difficult to define at this time.

The phase I clinical trial using 17-AAG (daily 1-hour intravenous infusion for 5 days every 3 weeks) as a single agent to treat advanced solid malignancies is in progress at the National Cancer Institute, and initial data indicate that hepatotoxicity is the dose-limiting factor as predicted from preclinical studies (Jean Grem and Richard

Wilson, National Cancer Institute, Bethesda, MD, personal communication). The peak plasma drug levels at maximally tolerated dose were 1 to 2 μmol/L, which are well above the concentrations required to achieve synergistic drug interaction in vitro. The acceptable drug toxicity profile derived from the phase I trial together with the powerful tumoricidal effect of this drug combination observed in our present studies support evaluation of 17-AAG in combination with paclitaxel in patients with NSCLC and esophageal cancers exhibiting high level HER2/neu expression.

We acknowledge the superb technical assistance of Shawn Farid, BS, and Arnold Mixon, BS, of the Flow Cytometry Core Facility, Surgery Branch, National Cancer Institute, National Institutes of Health.

References

1. Tsai CM, Dihua Y, Chang K-T, et al. Enhanced chemoresistance by elevation of p185neu levels in HER-2/neu-transfected human lung cancer cells. J Natl Cancer Inst 1995; 87:682–4.
2. Yu D, Liu B, Tan Ming L, Wang S-S, Hung M-C. Overexpression of c-erbB-2/neu in breast cancer cells confers increased resistance to Taxol via mdr-1-independent mechanisms. Oncogene 1996;13:1359–65.
3. You XL, Yen L, Zeng-Rong N, Al Moustafa AE, Alaoui-Jamali MA. Dual effects of erbB-2 depletion on the regulation of DNA repair and cell cycle mechanisms in non-small cell lung cancer cells. Oncogene 1998;17:3177–86.
4. Nguyen DM, Chen A, Mixon A, Schrump DS. Sequence-dependent enhancement of paclitaxel toxicity in non-small cell lung cancer by 17-allylamino 17-demethoxygeldanamycin. J Thorac Cardiovasc Surg 1999;118:908–15.
5. Supko JG, Hickman RL, Grever MR, Malspeis L. Preclinical pharmacologic evaluation of geldanamycin as an antitumor agent. Cancer Chemother Pharmacol 1995;36:305–15.
6. An WG, Schnur RC, Neckers L, Blagosklonny M. Depletion of p185/erbB-2, Raf-1, mutant p53 proteins by gendanamycin derivatives correlates with antiproliferative activity. Cancer Chemother Pharmacol 1997;40:60–4.
7. Schulte TW, Neckers L. The benzoquinone ansamycin 17-allylamino-17-demethoxygeldanamycin binds to HSP90 and shares important biologic activities with geldanamycin. Cancer Chemother Pharmacol 1998;42:273–9.
8. Slamon DJ, Clark GM, Wong SG, et al. Human breast cancer: correlation of relapse and survival with amplification of the HER-2/neu oncogene. Science 1987;235:177–82.
9. Diez M, Pollan M, Maestro M, et al. Prediction of recurrence by quantification of p185neu protein in non-small-cell lung cancer tissue. Br J Cancer 1997;75:684–9.
10. Hsieh CC, Chow KC, Fahn HJ, et al. Prognostic significance of HER-2/neu overexpression in stage I adenocarcinoma of lung. Ann Thorac Surg 1998;66:1159–63.
11. Yu D, Wang S-S, Dulski KM, et al. c-*erb*B-2/*neu* overexpression enhances metastatic potential of human lung cancer cells by induction of metastasis-associated properties. Cancer Res 1994;54:3250–6.
12. Petit AM, Rak J, Hung MC, et al. Neutralizing antibodies against epidermal growth factor and ErbB-2/neu receptor tyrosine kinases down-regulate vascular endothelial growth factor production by tumor cells in vitro and in vivo: angiogenic implications for signal transduction therapy of solid tumors. Am J Pathol 1997;151:1523–30.
13. Shiozaki H, Kadowaki T, Doki Y, et al. Effect of epidermal growth factor on cadherin-mediated adhesion in a human oesophageal cancer cell line. Br J Cancer 1995;71:250–8.
14. Nguyen DM, Desai S, Chen A, Weiser TS, Schrump DS. Modulation of metastasis phenotypes of non-small cell lung cancer cells by 17-allylamino 17-demethoxy geldanamycin. [In Process Citation]. Ann Thorac Surg 2000;70:1853–60.
15. Chou TC, Talalay P. Quantitative analysis of dose-effect relationships: the combined effects of multiple drugs or enzyme inhibitors. Adv Enzyme Regul 1984;22:27–55.
16. Rigberg DA, Blinman TA, Kim FS, Cole MA, McFadden DW. Antisense blockade of p21/WAF1 decreases radiation-induced G2 arrest in esophageal squamous cell carcinoma. J Surg Res 1999;81:6–10.
17. Klapper LN, Glathe S, Vaisman N, et al. The ErbB-2/HER2 oncoprotein of human carcinomas may function solely as a shared coreceptor for multiple stroma-derived growth factors. Proc Natl Acad Sci USA 1999;96:4995–5000.
18. Tsai CM, Levitzki A, Wu LH, et al. Enhancement of chemosensitivity by tyrphostin AG825 in high-p185(neu) expressing non-small cell lung cancer cells. Cancer Res 1996;56: 1068–74.
19. Lau DH, Xue L, Young LJ, Burke PA, Cheung AT. Paclitaxel (Taxol). an inhibitor of angiogenesis in a highly vascularized transgenic breast cancer. Cancer Biother Radiopharm 1999; 14:31–6.
20. Barboule N, Chadebech P, Baldin V, Vidal S, Valette A. Involvement of p21 in mitotic exit after paclitaxel treatment in MCF-7 breast adenocarcinoma cell line. Oncogene 1997; 15:2867–75.
21. Schmidt M, Lu Y, Liu B, et al. Differential modulation of paclitaxel-mediated apoptosis by p21Waf1 and p27Kip1. Oncogene 2000;19:2423–9.
22. Fang M, Liu B, Schmidt M, et al. Involvement of p21Waf1 in mediating inhibition of paclitaxel-induced apoptosis by epidermal growth factor in MDA-MB-468 human breast cancer cells. Anticancer Res 2000;20:103–11.
23. Zhong H, Chiles K, Feldser D, et al. Modulation of hypoxia-inducible factor 1alpha expression by the epidermal growth factor/phosphatidylinositol3-kinase/PTEN/AKT/FRAP pathway in human prostate cancer cells: implications for tumor angiogenesis and therapeutics. Cancer Res 2000;60:1541–5.
24. Herbst RS, Takeuchi H, Teicher BA. Paclitaxel/carboplatin administration along with antiangiogenic therapy in non-small-cell lung and breast carcinoma models. Cancer Chemother Pharmacol 1998;41:497–504.
25. Inoue K, Slaton JW, Davis DW, et al. Treatment of human metastatic transitional cell carcinoma of the bladder in a murine model with the anti-vascular endothelial growth factor receptor monoclonal antibody DC101 and paclitaxel [In Process Citation]. Clin Cancer Res 2000;6:2635–43.

DISCUSSION

DR HARVEY I. PASS (Detroit, MI): Very nice, Dr Nguyen.

I have a couple of questions. The relationship between erbB-2 and this whole situation, what is the evidence that AAG is actually working selectively through an erbB-2 mechanism and is not having other effects, and have you done experiments to block either with antibody or making it even better using Herceptin (Genentech, San Francisco, CA)?

The second question is, this could also be explained by overcoming resistance to paclitaxel. Do you have any data with regard to your cell line with regard to β tubulin mutations in this cell line?

DR NGUYEN: To answer your first question, in terms of the impact of 17-AAG on erbB-2-mediated signal transduction path-

way, you are perfectly right. This compound not only targets erbB-2, it also targets other signal transduction pathways as well as other oncoproteins. To specifically target erbB-2 pathway, we used Herceptin and we also used AG825, which is a selective erbB-2 antagonist. We observed similar enhancement of paclitaxel-mediated cytotoxicity in NSChC cells by AG825. Herceptin, on the other hand, we did not see such a powerful sensitization effect, and the reason for that is unclear at this point.

What is your second question, Dr Pass?

DR PASS: The question of whether this is simply an overcoming chemoresistance phenomenon. Do you have any data whether AAG has any effect on cell lines with β tubulin mutations, and does your cell line have β tubulin mutation?

DR NGUYEN: No, we have not done that. We recently looked at the mechanisms of this combination effect, and it is related to the ability of 17-AAG to suppress p21, and that allowed the cells to traverse the G2M check point and accumulate the cells in mitosis, and p21 actually inhibits cdC2/p34 kinase, which is known to play an important role in paclitaxel-mediated apoptosis. So we observed that by using this combination the p21 levels decreased, associated with higher fraction of cells in mitosis and augmentation of paclitaxel-mediated apoptosis.

DR PASS: Do you have any data with any other chemotoxics?

DR NGUYEN: It has been looked at before with 17-AAG-sensitized tumor cells to cisplatin and the other chemotherapeutics.

Notice From the American Board of Thoracic Surgery

The 2001 Part I (written) examination will be held at the Hotel Sofiel, 5500 North River Rd, Rosemont, IL 60018-5194, on November 18, 2001. The closing date for registration was August 1, 2001.

To be admissible to the part II (oral) examination, a candidate must have successfully completed the part I (written) examination.

A candidate applying for admission to the certifying examination must fulfill all the requirements of the Board in force at the time the application is received.

Please address all communications to the American Board of Thoracic Surgery, One Rotary Center, Suite 803, Evanston, IL 60201; telephone: (847) 475-1502; fax: (847) 475-6240; e-mail: abts_evanston@msn.com.

Modulation of Metastasis Phenotypes of Non-Small Cell Lung Cancer Cells by 17-Allylamino 17-Demethoxy Geldanamycin

Dao M. Nguyen, MD, Sudhen Desai, MD, Aaron Chen, MS, Todd S. Weiser, MD, and David S. Schrump, MD

Thoracic Oncology Section, Surgery Branch, Division of Clinical Sciences, National Cancer Institute, National Institutes of Health, Bethesda, Maryland

Background. Cancer cells that overexpress c-erbB oncogenes exhibit resistance to chemotherapy, enhanced tumorigenicity, as well as increased propensity for metastasis. The aim of this study was to investigate if depletion of erbB-1/EGFR and erbB-2/HER2neu oncogene products by 17-allylamino 17-demethoxy Geldanamycin (17AAGA) could diminish the metastatic potential of non-small cell lung cancer (NSCLC) cells that express varying levels of the erbB1/erbB2 oncogenes.

Methods. NSCLC cell lines (H460, H358, H322, or H661) were assayed for expression of erbB1 and erbB2, the cell adhesion molecule E-cadherin, secretion of the matrix metalloproteinase 9 (MMP-9), and vascular endothelial cell growth factor (VEGF), as well as their ability to invade Matrigel after 48-hour exposure to 17AAGA.

Results. 17AAGA significantly depleted erbB1 or erbB2 levels in NSCLC cells expressing high levels of these proteins, and effectively inhibited their growth with IC_{50} values ranging from 50 to 90 nmol/L. Moreover, drug treatment enhanced E-cadherin expression in H322 and H358 cells, and inhibited secretion of MMP-9 and VEGF secretion by tumor cells. 17AAGA diminished hypoxia-induced upregulation of VEGF expression as well as growth factor-mediated augmentation of MMP-9 secretion, and profoundly inhibited the ability of H322 and H358 cells to migrate through Matrigel in response to chemoattractants.

Conclusions. In addition to its known antiproliferative and chemosensitization effects, 17AAGA inhibits the metastatic phenotype of lung cancer cells. 17AAGA may be a novel pharmacologic agent for specific molecular intervention in lung cancer patients.

(Ann Thorac Surg 2000;70:1853–60)

Patients with non-small cell lung cancer (NSCLC) frequently present with either locally advanced (stage IIIA/B) or systemic disease (stage IV). The overall prognosis for these individuals is very poor, with the median survival less than 9 to 12 months despite an aggressive combination of chemo and radiotherapy. More importantly, the main mode of treatment failure after curative-intent therapy for early-stage NSCLC is systemic metastasis [1]. Acknowledging the fact that mature data of phase II/III clinical trials addressing the values of adjuvant chemotherapy for completely resected early-stage NSCLC are still forthcoming, there is no evidence that adjuvant therapy has any impact on the outcome of surgically treated NSCLC [2]. Micrometastases derived from lung cancers may have low proliferative activity, rendering them insensitive to standard cytotoxic agents. Hence, there is an urgent need for novel antineoplastic agents that exhibit strong antiproliferative effects as well as a capacity to inhibit the metastatic potential of tumor cells.

Solid tumor metastases arise by a multistep process regulated by complex interactions between tumor cells and adjacent stromal tissues [3]. In association with altered expression of adhesion molecules such as E-cadherin, cells detach from the main tumor mass and migrate through the extracellular matrix, degraded by tumor-derived matrix metalloproteinases (MMPs). After dissemination, cells exit from the vasculature and establish metastatic deposits, facilitated by the expression of integrin or hyaluronate (CD44) receptors, and the secretion of angiogenesis factors such as vascular endothelial cell growth factor (VEGF).

Experimental and clinical data have indicated that overexpression of erbB1 and erbB2 protooncogenes encoding the epidermal growth factor receptor (EGFR) and the orphan receptor (HER2/neu), respectively, correlates with locally advanced disease, distant metastases, and diminished survival in patients with breast, lung, esophageal, and ovarian carcinomas [4–7]. Tumor cells overexpressing these protooncogenes exhibit one or more phenotypes correlating with enhanced metastatic potential

Presented at the Thirty-sixth Annual Meeting of The Society of Thoracic Surgeons, Fort Lauderdale, FL, Jan 31–Feb 2, 2000.

Address reprint requests to Dr Nguyen, Thoracic Oncology Section, Surgery Branch, Division of Clinical Sciences, National Cancer Institute, Room 2B07, Building 10, 10 Center Dr, Bethesda, MD 20892; e-mail: dao_nguyen@nih.gov.

Published by Elsevier Science Inc

0003-4975/00/$20.00
PII S0003-4975(00)01810-5

Exhibit H

including downregulation of E-cadherin expression, increased secretion of MMP-9 and VEGF, and accelerated invasion through extracellular matrix [8–10]. Therapeutic strategies that specifically target erbB should inhibit mitogenic signaling via erbB1 and erbB2 pathways and may reduce the proliferation and metastatic potential of cancer cells; indeed, treatment of cells overexpressing the erbB1 or erbB2 gene products with antagonistic monoclonal antibodies significantly inhibits their metastatic phenotype [10, 11].

The benzoquinone ansamycin antibiotic geldanamycin (GA) and its less toxic synthetic derivative, 17-allylamino 17-demethoxygeldanamycin (17AAGA), have been recently selected for clinical development at the National Cancer Institute based upon their activity against cell lines derived from a variety of human malignancies [12, 13]. The growth inhibitory effects of geldanamycin and 17AAGA appear related to their ability to inhibit the expression of several cellular oncoproteins, including erbB1 and erbB2 [13]. In the present study, we sought to evaluate if 17AAGA could modulate the metastatic potential of lung cancer cells overexpressing the erbB1 and erbB2 gene products. Herein, we demonstrate that treatment of NSCLC cells with 17AAGA results in significant reduction of erbB1 or erbB2 expression, profound inhibition of cell proliferation, upregulation of E-cadherin expression, and downregulation of VEGF and MMP-9 secretion, paralleling with diminished capacity to invade extracellular matrix in vitro.

Material and Methods

Cells and Reagents

The NSCLC cells H460, H358, H661, and H322 were purchased from ATCC (Manassas, VA), and were grown in RPMI-1640 medium supplemented with glutamine (1 mmol/L), penicillin (100 U/mL)/streptomycin (100 μg/mL), and 10% fetal bovine serum (FBS) (all purchased from Biofluids, Rockville, MD). Normal human bronchial epithelial (NHBE) cells were purchased from Clonetics, Inc (Walkerville, MD) and maintained in bronchial epithelial cell basal media (Clonetics, Inc). 17AAGA was obtained from the Drug Synthesis and Chemistry Branch, Developmental Therapeutics Program, Division of Cancer Treatment, National Cancer Institute, and dissolved in dimethyl sulfoxide to yield a 100 μmol/L stock solution, which was stored at −70°C. All experiments using this compound were performed under subdued lighting conditions. Recombinant human epidermal growth factor (EGF) and heregulin-α (HRG) (purchased from R&D, Minneapolis, MN), and the anti-erbB1 and anti-erbB2 monoclonal antibodies (purchased from Calbiochem/Oncogene Research Products, Cambridge, MA), were constituted in phosphate-buffered saline (PBS), and stored at 4°C as recommended by the manufacturers. The E-cadherin antibody was obtained from ICN Biomedicals, Inc (Aurora, OH).

Immunofluorescent Staining and Flow Cytometric Analysis of erbB1, erbB2, and E-cadherin

Expression of erbB1, erbB2, and E-cadherin in NSCLC cell lines was quantitated by flow cytometry using a Becton-Dickinson (San Jose, CA) fluorescence-activated cell sorter (FACS). In brief, cells grown in either normal media with or without 17AAGA were harvested by trypsin/EDTA. To prevent proteolysis of surface adhesion molecules, cells harvested for E-cadherin staining were treated with 0.01% crystallized trypsin in the presence of 1 mmol/L of calcium, then washed in Ca/Mg-free PBS. Single-cell suspensions were incubated with either anti-erbB1, anti-erbB2, or anti-E-cadherin monoclonal antibodies for 60 minutes at room temperature. Cells were then washed with PBS, and incubated with fluorescent isothiocyanate (FITC)-conjugated goat anti-mouse IgG antibody at room temperature for 60 minutes in the dark. An irrelevant mouse IgG isotype monoclonal antibody was used as a negative control for FACS analysis. A minimum of 10^4 cells were analyzed by FACS flow cytometry. The magnitude of surface expression of these proteins was indicated by the mean fluorescence intensity (MFI) of positively stained cells. The MFI of isotype IgG control samples was always less than 10.

In Situ Immunofluorescent Staining of E-cadherin

Cells were cultured in chamber slides (Nalge Nunc International Corp, Naperville, IL) until 80% confluent, washed with PBS, fixed with 1% paraformaldehyde for 10 minutes, and permeabilized with acetone for 5 minutes. Immunofluorescent staining for E-cadherin was performed similar to that described for flow cytometry. Slides were examined under the fluorescence microscope. Fluorescent photomicrographs were taken at 200× magnification.

MMP-9 Assay

Cells were grown to confluence in six-well plates, washed twice with PBS, and then incubated with 2 mL of fresh serum-free RPMI-1640 medium. In the 17AAGA treatment group, cells were replenished with media containing either 20 or 80 nmol/L of 17AAGA. After 48 hours of incubation, conditioned media were harvested and frozen at −70°C until assayed for MMP-9 expression using an enzyme-linked immunosorbent assay (ELISA) kit (Calbiochem/Oncogene Research Products, Cambridge, MA). Cells from each well were collected, and total cellular protein was assayed by bicinchoninic acid (BCA) technique (Pierce, Rockford, IL). MMP-9 levels in the conditioned media were expressed as pg/mL/24 h/mg of total cellular protein.

VEGF Assay

Cells were grown to 80% confluence in 24-well plates, washed once with PBS, and replenished with 2 mL of fresh RPMI-1640 alone or containing either 50 μmol/L or 100 μmol/L Cobalt Chloride ($CoCl_2$) to simulate hypoxia [14]. In the 17AAGA treatment groups, appropriate aliquots of 100× 17AAGA stock were added to the culture

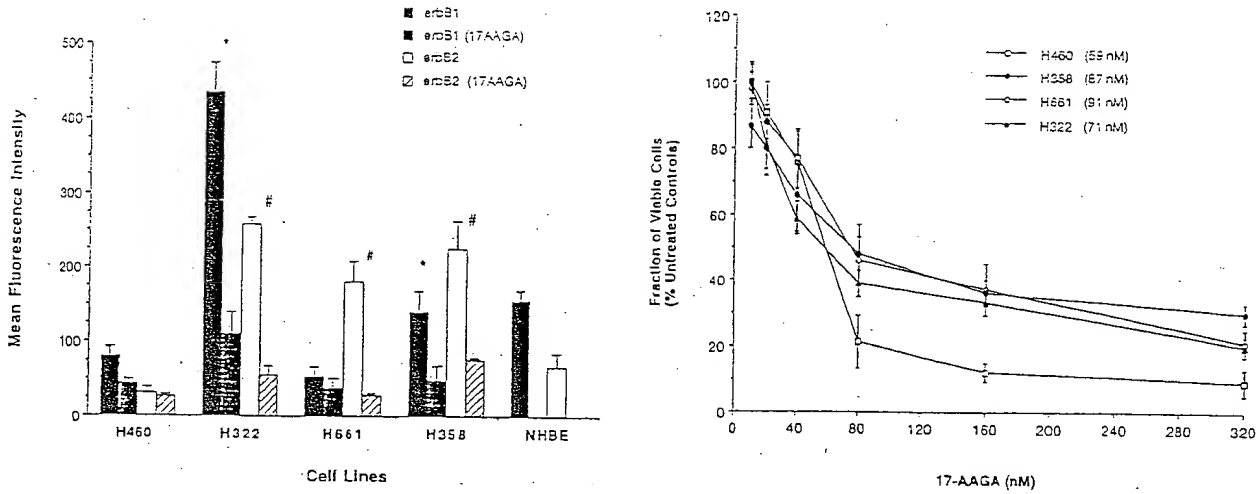

Fig 1. (A) Flow cytometric analysis of basal expression and 17AAGA-mediated depletion of erbB1 and erbB2 surface receptors in 4 NSCLC cell lines and normal human epithelial cells (NHBE). *Exposure of these cells to 80 nmol/L of 17AAGA for 48 hours resulted in significant reduction of surface expression of these two receptors. Data are expressed as means ± SD of three independent experiments* (*$p < 0.0001$, #$p < 0.001$). *(B) Dose-dependent growth inhibition of NSCLC cells in vitro by 17AAGA. Cells were seeded in 96-well plates and, after an overnight incubation, were continuously exposed to varying doses of 17AAGA for 96 hours. Viable cells were quantitated by MTT assay. IC_{50} values, estimated from these dose-response curves, are indicated in parentheses. Data are expressed as means ± SD of three independent experiments.*

media to yield a final concentration of 80 nmol/L. After 48-hour incubation, conditioned media were harvested and frozen at −70°C until assayed for VEGF. VEGF levels in the conditioned media were evaluated using an ELISA kit (R&D) and expressed as ng/mL/24 h/10^6 cells.

Matrigel Invasion Assay

The chemoinvasion assay was performed as previously described [15]. Briefly, polyvinylpyrrolidone-free polycarbonate filters (10-μm pore size; Neuroprobe, Gaithersburg, MD) coated with 500 μg/mL of Englebreth-Holm-Swarm murine sarcoma basement membrane extract (Matrigel; Sigma Chemical Co, St. Louis, MO) were placed in a modified Boyden chamber (Neuroprobe, Gaithersburg, MD). Matrigel was diluted to the desired final concentration using cold (4°C) serum-free RPMI-1640 media. Filters were then placed in 15 mL of 500-μg/mL Matrigel in 100 × 15-mm Petri dishes and rotated at 45 rpm overnight at 4°C. Filters were air dried under a sterile hood immediately before use. Cells (6×10^5/mL) were suspended in serum-free RPMI and added to the upper chamber (30,000 cells/well). The lower chamber contained serum-free conditioned media from cultures of NIH 3T3 cells as a chemoattractant. Chambers were incubated at 37°C in 5% CO_2 for 6 hours. At the end of the incubation, cells on the upper surface of the filter were aspirated off and the filters were fixed in methanol and stained with Diff-Quik II, a Wright-Geimsa stain (Baxter, McGaw Park, IL). Cells that had invaded the lower surface of the filter were counted by light microscopy and data were expressed as cells/5 high-power fields (HPF)/well.

Data Analysis

Data are expressed as means ± standard deviation (SD). Student's *t* test and one-way analysis of variance (with Bonferroni test for pairwise comparisons) were used for statistical analysis using Prism 2.0 software package from Graphpad Software, Inc (San Diego, CA).

Results

Constitutive Expression of erbB1 and erbB2 in 4 NSCLC Cells Lines

The NSCLC cell lines used in this study express different levels of erbB1 and erbB2 surface receptors as determined by flow cytometric analysis (Fig 1A). In comparison with the receptor levels expressed in confluent NHBE, H460 cells express low levels of both erbB1 and erbB2; H661 and H358 cells express high levels of erbB2, but not erbB1, whereas H322 cells overexpress both erbB1 and erbB2. Forty-eight-hour exposure of these cells to 80 nmol/L 17AAGA resulted in significant reduction of surface expression of erbB1 or erbB2 in cells exhibiting elevated levels of these receptors. In parallel with inhibition of erbB1 or erbB2 expression, continuous exposure of these cells to 17AAGA for 96 hours resulted in a dose-dependent inhibition of cell proliferation, with estimated IC_{50} (concentrations of drug that inhibit 50% of cell proliferation) values ranging from 60 to 90 nmol/L (Fig 1B).

Upregulation of E-Cadherin by 17AAGA

Expression of the calcium-dependent epithelial cell adhesion molecule E-cadherin was readily detectable by

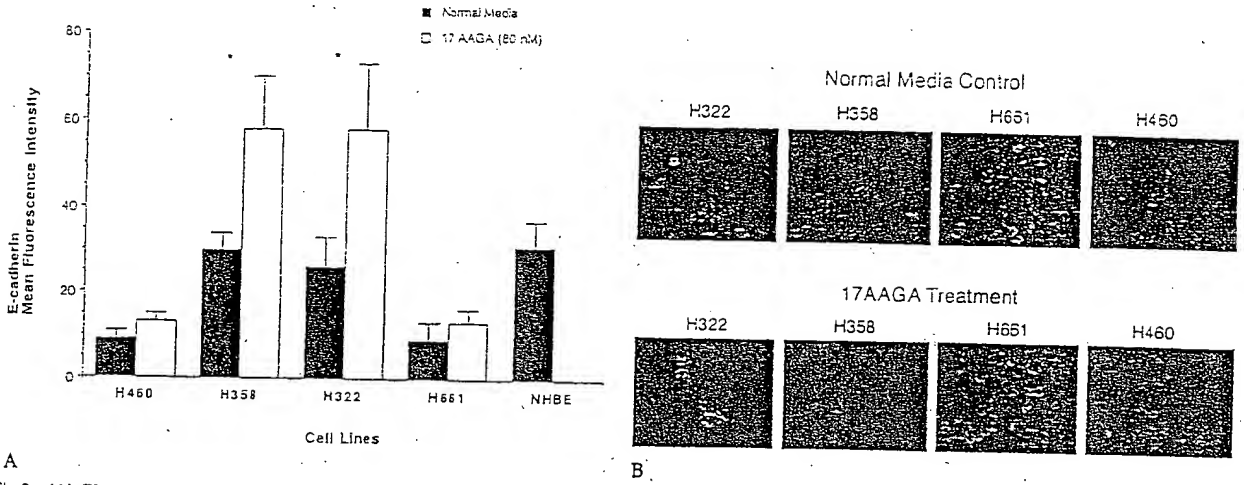

Fig 2. (A) Flow cytometric analysis of surface expression of E-cadherin on NSCLC cells under normal or 17AAGA condition. Similar levels of surface expression of E-cadherin were noted on H322, H358, and normal human bronchial epithelial cells (NHBE); E-cadherin was undetectable on H460 and H661 cells. Significant upregulation of E-cadherin expression was observed in H358 and H322 cells after 48-hour exposure to 17AAGA (80 nmol/L). Data are expressed as means ± SD of four independent experiments ($p < 0.01$). (B) Immunofluorescent analysis of lung cancer cells grown in normal media or media containing 17AAGA. After exposure to 17AAGA, H358 and H322 cells exhibit increased membrane localization of E-cadherin.*

flow cytometry in NHBE, H322, and H358 cells and not in H460 or H661 cells; results that were consistent with previously published data concerning E-cadherin expression in these cells [11]. The mean fluorescence intensity of E-cadherin in H322 and H358 cells increased 1.5- to 2-fold after treatment with 17AAGA (80 nmol/L for 48 hours) (Fig 2A). The percentages of positively stained cells also increased significantly after 17AAGA treatment in these cell lines (63% ± 13% and 58% ± 10% of 17AAGA-treated cells vs 47% ± 7% and 38% ± 8% of untreated H358 and H322 cells; $p = 0.05$ and $p = 0.02$, respectively). No upregulation of this adhesion molecule was noted in H460 and H661 cells. Although diffuse cytoplasmic staining for E-cadherin was noted both in control and 17AAGA-treated cells, intense fluorescence indicating localization of E-cadherin to the cell membrane was only observed in treated H358 and H322 cells. No such membrane localization was noted in H460 or H661 cells after 17AAGA treatment (Fig 2B).

Downregulation of MMP-9 Secretion

Continuous exposure of NSCLC cells to either 20 or 80 nmol/L of 17AAGA significantly inhibited MMP-9 secretion in a dose-dependent manner, with an overall reduction of up to 50% relative to baseline control levels (Fig 3A). Moreover, incubation of H358 and H322 cells, which express high levels of both erbB1 and erbB2 receptors with agonistic recombinant human EGF or heregulin-α, augmented secretion of MMP-9 by 35% to 50% relative to baseline. 17AAGA treatment completely blocked ligand-mediated upregulation of MMP-9 production in these two cell lines (Fig 3B).

Suppression of VEGF Secretion by 17AAGA

NSCLC cells differed widely in their ability to secrete VEGF into the culture media. Values ranged from approximately 1,000 pg/mL/24 h/10^6 cells (H460, H322) to as high as 15,000 pg/mL/24 h/10^6 cells (H358) (Fig 4A). Cobalt chloride ($CoCl_2$), which simulates hypoxic conditions by interfering with cellular oxygen sensing mechanisms [14], induced significant upregulation of VEGF secretion (Fig 4A). Forty-eight-hour exposure to 17AAGA (80 nmol/L) significantly suppressed basal VEGF secretion in cultured lung cancer cells, with the magnitude of inhibition ranging from 10% to 50%. Furthermore, 17AAGA suppressed hypoxia-induced upregulation of VEGF secretion; the magnitude of inhibition in treated cells ranged from 30% to 45% relative to untreated "hypoxic" cells. To confirm these findings, cells were incubated in a hypoxic chamber (95% N_2 and 5% O_2). As expected, profound augmentation of VEGF secretion was noted in response to hypoxia, which could be effectively inhibited by 17AAGA (either 80 or 160 nmol/L) in a dose-dependent manner in all cell lines examined (Fig 4B).

Inhibition of Matrigel Membrane Invasion

The ability of cancer cells to migrate through the artificial extracellular matrix membrane, Matrigel, frequently correlates with their invasiveness in vivo [16]. Forty-eight-hour exposure to 17AAGA (80 nmol/L) significantly inhibited the ability of H322 and H358 cells to migrate through Matrigel. This inhibitory effect of 17AAGA was profound in H322 cells, with up to a 60% reduction in the number of cells invading through the membrane (109 ± 28 cells/5 HPF of 17AAGA-treated cells vs 293 ± 42 cells/5 HPF in untreated control cells; $p < 0.001$) (Fig 5). 17AAGA inhibited the invasiveness of H358 cells by approximately 40% (116 ± 8 cells/5 HPF of 17AAGA-treated cells vs 190 ± 14 cells/5 HPF of control cells; $p < 0.01$).

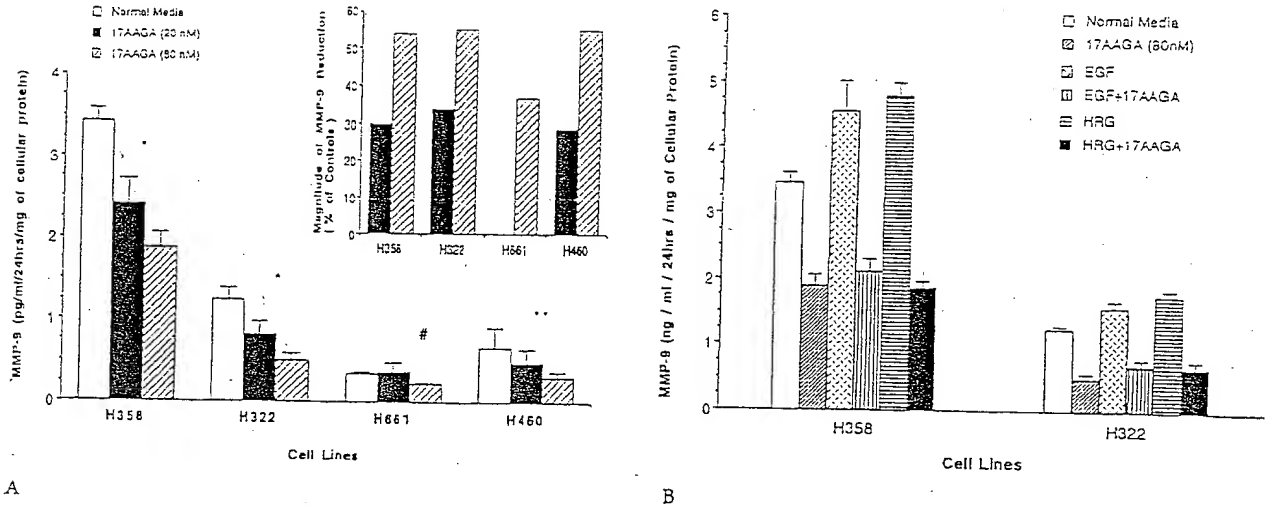

*Fig 3. (A) ELISA analysis of MMP-9 secretion by NSCLC cells, grown in the absence or presence of 17AAGA. Exposure of NSCLC cells to 17AAGA resulted in a dose-dependent reduction of MMP-9 levels in the conditioned media (*p < 0.001 vs normal media, #p < 0.01 17AAGA [80 nmol/L] vs normal media, ¯p < 0.05 17AAGA [80 nmol/L] vs normal media). The magnitude of inhibition of MMP-9 production is displayed in the upper right graph. Results are mean ± SD of four independent experiments. (B) Suppression of growth factor-mediated upregulation of MMP-9 secretion by 17AAGA (80 nmol/L) in H322 and H358 cells. Incubating H322 or H358 cells with 20 ng/mL of either epidermal growth factor (EGF) or heregulin α (HRG) for 48 hours induced 25% to 40% upregulation of MMP-9 secretion, which was effectively inhibited by 17AAGA. Results are means ± SD of three independent experiments.*

Comment

Better appreciation of the genetic and epigenetic factors that govern malignant transformation and metastasis may facilitate the development of more specific anticancer therapies. In addition to the development of drugs that specifically target the cell cycle machinery, considerable efforts have been focused on the evaluation of novel biologic or pharmacologic agents that suppress tumor growth or invasion by inhibiting neoangiogenesis or matrix metalloprotease activity. Activation of erbB protooncogenes profoundly disrupts cell cycle regulation [17], and enhances the expression of "pro-metastasis" phenotypes, namely decreased E-

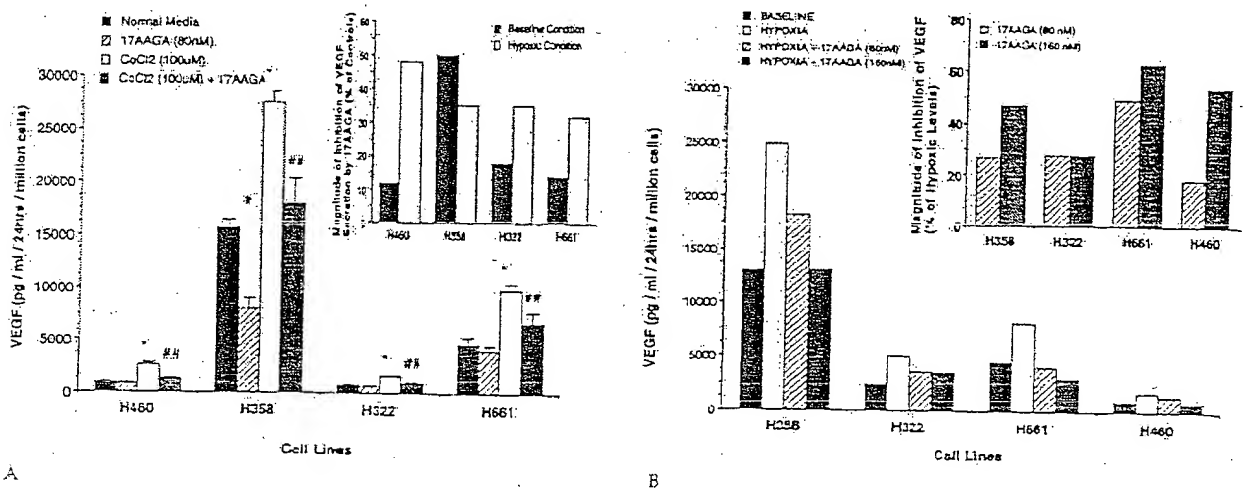

*Fig 4. (A) ELISA analysis of basal and hypoxia-stimulated VEGF secretion by 17AAGA. Significant upregulation of VEGF secretion into the culture supernatants by $CoCl_2$-simulated hypoxic condition was observed in all cell lines (*p < 0.001). 17AAGA at 80 nmol/L substantially suppressed the baseline (in H358 cells) and hypoxia-induced VEGF (in all four cell lines) secretion (*p < 0.001 vs baseline controls and **p < 0.001 versus hypoxia controls). The magnitude of inhibition of VEGF secretion by 17AAGA (expressed as percentages of baseline or hypoxia controls) is displayed in the upper right graph. Data are mean ± SD of three independent experiments. (B) ELISA analysis of VEGF levels in culture supernatants after physical hypoxia (< 5% O_2) with or without 17AAGA (80 or 160 nmol/L). The magnitude of 17AAGA-mediated inhibition of VEGF secretion (expressed as percentages of hypoxia controls) is displayed in the upper right graph. Data from a representative experiment are shown in this graph.*

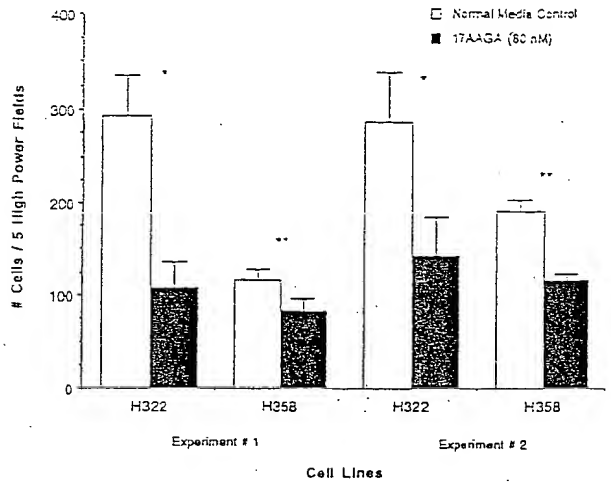

Fig 5. Inhibition of H322 and H358 cell invasion through Matrigel. Exposure of cells to 80 nmol/L 17AAGA for 48 hours reduced their invasion potential by 25% to 50% of that of normal cells. Data are means ± SD; each independent experiment was done in quadruplicate ($p < 0.005$, **$p < 0.05$).*

cadherin expression, increased VEGF and MMP secretion, as well as increased invasion through Matrigel [8–10]. These experimental results correlate closely with observations regarding c-erbB overexpression and aggressive clinical behavior of solid tumors [4–7]. These data provide the rationale for the development of treatment strategies specifically designed to abrogate expression or function of the c-erbB signal transduction pathways. Antagonistic anti-erbB1 and anti-erbB2 monoclonal antibodies, although not always effectively inhibiting tumor cell proliferation, have been shown to significantly upregulate E-cadherin expression, diminish VEGF and MMPs secretion, and reduce chemotaxis through extracellular matrix in vitro [10, 11]. Whereas these monoclonal antibodies may have limited clinical use from technical issues pertaining to delivery of macromolecules to tumor cells, low-molecular weight compounds such as 17AAGA that specifically inhibit erbB-mediated signal transduction pathways at nanomolar concentrations are of particular relevance.

In the present study, we sought to investigate the ability of 17AAGA to modulate expression of E-cadherin, MMP-9, and VEGF, each of which has been implicated in regulation of metastatic potential in tumor cells. The initial step of invasion and metastasis is the dissociation of cancer cells from the primary tumor mass resulting from aberrant expression of a variety of cell surface adhesion molecules, including integrin, immunoglobulins, secretins, and cadherins; the cadherins appear to be critical regulators of this process [18]. Cadherins are calcium-dependent transmembrane glycoproteins that mediate homophilic adhesion between cells. E-cadherin plays an important role in maintaining integrity of epithelial tissue; decreased E-cadherin expression or function correlates with tumor dedifferentiation, increased invasiveness, and lymph node metastases in a number of human carcinomas including lung, breast, esophagus, and prostate [16, 18]. E-cadherin has been referred to as an "antimetastasis" adhesion molecule, because the high propensity for metastasis formation in E-cadherin-negative cells can be reversed by restoration of expression of this adhesion molecule [19]. Previous studies have indicated an inverse relationship between erbB1 activation and E-cadherin expression in squamous cell cancers of skin and esophagus, as well as breast carcinomas [11, 20]. Upregulation of E-cadherin expression and inhibition of chemotaxis has been observed in H322 cells after exposure to an antagonistic monoclonal antibody directed against the erbB1 receptor [11].

MMPs are enzymes secreted by normal as well as cancer cells that degrade extracellular matrix and influence cell motility, tissue implantation, and angiogenesis. Considerable evidence indicates that MMP expression is increased in cancers relative to adjacent normal tissue, and levels of MMP expression correlate with tumor invasiveness and distant metastases [21]. There exist at least 10 isoforms of these proteases, each of which has unique substrate specificity. Secretion of MMPs is regulated by growth factors, some of which activate erbB1 or erbB2 mitogenic pathways. Inhibition of MMP activity either by recombinant tissue inhibitor of MMP or pharmacologic agents such as batimastat or marimastat decreases tumor growth, invasion, and metastasis in vivo [21]. More interestingly, reduction of MMP levels or inhibition of MMP activity has also been shown to suppress angiogenesis in vitro and in vivo [21].

Tumors smaller than 1 to 2 mm in diameter can receive nutrients by diffusion, but continued growth of the lesions is predicated on neoangiogenesis, which is regulated by complex mechanisms mediated by a balance between proangiogenic and antiangiogenic cytokines present simultaneously in the tumor and normal stromal tissues [22]. VEGF is one of the most potent proangiogenic cytokines, and secretion of VEGF by tumor cells may be sufficient to ensure neovascularization. The extent of neovascularization correlates with aggressive chemical behavior in a variety of malignancies including breast or prostate cancers and melanomas; vascular density and VEGF levels in tumor tissue are significant, independent predictors of systemic recurrence and diminished survival in patients with stage I NSCLC.

Although tumor dissemination, itself, does not require angiogenesis, interruption of angiogenesis should prevent the growth of metastatic deposits [22]. This is the basis of antiangiogenesis therapies using monoclonal antibodies against circulating VEGF or VEGF receptors on endothelial cells. Another strategy to inhibit angiogenesis involves targeting oncogene or tumor suppressor gene mutations directly influencing VEGF transcription through the use of Herceptin in breast cancer patients whose tumors overexpress erbB2, or potentially, by restoration of p53 expression using gene therapy techniques [10, 23]. Our approach

has been to use a pharmacologic agent to achieve similar endpoints while avoiding monoclonal antibodies or cumbersome, inefficient adenoviral vectors that may have limited use in clinical settings. Conceivably, the in vivo antiangiogenesis effect of 17AAGA may be more pronounced than anticipated on the basis of our in vitro data because this compound suppresses VEGF expression as well as MMP-9, another potent mediator of neoangiogenesis.

Migration through Matrigel depends on a cell's ability to detach from a multicellular aggregate, degrade extracellular matrix, and undergo chemotaxis. The relative contribution of each of these phenotypes to cell invasiveness is not known. 17AAGA-mediated inhibition of cell invasion through Matrigel is the most concrete in vitro evidence of the antimetastatic activity of this compound. The mechanisms responsible for 17AAGA-mediated upregulation of E-cadherin, as well as inhibition of tumor-derived VEGF and MMP-9 secretion, most likely depend on the depletion of erbB2 or erbB1 proteins and subsequent decreased mitogenic stimulation via erbB pathways. This notion is supported by the fact that these effects have been observed in cancer cells after treatment with antagonistic monoclonal antibodies against erbB1 and erbB2 receptors [10, 11]. However, additional mechanisms unrelated to inhibition of erbB signal transduction may be relevant given the effects of 17AAGA on a variety of other cell cycle regulatory proteins, including Raf-1 and cyclin-dependent kinase 4 [13].

In vivo toxicity profiles of geldanamycin and 17AAGA have been documented in small-animal models; renal and hepatic toxicities are dose-limiting events [24]. However, the nanomolar concentrations required to mediate the "antimetastasis" effects are well below the maximal tolerable doses reported in animal toxicity studies [24]. Underlying mechanisms notwithstanding, our findings extend those pertaining to the antiproliferative effects of 17AAGA. These current data, together with our previous observations concerning the ability of 17AAGA to sensitize NSCLC cells to paclitaxel [25], provide impetus for the evaluation of 17AAGA in lung cancer patients.

References

1. Walsh GL, O'Connor M, Willis KM, et al. Is follow-up of lung cancer patients after resection medically indicated and cost-effective? Ann Thorac Surg 1995;60:1563–70.
2. Logan DM, Lochrin CA, Darling G, et al. Adjuvant radiotherapy and chemotherapy for stage II or IIIA non-small-cell lung cancer after complete resection. Provincial Lung Cancer Disease Site Group. Cancer Prev Control 1997;1:366–78.
3. Meyer T, Hart IR. Mechanisms of tumour metastasis. Eur J Cancer 1998;34:214–21.
4. Veale D, Kerr N, Gibson GJ, Kelly PJ, Harris AJ. The relationship of quantitative epidermal growth factor receptor expression in non-small cell lung cancer to long term survival. Br J Cancer 1993;162–5.
5. Volm M, Drings P, Wodrich W. Prognostic significance of the expression of c-fos, c-jun and c-erbB-1 oncogene products in human squamous cell lung carcinomas. J Cancer Res Clin Oncol 1993;119:507–10.
6. Slamon DJ, Clark GM, Wong SG, et al. Human breast cancer: correlation of relapse and survival with amplification of the HER-2/neu oncogene. Science 1987;235:177–82.
7. Hsieh CC, Chow KC, Fahn HJ, et al. Prognostic significance of HER-2/neu overexpression in stage I adenocarcinoma of lung. Ann Thorac Surg 1998;66:1159–63.
8. Xu F-J, Stack S, Boyer C, et al. Heregulin and agnostic anti-p-185c-erbB2 antibodies inhibit proliferation but increase invasiveness of breast cancer cells that overexpress p185c-erbB2: increased invasiveness may contribute to poor prognosis. Clin Cancer Res 1997;3:1629–34.
9. Yu D, Wang S-S, Dulski KM, et al. c-erbB-2/neu overexpression enhances metastatic potential of human lung cancer cells by induction of metastasis-associated properties. Cancer Res 1994;54:3260–6.
10. Petit AM, Rak J, Hung MC, et al. Neutralizing antibodies against epidermal growth factor and ErbB-2/neu receptor tyrosine kinases down-regulate vascular endothelial growth factor production by tumor cells in vitro and in vivo: angiogenic implications for signal transduction therapy of solid tumors. Am J Pathol 1997;151:1523–30.
11. Al Moustafa AE, Yansouni C, Alaoui-Jamali MA, O'Connor-McCourt M. Up-regulation of E-cadherin by an anti-epidermal growth factor receptor monoclonal antibody in lung cancer cell lines. Clin Cancer Res 1999;5:681–6.
12. Supko JG, Hickman RL, Grever MR, Malspeis L. Preclinical pharmacologic evaluation of geldanamycin as an antitumor agent. Cancer Chemother Pharmacol 1995;36:305–15.
13. An WG, Schnur RC, Neckers L, Blagosklonny M. Depletion of p185/erbB-2, Raf-1, mutant p53 proteins by geldanamycin derivatives correlates with antiprolifeartive activity. Cancer Chemother Pharmacol 1997;40:60–4.
14. Goldberg MA, Schneider TJ. Similarities between the oxygen-sensing mechanisms regulating the expression of vascular endothelial growth factor and erythropoietin. J Biol Chem 1994;269:4355–9.
15. Albini A, Iwamoto Y, Kleinman HK, et al. A rapid in vitro assay for quantitating the invasive potential of tumor cells. Cancer Res 1987;47:3239–45.
16. Luo J, Lubaroff DM, Hendrix MJ. Suppression of prostate cancer invasive potential and matrix metalloproteinase activity by E-cadherin transfection. Cancer Res 1999;59:3552–6.
17. Lukas J, Bartkova J, Bartek J. Convergence of mitogenic signalling cascades from diverse classes of receptors at the cyclin D-cyclin-dependent kinase-pRb-controlled G1 checkpoint. Mol Cell Biol 1996;16:17–25.
18. Shibanuma H, Hirano T, Tsuji K, et al. Influence of E-cadherin dysfunction upon local invasion and metastasis in non-small cell lung cancer. Lung Cancer 1998;22:85–95.
19. Saiki I. Cell adhesion molecules and cancer metastasis. Jpn J Pharmacol 1997;75:215–42.
20. Tamura S, Shiozaki H, Miyata M, et al. Decreased E-cadherin expression is associated with haematogenous recurrence and poor prognosis in patients with squamous cell carcinoma of the oesophagus. Br J Surg 1996;83:1608–14.
21. Yu AE, Hewitt RE, Connor EW, Stetler-Stevenson WG. Matrix metalloproteinases. Novel targets for directed cancer therapy. Drugs Aging 1997;11:229–44.
22. Fidler IJ. Modulation of the organ microenvironment for treatment of cancer metastasis. J Natl Cancer Inst 1995;87:1588–92.
23. Bouvet M, Ellis LM, Nishizaki M, et al. Adenovirus-mediated wild-type p53 gene transfer down-regulates vascular endothelial growth factor expression and inhibits angiogenesis in human colon cancer. Cancer Res 1998;58:2288–92.
24. Eiserman JL, Sentz DL, Zuhowski EG, Ramsland TS. Plasma pharmacokinetics and tissue distribution of 17-allylaminogeldanamycin (NSC330507), a prodrug for geldanamycin, in

CD2F1 mice and Fisher 344 rats [Abstract]. Proceedings of the American Association for Cancer Research 1997;38:308.
25. Nguyen DM, Chen A, Mixon A, Schrump DS. Sequence-dependent enhancement of paclitaxel toxicity in non-small cell lung cancer by 17-allylamino 17-demethoxygeldanamycin. J Thorac Cardiovasc Surg 1999;118:908–15.

DISCUSSION

DR ROBERT J. KEENAN (Pittsburgh, PA): One of the things that struck me was the effect or lack of effect on normal human bronchial epithelium. There were at least a couple of cell lines that seemed to have similar erbB-1 and erbB-2 expression to the normals, and yet there was no effect of your treatment on normal tissue. Can you comment on what the potential is for toxicity to normal tissues when there is expression of these genes in normals?

DR NGUYEN: Thank you. I am glad you brought up that issue. In the two graphs that I showed where we used normal human bronchial epithelial cells as a normal control, I did not show the effect of 17AAGA. First of all, I can say that when the normal human bronchial epithelial cells are grown for 96 hours in vitro to reach confluence to mimic the normal condition in vivo, in which there are very few mitotic activities, treating these cells with 17AAGA has no effect on their viability. Treating these cells with 17AAGA indeed does decrease the erbB-1 and erbB-2 expression, but that does not affect cell viability. So we know from our experiments that this drug is not toxic to normal human cells grown to confluence in vitro. I have not tested normal human cells in terms of their ability to secrete MMP-9 or VEGF at all.

DR KEENAN: Sometimes there is differential gene expression in the metastasis compared with the primary tumor. Do you have any data on whether or not some of the antimetastatic effect might be related to those differences in gene expression and whether your treatment might be more or less effective because of that?

DR NGUYEN: That is a very insightful question. No, I have not looked into all the phenotypes. That might contribute to it. The "prometastasis" phenotypes evaluated in this project are those that have been shown to associate with or actively play a role in the process of metastasis formation, but not the metastasis deposit itself.

DR JOHN R. BENFIELD (Los Angeles, CA): Could you tell us a bit more about the cell lines that you used? There is always the problem as to whether cultured cell lines for lung cancer, which, are hard to perpetuate, do in fact represent what happens in lung cancer in humans. What were the cell lines that you used?

DR NGUYEN: The H460 is a large-cell carcinoma, the H322 and H358 cells are bronchoalveolar carcinoma, and H661 is a large-cell carcinoma. So they are all non-small cell lung cancer of different subtypes.

DR BENFIELD: And they have been perpetuated for how many passages? Are these well-established cell lines?

DR NGUYEN: Yes, these cells are well-established, available from ATCC.

DR BENFIELD: Thank you. You alluded to the fact that you are ready now for in vivo testing of the agent. There are at least two ways in which you could do that preclinically. There are hamsters, non-small cell lung cancer models that are rather well established (Benfield JR, Malkinson AM, Schuller HM, Sunday ME. Animal models of lung cancer. In: Kane MA, Bunn PA Jr., eds. Biology of Lung Cancer. New York: Marcel Dekker, 1998: 247–93). The other thing that you might want to consider is placing some of the human tumors into nude mice, and then trying the agent while the nude mice are accepting the tumor.

DR NGUYEN: Thank you very much. I appreciate your suggestion.

To be specific about what we are doing, we create either a tumor mass in the flank or actually inject the H358 cells intravenously via lateral tail veins of nude mice to create a metastasis model and then treat the animals at a different time point after tumor cell inoculation with 17AAGA. So this is the experiment that we are carrying out right now.

Cell, Vol. 89, 239–250, April 18, 1997, Copyright ©1997 by Cell Press

Crystal Structure of an Hsp90-Geldanamycin Complex: Targeting of a Protein Chaperone by an Antitumor Agent

Charles E. Stebbins,*‖ Alicia A. Russo,*‖
Christine Schneider,† Neal Rosen,§
F. Ulrich Hartl,‡ and Nikola P. Pavletich*
*Department of Biochemistry and Structural Biology
Cornell University Graduate School of Medical Sciences
New York, New York 10021
†Cellular Biochemistry and Biophysics Program
Memorial Sloan-Kettering Cancer Center
New York, New York 10021
‡Cellular Biochemistry and Biophysics Program and Howard Hughes Medical Institute
Memorial Sloan-Kettering Cancer Center
New York, New York 10021
§Cell Biology and Genetics Program and Department of Medicine
Memorial Sloan-Kettering Cancer Center
New York, New York 10021

Summary

The Hsp90 chaperone is required for the activation of several families of eukaryotic protein kinases and nuclear hormone receptors, many of which are proto-oncogenic and play a prominent role in cancer. The geldanamycin antibiotic has antiproliferative and antitumor effects, as it binds to Hsp90, inhibits the Hsp90-mediated conformational maturation/refolding reaction, and results in the degradation of Hsp90 substrates. The structure of the geldanamycin-binding domain of Hsp90 (residues 9–232) reveals a pronounced pocket, 15 Å deep, that is highly conserved across species. Geldanamycin binds inside this pocket, adopting a compact structure similar to that of a polypeptide chain in a turn conformation. This, and the pocket's similarity to substrate-binding sites, suggest that the pocket binds a portion of the polypeptide substrate and participates in the conformational maturation/refolding reaction.

Introduction

Geldanamycin, and its closely related analogs herbimycin and macbecin, are naturally occurring antitumor antibiotics (DeBoer et al., 1970; Omura et al., 1979; Ono et al., 1982). In the National Cancer Institute's (NCI) in vitro screen for antitumor agents, geldanamycin has shown potent activity, achieving 50% growth inhibition (GI_{50}) at concentrations as low as 13 nM against the most responsive cell lines, with a mean GI_{50} of 180 nM against all 60 of the tumor cell lines (Supko et al., 1995). Geldanamycin is active in mouse tumor models as well (Sasaki et al., 1979; Ono et al., 1982), and it has been selected for preclinical development as an antitumor agent by the NCI (Supko et al., 1995).

‖ These authors contributed equally to this work.

The antitumor effects of geldanamycin likely result from its ability to deplete cells of two broad classes of growth-regulatory signaling proteins: (1) proto-oncogenic protein kinases, including the erbB2 (Miller et al., 1994; Chavany et al., 1996) and EGF (Murakami et al., 1994) receptor tyrosine kinases, the v-src family of nonreceptor tyrosine kinases (June et al., 1990; Xu and Lindquist, 1993; Hartson and Matts, 1994; Whitesell et al., 1994), and the Raf-1 (Schulte et al., 1995; Schneider et al., 1996) and CDK4 Ser/Thr kinases (Stepanova et al., 1996), whose overexpression, or otherwise deregulation, has been observed in diverse human cancers (Bouchard et al., 1989; Hunter and Pines, 1994; Tronick and Aaronson, 1995); and (2) the nuclear hormone receptor family, including the estrogen and androgen hormone receptors (Smith et al., 1995; Nair et al., 1996; Whitesell and Cook, 1996), which can drive the growth of hormone-dependent cancers of the breast (Osborne et al., 1980) and prostate (Isaacs and Coffey, 1979), respectively.

Initially thought to be a nonspecific kinase inhibitor, geldanamycin's target has only recently been identified as the heat shock protein Hsp90 (Whitesell et al., 1994) and its endoplasmic reticulum homolog GP96 (Chavany et al., 1996). In eukaryotes, Hsp90 has dual chaperone functions participating both in the conformational maturation of the nuclear hormone receptors and the aforementioned protein kinases, and in the cellular stress response (Bohen and Yamamoto, 1994; Jakob and Buchner, 1994; Pratt and Welsh, 1994). These two processes are likely to have in common the ability of Hsp90, in cooperation with Hsp70 and other factors, to prevent protein aggregation and mediate the ATP-dependent refolding of heat-denatured proteins in vitro and in vivo (Freeman and Morimoto, 1996; Schneider et al., 1996).

The best-studied Hsp90-mediated conformational maturation is that of the nuclear hormone receptors, which require the Hsp90 system in order to acquire or maintain a state competent to bind hormone (Bresnick et al., 1989; Picard et al., 1990; Nathan and Lindquist, 1995). In this ATP-dependent reaction, an initial hormone receptor complex that contains Hsp90, Hsp70, and at least two cochaperones, p60 and Hip (p48), is in equilibrium with a complex in which the receptor is in a metastable, nearly mature state competent to bind hormone (Smith et al., 1995; Dittmar et al., 1996). This nearly mature complex lacks Hsp70, p60, and Hip, but contains two new proteins, p23 and one of the three large immunophilins, FKBP52, FKBP54, or CyP40 (Smith et al., 1995; Dittmar et al., 1996). Upon hormone binding, the receptor is released as an active transcription factor (Smith et al., 1995; Dittmar et al., 1996). Treatment with geldanamycin appears to block the conversion to the nearly mature complex, preventing hormone binding and activation, and results in the degradation of the hormone receptor (Whitesell and Cook, 1996).

The requirement for Hsp90 in the activation of the aforementioned protein kinases has been demonstrated both genetically (Xu and Lindquist, 1993; Aligue et al., 1994; Nathan and Lindquist, 1995) and biochemically

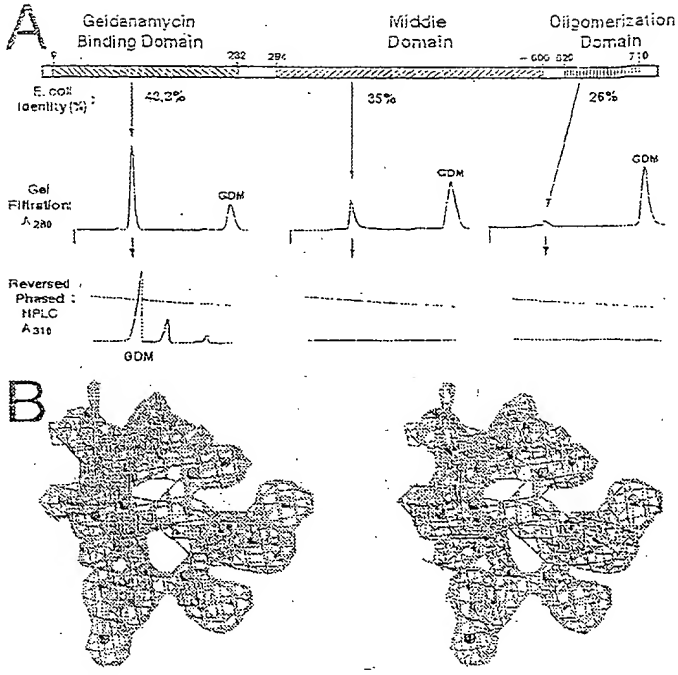

Figure 1. Geldanamycin Binds the N-Terminal Structural Domain of Hsp90

(A) The three structural domains of Hsp90, identified by proteolytic digestion, are indicated, together with their percent identity in the E. coli homolog. The oligomerization activity at the C-terminal portion has been described (Wearsch and Nicchitta, 1996). The digestion of residues 1–9 is consistent with this region being absent from most Hsp90 sequences except mammalian ones. To identify the geldanamycin-binding domain, the purified structural domains, at 1 μM, were incubated with 2.0 μM geldanamycin (GIBCO-BRL) each; the free drug was then separated on a gel filtration column, monitoring absorption at 280 nm, and the protein peaks (the C-terminal domain absorbed weakly at 280 nm for lack of tryptophans) were analyzed for the presence of geldanamycin by reverse-phase HPLC, with monitoring at 310 nm. The gel filtration protein peak of the N-terminal domain was the only one that contained geldanamycin; the molar ratio was determined to be approximately 1:1 based on UV absorption. The composition of the two secondary geldanamycin peaks observed in the reversed-phase chromatography is not clear, but they could also be produced by the addition of dithiothreitol in the absence of protein. Geldanamycin is abbreviated as GDM.

(B) Stereo view of the geldanamycin 2Fo-Fc electron density before any geldanamycin atoms were built into the Hsp90 model. The map was calculated at 2.0 Å and contoured at 1.0 sigma; also shown is the refined geldanamycin model in a ball-and-stick representation.

(Hartson and Matts, 1994; Chavany et al., 1996; Stepanova et al., 1996). This reaction is not as well understood, but it appears to involve a subset of the molecules found in the complexes with hormone receptors, as well as a protein kinase–specific cofactor, $p50^{Cdc37}$ (Whitelaw et al., 1991; Stancato et al., 1993; Cutforth and Rubin, 1994; Stepanova et al., 1996). For some of these kinases, such as Raf-1, Hsp90 association is a prerequisite for their trafficking to the plasma membrane (Schulte et al., 1995); for others, the mechanism of Hsp90-mediated activation is not yet understood. Again, geldanamycin interferes with Hsp90 function and induces the rapid degradation of these kinases by the proteosome system (Murakami et al., 1994; Schulte et al., 1995; Schneider et al., 1996; Stepanova et al., 1996).

In addition to its role in the conformational maturation of signal transduction molecules, the eukaryotic Hsp90 system participates in the refolding of certain thermally denatured polypeptides during the recovery of cells from heat stress (Borkovich et al., 1989). Using firefly luciferase as a model substrate, it was demonstrated that Hsp90 cooperates in this process with Hsp70, Hsp40 (a DnaJ homolog), p60, Hip, and p23 (Schumacher et al., 1994; Schneider et al., 1996). Thus, the Hsp90 complexes formed with the thermally denatured polypeptide resemble those of hormone receptors and protein kinases. Geldanamycin inhibits the Hsp90-mediated refolding of luciferase, both in vitro and in vivo, and, as a result, luciferase is retained in the Hsp90 complex in an unfolded, degradation-sensitive state (Schneider et al., 1996). This shifts the balance from refolding to the proteolytic degradation of the protein (Schneider et al., 1996). Such a mechanism might also explain how, under nonstress conditions, geldanamycin and its homologs cause the degradation of the signaling molecules.

To obtain insights into the function of Hsp90 in these conformational maturation/refolding processes and its inhibition by geldanamycin, we identified the geldanamycin-binding domain of Hsp90 (henceforth Hsp90-GBD), and we determined the crystal structures of this domain and of its complex with geldanamycin.

Results and Discussion

Isolation of the Geldanamycin-Binding Domain of Hsp90

To facilitate the structural study of the geldanamycin-Hsp90 interaction, we first used proteolytic digestion and determined that the bovine Hsp90 contains three structural domains (Figure 1A): an N-terminal domain of approximately 25 kDa, a middle domain of approximately 35 kDa, and a C-terminal domain of approximately 10 kDa. We then assayed the three corresponding recombinant domains of human Hsp90 for geldanamycin binding using gel filtration chromatography to remove excess drug and reverse-phase HPLC to detect the bound drug,

Table 1. Summary of Crystallographic Analysis

Diffraction Data and MIR Analysis

Crystal	Crystal Description	Resolution (Å)	Unique Reflections	Measured Reflections	Coverage (%)	R_{sym} (%)	R_{iso} (%)	Phasing Power	R_c
Native1	I222 (10°C)	2.30	13532	43812	98.0	4.4	—	—	—
Native2	I222 (−160°)	1.65	34516	361958	98.2	3.8	—	—	—
Native3	$P2_1$-Mg (−160°C)	2.20	11381	51794	97.7	3.5	—	—	—
GDM Complex	$P2_1$ (−160°C)	1.90	16906	86335	92.2	2.5	—	—	—
K_2AuCl_4	I222 (10°C)	2.50	10254	49642	94.6	5.7	17	2.43	0.54
K_2PtCl_4	I222 (10°C)	3.20	4713	20129	91.6	5.8	28	1.07	0.83
K_2PtBr_6	I222 (10°C)	3.20	4831	25025	93.1	4.7	22	0.75	0.90
$Sm(OAc)_3$	I222 (10°C)	3.20	4442	16281	86.0	7.1	30	0.65	0.92

Refinement and Analysis of Atomic Models

Crystal	Resolution (Å)	Reflections ($\|F\| > 2\sigma$)	Atoms Modeled (Protein, Water)	R_{cryst}/R_{free} (%, %)	rms Deviations (Bonds [Å], Angles [°], B Factor [Å²])
Native1	7.0–2.30	12445	1626, 96	16.9, 25.2	0.012, 1.7, 3.2
Native2	6.0–1.65	32524	1626, 335	19.4, 24.4	0.007, 1.6, 3.3
Native3	7.0–2.20	10845	1679, 246	18.9, —	0.010, 1.7, 3.2
GDM Complex	6.0–1.90	16080	1679, 288	18.9, —	0.009, 1.8, 3.2

Coverage is the percentage measured of the total reflections theoretically observable. $R_{sym} = \Sigma_h\Sigma_i \, |I_{hi} - I_h| \, / \, \Sigma_h\Sigma_i \, I_{hi}$, where I_h is the mean intensity of the i observations of the unique reflection h. $R_{iso} = \Sigma \, | F_{PH} - F_P | \, / \, \Sigma |F_P|$, where F_P and F_{PH} are the native and derivative structure factor amplitudes, respectively. Phasing power $= [F_{H(calc)}{}^2 \, / \, (F_{PH(obs)} - F_{PH(calc)})^2]^{1/2}$, where $F_{PH(obs)}$ and $F_{PH(calc)}$ are the observed and calculated derivative structure factors, respectively. $R_c = \Sigma \| F_{PH} \pm F_P | - F_{H(calc)} | \, / \, \Sigma | F_{PH} \pm F_P |$, for centric reflections only, where $F_{H(calc)}$ is the calculated heavy atom structure factor. Figure of merit $= \langle \Sigma \, P(\alpha) \exp(i\alpha) \, / \, \Sigma \, P(\alpha) \rangle$, where $P(\alpha)$ is the probability distribution for the phase α. Atoms modeled discounts hydrogen atoms. $R = \Sigma | F_o - F_{calc} | \, / \, \Sigma F_o$, where F_{calc} is the calculated protein structure factor from the atomic model; R_{free} is the R factor calculated using 10% of the reflection data chosen randomly and omitted from the refinement process, whereas R_{cryst} is calculated with the remaining data used in the refinement. rms, bond lengths and angles are the deviations from ideal values; the rms deviation in B factors is calculated between covalently bonded atoms.

and determined that the N-terminal domain, which has the highest sequence conservation among the three domains, binds geldanamycin at an approximately one molar ratio (Figure 1A).

In crystallization experiments, the geldanamycin-binding domain of human Hsp90 (Hsp90-GBD, residues 9–236) produced two distinct crystal forms in which the structure differs by a local conformational change. The geldanamycin–Hsp90-GBD complex crystallized in only one of the two forms. The two apo-Hsp90-GBD structures have been determined at 1.65 and 2.2 Å resolution, respectively, and the structure of the geldanamycin complex at 1.9 Å resolution (Table 1, Figure 1B).

Overall Structure of the Geldanamycin–Hsp90-GBD Complex

The Hsp90-GBD has nine helices and an antiparallel β sheet of eight strands that together fold into an α+β sandwich (Figures 2A–2D). One face of the β sheet is hydrophobic and packs against a layer of five helices; four of these helices (H1, H2, H4, and H9) pack flatly against the β sheet, with their axes parallel to the β strands, while H7 packs against the β sheet at a steeper, almost perpendicular angle. The structure has a second layer of helices that pack on the first layer (H5 and H6), and two smaller helices (H3 and H8) at the periphery of the sandwich (Figures 2A–2D). It is noteworthy that four of the nine helices are of the 3_{10} type and comprise 11.2% of the amino acids, which is significantly higher than the 3.4% average in the protein database (Barlow and Thornton, 1988). At its center, the helical face of the sandwich has a wide opening that extends into the hydrophobic core of the structure and results in a pronounced pocket, about 15 Å deep (Figures 2B–2D). The pocket has the β sheet as its base and three helices and a loop as its walls, and contains residues highly conserved across species (Figure 3). The helical face of the sandwich also has a surface groove that leads into the pocket.

In the complex, the 560 Da geldanamycin adopts a compact conformation and binds inside the pocket, filling all but its deepest portion (Figures 2A–2E). The benzoquinone group of geldanamycin binds near the entrance of the pocket, whereas the ansamycin ring, having dimensions similar to those of a five amino acid polypeptide in a turn conformation, inserts into the pocket. There is extensive, though not complete, surface complementarity between geldanamycin and the pocket, and this allows for a high density of van der Waals contacts. Although hydrogen bond contacts are fewer, there being only five of them, one pair from the geldanamycin carbamate group (Figure 2E) can be reasonably described as one of the most important intermolecular interactions in the complex.

The entrance and width of the pocket are likely regulated by a conformational change, as evidenced by structural and positional changes in three helices and a loop in the two different apo-Hsp90-GBD crystal forms (Table 1). One of the conformations, which is essentially identical to that observed in the crystals of the geldanamycin–Hsp90-GBD complex, has a wide enough entrance to allow geldanamycin binding. The other conformation has a narrower entrance, and it would be incompatible with geldanamycin binding.

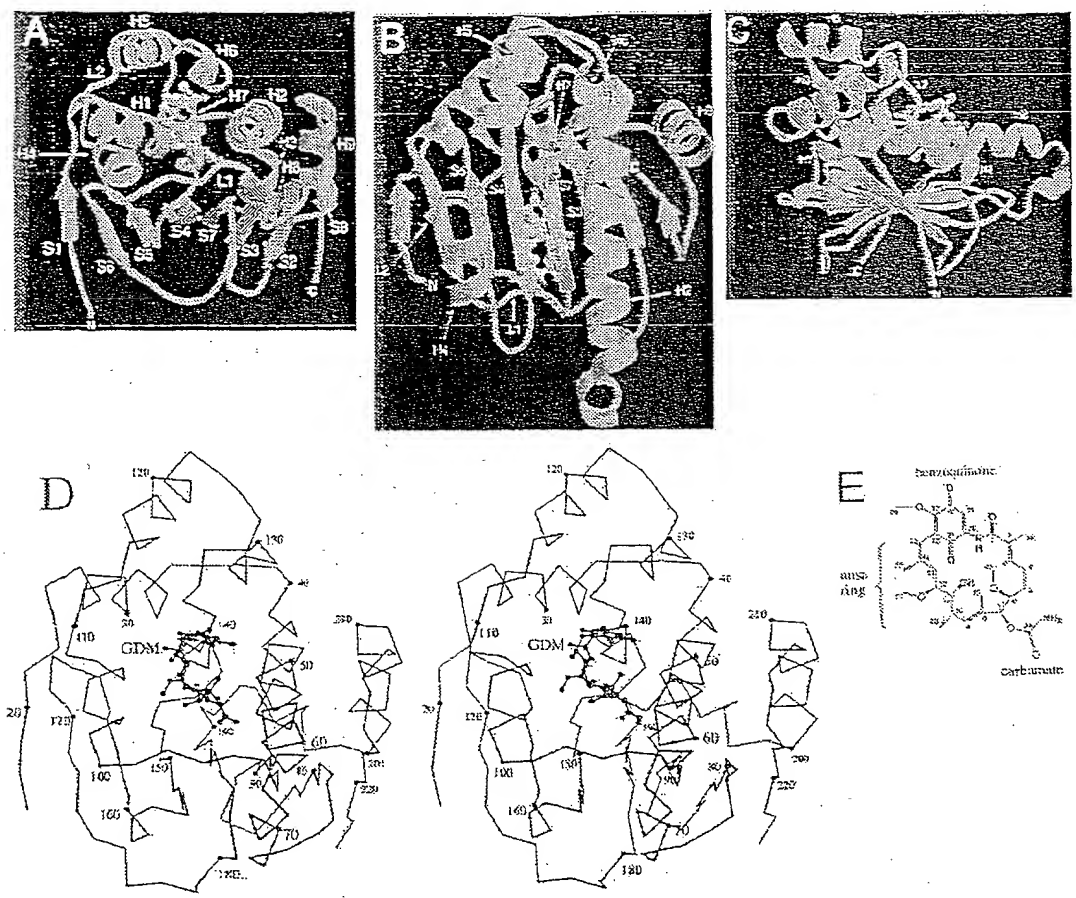

Figure 2. The Hsp90-GBD Is an α+β Sandwich with a Deep, Conserved Pocket where Geldanamycin Binds

(A–C) Three approximately orthogonal views of the complex. Geldanamycin atoms are colored yellow for carbon, red for oxygen, and blue for nitrogen. In (A), all secondary structure elements are labeled, whereas in (B) and (C), only those discussed in the text are labeled for clarity. Images were prepared with the programs MOLSCRIPT (Kraulis, 1991) and RASTER3D (Merritt and Murphy, 1994).

(D) Stereo view of the Cα trace of the complex, with every 10th residue numbered and its Cα atom highlighted as a sphere.

(E) Chemical structure of geldanamycin.

Architecture and Properties of the Geldanamycin-Binding Pocket

The pocket can be described as a flat-bottomed cone: it is about 15 Å deep, 12 Å in diameter near its entrance, 8 Å midway down, and wide enough at the bottom to hold three water molecules (Figure 4A). The bottom of the pocket is formed by the central portion of the antiparallel β sheet (strands S3, S4, and S7), and the walls by the H2, H4, and H7 helices and the L1 loop (Figure 3). The pocket is deepest by the H7 helix, which packs at an almost perpendicular angle to the β sheet bottom, and is shallowest by the L1 loop. The pocket is of mixed hydrophobic and polar character, with roughly half of the 17 amino acids lining its interior being hydrophobic, a quarter polar, and a quarter charged (these residues are Leu48, Asn51, Asp54, Ala55, Lys58, Ile91, Asp93, Ile96, Gly97, Met98, Asn106, Leu107, Lys112, Gly135, Phe138, Val150, Thr184, and Val186; Figure 3). Although the pocket becomes increasingly hydrophobic toward the bottom, it retains one charged and one polar residue at its deepest portion (Asp93 and Thr184 from the β sheet).

The Hsp90-GBD domain is highly conserved across species, with 43% of its residues identical in the Escherichia coli Hsp90 homolog. The structure reveals that the conserved residues are not distributed homogeneously on the structure, but instead show a striking tendency to cluster in and around the pocket, with 82% of the residues lining the interior of the pocket being invariant from E. coli to humans (Figures 3 and 4B). This identifies the pocket as holding the key to understanding the function of this domain. Of particular interest is Asp93, because it is at the pocket bottom in an otherwise mostly hydrophobic environment, and because it is conserved in all known Hsp90 homologs from 35 species.

Supporting a functional significance for this pocket are mutations in the yeast homolog of Hsp90 (Hsp82) that result in either temperature-sensitive or reduced activity phenotypes (Bohen and Yamamoto, 1993; Sullivan and Toft, 1993; Kimura et al., 1994; Nathan and

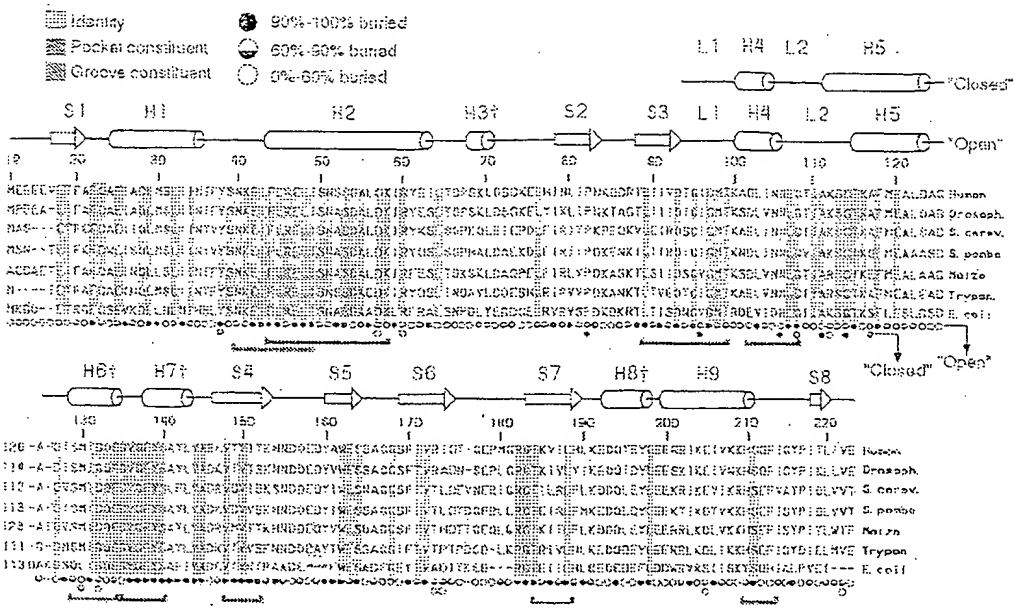

Figure 3. Alignment of Hsp90-GBD Sequences from Several Diverse Species

Secondary structure elements for the $P2_1$ (open) form are indicated above the sequence together with the changes observed in the 1Z22 (closed) form. Invariant residues are highlighted in yellow, residues that make up the pocket are underlined in red, and residues that make up the surface groove are underlined in blue. Residue solvent accessibilities are indicated with circles (open, half-closed, or closed). The dagger symbol indicates 3_{10} helices.

Lindquist, 1995), as well as a mutation in the Drosophila Hsp90 (Hsp83) that impairs signaling by the Sevenless receptor tyrosine kinase (Cutforth and Rubin, 1994). These mutations map either in the pocket (Ala55Val, Gly95Ser, Gly183Asp) or in the immediate vicinity of the pocket (Thr36Asn, Ser50Leu, Ala111Thr, Thr115Ile), and

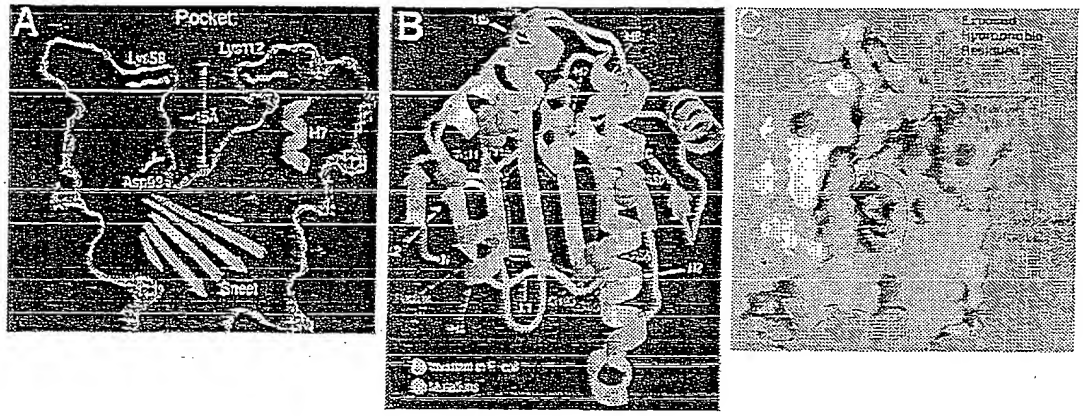

Figure 4. The Hsp90-GBD Has a Conserved Pocket That Is 15 Å Deep

(A) A thin slice of the Hsp90-GBD molecular surface, depicted as a white net, stressing the pocket dimensions. Red indicates surface portions with a negative electrostatic potential, and blue those with a positive potential. The pocket is mostly polar at its entrance (Lys58 and Lys112 are shown), and it becomes predominantly hydrophobic near the bottom, except for Asp93. The approximate locations of the β sheet and of the H7 helix are indicated; the H2 helix would be approximately above the plane of the figure, whereas the H4 helix would be below. This image was prepared with the program GRASP (Nicholls et al., 1991).

(B) Yellow highlights the positions of residues invariant in the E. coli Hsp90 homolog; magenta highlights residues, shown in space filling representation, where either temperature-sensitive or inactivating mutations map.

(C) Surface representation indicating the pocket and groove. Also indicated, in yellow, are several patches of exposed hydrophobic amino acids in the vicinity of the pocket and groove. These hydrophobic residues are: Phe213 to the right of the groove in this view; Ala117, Ala121, Ala124, Ala126, Met130, and Phe134 to the left of the groove; and Phe20, Ile104, Ala111, and Ile112 to the left of the pocket (prepared with the program GRASP).

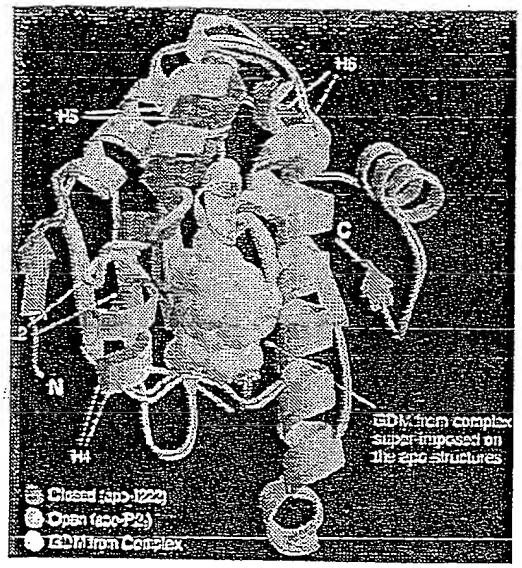

Figure 5. A Conformational Change Alters the Size and Accessibility of the Pocket in the Absence of Geldanamycin

The secondary structural elements that undergo positional and conformational changes are shown in red for the I222 (closed) and in cyan for the P2, (open) apo-Hsp90-GBD crystal forms. Geldanamycin, in space-filling representation, is superimposed on the figure to stress the effects that the conformational change has on the pocket size.

the structure suggests that most of these mutations would disrupt the structural integrity of the pocket (Figures 3 and 4B).

Leading to the pocket, there is a surface groove formed by the H6 and H9 helices on the sides, and the H2 helix at its bottom (Figure 4C). Its shape is not as pronounced as the pocket, being shallower (about 7–8 Å), broader (about 15 Å), and mostly polar. This groove is conserved, although not as well as the pocket, with 73% of the residues lining its concave surface identical in the E. coli homolog (these residues are Asn40, Glu42, Ile43, Arg46, Glu47, Ser50, Ser129, Gln133, His210, Ser211, and Ile214; Figure 3). Since many of these residues are polar or charged, without any significant roles in the structural integrity of this domain, their conservation suggests that the groove may participate in intermolecular interactions important for Hsp90 function.

Conformational Change Alters the Size and Accessibility of the Pocket

An approximately 35 amino acid region of the Hsp90-GBD structure, consisting of the H4-L2-H5-H6 secondary structure elements (residues 100–134), has two different conformations in the two different Apo-Hsp90-GBD crystal forms (Table 1, Figures 3 and 5). We have termed these the "open" and "closed" conformations because they result in different pocket size and accessibility, with only the open conformation being compatible with geldanamycin binding.

At the center of the open-to-closed conformational change is a displacement of the L2 loop into the pocket by more than 9 Å (Cα–Cα distance), whereupon the L2 loop replaces the H4 helix as one of the pocket walls. The motion of the L2 loop is facilitated by portions of the H4 and H5 helices undergoing helix-to-coil and coil-to-helix transitions, respectively (Figures 3 and 5). The H4 and H5 helices also are displaced, by up to 6 Å. The functional consequence of this conformational change is that the L2 loop acts as a gate that constricts the pocket entrance from a width of 12 Å to 8 Å (Figure 5).

These two alternate conformations have clear electron density in their respective crystal forms and are associated with well-packed side chain arrangements (Figure 3). It is conceivable that this conformational change in vitro may mimic a process that occurs in vivo and may be involved in the regulation or functioning of the pocket. Supporting an in vivo role for the closed conformation is the Ala111Thr mutation on the L2 loop that results in a temperature-sensitive phenotype in yeast (Kimura et al., 1994). This mutation would disrupt the closed conformation structure where Ala111 is fully buried and participates in the hydrophobic packing of the loop, but not the open conformation structure where Ala111 is fully solvent exposed with no apparent structure-stabilizing role.

Structure of Geldanamycin

Geldanamycin consists of a closed ansa ring with a planar benzoquinone embedded in it (Figure 2E). The ansa ring is sterically hindered because (1) its backbone consists of a planar amide and three carbon-carbon double bonds (two of them arranged in a 1,3 diene), and (2) of its sixteen backbone atoms, nine carry nonhydrogen substituents: a carbonyl, a carbamate ($-OC(O)NH_2$), a hydroxyl, two methoxy, and four methyl groups (Figure 2E).

Hsp90-bound geldanamycin is highly compact and internally well packed (overall dimensions of about 9 × 9 × 9 Å). Its ansa ring is folded over the benzoquinone, forming a C-clamp-like structure, with the benzoquinone forming the top of the (C) and the ansa ring forming the stem and bottom of the (C) (Figure 6A). Two of the methyl groups from the ansa ring are centrally positioned to maximize intramolecular van der Waals contacts: the C25 methyl group from the tip of the ansa ring packs with the benzoquinone, thus bridging the top and bottom halves of the (C), and the C28 methyl group packs with the diene carbon atoms, bridging the two sides of the ansa ring (Figure 6A).

This compact conformation differs from those observed with free geldanamycin (Rinehart and Shield, 1976) or herbimycin (Furusaki et al., 1980), which crystallize from organic solvents in significantly more open, extended conformations. The differences are likely due, in part, to the loss of coplanarity between the amide group and the benzoquinone in Hsp90-bound geldanamycin, as well as to the differences in the crystallization solvents.

Geldanamycin–Hsp90 Contacts

The tip of the geldanamycin ansa ring (bottom of [C]), which has the carbamate, C23 methoxy, and C25 and

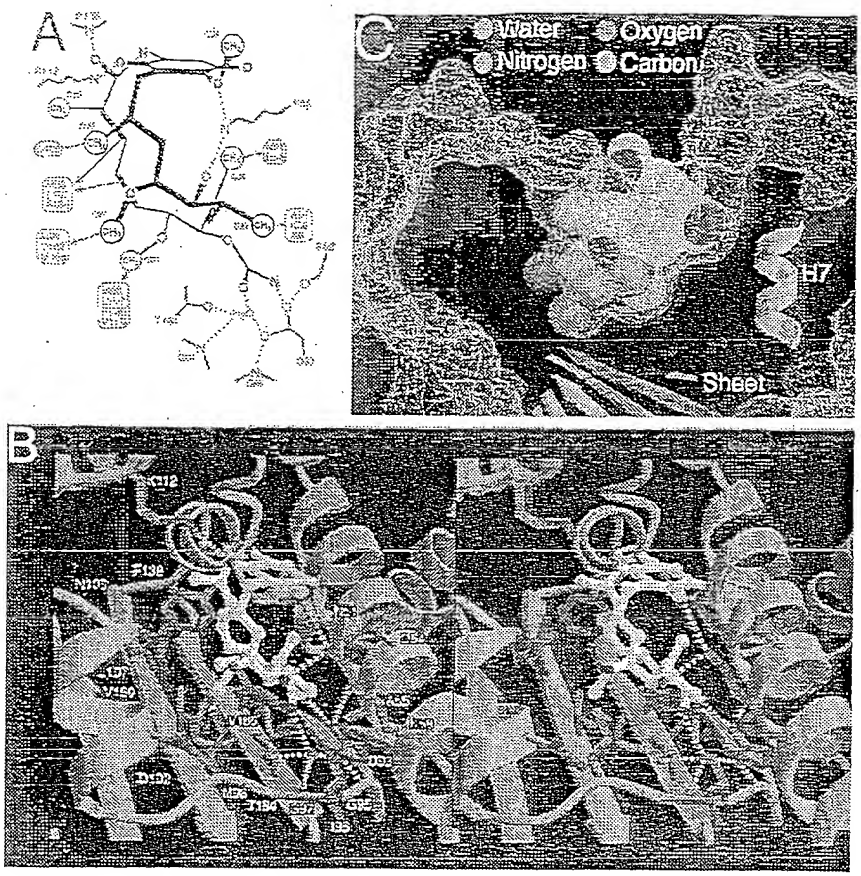

Figure 6. Hsp90-Bound Geldanamycin Adopts a Compact Conformation Reminiscent of the Letter (C) and Binds Hsp90 by Inserting the Tip of Its Ansa Ring inside the Pocket

(A) Diagram of the bound geldanamycin conformation summarizing the hydrogen bond (dotted lines) and van der Waals (arrows) contacts it makes with Hsp90 residues, colored brown. The oxygen atoms of geldanamycin are shown in red, nitrogen atoms in blue, and methyl groups as closed circles; the remaining carbon atoms are not explicitly shown.

(B) Stereo view of the geldanamycin–Hsp90-GBD interactions. Geldanamycin is colored as in Figure 2A, and Hsp90 residues that make up the pocket are colored magenta. Hydrogen bonds are indicated by green dotted lines, and the water molecule that bridges the geldanamycin carbamate group with Asp93 is shown as a red sphere.

(C) Geldanamycin, in space-filling representation, adopts a structure that is, overall, complementary to the pocket, shown as a blue molecular surface net. Although the fit is extensive, there remains a buried cavity at the interface with three trapped water molecules in it (colored magenta), while a fourth water molecule hydrogen bonds with the carbamate group and Asp93. The reduced complementarity near the pocket entrance is evident as gaps between the geldanamycin atoms and the Hsp90-GBD surface. Orientation is similar to that of Figure 4A.

C26 methyl group substituents, binds near the bottom of the Hsp90 pocket and makes a high density of van der Waals contacts, whereas the benzoquinone (top of [C]) is positioned near the entrance of the pocket and makes only a few contacts (Figures 6A and 6B). There is extensive surface complementarity between the compact geldanamycin structure and the pocket, as attested by the fact that a remarkable 85% of the surface area of geldanamycin is buried in the complex (609 Å^2 out of 719 Å^2).

The most critical portion of the interface is likely to be a hydrogen bond network between the geldanamycin carbamate group and the Asp93 side chain from Hsp90, which are buried at the pocket bottom in an otherwise mostly hydrophobic environment. The carbamate amino group makes a hydrogen bond to one of the Asp93 side chain oxygen atoms, and its carbonyl oxygen atom makes a water-bridged hydrogen bond with the other Asp93 side chain oxygen atom (Figures 6A and 6B). The Asp93 side chain, which has an identical conformation in the Apo-Hsp90 structures, also hydrogen bonds to the Ser52 OH and the backbone amide of residue 95. This hydrogen bond network is buried about 10 Å away from the nearest solvent surface, and the low dielectric constant of this environment would significantly increase the coulombic attraction due to the partial charges. The importance of this hydrogen bond network is supported by structure activity studies demonstrating

that the removal of the carbamate group, or the attachment of additional atoms to it, completely abolished geldanamycin activity (Schnur et al., 1995b).

At the tip of the ansa ring, the carbamate group contact is flanked by the C23 methoxy and C25 and C26 methyl groups making high density van der Waals contacts with the bottom and sides of the pocket (Figures 6A and 6B). Although the surface complementarity at the pocket bottom is extensive, there remains a buried cavity filled with three water molecules near the C23 methoxy and the carbamate groups (Figure 6C). It is conceivable that the cellular substrates of Hsp90 can fill this cavity as well. Modifications to this portion of geldanamycin, for example by adding to the C23 position a group of 4–6 nonhydrogen atoms, could increase the steric and hydrogen bond complementarity and may yield derivatives with increased affinity for Hsp90.

Halfway between the pocket bottom and the surface, the widening of the pocket causes a decrease in the complementarity and contact density, although the fit is still adequate to exclude bulk solvent (Figure 6C). In this region, the diene and the C27 methoxy groups make van der Waals contacts, and the O5 hydroxyl group makes a hydrogen bond contact with Lys58 (Figures 6A and 6B). As we get closer to the surface, the contact density decreases further. In this region, the C28 methyl group appears to be in an overall unfavorable environment, being within van der Waals contact distance to a backbone carbonyl oxygen atom and a partially buried water molecule (Figures 6A and 6B). The loose fit in this region, both sterically and electrostatically, points to a potential for a significant improvement of the affinity of geldanamycin for Hsp90 (Figure 6C).

At the pocket entrance, the carbonyl oxygen atom of the ansa ring makes a hydrogen bond to a backbone amide (Phe138) at the N-terminal portion of the H7 helix (Figures 6A and 6B). The benzoquinone, which is at the pocket entrance with one face solvent-exposed, makes only a few contacts, and these are primarily solvent-exposed hydrogen bonds made to long lysine chains: one of the benzoquinone oxygen atoms hydrogen bonds with Lys112, and the C29 methoxy group oxygen atom makes a long-distance (3.5 Å) hydrogen bond with Lys58.

Geldanamycin Derivatives

Among the naturally occurring homologs, geldanamycin is the most potent. Compared to herbimycin, for example, geldanamycin is more potent by a factor of about four in achieving a 50% reduction (IC_{50}) of erbB-2 kinase activity in human SKBr3 breast cancer cells (Miller et al., 1994). The structure suggests that this may be due to the hydrogen bond that the C29 methoxy oxygen atom of geldanamycin makes with Lys58, because herbimycin does not have the C29 methoxy group.

Among the published synthetic derivatives (Schnur et al., 1995a, 1995b), the highest potency, reflecting an improvement in the IC_{50} of a factor of 4–5, was achieved by an amino group substitution at the C17 position of the benzoquinone (Schnur et al., 1995a). It was proposed that this and several related substitutions at the C17 position improved cellular activity indirectly, by stabilizing the quinone form over the reduced hydroquinone (Schnur et al., 1995a). The structure supports this hypothesis, as this position is highly solvent exposed in the complex and is a poor candidate for additional Hsp90 contacts.

Overall, however, most modifications decreased or eliminated activity (Schnur et al., 1995a, 1995b). The maintenance of the carbamate group and of the closed, cyclic nature of the ansa ring proved necessary for activity (Schnur et al., 1995b), consistent with the extended hydrogen bond network that the carbamate group makes and with the importance of a closed cyclic ring in limiting conformational flexibility, respectively. Modifications at other positions either had little effect or reduced the activity of geldanamycin in line with space considerations revealed by the crystal structure. For example, additions of small groups to the amide nitrogen and to the C19 position of the benzoquinone, which are juxtaposed in a partially solvent-exposed region of the complex, were tolerated (Schnur et al., 1995a, 1995b), whereas bulky substituents at these positions reduced or eliminated activity (Schnur et al., 1995b).

Our crystal structure suggests modifications, such as those at the C23 methoxy and C22 methyl groups discussed earlier, that could improve the steric and hydrogen bond complementarity between geldanamycin and Hsp90 and could thus provide analogs with increased Hsp90 affinity (a total synthesis of geldanamycin has recently been reported [Miller, 1995]). In addition, by identifying which modifications are compatible with Hsp90 binding, the structure should also help with the improvement of geldanamycin's low plasma half-life (Supko et al., 1995) and other pharmacological properties as well.

Implications for Understanding Hsp90 Function

The pocket is best considered as a substrate-binding site, for there are extensive similarities between the pocket and a typical enzyme active site, though no covalent chemistry is implied by the similarities. We note that: (1) the pocket has adequate space and hydrophobic content, and is adequately shielded from bulk solvent to tightly bind substrates of a few hundred daltons; (2) there is a nonuniform electrostatic distribution resulting from an aspartic acid at the otherwise hydrophobic bottom of the pocket; (3) the shape and size of the pocket entrance is likely to be regulated by a conformational change; (4) the geldanamycin-binding domain of Hsp90 is the best conserved among its three structural domains, and within this domain, the conserved residues cluster in and around the pocket; (5) mutations that inactivate Hsp90 map in and around the pocket; and, finally, (6) the geldanamycin inhibitor of Hsp90 function binds inside this pocket.

Assuming that the Hsp90 pocket is a substrate binding site, it can then directly follow that its substrate is the protein, or more precisely, a segment of the protein, whose conformational maturation/refolding is mediated by the Hsp90 chaperone system. This pocket-polypeptide association is likely to occur as a late step in the reaction pathway because Hsp70, which is present in all of the early Hsp90 complexes (Smith, 1993; Smith et

al., 1995; Dittmar et al., 1996; Johnson et al., 1996), can bind unfolded proteins (Flynn et al., 1991; Zhu et al., 1996) and is thus the likely initial recruiter of the unfolded polypeptide to the Hsp90 complex. That a polypeptide portion is the substrate for the pocket is supported by the ability of the endoplasmic reticulum homolog, GP96, to associate with a specific viral peptide, though it is not yet known with which domain of GP96 this peptide is associated (Nieland et al., 1996).

Further support is provided by the general similarities between the geldanamycin ansa ring and a peptide. A five amino acid polypeptide in a turn conformation could closely trace the geldanamycin ansa ring backbone, with its amino acid side chains broadly corresponding to the carbamate, methyl, and methoxy groups of geldanamycin (Figure 7). Furthermore, and intended only as an example, steric and hydrogen bond complementarity considerations suggest that a tryptophan amino acid could be accommodated at the polypeptide position corresponding to that of the geldanamycin carbamate group (Figure 7). The tryptophan indole amino group could donate a hydrogen bond to Asp93, in a manner analogous to that of the carbamate amino group, perhaps explaining why Asp93 is conserved, and the hydrophobic portion of the tryptophan could fill the buried cavity that is now occupied by water molecules in the geldanamycin complex (Figure 7). In this region, backbone amide groups, as well as other hydrogen bond donor amino acids, could also satisfy the hydrogen bond potential of Asp93, although they may not have as good of a fit as a tryptophan in the buried cavity.

It is conceivable that the pocket binds a family of related polypeptide sequences, and this could explain the conservation of the pocket residues, because a large family of peptide sequences, in contrast to a single sequence, could not coevolve with amino acid changes in the pocket. This has precedence in the Hsp70 chaperone, which has a peptide-binding channel highly conserved between E. coli and humans (Zhu et al., 1996), and binds unfolded proteins by interacting with seven-residue segments, having exposed hydrophobic amino acids at their central positions (Flynn et al., 1991; Zhu et al., 1996).

A model in which the polypeptide substrate binds in the pocket along the reaction pathway would be supported by the observation that geldanamycin causes the dissociation of the v-src–Hsp90 complex in transformed cells (Whitesell et al., 1994). Also consistent are observations from the in vitro conformational maturation of the steroid receptors. In this reaction, a transient complex of the receptor that includes Hsp90, Hsp70, and several other cofactors is in equilibrium with the hormone-responsive state of the receptor, which is bound to Hsp90, p23, and an immunophilin (Smith et al., 1995; Dittmar et al., 1996; Nair et al., 1996). Geldanamycin blocks the formation of the latter complex, consistent with receptor–pocket interactions being required to either arrive at or to maintain the hormone-responsive state of the receptor (Smith et al., 1995; Nair et al., 1996). In principle, the interruption of this reaction by geldanamycin can be interpreted in other ways, for example, to mean that geldanamycin directly competes with p23 (Smith et al., 1995) binding to the pocket. This

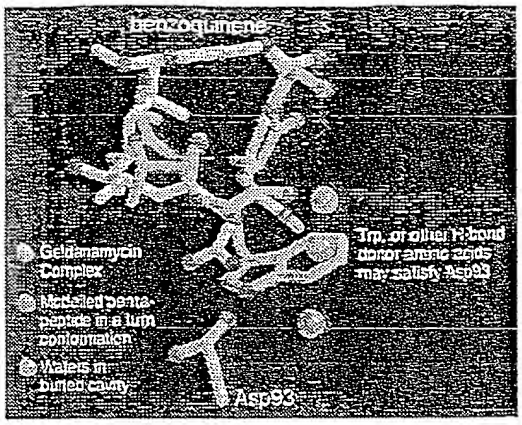

Figure 7. The Geldanamycin Ansa Ring Adopts a Structure Reminiscent of a Pentapeptide in a Turn Conformation

Geldanamycin and Asp93 of Hsp90 are in yellow, the buried water molecules at the geldanamycin–Hsp90-GBD interface are in magenta, and the modeled polypeptide is in cyan. Red and blue indicate oxygen and nitrogen atoms, respectively. A tryptophan at the peptide position corresponding to that of the carbamate group in geldanamycin could donate a hydrogen bond to Asp93 of Hsp90 and also pack in the hydrophobic cavity now occupied by the three water molecules. Backbone amide groups and several other amino acids could also hydrogen bond to Asp93, but their fit in the pocket would not be as good as that of a Trp.

is possible; however, we note that: (1) it is unlikely that such an unusual pocket would have evolved to bind a protein cofactor; (2) p23 and the pocket could have coevolved resulting in far lesser sequence conservation at the pocket; and (3) E. coli and lower eukaryotes do not seem to have p23, at least not one that is as conserved as the Hsp90-GBD.

On the other hand, the isolation of complexes of heat-denatured luciferase and of Raf with Hsp90 in the presence of geldanamycin (Schneider et al., 1996) at first appears to be inconsistent with the pocket binding these substrates. It is conceivable, however, that Hsp90 contains additional polypeptide-interacting sites that are not blocked by geldanamycin and that act at an earlier stage. These additional sites can be either within its geldanamycin-binding domain (for example, the conserved surface groove) or in the rest of the 732 residue protein. Alternatively, the observed association of geldanamycin-bound Hsp90 with the protein substrate may be indirect, since these complexes contain several other protein cofactors, such as Hsp70, which may contribute to polypeptide binding (Bose et al., 1996; Duina et al., 1996; Freeman et al., 1996; Schneider et al., 1996). In any case, geldanamycin blocks the refolding of the heat-denatured Raf and luciferase substrates, and this ultimately results in their degradation (Schneider et al., 1996).

The crystal structure of the Hsp90-GBD reveals a pocket whose properties indicate that it is a likely binding site for the polypeptide substrate. That geldanamycin, by binding in this pocket, inhibits the Hsp90-catalyzed conformational reaction both in vitro and in

vivo strongly argues that the pocket–substrate interaction is a required step in this reaction. The crystal structure of this pocket, as well as that of the geldanamycin–pocket complex, also provides a rational basis for the development of geldanamycin derivatives with improved antitumor activity.

Experimental Procedures

Identification of the Geldanamycin-Binding Domain of Hsp90

Bovine Hsp90, prepared from brains as described (Koyasu et al., 1986), was digested by subtilisin, and the products were delineated by N-terminal sequencing and mass spectroscopy. The C terminus of the middle domain is estimated based on its mobility in SDS–PAGE because this fragment was not amenable to mass spectroscopic analysis. The corresponding fragments of human Hsp90 were overexpressed in E. coli using the pET3d vector (Novagen), and the recombinant domains were purified by ion exchange and gel filtration chromatography.

Crystallization and Data Collection

For crystallization, the recombinant human Hsp90-GBD (residues 9–236) was concentrated by ultrafiltration to 30 mg/ml and was further purified by gel filtration chromatography. The geldanamycin–Hsp90-GBD complex was prepared by mixing the purified protein with a 2-fold molar excess of geldanamycin (GIBCO-BRL), fractionation by gel filtration, and concentration by ultrafiltration to 17 mg/ml. Two crystal forms were grown at 7°C using the method of hanging-drop vapor diffusion. One form (Native1 and Native2 in Table 1) grew from a buffer of 0.1 M sodium cacodylate (pH 6.5), 0.2 M ammonium sulfate, and 30 percent w/v polyethylene glycol 8000 (PEG8000) in spacegroup I222 with a = 66.2 Å, b = 90.1 Å, c = 101.2 Å. Another form (Native3) grew from 0.1 M Tris–HCl, 0.2 M magnesium chloride, and 30% PEG4000 (pH 8.5) in spacegroup $P2_1$ with a = 53.4 Å, b = 44.1 Å, c = 54.0 Å, β = 115.7°. Crystals of the geldanamycin–Hsp90-GBD complex (GDM complex in Table 1) grew from a buffer of 0.1 M Tris–HCl, 0.2 M sodium acetate, and 33% w/v PEG4000 (pH 8.5) in spacegroup $P2_1$, with a = 53.7 Å, b = 44.3 Å, c = 54.6 Å, β = 116.1° (same space group as Native3), and had a violet coloring. Data were collected on an R-AXISIIC imaging plate detector mounted on a Rigaku 200HB X-ray generator, at 10°C for Native1 and the derivatized crystals. For the other data sets, crystals were flash frozen at −160.0°C either in 30% PEG8000 and 20% glycerol (Native2) or in 35% PEG4000 (Native3 and GDM complex).

Structure Determination and Refinement

The heavy atom derivatives were prepared by soaking I222 form crystals in a buffer of 75 mM sodium cacodylate, 0.15 M ammonium sulfate, and 40% PEG8000 (pH 6.5) containing one of the following heavy atom solutions: saturated K_2AuCl_4 for 52 hr, 20 mM K_2PtCl_4 for 24 hr, and 20 mM K_2PtBr_6 for 60 hr. An additional derivative was obtained in 5 mM sodium cacodylate, 250 mM NaCl, 33% PEG8000 with 0.5 mM $Sm(OAc)_3$ (pH 7.0) for 14 hr. The multiple isomorphous replacement (MIR) analysis was performed using the CCP4 suite of programs (Collaborative Computational Project, Number 4, 1994). MIR phases had a mean figure of merit of 0.66 to 3.2 Å and were improved by solvent flattening and histogram matching. The initial model building was followed by several cycles of refinement with the program X-PLOR (Brunger, 1991) and by weighted combination between model phases and MIR phases, and this allowed for a continuous trace of residues 17–223. Amino acids 9–16 and 224–236 in the I222 form were not visible in the electron density maps and are presumed to be disordered. The $P2_1$ crystal form was solved by molecular replacement with X-PLOR. Difference density maps revealed that amino acids 105–132, and especially 105–112, had undergone significant structural rearrangement compared to the I222 form. In the crystals of the complex, geldanamycin was prominent in the early difference electron density maps and was built using the crystal structure of free herbimycin (Furusaki et al., 1980) as a starting point. In addition, in both $P2_1$ forms, the amino-terminal residues 11–16 were visible and modeled, whereas two solvent-exposed loops, 121–130 and 212–214, became partially disordered relative to the I222 crystals. Residues in all models were in the allowed regions of the Ramachandran plot, with 89% or more in the most favored regions. It is not clear what causes the conformational change in vitro; the L2 loop, which changes the most, is not involved in any significant crystal-packing contacts, though the H5 and H6 helices are in both crystal forms. In addition to magnesium and geldanamycin, the growth of the $P2_1$ form can be induced by acidic pH as well.

Acknowledgments

We thank S. Geromanos and H. Erdjument-Bromage of the Sloan-Kettering Microchemistry Facility for NH_2-terminal sequence and mass spectroscopic analyses, and O. Ouerfelli for helpful discussions about geldanamycin. This research was supported by the National Institutes of Health, the Pew Charitable Trusts, the Arnold and Mabel Beckman Foundation, the Dewitt Wallace Foundation, and the Samuel and May Rudin Foundation. Correspondence and requests for materials should be addressed to N. P. P. (nikola@xray2.mskcc.org). Coordinates have been deposited in the Brookhaven Protein Data Bank (ID codes 1YER, 1YES, and 1YET).

Received February 27, 1997; revised March 17, 1997.

References

Allgue, R., Akhavan-Niak, H., and Russell, P. (1994). A role for Hsp90 in cell cycle control: Wee1 tyrosine kinase activity requires interaction with Hsp90. EMBO J. *13*, 6099–6106.

Barlow, D.J., and Thornton, J.M. (1988). Helix geometry in proteins. J. Mol. Biol. *201*, 601–619.

Bohen, S.P., and Yamamoto, K.R. (1994). The Biology of Heat Shock Proteins and Molecular Chaperones, R.I. Morimoto, A. Tissieres and C. Georgopoulos, eds. (Cold Spring Harbor, NY: Cold Spring Harbor Laboratory Press).

Bohen, S.P., and Yamamoto, K.R. (1993). Isolation of Hsp90 mutants by screening for decreased steroid receptor function. Proc. Natl. Acad. Sci. USA *90*, 11424–11428.

Borkovich, K.A., Farrelly, F.W., Finkelstein, D.B., Taulien, J., and Lindquist, S. (1989). hsp82 is an essential protein that is required in higher concentrations for growth of cells at higher temperatures. Mol. Cell. Biol. *9*, 3919–3930.

Bose, S., Weiki, T., Bugl, H., and Buchner, J. (1996). Chaperone function of hsp90-associated proteins. Science *274*, 1715–1717.

Bouchard, L., Lamarre, L., and Tremblay, P.J. (1989). Stochastic appearance of mammary tumors in transgenic mice carrying the MMTV/c-*neu* oncogene. Cell *57*, 931–940.

Bresnick, E.H., Dalman, F.C., Sanchez, E.R., and Pratt, W.B. (1989). Evidence that the 90-kDa heat shock protein is necessary for the steroid binding conformation of the L cell glucocorticoid receptor. J. Biol. Chem. *264*, 4992–4997.

Brunger, A.T. (1991). X-PLOR, a system for X-ray crystallography and NMR, Version 3.1, Yale University. (New Haven, CT: Yale Univ. Press).

Chavany, C., Mimnaugh, E., Miller, P., Bitton, R., Nguyen, P., Trepel, J., Whitesell, L., Schnur, R., Moyer, J.D., and Neckers, L. (1996). p185(erbB2) binds to GRP94 in vivo—dissociation of the p185(erbB2)/GRP94 heterocomplex by benzoquinone ansamycins precedes depletion of p185(erbB2). J. Biol. Chem. *271*, 4974–4977.

Collaborative Computational Project, Number 4. (1994). The CCP4 suite: programs for protein crystallography. Acta Cryst. *D50*, 760–763.

Cutforth, T., and Rubin, G.M. (1994). Mutations in *Hsp83* and *cdc37* impair signaling by the Sevenless receptor tyrosine kinase in Drosophila. Cell *77*, 1027–1036.

DeBoer, C., Meulman, P.A., Wnuk, R.J., and Peterson, D.H. (1970). Geldanamycin, a new antibiotic. J. Antibiot. (Tokyo) *23*, 442–447.

Dittmar, K.D., Hutchison, K.A., Owens-Grillo, J.K., and Pratt, W.B.

(1996). Reconstitution of the steroid receptor-hsp90 heterocomplex assembly system of rabbit reticulocyte lysate. J. Biol. Chem. *271*, 12833–12839.

Duina, A.A., Chang, H.J., Marsh, J.A., Lindquist, S., and Gaber, R.F. (1996). A cyclophilin function in hsp90-dependent signal transduction. Science *274*, 1713–1715.

Flynn, G.C., Pohl, J., Flocco, M.T., and Rothman, J.E. (1991). Peptide-binding specificity of the molecular chaperone BiP. Nature *353*, 726–730.

Freeman, B.C., and Morimoto, R.I. (1996). The human cytosolic molecular chaperones hsp90, hsp70 (hsc70) and hdj-1 have distinct roles in recognition of a non-native protein and protein refolding. EMBO J. *15*, 2969–2979.

Freeman, B.C., Toft, D.O., and Morimoto, R.I. (1996). Molecular chaperone machines: chaperone activities of the cyclophilin cyp-40 and the steroid aporeceptor-associated protein p23. Science *274*, 1718–1720.

Furusaki, A., Matsumoto, T., Nakagawa, A., and Omura, S. (1980). Herbimycin A: an ansamycin antibiotic; X-ray crystal structure. J. Antibiot. (Tokyo) *33*, 781–782.

Hartson, S.D., and Matts, R.L. (1994). Association of Hsp90 with cellular Src-family kinases in a cell-free system correlates with altered kinase structure and function. Biochemistry *33*, 8912–8920.

Hunter, T., and Pines, J. (1994). Cyclins and cancer II: cyclin D and CDK inhibitors come of age. Cell *79*, 573–582.

Isaacs, J.T., and Coffey, D.S. (1979). Androgenic control of prostatic growth: regulation of steroid levels. UICC Monograph (Prostatic Cancer) *48*, 112–122.

Jakob, U., and Buchner, J. (1994). Assisting spontaneity: the role of Hsp90 and small Hsps as molecular chaperones. Trends Biochem. Sci. *19*, 205–211.

Johnson, J., Corbisier, R., Stensgard, B., and Toft, D. (1996). The involvement of p23, hsp90, and immunophilins in the assembly of progesterone receptor complexes. J. Steroid Biochem. Mol. Biol. *56*, 31–37.

June, C.H., Fletcher, M.C., Ledbetter, J.A., Schieven, G.L., Siegel, J.N., Phillips, A.F., and Samelson, L.E. (1990). Inhibition of tyrosine phosphorylation prevents T-cell receptor–mediated signal transduction. Proc. Natl. Acad. Sci. USA *87*, 7722–7726.

Kimura, Y., Matsumoto, S., and Yahara, I. (1994). Temperature-sensitive mutants of hsp82 of the budding yeast Saccharomyces cerevisiae. Mol. Gen. Genet. *242*, 517–527.

Koyasu, S., Nishida, E., Kadowaki, T., Matsuzaki, F., Iida, K., Harada, F., Kasuga, M., Sakai, H., and Yahara, I. (1986). Two mammalian heat shock proteins, HSP90 and HSP100, are actin-binding proteins. Proc. Natl. Acad. Sci. USA *83*, 8054–8058.

Kraulis, P.J. (1991). Molscript: a program to produce both detailed and schematic plots of protein structures. J. Appl. Cryst. *24*, 946–950.

Merrit, E.A., and Murphy, M.E. (1994). Raster3D Version 2.0: a program for photorealistic molecular graphics. Acta Cryst. *D50*, 869–873.

Miller, P., DiOrio, C., Moyer, M., Schnur, R.C., Bruskin, A., Cullen, W., and Moyer, J.D. (1994). Depletion of the erbB-2 gene product p185 by benzoquinoid ansamycins. Cancer Res. *54*, 2724–2730.

Miller, S.J. (1995). I. The asymmetric synthesis of the antitumor antibiotic macbecin. Diss. Abstr. Int. [B] *55*, 3313.

Murakami, Y., Mizuno, S., and Uehara, Y. (1994). Accelerated degradation of 160 kDa epidermal growth factor (EGF) receptor precursor by the tyrosine kinase inhibitor herbimycin A in the endoplasmic reticulum of A431 human epidermoid carcinoma cells. Biochem. J. *301*, 63–68.

Nair, S.C., Toran, E.J., Rimerman, R.A., Hjermstad, S., Smithgall, T.E., and Smith, D.F. (1996). A pathway of multi-chaperone interactions common to diverse regulatory proteins: estrogen receptor, Fes tyrosine kinase, heat shock transcription factor Hsf1, and the aryl hydrocarbon receptor. Cell Stress and Chaperones *1*, 237–250.

Nathan, D.F., and Lindquist, S. (1995). Mutational analysis of Hsp90 function: interactions with a steroid receptor and a protein kinase. Mol. Cell. Biol. *15*, 3917–3925.

Nicholls, A., Sharp, K.A., and Honig, B. (1991). Protein Folding and association: insights from the interfacial and thermodynamic properties of hydrocarbons. Proteins Struct. Funct. Genet. *11*, 281–296.

Nieland, T.J.F., Tan, M.C.A.A., Monne-van Muijen, M., Koning, F., Kruisbeek, A.M., and Vanbleek, G.M. (1996). Isolation of an immunodominant viral peptide that is endogenously bound to the stress protein GP96/GRP94. Proc. Natl. Acad. Sci. USA *93*, 6135–6139.

Omura, S., Iwai, Y., Takahashi, Y., Sadakane, N., Nakagawa, A., Oiwa, H., Hasegawa, Y., and Ikai, T. (1979). Herbimycin, a new antibiotic produced by a strain of Streptomyces. J. Antibiot. (Tokyo) *32*, 255–261.

Ono, Y., Kozai, Y., and Ootsu, K. (1982). Antitumor and cytocidal activities of a newly isolated benzenoid ansamycin, macbecin I. Gann. *73*, 938–944.

Osborne, C.K., Yochmowitz, M.G., Knight, W.A., and McGuire, W.L. (1980). The value of estrogen and progesterone receptors in the treatment of breast cancer. Cancer *46*, 2884–2888.

Picard, D., Khursheed, B., Garabedian, B., Fortin, M.G., Lindquist, S., and Yamamoto, K.R. (1990). Reduced levels of hsp90 compromise steroid receptor action *in vivo*. Nature *348*, 166–168.

Pratt, W.B., and Welsh, M.J. (1994). Chaperone functions of the heat shock proteins associated with steroid receptors. Semin. Cell Biol. *5*, 83–93.

Rinehart, K.L., Jr., and Shield, L.S. (1976). Chemistry of the ansamycin antibiotics. Fortschr. Chem. Org. Naturst. *33*, 231–307.

Sasaki, K., Yasuda, H., and Onodera, K. (1979). Growth inhibition of virus transformed cells in vitro and antitumor activity in vivo of geldanamycin and its derivatives. J. Antibiot. (Tokyo) *32*, 849–851.

Schneider, C., Sepp-Lorenzino, L., Nimmesgern, E., Ouerfelli, O., Danishefsky, S., Rosen, N., and Hartl, F.U. (1996). Pharmacologic shifting of a balance between protein refolding and degradation mediated by Hsp90. Proc. Natl. Acad. Sci. USA *93*, 14536–14541.

Schnur, R.C., Corman, R.J., Gallaschum, R.J., Cooper, B.A., Dee, J.L., Doty, J.L., Muzzi, M.L., DiOrio, C.I., Barbacci, E.G., et al. (1995a). erbB-2 oncogene inhibition by geldanamycin derivatives: synthesis, mechanism of action, and structure-activity relationships. J. Med. Chem. *38*, 3813–3820.

Schnur, R.C., Corman, R.J., Gallaschum, R.J., Cooper, B.A., Dee, J.L., Doty, J.L., Muzzi, M.L., Moyer, J.D., DiOrio, C.I., Barbacci, E.G., et al. (1995b). Inhibition of the oncogene product p185(erbB-2) in vitro and in vivo by geldanamycin and dihydrogeldanamycin derivatives. J. Med. Chem. *38*, 3806–3812.

Schulte, T.W., Blagosklonny, M.V., Ingui, C., and Neckers, L. (1995). Disruption of the Raf-1–Hsp90 molecular complex results in destabilization of Raf-1 and loss of Raf-1–Ras association. J. Biol. Chem. *270*, 24585–24588.

Schumacher, R.J., Hurst, R., Sullivan, W.P., McMahon, N.J., Toft, D.O., and Matts, R.L. (1994). ATP-dependent chaperoning activity of reticulocyte lysate. J. Biol. Chem. *269*, 9493–9499.

Smith, D.F. (1993). Dynamics of heat shock protein 90–progesterone receptor binding and the disactivation loop model for steroid receptor complexes. Mol. Endocrinol. *7*, 1418–1429.

Smith, D.F., Whitesell, L., Nair, S.C., Chen, S.Y., Prapapanich, V., and Rimerman, R.A. (1995). Progesterone receptor structure and function altered by geldanamycin, an hsp90-binding agent. Mol. Cell Biol. *15*, 6804–6812.

Stancato, L.F., Chow, Y.H., Hutchison, K.A., Perdew, G.H., Jove, R., and Pratt, W.B. (1993). Raf exists in a native heterocomplex with hsp90 and p50 that can be reconstituted in a cell-free system. J. Biol. Chem. *268*, 21711–21716.

Stepanova, L., Leng, X., Parker, S.B., and Harper, J.W. (1996). Mammalian p50Cdc37 is a protein kinase-targeting subunit of Hsp90 that binds and stabilizes Cdk4. Genes Dev. *10*, 1491–1502.

Sullivan, W.P., and Toft, D.O. (1993). Mutational analysis of hsp90 binding to the progesterone receptor. J. Biol. Chem. *268*, 20373–20379.

Supko, J.G., Hickman, R.L., Grever, M.R., and Malspeis, L. (1995). Preclinical pharmacologic evaluation of geldanamycin as an antitumor agent. Cancer Chemother. Pharmacol. *36*, 305–315.

Tronick, S.R., and Aaronson, S.A. (1995). Growth factors and signal transduction. In The Molecular Basis of Cancer, J. Mendelsohn, P. Howley, M. Israel and L. Liotta, eds., pp. 117–140.

Wearsch, P.A., and Nicchitta, C.V. (1996). Endoplasmic reticulum chaperone GRP94 subunit assembly is regulated through a defined oligomerization domain. Biochemistry *35*, 16760–16769.

Whitelaw, M.L., Hutchison, K., and Perdew, G.H. (1991). A 50-kDa cytosolic protein complexed with the 90-kDa heat shock protein (hsp90) is the same protein complexed with pp60v-src hsp90 in cells transformed by the Rous sarcoma virus. J. Biol. Chem. *266*, 16436–16440.

Whitesell, L., and Cook, P. (1996). Stable and specific binding of heat shock protein 90 by geldanamycin disrupts glucocorticoid receptor function in intact cells. Mol. Endocrinol. *10*, 705–712.

Whitesell, L., Mimnaugh, E.G., De Costa, B., Myers, C.E., and Neckers, L.M. (1994). Inhibition of heat shock protein HSP90–pp60v-src heteroprotein complex formation by benzoquinone ansamycins: essential role for stress proteins in oncogenic transformation. Proc. Natl. Acad. Sci. USA *91*, 8324–8328.

Xu, Y., and Lindquist, S. (1993). Heat-shock protein hsp90 governs the activity of pp60v-src kinase. Proc. Natl. Acad. Sci. USA *90*, 7074–7078.

Zhu, X., Zhao, X., Burkholder, W.F., Gragerov, A., Ogata, C.M., Gottesman, M.E., and Hendrickson, W.A. (1996). Structural analysis of substrate binding by the molecular chaperone DnaK. Science *272*, 1606–1614.

Antibiotics with Ansa Rings

KENNETH L. RINEHART, JR.

Department of Chemistry, University of Illinois, Urbana, Illinois 61801

Received July 27, 1971

Often when an antibiotic of a new structural type appears on the chemotherapeutic scene it is soon joined by additional representatives of the same type, so that one can begin to speak of a class of antibiotics. This is the case with a new class of antibiotics containing an aliphatic ansa bridge,[1] a bridge connecting two nonadjacent positions of an aromatic nucleus, for which the term "ansamycins" has been suggested by Prelog.

Thus far four representatives of this class of antibiotics have been identified—the rifamycins, produced by *Streptomyces mediterranei*,[2] the streptovaricins, from *Streptomyces spectabilis*,[3] the tolypomycins, from *Streptomyces tolypophorus*,[4] and geldanamycin, from *Streptomyces hygroscopicus* var. *geldanus* var. *nova*.[5] The first three exist as complexes of closely related components; more than a dozen individual compounds have been assigned to the class. Moreover, some of the antibiotics have been isolated by more than one group; the nancimycins[6a] have been reported [6b] to be the same as the rifamycins, and the streptovaricins are apparently identical with antimicrobial substance B44P[7] as well as the austmycins.[8]

Structures assigned to components of the rifamycin complex, rifamycins B,[9,10] L,[11] and Y,[12,13] are shown in Figure 1, those assigned to the streptovaricins, streptovaricins A, B, C, D, E, G, and F,[14,15] in Figure 2, that of tolypomycin Y[16] in Figure 3, and that of geldanamycin in Figure 4.[17,18] Rifamycins O[21] and SV,[22a] originally obtained as degradation products of rifamycin B (Figure 5), have been isolated from *Streptomyces* 4107A2 and a mutant of *Streptomyces mediterranei*, respectively.

Biological Activity

The ansamycins are notably active[22b] against gram-positive bacteria. Some broad spectrum activity has been noted for certain rifamycin derivatives[20] and some activity against gram-negative bacteria for the streptovaricins.[3] The streptovaricins repress *Mycobacterium tuberculosis*[23] and murine leprosy,[24] and rifamycin derivatives[25,26] are reported to be clinically useful, especially in the treatment of tuberculosis. Geldanamycin differs from the other ansamycins in that its principal activity is against protozoa rather than against bacteria.[5]

Curiously, the antibacterial activity of the ansamycin antibiotics withstands considerable variation in structure. Several of the streptovaricins have antibacterial activity,[3,27] and all the rifamycins (A, B, C,

K. L. Rinehart, Jr., is Professor of Chemistry at the University of Illinois, Urbana, where he has been employed since receiving his doctorate (with James Cason) at the University of California, Berkeley, in 1954. His present research interests center around bioorganic chemistry, especially structural, biosynthetic, and synthetic aspects of antibiotics, and mass spectrometry as applied to biologically interesting compounds. Former research efforts have included forays into ferrocene and cycloprene chemistry.

(1) The term *ansa* compounds was originally proposed by Lüttringhaus [A. Lüttringhause and H. Gralheer, *Justus Liebigs Ann. Chem.*, 550, 67 (1942)] for compounds of this general structural type, usually meta- and para-bridged benzenes.

(2) P. Sensi, P. Margalith, and M. T. Timbal, *Farmaco, Ed. Sci.*, 14, 146 (1959).

(3) P. Siminoff, R. M. Smith, W. T. Sokolski, and G. M. Savage, *Amer. Rev. Tuberc. Pulm. Dis.*, 75, 576 (1957).

(4) (a) T. Kishi, M. Asai, M. Muroi, S. Harada, E. Mizuta, S. Terao, T. Miki, and K. Mizuno, *Tetrahedron Lett.*, 91 (1969); (b) M. Shibata, T. Hasegawa, and E. Higashide, *J. Antibiot.*, 24, 810 (1971).

(5) C. De Boer, P. A. Meulman, R. J. Wnuk, and D. H. Peterson, *J. Antibiot.*, 23, 442 (1970).

(6) (a) R. Donovick, J. F. Pagano, and J. Vandeputte, U. S. Patent 2,999,048 (Sept 5, 1961); *cf. Chem. Abstr.*, 55, 27792e (1961); (b) J. S. P. Schwarz, *J. Antibiot., Ser. A*, 20, 238 (1967).

(7) H. Yamazaki, *ibid.*, 21, 204, 209, 222 (1968).

(8) Dr. Heiichi Sakai, Fujisawa Pharmaceutical Co., personal communication to Dr. G. B. Whitfield, The Upjohn Co.

(9) (a) W. Oppolzer, V. Prelog, and P. Sensi, *Experientia*, 20, 336 (1964); (b) J. Leitich, W. Oppolzer, and V. Prelog, *ibid.*, 20, 343 (1964).

(10) M. Brufani, W. Fedeli, G. Giacomello, and A. Vaciago, *ibid.*, 20, 339 (1964).

(11) G. C. Lancini, G. G. Gallo, G. Sartori, and P. Sensi, *J. Antibiot.*, 22, 369 (1969).

(12) J. Leitich, V. Prelog, and P. Sensi, *Experientia*, 23, 505 (1967).

(13) M. Brufani, W. Fedeli, G. Giacomello, and A. Vaciago, *ibid.*, 23, 508 (1967).

(14) (a) K. L. Rinehart, Jr., and F. J. Antosz, *J. Antibiot.*, in press; (b) A. H.-J. Wang, I. C. Paul, K. L. Rinehart, Jr., and F. J. Antosz, *J. Amer. Chem. Soc.*, 93, 6275 (1971).

(15) K. L. Rinehart, Jr., M. L. Maheshwari, F. J. Antosz, H. H. Mathur, K. Sasaki, and R. J. Schacht, *ibid.*, 93, 6273 (1971).

(16) (a) T. Kishi, S. Horanda, M. Asai, M. Muroi, and K. Mizuno, *Tetrahedron Lett.*, 97 (1969); (b) K. Kamiya, T. Sugiro, Y. Wada, M. Nishikawa, and T. Kishi, *Experientia*, 25, 901 (1969).

(17) K. Sasaki, K. L. Rinehart, Jr., G. Slomp, M. F. Grostic, and E. C. Olson, *J. Amer. Chem. Soc.*, 92, 7591 (1970).

(18) In addition to the components shown in Figures 1 and 2, rifamycins A, C, D, and E[19] and streptovaricins H and I[20] have been reported. Both relative and absolute stereochemistry of rifamycins B and Y has been assigned, based on X-ray data[10,11] and degradation products.[9b] The relative stereochemistry of tolypomycin Y has also been determined by X-ray crystallography.[16b] The relative stereochemistry shown for the streptovaricins has very recently been established for a streptovaricin C derivative by X-ray crystallography.[14b] It is of interest that the stereochemistry of rifamycins B and Y, of tolypomycin Y, and of streptovaricin C is the same at all the asymmetric carbon atoms. Stereochemical assignments have not yet been made for geldanamycin; the pattern shown would accord (in part) with the patterns of the other ansamycins.

(19) P. Sensi, A. M. Greco, and R. Ballotta, *Antibiot. Annu.*, 1959–1960, 262 (1960).

(20) G. B. Whitfield, Jr., P. K. Martin, and M. L. Maheshwari, unpublished observations.

(21) S. Sugawara, K. Karasawa, M. Watanabe, and T. Hidaka, *J. Antibiot., Ser. A*, 17, 29 (1964).

(22) (a) G. Lancini and C. Hengeller, *J. Antibiot.*, 22, 637 (1969); (b) the biological activities of the rifamycins have been reviewed very recently [W. Wehrli and M. Staehelin, *Bacteriol. Rev.*, 35, 290 (1971)].

(23) L. E. Rhuland, K. F. Stern, and H. R. Reames, *Amer. Rev. Tuberc. Pulm. Dis.*, 75, 588 (1957).

(24) Y. T. Chang, *ibid.*, 79, 673 (1959).

(25) (a) S. Furesz and R. Scotti, *Antibiot. Annu.*, 1959–1960, 285 (1960); (b) S. Furesz and R. Scotti, *Farmaco, Ed. Sci.*, 16, 262 (1961).

(26) T. M. Daniel, *New Engl. J. Med.*, 280, 615 (1969).

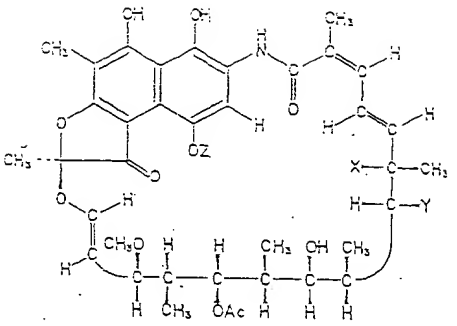

RIFAMYCIN	X	Y	Z
B	H	OH	CH_2COOH
Y	OH	O=	CH_2COOH
L	H	OH	$COCH_2OH$

Figure 1. Structures assigned to rifamycins.

D, E,) are biologically active.[22,28] Moreover, a number of the derivatives of rifamycin B are more active than the antibiotic itself. The biological activity of rifamycin B is retained through the sequence (Figure 5) of oxidation to rifamycin O (which forms the lactone), hydrolysis to rifamycin S (which removes the glycolic acid), and reduction to rifamycin SV (which reforms the hydroquinone).

Acyl derivatives of rifamycins B, O, S, and SV with the phenolic hydroxyl substituted show activity.[29] Amides of the glycolic acid acid group of rifamycin B, such as rifamide,[30] are also active. Condensation of rifamycin O (at the less hindered quinone carbonyl of rifamycin S) with various amines gave active derivatives, of which the aminoguanidine derivative was reported to be the most active.[29,31] Condensations with *o*-diamino aromatic compounds gave active derivatives such as rifazine.[32] An even more remarkable transformation with retention of biological activity involves a Mannich reaction at the unsubstituted hydroquinone position and oxidation to the formyl derivative, followed by condensation of the formyl group with amines (Figure 6). In these derivatives, such as rifampicin, the antibacterial activity of the antibiotic is considerably enhanced.[33]

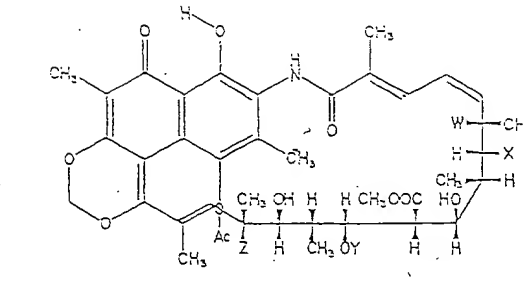

STREPTOVARICIN	W	X	Y	Z
A	OH	OH	Ac	OH
B	H	OH	Ac	OH
C	H	OH	H	OH
D	H	OH	H	H
E	H	O=	H	OH
G	OH	OH	H	OH

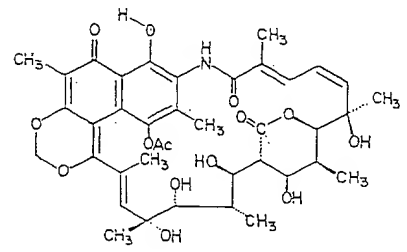

STREPTOVARICIN F

Figure 2. Structures assigned to streptovaricins.

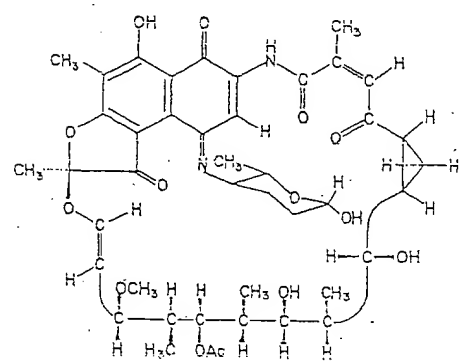

TOLYPOMYCIN Y

Figure 3. Structure assigned to tolypomycin Y.

The modes of action of rifamycin[34,35] and streptovaricin[36,37] as antibacterial agents are very similar. Both antibiotics inhibit DNA-directed RNA polymerase in bacterial cells more strongly than any other known agent.[38] It seems likely that both antibiotics act at a similar site, since *E. coli* resistant to one of the antibiotics is also resistant to the other.[39] Specific

(27) J. P. Folkertsma, W. T. Sokolski, and J. W. Snyder, *Antibiot. Annu.*, 1957–1958, 114 (1958).

(28) Under some conditions of fermentation, notably on addition of diethylbarbituric acid to the medium, the normally occurring complex of rifamycins (predominantly rifamycins C and D) is replaced by what is mostly a single entity, rifamycin B, differing from the other rifamycins in solubility properties.[19] Rifamycin B is acidic, whereas the other rifamycins are essentially neutral. This ability to obtain one component, and the most stable component at that, aided considerably in the structural investigations of the rifamycins, since the tedious separation, preliminary to the structural investigations of the streptovaricins, for example, was obviated.

(29) (a) P. Sensi, *Res. Progr. Org.-Biol. Med. Chem.*, 1, 338 (1964); (b) apparently, however, the activity of acyl derivatives in antibacterial assays is due to their hydrolysis during incubation [W. Wehrli and M. Staehelin, *Biochim. Biophys. Acta*, 182, 24 (1969)].

(30) P. Sensi, N. Maggi, R. Ballotta, S. Furesz, R. Pallanza, and V. Ariola, *J. Med. Chem.*, 7, 596 (1964).

(31) P. Sensi, M. T. Timbal, and A. M. Greco, *Antibiot. Chemother.*, 12, 488 (1962).

(32) (a) G. G. Gallo, C. R. Pasqualucci, N. Maggi, R. Ballotta, and P. Sensi, *Farmaco, Ed. Sci.*, 21, 68 (1966); (b) H. Bickel, F. Knüsel, W. Kump, and L. Neipp, *Antimicrob. Ag. Chemother.*, 1966, 352 (1967).

(33) N. Maggi, R. Pallanza, and P. Sensi, *ibid.*, 1965, 765 (1966).

(34) G. Hartmann, K. O. Honikel, F. Knüsel, and J. Nüesch, *Biochim. Biophys. Acta*, 145, 843 (1967).

(35) H. Umezawa, S. Mizuno, H. Yamazaki, and K. Nitta, *J. Antibiot.*, 21, 235 (1968).

(36) H. Yamazaki, S. Mizuno, K. Nitta, R. Utahara, and H. Umezawa, *ibid.*, 21, 63 (1968).

(37) S. Mizuno, H. Yamazaki, K. Nitta, and H. Umezawa, *Biochim. Biophys. Acta*, 157, 322 (1968).

(38) G. Hartmann, W. Behr, K.-A. Beissner, K. Honikel, and A. Sippel, *Angew. Chem.*, 80, 710 (1968).

(39) K. Nitta, S. Mizuno, H. Yamazaki, and H. Umezawa, *J. Antibiot.*, 21, 521 (1968).

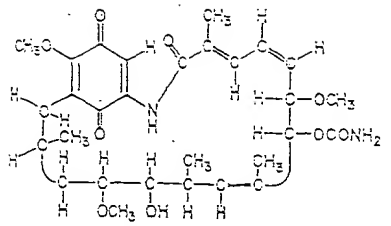

Figure 4. Structure assigned to geldanamycin.

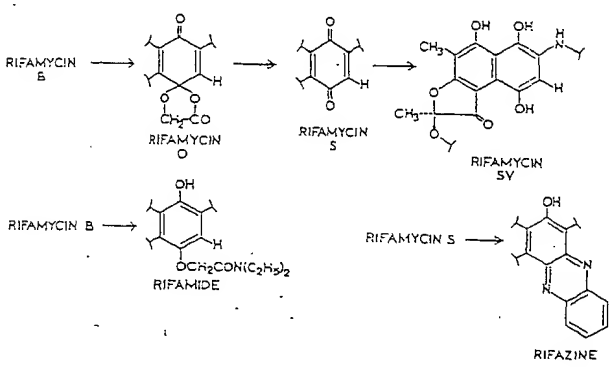

Figure 5. Conversion of rifamycin B to related biologically active compounds.

structural requirements needed to ensure activity have not been ascertained. In view of the wide variety of rifamycin derivatives which retain antibacterial activity, the principal requisite feature may be the ansa bridge. Unfortunately, reports of the mode of action of tolypomycin and geldanamycin are not available.

The effect of rifamycin and streptovaricin in inhibiting RNA polymerase recalls the similar activity of actinomycin; however, the mode of action appears to differ. Whereas actinomycin interacts with the DNA, rifamycin appears to interact directly with the polymerase itself.[40] In the case of rifamycin, the antibiotic and enzyme form a very stable complex.[41] As expected, RNA polymerase from rifamycin-resistant mutants does not form a similar complex.[41] The action of chromomycin is the same as that of actinomycin.[42] In keeping with this difference in mode of action between streptovaricin–rifamycin and actinomycin–chromomycin: (1) the former antibiotics do not interfere with DNA-dependent DNA synthesis,[35a] (2) their effect on RNA synthesis is independent of the base composition of the DNA template,[35a] (3) they must be added prior[37,42] to the initiation of the polymerization reaction since their specific action lies in blocking initiation of the RNA synthesis,[42,43] and (4) the activity is much greater aginst bacterial RNA polymerase than against mammalian[40] or tumor[37] RNA polymerase.

In bacterial polymerase studies rifampicin (Figure 6) usually is used, although rifamycins B and SV (Figures

(40) W. Wehrli, J. Nüesch, F. Knüsel, and M. Staehelin, *Biochim. Biophys. Acta*, 157, 215 (1968).
(41) W. Wehrli, F. Knüsel, K. Schmid, and M. Staehelin, *Proc. Nat. Acad. Sci. U. S.*, 61, 667 (1968).
(42) A. Sippel and G. Hartmann, *Biochim. Biophys. Acta*, 157, 218 (1968).
(43) S. Mizuno, H. Yamazaki, K. Nitta, and H. Umezawa, *Biochem. Biophys. Res. Commun.*, 30, 379 (1968).

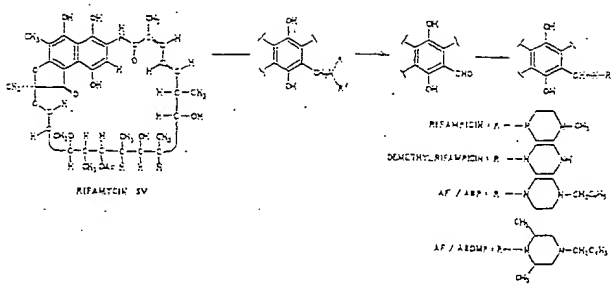

Figure 6. Biologically important compounds derived from rifamycin SV.

1 and 5) also appear to be effective. Other organisms are inhibited by rifamycin derivatives as well. Growth of *Anacystis montana* (a blue-green algae representative) was completely blocked by rifamycins B and S and rifampicin, while growth of *Chlorella pyrenoidosa* (green algae) was unaffected.[44] On the other hand, development of trachoma agent was markedly inhibited by rifampicin and rifamycin SV but not by rifamycin B.[45]

The ansamycins are also antiviral agents; the activity of rifampicin has been tested with human volunteers.[46] Rifampicin (Figure 4) inhibits replication of vaccinia poxvirus,[47–49] and the same effect is manifested by at least one (but not by all) of the streptovaricin components.[50] More recently *N*-demethylrifampicin and AF/ABDMP (2,6-dimethyl-*N*-demethyl-*N*-benzylrifampicin), other derivatives of formylrifamycin SV (Figure 6), have been shown to be much more potent than rifampicin in inhibiting vaccinia virus, *Herpes simplex*, and pseudorabies.[51] The mode of action of rifampicin in this inhibition of viral replication appears to be different[49,52] from that described in the preceding paragraphs for bacteria. The gross effect is inhibition of virus particle formation, and this appears to proceed by prevention of the conversion of one polypeptide to another.[52]

Most dramatic (and most recent) of the activities of the ansamycins is that as potential antitumor agents. A number of derivatives of formylrifamycin SV (Figure 6) have been shown[53] to inhibit the RNA-dependent DNA polymerase activity[54,55] of several RNA tumor viruses. In this system rifampicin was without effect, but *N*-demethylrifampicin, AF/ABP (*N*-demethyl-

(44) M. Rodriguez-López, M. L. Muñoz, and D. Vazquez, *FEBS (Fed. Eur. Biochem. Soc.) Lett.*, 9, 171 (1970).
(45) Y. Becker, *Nature (London)*, 231, 115 (1971).
(46) A. Moshkowitz, N. Goldblum, and E. Heller, *ibid.*, 229, 422 (1971).
(47) E. Heller, M. Argaman, H. Levy, and N. Goldblum, *ibid.*, 222, 273 (1969).
(48) J. H. Subak-Sharpe, M. C. Timbury, and J. F. Williams, *ibid.*, 222, 341 (1969).
(49) B. R. McAuslan, *Biochem. Biophys. Res. Commun.*, 37, 289 (1969).
(50) (a) N. A. Quintrell and B. R. McAuslan, *J. Virol.*, 6, 485 (1970); (b) K. B. Tan and B. R. McAuslan, *Biochem. Biophys. Res. Commun.*, 42, 230 (1971).
(51) G. L. Lancini, R. Cricchio, and L. Thiry, *J. Antibiot.*, 24, 64 (1971).
(52) (a) B. Moss, E. N. Rosenblum, E. Katz, and P. M. Grimley, *Nature (London)*, 224, 1280 (1969); (b) E. Katz and B. Moss, *Proc. Nat. Acad. Sci. U. S.*, 66, 677 (1970).
(53) C. Gurgo, R. K. Ray, L. Thiry, and M. Green, *Nature (New Biol.)*, 229, 111 (1971).
(54) E. M. Temin and S. Mizutani, *Nature (London)*, 226, 1211 (1970).
(55) D. Baltimore, *ibid.*, 226, 1209 (1970).

N-benzylrifampicin), and AF/ABDMP (2,6-dimethyl-*N*-demethyl-*N*-benzylrifampicin) were highly active.[53] For inhibition of RNA-dependent DNA polymerase activity in murine leukemia virus, the streptovaricin complex is reported to be highly active, considerably more so than purified streptovaricins A or C, or rifamycin SV, which in turn are reportedly more active than rifampicin.[55] The clinical utility of these ansamycins as antitumor agents remains unknown.

Structural Studies on Streptovaricins

Studies leading to the assignment of structure to rifamycin B have been reviewed elsewhere.[9,10,57] Similarly, evidence for the structures of rifamycin Y[12,13] and tolypomycin Y[4,16,17] can be found in other sources. The structure assigned to geldanamycin is based nearly entirely on interpretation of the nmr spectra of geldanamycin and simple derivatives or degradation products.[18] Consequently, we shall here exercise an author's prerogative and concentrate our attention on our own studies of the streptovaricins.

The streptovaricin complex was initially characterized in work at the Upjohn Company, where the antibiotic was demonstrated to consist of a mixture of related components[58] separable by countercurrent distribution, partition chromatography, and paper chromatography. In our work, we have made extensive use of thin (and thick) layer chromatography in separating these orange antibiotics.[59] In the normal fermentation products streptovaricins A and C are the principal components, while a number of other components can be identified in concentrates from which most of the A or C components have been removed.

Difficulty was initially encountered in establishing molecular formulas for the streptovaricins due to their formation of stable complexes with solvents. However, mass spectrometry, combined with elemental analyses of samples from which solvent had been scrupulously removed under high vacuum, allowed assignment of molecular formulas. The molecular formulas indicated immediately that the streptovaricins are closely related, being either C_{40} or C_{42} compounds with varying numbers of oxygen atoms. Significantly, the C_{42} compounds contain ten *C*-methyl groups (including two acetate groups), while the C_{40} compounds contain nine *C*-methyl groups (including one acetate group). Accordingly, it was felt that the streptovaricins all contain an identical carbon skeleton and that they differ from one another in the degree of oxygenation and degree of acetylation.[59] This supposition was supported by the fact that the ultraviolet spectra of the streptovaricins[58] are nearly identical.

Because the compounds share a common chromophoric system, initial attempts centered on degrading the streptovaricins to a structural entity in which the chromophore was retained. However, attempts to degrade the compound by standard hydrolytic techniques were singularly unsuccessful. The failure to hydrolyze contrasts with the successful hydrolyses of rifamycin B[9] and tolypomycin Y[4] and can be attributed to the replacement of the enol ether function of the rifamycins and tolypomycins by a carbon–carbon bond in the streptovaricins.

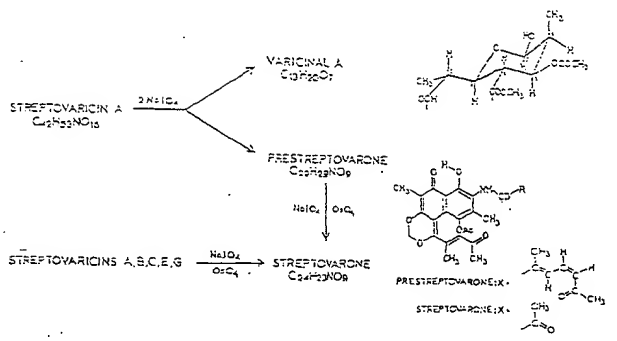

Figure 7. Degradation products derived from the streptovaricins.

Initial attempts at oxidative degradation of streptovaricins also yielded little information, but ultimately streptovaricin A was shown (Figure 7) to react with 2 moles of sodium periodate to give a colorless water-soluble product, varicinal A,[60,61] and a water-insoluble orange product, prestreptovarone.[15,62] Of the other streptovaricins, only streptovaricin G gave prestreptovarone on treatment with periodate. However, all the streptovaricins except streptovaricin D, on treatment with a mixture of sodium periodate and osmium tetroxide, gave streptovarone, a somewhat smaller orange compound, which was shown to be related to prestreptovarone by conversion of the latter compound to the former on oxidation with periodate–osmium tetroxide. Since both compounds contain the chromophore of the streptovaricins,[63] attention was directed initially to the smaller compound, streptovarone.[62,64]

On mild acidic hydrolysis, streptovarone was converted to a deep red compound lacking nitrogen, and other hydrolyses of streptovarone yielded formaldehyde and pyruvic acid, isolated as suitable derivatives (Figure 8).[62] A third group of streptovarone absent in the deep red compound was an enol acetate function, identified by infrared and nmr spectra. Accordingly, the new aromatic compound was referred to as dapmavarone (*deacetyldepyruvyldemethylenedioxystreptovarone*).

Dapmavarone in turn was further degraded, by a serendipitous Dakin reaction, to 3,7-dimethyl-2,5,6,8-tetrahydroxynaphthoquinone and 2-methyl-4-oxo-

(56) W. W. Brockman, W. A. Carter, L.-H. Li, F. Reusser, and F. R. Nichol, *Nature (London)*, 230, 249 (1971).
(57) V. Prelog, *Pure Appl. Chem.*, 7, 551 (1963).
(58) G. B. Whitfield, Jr., E. C. Olson, R. R. Herr, J. A. Fox, M. E. Bergy, and G. A. Boyack, *Amer. Rev. Tuberc. Pulm. Dis.*, 75, 584 (1957).
(59) K. L. Rinehart, Jr., P. K. Martin, and C. E. Coverdale, *J. Amer. Chem. Soc.*, 88, 3149 (1966).
(60) K. L. Rinehart, Jr., and H. H. Mathur, *ibid.*, 90, 6340 (1968).
(61) K. Sasaki, K. L. Rinehart, Jr., and F. J. Antosz, *J. Antibiot.*, in press.
(62) K. L. Rinehart, Jr., C. E. Coverdale, and P. K. Martin, *J. Amer. Chem. Soc.*, 82, 3150 (1960).
(63) P. K. Martin, Ph.D. Thesis, University of Illinois, Urbana, 1965.
(64) K. L. Rinehart, Jr., and F. J. Antosz, *J. Antibiot.*, in press.

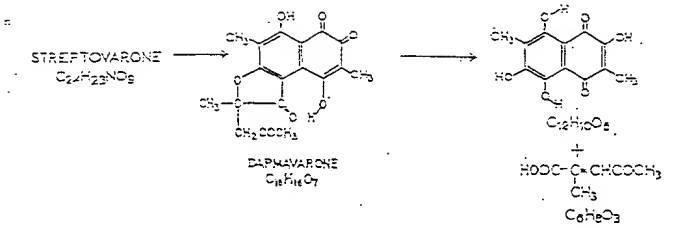

Figure 8. Degradation products derived from streptovarone.

2-pentenoic acid. The hydroxyl and methyl groups in the quinone were located by consideration of its nmr and mass spectra[62] and by comparison of these spectral properties with those of similar compounds prepared in the extensive studies of Scheuer and Moore on spinochromes.[65] The keto unsaturated acid was initially identified from its nmr spectrum[62] and subsequently compared to a synthetic sample, prepared by a known route.[66]

With all the carbon atoms in streptovarone identified, there remained only the problem of putting the pieces together again. Since the quinone and the keto unsaturated acid had been isolated from a Dakin reaction, they could be assumed to be formed by the introduction of 1 mole of hydrogen peroxide between an aromatic ring and a carbonyl group of dapmavarone. Because the quinone has a center of symmetry, only three positions needed to be considered for attaching the carbonyl group. Ultimately, the decision rested on the nmr spectrum of dapmavarone. Indeed, many of the structural assignments from this point on rest on the shifting positions and splitting patterns of certain protons observed initially in the nmr spectrum of the keto unsaturated acid (a, Figure 9).

The olefinic proton of the unsaturated acid is lacking in the nmr spectrum of dapmavarone (b, Figure 9), being replaced by absorption of a new methylene group. Moreover, the olefinic methyl group has been shifted to a position more appropriate to a methyl group on a quaternary aliphatic carbon. These changes imply addition of an oxygen function across the carbon–carbon double bond to give an additional ring, an implication supported by the appearance of a saturated ketone's infrared absorption at 1725 cm^{-1}. The very low frequency of the aromatic ketone band (below 1635 cm^{-1}) indicates hydrogen bonding and requires the aromatic carbonyl (removed in the Dakin reaction) to be located in the central position (for hydrogen bonding) among the three hydroxyl groups of the quinone (Figure 8). Comparison of the properties of dapmavarone to those of synthetic model compounds confirms the structure shown for dapmavarone in Figure 8.[67]

(65) (a) C. W. J. Chang, R. E. Moore, and P. J. Scheuer, *J. Amer. Chem. Soc.*, 86, 2959 (1964); (b) R. E. Moore and P. J. Scheuer, *J. Org. Chem.*, 31, 3272 (1966); (c) I. Singh, R. T. Ogata, R. E. Moore, C. W. J. Chang, and P. J. Scheuer, *Tetrahedron*, 24, 6053 (1968).

(66) C. Armengaud, G. Wermuth, and J. Schreiber, *C. R. Acad. Sci.*, 254, 2181 (1962).

(67) D. C. Schlegel, Ph.D. Thesis, University of Illinois, 1969.

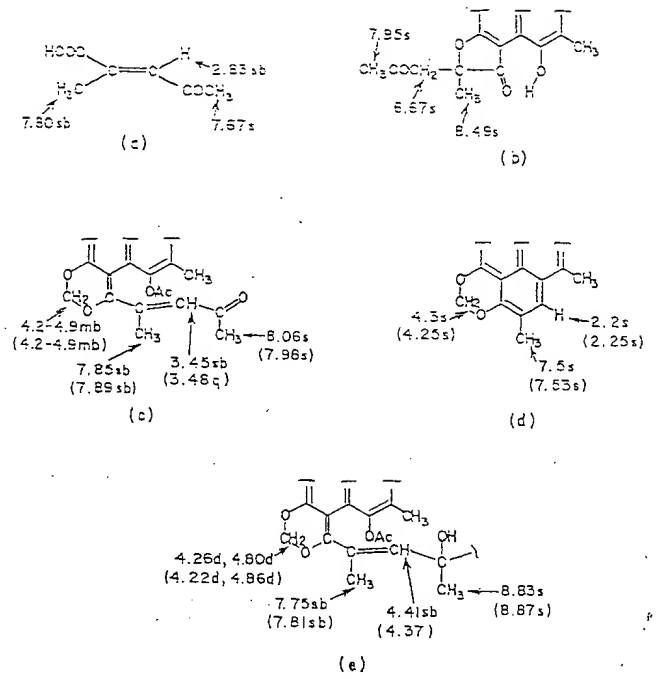

Figure 9. Chemical shifts of characteristic protons of streptovaricins and their degradation products: (a) 3-oxo-*trans*-2-pentenoic acid, (b) dapmavarone, (c) streptovarone (prestreptovarone), (d) photostreptovarone (deptovarone), (e) streptovaricin A (C).

In streptovarone (c, Figure 9), the olefinic hydrogen and an olefinic methyl group are found again. The ketone group in the side chain was confirmed by the formation of a dioxime of streptovarone, the other ketone being in the pyruvamide group.[64] The functional group in streptovarone which is hydrolyzed to formaldehyde was identified as a methylenedioxy group by its appearance at low field in the nmr spectrum, with the methylene protons being deshielded by two oxygen atoms. The amide function was identified by the nitrogen atom's neutrality and hydrogen exchange and located by comparison of its properties to those of 2-aminonaphthoquinone and 8-hydroxynaphthoquinone.[62]

Although the partial structure in the enolic portion of the molecule obviously involved a methylenedioxy group and enol acetate, as shown here, it was not clear

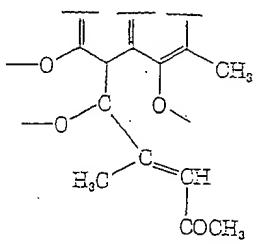

which two of the three oxygens the methylene group was spanning or, by difference, which oxygen was involved in the enol acetate group. This was ultimately assigned by consideration of the structure of photostreptovarone, discussed below, which was first observed as a yellow spot appearing on thin layer plates during chromatography of the orange streptovarone.

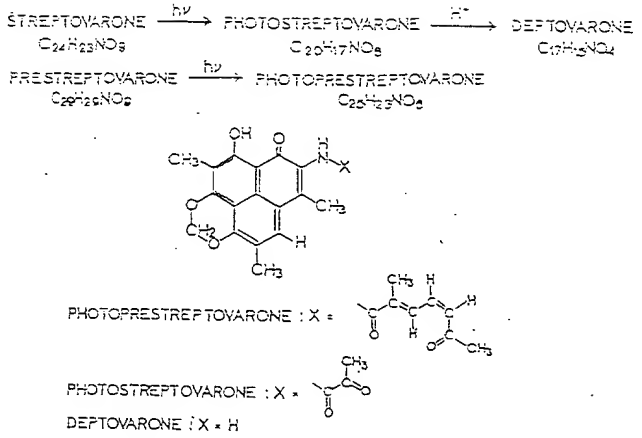

Figure 10. Structures of photostreptovarone and related products.

More careful radiation studies in solution allowed the isolation of photostreptovarone.[68] The molecular formula of photostreptovarone indicated loss of $C_4H_6O_3$ (the elements of acetic anhydride) from streptovarone and, indeed, acetic anhydride could be identified as a product of the photolysis. The yellow compound itself was shown, by comparison of its ultraviolet spectrum to those of related compounds, to be an 8-hydroxyphenalenenone (Figure 10), which would be formed *via* the intermediate dihydrophenalenone shown. A hydrolysis product, deptovarone (*dep*yruvylphotostreptovarone), was also prepared. The methyl and hydrogen groups empolyed in assigning the structures of dapmavarone and streptovarone appear at the appropriate aromatic positions in photostreptovarone (d, Figure 9). The isolation of photostreptovarone and its assigned structure define the locations of the methylenedioxy and enol acetate groups in streptovarone. Taken together, these lines of argument allowed assignment of the structure of streptovarone.[62,64]

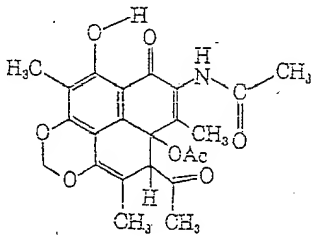

The structure of the immediate precursor of streptovarone, prestreptovarone, was apparent once the structure of streptovarone was established, since the nmr spectrum of prestreptovarone indicated an additional unsaturated methyl group and three olefinic hydrogens. The chemical shifts and coupling constants of these hydrogens indicated the stereochemistry shown here.[15,69,70] Photoprestreptovarone, with structure analogous to photostreptovarone, was obtained from photolysis of prestreptovarone (Figure 10).

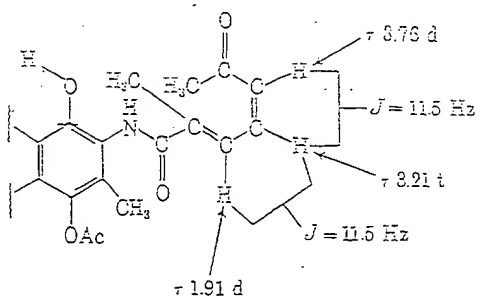

With the structure of prestreptovarone in hand, attention was directed toward the colorless water-soluble product from periodate oxidation of streptovaricin A, varicinal A.[60,61] Although the electron-impact-produced mass spectrum of varicinal A did not give a molecular ion, its molecular formula could be assigned from the occurrence of peaks at M − 31 and M − 18 whose juxtaposition indicated them to be fragment ions rather than molecular ions. A field-emission mass spectrum of varicinal A gave a strong molecular ion and confirmed the molecular formula.[71]

The structure of varicinal A (Figure 7) rests on its nmr spectrum and those of related compounds derived from streptovaricin C.[61] Individual peaks in the spectra occur at appropriate positions, and spin decoupling (Figure 11) indicates which of the protons are on adjacent carbon atoms. From the nmr spectrum of varicinal A relative stereochemistry at the atoms in the six-membered ring can be assigned (Figure 7); it is the same as that found in the rifamycins (Figure 1).

From the structures of prestreptovarone and varicinal A one can develop the structure of streptovaricins A and C,[15,64,69] remembering that 2 moles of periodate is required to cleave streptovaricin A to prestreptovarone and varicinal A. The nmr spectra of the streptovaricins indicate that all the oxygens of the streptovaricins which are found in varicinal A are present in the streptovaricins as hydroxyl, acetate, or carbomethoxyl groups, leaving as the only positions available for attachment to the prestreptovarone part of the molecule the terminal carbons, as shown in Figure 11. One point of attachment must be the ϵ carbon of the oxo dienamide unit in prestreptovarone. The carbonyl group at that position must have existed as a tertiary alcohol in streptovaricin A. In principle, that carbon could have been attached to either aldehyde carbon of varicinal A. However, spin-decoupling experiments carried out on streptovaricins A and C and related compounds (Figure 11)[69] completed the linking of the carbon atoms of varicinal A with those of the prestreptovarone dienamide unit.

The second point of attachment (and the second point of periodate cleavage) was more difficult to locate. It is particularly significant that one of the olefinic methyl groups of streptovarone appears in streptovaricin A (e, Figure 9) as a deshielded aliphatic methyl

(68) R. J. Schacht and K. L. Rinehart, Jr., *J. Amer. Chem. Soc.*, 89, 2239 (1967).

(69) K. L. Rinehart, Jr., H. H. Mathur, K. Sasaki, P. K. Martin, and C. E. Coverdale, *ibid.*, 90, 6241 (1968).

(70) The stereochemistry of an early sample of prestreptovarone was assigned[62] as trans,trans instead of the trans,cis stereochemistry shown which is also that of the streptovaricins.[69] Apparently the dienamide system isomerizes readily.

(71) E. M. Chait, T. W. Shannon, J. W. Amy, and F. W. Mc-

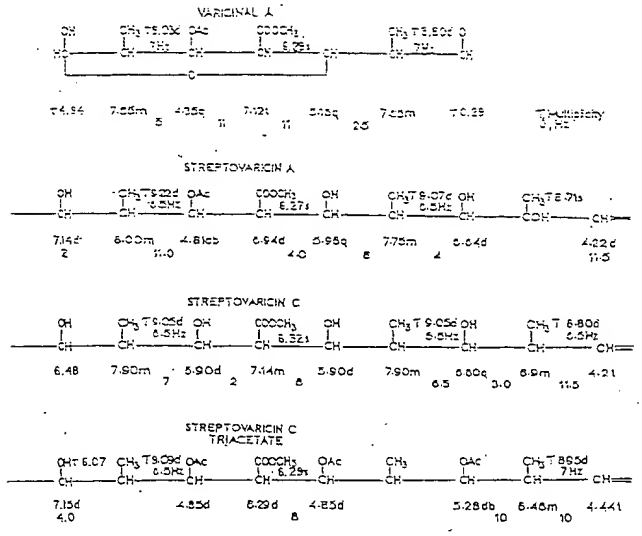

Figure 11. Chemical shifts and coupling of varicinal A protons and related protons in streptovaricins.

group, indicating the tetragonal nature of the carbon to which it is attached and suggesting an oxygen substituent. The latter point was confirmed by the appearance of the quaternary carbon at 82.9 ppm from tetramethylsilane in the ^{13}C nmr spectrum of streptovaricin C, a region appropriate for a hydroxyl-substituted carbon atom.[64] The only carbon in the diene side chain of streptovarone which is appropriate for a $>C(CH_3)O-$ group is C-4′, as shown in the partial structure here. The methylenedioxy group appears

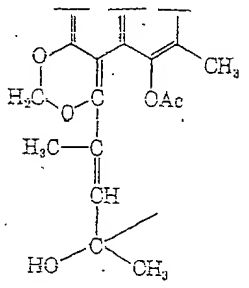

as an AB quartet. In the spectrum of streptovarone that group appeared as a very broad absorption which could be sharpened to a singlet on heating or split into an AB quartet on cooling. In photostreptovarone, the peak occurs as a singlet (d, Figure 9). Thus the structures of streptovaricins A and C are assigned as shown in Figure 2.

With the structures of streptovaricins A and C in hand, we turn to the structures of the other streptovaricins. As mentioned, these compounds must all be closely related in light of their similar molecular formulas—most likely by a common carbon skeleton differing in degree of oxygenation and acetylation.

A useful tool in assigning structures to the streptovaricins was mass spectrometry. Mass spectra of nearly all the streptovaricins contain strong peaks in the lower mass region at *m/e* 390, 324, 297, and 269. These peaks were initially a source of perplexity, even after determination of high-resolution spectra and assignment of structures to streptovaricins A and C in that there is no contiguous set of atoms in streptovaricins A and C which could lead to fragment ions having this composition. However, the perplexity was resolved with the observations that prestreptovarone and photoprestreptovarone give intense ions at *m/e* 390, 297, and 269, that streptovarone and photostreptovarone give peaks at *m/e* 324, 297, and 269, and that deptovarone gives peaks at *m/e* 297 and 269.[15,72] These results indicate a process occurring in the mass spectrometer akin to the photolytic process observed in solution (Figure 10) and the streptovaricin fragmentation joins the growing list of mass spectral–photochemical analogies.[73] Indeed, a metastable ion has been found indicating the one-step loss of $C_4H_6O_3$ (acetic anhydride) from the M − 43 ion (*m/e* 426) of streptovarone.[72] Since not only streptovaricins A and C but streptovaricins B, E, F, and G all give the *m/e* 390, 324, 297, and 269 peaks, the other streptovaricins must also contain the structural unit of streptovaricins A and C giving rise to the peaks.

A second useful tool was periodate oxidation, both in assigning the amount of periodate consumed and in establishing the formation of prestreptovarone or the lack thereof. Thus, only streptovaricin G besides streptovaricin A gives prestreptovarone on treatment with sodium periodate, consuming 2 moles of oxidant. This cleavage indicates a hydroxyl in the ϵ position of the dienamide for streptovaricin G. Lacking an acetate of streptovaricin A, it is assigned the structure in Figure 2. Streptovaricins B, C, E, and F do not give prestreptovarone on cleavage with periodate but react with 1 mole of periodate to give compounds which retain both the chromophoric unit and the complete side chain. Streptovaricins B, C, and E do not have a hydroxyl at C-6 of the macrolide ring; F has a protected hydroxyl at C-7 of the ring.

In assigning structures to the other streptovaricins, 100- and 220-MHz nmr spectroscopy were employed throughout, and essentially every proton could be located and assigned. The spectrum of streptovaricin C (Figure 11), as the most abundant streptovaricin, has been studied most extensively and has been compared carefully to those of the other streptovaricins. Structural parameters deduced by these nmr spectral comparisons have been confirmed by chemical evidence. Streptovaricin B has one acetate unit lacking in streptovaricin C; it is located at the same position as in streptovaricin A. Acetylation of streptovaricins B and C gives a common product, as does acetylation of streptovaricins A and G.[15] Streptovaricin E has a molecular formula two hydrogen atoms less than that of streptovaricin C and its infrared spectrum contains an extra carbonyl group, which its nmr spectrum locates

(72) R. J. Schacht, Ph.D. Thesis, University of Illinois, 1969.

(73) *Inter alia:* A. L. Burlingame, C. Fenselau, W. J. Richter, W. G. Dauben, G. W. Shaffer, and N. D. Vietmeyer, *J. Amer. Chem. Soc.*, 89, 3848 (1967); N. J. Turro, D. W. Weiss, W. F. Haddon, and F. W. McLafferty, *ibid.*, 89, 3870 (1967); R. C. Dougherty, *ibid.*, 90, 5780 (1968); M. K. Hoffmann, M. M. Bursey, and R. E. K. Winter, *ibid.*, 92, 727 (1970); C. Fenselau, G. W. Shaffer, and W. G. Dauben,

at C-7 of the side chain. On reduction with sodium borohydride streptovaricin E gives streptovaricin C.[15]

The most distinctly different streptovaricins are streptovaricins D and F. Streptovaricin D has one oxygen atom less than streptovaricin C and one of the aliphatic singlet methyl groups in the nmr spectra of the other streptovaricins is replaced by a methyl doublet at higher field. Streptovaricin D is not cleaved by sodium periodate at all, in accord with its lack of hydroxyl groups at C-6 and C-4′. The mass spectrum of streptovaricin D lacks the characteristic peaks at *m/e* 390, 324, 297, and 269 found in the spectra of the other streptovaricins and its structure is assigned as shown in Figure 2.[15]

The molecular formula of streptovaricin F suggests it to be related to streptovaricin G but lacking the elements of methanol. This is confirmed by their respective nmr spectra in that the methoxyl group absorption of the other streptovaricins is absent in the spectrum of streptovaricin F and the C-7 proton is shifted downfield (due to acylation of the C-7 hydroxyl) relative to the spectra of other streptovaricins.[15]

Biosynthesis

Little work has been reported dealing with the biosynthesis and bioconversion of the ansamycins. Inspection of their formulas suggests the highly branched side chains are likely formed from acetate and propionate (malonate and methylmalonate) units,[74] or, possibly, from acetate with subsequent methylation of the polyacetate chain by methionine or another one-carbon unit. Preliminary results concerning the primary source of the carbon atoms of rifamycin B indicate that propionate is a good precursor but that methionine is incorporated only in the methoxyl group.[74–76] The naphthoquinone rings may also be derived from acetate-propionate or from acetate with subsequent methylation.[74] However, an alternative pathway to naphthoquinone rings could be involved, such as that involving shikimic and glutamic acids.[77,78]

Bioconversions of some of the rifamycins have been reported. Labeled rifamycin B added to the fermentation medium has been shown to be converted to rifamycin Y, by hydroxylation and oxidation.[79] Rifamycin B itself is derived from rifamycin S, as is rifamycin L, the isomer of rifamycin B.[11] The latter two components appear to interconvert, but not directly, since aromatic ring-labeled rifamycin L gives labeled rifamycin B but label in the glycolate unit of rifamycin L is not retained in rifamycin B. Rifamycin O has been proposed to be an intermediate for both.[11]

Future Directions

The ansamycins represent some of the most complex antibiotics thus far isolated, and further members of this family will presumably be reported. The very high activity of the compounds promises continuing interest in them, both as tools of molecular biology through study of their mode of action and as potentially useful chemotherapeutic agents. In the latter capacity, it seems likely that the remarkable latitude allowed in structural modification with retention of biological activity will prompt further investigation along these lines. Moreover, the demonstrated ability to direct *Streptomyces mediterranei* toward production of one selected component of the rifamycins suggests the promising nature of continuing efforts toward biological modification of all these antibiotics.

It is a pleasure to express here my sincere appreciation to my collaborators whose work is discussed here—F. J. Antosz, C. E. Coverdale, M. L. Maheshwari, P. K. Martin, H. H. Mathur, K. Sasaki, R. J. Schacht, and D. C. Schlegel; to the Upjohn Co. for streptovaricin samples; and to the National Institute of Allergy and Infectious Diseases for their grants (AI 01278 and AI 04769) in support of this work.

(74) J. W. Corcoran and M. Chick in "Biosynthesis of Antibiotics," Vol. I, J. F. Snell, Ed., Academic Press, New York, N. Y., 1966, p 159.
(75) P. Sensi, unpublished results.
(76) V. Prelog, personal communication.
(77) P. Dansette and R. Azerad, *Biochem. Biophys. Res. Commun.*, 40, 1090 (1970), and earlier papers.
(78) D. J. Robbins, I. M. Campbell, and R. Bentley, *ibid.*, 39, 1081 (1970), and earlier papers.
(79) G. C. Lancini, J. E. Thiemann, G. Sartori, and P. Sensi, *Experientia*, 23, 899 (1967).

Related Proceedings Appendix

none